

2009

APPLICATION OF A MULTI-SEGMENT FOOT MODEL DURING RUNNING

Rebecca Shultz

Follow this and additional works at: <https://ir.lib.uwo.ca/digitizedtheses>

Recommended Citation

Shultz, Rebecca, "APPLICATION OF A MULTI-SEGMENT FOOT MODEL DURING RUNNING" (2009).
Digitized Theses. 3797.
<https://ir.lib.uwo.ca/digitizedtheses/3797>

This Thesis is brought to you for free and open access by the Digitized Special Collections at Scholarship@Western. It has been accepted for inclusion in Digitized Theses by an authorized administrator of Scholarship@Western. For more information, please contact wlsadmin@uwo.ca.

APPLICATION OF A MULTI-SEGMENT FOOT MODEL DURING RUNNING

(Spine Title:) "Applications of a Multi-Segment Foot Model during Running."

(Thesis format: Integrated-Article)

by

Rebecca Shultz

Graduate Program in Kinesiology

A thesis submitted in partial fulfillment
of the requirements for the degree of
Doctor of Philosophy

The School of Graduate and Postdoctoral Studies
The University of Western Ontario
London, Ontario, Canada

© Rebecca Shultz 2009

Abstract (including key words)

Standard gait analysis using optical motion capture systems involves modeling the foot as a single segment which limits the information on inter-segmental foot motion. Foot models have been shown to be reliable, but limited research is available that uses these foot models in conjunction with shoes. There are methodology issues that arise when the subject is wearing a shoe.

The primary objective of this dissertation is to develop a method to analyze the relative motion of the foot bones within multiple shoes during a variety of activities. The secondary objective is to apply this method in clinical studies to investigate the effect on foot kinematics due to shoe modifications or during different movements. Before any clinical research could be conducted, three methodology studies needed to be performed. Firstly, a method for validating holes in the shoe was developed and used to demonstrate that a 2.5 cm hole is valid for three different shoe types. Secondly, static trials from four different shoe conditions were found to exceed a minimum important difference (5°). Consequently, single static trials are important from an injury perspective since the absolute angular range is calculated. Per-condition static trials are necessary, however, if the study objective is to examine the symmetry of the range of motion around the joint. Lastly, in a single-plane fluoroscopy study, soft tissue artifact (STA) was found to range from 6.46mm and 16.72mm for the hindfoot and midfoot triad markers, which was comparable to previous values found in literature.

Two clinical studies were then conducted and demonstrated that foot kinematics are influenced by a directional change but appear to be unaffected by a change in longitudinal torsional stiffness and forefoot flexion. Many possible hypotheses for these results are discussed, including the possibility that the foot has a pre-determined kinematic pattern while traveling in a straight line that may be controlled by a pre-determined muscle activation pattern. The hypothesis that soft tissue is susceptible to injury past its "end-of-range" is also discussed in reference to foot injuries and the use of interventions. The method used in this dissertation will assist researchers in their investigations to find the mechanisms behind how the foot adapts to perturbations.

Keywords: Foot kinematics, running shoes, multi-segmented foot model, running, lateral cutting, skin artifact error, longitudinal torsional stiffness

Acknowledgments

Firstly, I would like to thank my supervisor, Thomas Jenkyn, for supporting and helping me through this process. I would also like to thank Trevor Birmingham and Ian Jones who helped me over the last four years offering me much needed advice. To my labmates, who have become my good friends, thank you for listening and helping me when I was not present in the lab. I hope I can repay you for all the favours you have granted me.

The employees of the Nike Sport Research lab, specifically Kelly, Matt, Martine, Mike and Tyler, were tremendously welcoming and knowledgeable. Thank you for teaching me so much in so little time.

I would like to first thank the UWO kinesiology department, specifically Jenn Symmes and Charles Rice, for helping me finish my thesis while taking on great career opportunities at Stanford. I truly appreciate the extra effort you have done on my behalf.

To my friends and family that have been on my side during my struggles over the last four years, thank you for listening and supporting me through the hard work and difficult decisions I have faced. I could not have accomplished this without your support and encouragement.

TABLE OF CONTENTS

CERTIFICATE OF EXAMINATION.....	II
ABSTRACT (INCLUDING KEY WORDS).....	III
TABLE OF TABLES.....	X
TABLE OF FIGURES.....	XII
LIST OF APPENDICES.....	XIX
LIST OF ABBREVIATIONS AND SYMBOLS.....	XX
1 CHAPTER 1: ANATOMY OVERVIEW OF THE FOOT AND REVIEW OF FOOT KINEMATIC RESEARCH.....	1
1.1 Anatomical Overview of the Foot.....	2
1.2 Bones of the foot.....	4
1.2.1 Rearfoot.....	4
1.2.2 Midfoot.....	6
1.2.3 Forefoot.....	7
1.2.4 Medial Longitudinal Arch.....	8
1.3 Brief Technical Note.....	9
1.4 Ligaments.....	11
1.4.1 Plantar Fascia.....	11
1.4.2 Intrinsic ligaments.....	12
1.5 Muscles and Tendons.....	14
1.5.1 Plantarflexors and Dorsiflexors.....	15
1.5.2 Invertors and Evertors.....	15
1.5.3 Intrinsic muscles of the foot.....	16
1.6 Functional Biomechanics.....	20
1.6.1 Gait Cycle.....	20
1.6.2 Locking mechanism of the foot during gait.....	23
1.6.3 Forefoot movement during Gait.....	24
1.7 Methods for Measuring Kinematics of the Foot during gait.....	24
1.7.1 Optical Motion Analysis Systems.....	25
1.7.2 Fluoroscopy.....	28
1.7.3 Other Methods.....	31

1.8	Previous Research Methods	33
1.8.1	Foot Kinematics during Gait	33
1.8.2	Foot Models	36
1.8.3	Multi-Segment Foot Model	42
1.9	Clinical Relevance	53
1.10	Thesis Objective and Chapter Overview	56
1.10.1	Outline	57
1.11	References	60
CHAPTER 2 – VALIDATION OF HOLES FOR EXAMINING KINEMATICS OF THE FOOT USING A MULTI-SEGMENT FOOT MODEL		66
2	ABSTRACT	67
2.1	Introduction	68
2.2	Methods	70
2.2.1	Subject and equipment	70
2.2.2	Multi-segment foot model marker set	72
2.2.3	Testing protocol	72
2.2.4	Shoe deformation analysis	74
2.2.5	Foot kinematic analysis	75
2.3	Results	75
2.4	Discussion	83
2.5	References	87
CHAPTER 3 – EFFECT OF NEUTRAL TRIAL ON FOOT KINEMATICS		89
3	ABSTRACT	90
3.1	Introduction	92
3.2	Methods and Procedures	94
3.2.1	Subjects	94
3.2.2	Gait Analysis and Data Collection	94
3.2.3	Data Analysis	97
3.2.4	Statistical Analysis	98
3.3	Results	98
3.4	Discussion	102

3.5	References	106
CHAPTER 4 – QUANTIFYING SKIN MOTION ERROR IN OPTICAL TRACKING OF A MULTI-SEGMENT FOOT MODEL USING SINGLE-PLANE FLUOROSCOPY		
4	ABSTRACT.....	109
4.1	Introduction	111
4.2	Methods	114
	4.2.1 Subjects	114
	4.2.2 Equipment.....	115
	4.2.3 Testing Procedure.....	116
	4.2.4 Analysis.....	118
4.3	Results	124
4.4	Discussion.....	131
4.5	References.....	135
CHAPTER 5 – EFFECT OF LONGITUDINAL TORSION AND FOREFOOT FLEXION OF RUNNING SHOES ON FOOT KINEMATICS.....		
5	ABSTRACT.....	140
5.1	Introduction	142
5.2	Methods	146
	5.2.1 Subjects	146
	5.2.2 Experimental equipment.....	146
	5.2.3 Multi-segment foot model.....	150
	5.2.4 Procedure.....	150
	5.2.5 Data and statistical analysis.....	152
5.3	Results	153
5.4	Discussion.....	164
5.5	References.....	171
CHAPTER 6 – KINEMATICS OF THE SEGMENTS OF THE FOOT DURING LEVEL RUNNING AND MEDIAL CUTTING TURNS USING A MULTI-SEGMENT FOOT MODEL.....		
6	ABSTRACT.....	175
6.1	Introduction	177
6.2	Methods	179

6.2.1	Subjects	179
6.2.2	Experimental equipment.....	180
6.2.3	Multi-segment foot model.....	181
6.2.4	Experimental Protocol.....	183
6.2.5	Data Reduction and Analysis	185
6.3	Results	186
6.4	Discussion.....	192
6.5	References.....	196
7	CHAPTER 7: CONCLUSION	199
7.1	Addition to current research – The theory of Excessive Pronation	205
7.2	Reference.....	211
8	APPENDIX A	212
8.1	Minimum important difference, including the calculation of a value for the Medial Longitudinal Arch	212
	APPENDIX B	214
8.2	Support for Fluoroscopy Study (chapter 4).....	214
	APPENDIX C	216
8.3	Support for Longitudinal Torsional Study (chapter 6).....	216
	APPENDIX D	228
8.4	Calculation of Torsional Stiffness and Bending Stiffness (chapter 6).....	228
8.4.1	Torsional Stiffness.....	228
8.4.2	Forefoot Stiffness.....	228
	APPENDIX E	229
8.5	Permission Wiley-Blackwell.....	229
8.5.1	Permission from Elsevier.....	230
	APPENDIX F - CODE	232
8.6	Deformation of the shoe	232
8.7	Soft tissue error translation and rotation.....	243
8.7.1	Sub-Function.....	245
	APPENDIX G – ETHICS	247
	CURRICULUM VITAE	249

Table of Tables

TABLE 1.1: PLACEMENT SITE DESCRIPTIONS FOR THE EIGHT MARKER CLUSTERS ON THE RIGHT LEG AND FOOT. EACH SEGMENT HAS A SINGLE CLUSTER EXCEPT THE LOWER LEG AND THE MIDFOOT SEGMENTS WHICH HAD TWO CLUSTERS (REPRINTED WITH PERMISSION FROM JENKYN ET AL., 2007)	43
TABLE 1.2: THE FOLLOWING IS A FULL DESCRIPTION OF THE BONY LANDMARK LOCATIONS USED TO CALCULATE THE ANATOMICAL REFERENCE FRAMES USED IN THIS DISSERTATION. IT IS ADAPTED FROM THE JENKYN ET AL. MODEL. THIS INCLUDES THE ANKLE COMPLEX AND SUBTALAR JOINT. (REPRINTED WITH PERMISSION FROM JENKYN ET AL., 2007)	46
TABLE 2.1: DIMENSIONS OF THE FOUR HOLE SIZES TESTED. EACH HOLE WAS AN OVAL WITH THE LONG AND SHORT AXIS DIMENSIONS. SINCE MATERIAL WAS PERMANENTLY CUT FROM THE SHOE TO MAKE THE HOLES, THE HOLE CONDITIONS PROGRESSED FROM SMALLEST TO LARGEST SIZE. IT WAS NOT POSSIBLE TO RANDOMIZE THE HOLE SIZES.	74
TABLE 3.1: SUMMARY OF NEUTRAL POSITIONS: THE MEANS AND STANDARD DEVIATIONS (SD) FOR EACH OF THE FOOTWEAR CONDITIONS ACROSS EACH OF THE FOUR INTER-SEGMENTAL JOINTS TESTED. STATISTICALLY SIGNIFICANT DIFFERENCE BETWEEN THE CONTROL SHOE (CO) CONDITION AND THE BAREFOOT CONDITION (BARE) WERE FOUND FOR THE HEIGHT-TO-LENGTH MEDIAL LONGITUDINAL ARCH AND THE HALLUX ANGLE AT $P < 0.05$. DIFFERENCES WERE FOUND BETWEEN THE SHOE CONDITIONS AND THE BAREFOOT CONDITION FOR THE OTHER TWO INTER-SEGMENTAL JOINTS, BUT THESE WERE NOT SIGNIFICANT.	99
TABLE 3.2: SUMMARY OF STRENGTHS AND WEAKNESSES OF SINGLE VERSUS PER-CONDITIONS STATIC TRIALS AND NEUTRAL POSITIONS.	105
TABLE 4.1. LOCATION OF THE MANUALLY DIGITIZED LANDMARKS FOR THE NAVICULAR AND THE CALCANEUS.	118
TABLE 4.2. ROOT MEAN SQUARE (RMS) ERRORS FOR INTRA-RATER REPEATABILITY TESTING. THE NUMBERED LANDMARKS CORRESPOND TO THE DESCRIPTIONS LISTED IN TABLE 4.1. IN GENERAL, THE CALCANEUS LANDMARKS SHOWED BETTER RESULTS THAN THE NAVICULAR. THE PERIPHERY OF THE FLUOROSCOPE IMAGE WAS CLEARER THAN THE CENTRE, MAKING THE CALCANEUS LANDMARKS EASIER TO VISUALIZE AND DIGITIZE.	127
TABLE 4.3. THE DIFFERENCE IN ORIGIN DISPLACEMENT LENGTH BETWEEN THE STANCE PHASE INSTANCES OF HEEL STRIKE (HS), MID-STANCE (MS) AND TOE-OFF (TO) WITH RESPECT TO THE QUIET STANDING (QS) REFERENCE POSITION. THIS IS THE CHANGE IN DISTANCE BETWEEN THE ORIGIN OF THE BONE-FIXED COORDINATE SYSTEM AND THE MARKER-FIXED COORDINATE SYSTEM WITH RESPECT TO QS. THESE ARE SHOWN FOR EACH OF THE TEST SUBJECTS, WITH THE AVERAGE, STANDARD DEVIATION AND RANGE STATED IN THE BOTTOM FOUR ROWS. THE LARGEST DIFFERENCES FOR BOTH THE CALCANEUS AND THE NAVICULAR WERE SEEN AT TOE-OFF (TO).	128
TABLE 4.4. THE DIFFERENCE IN SEGMENT ANGLE BETWEEN THE STANCE PHASE INSTANCES OF HEEL STRIKE (HS), MID-STANCE (MS) AND TOE-OFF (TO) WITH RESPECT TO THE QUIET STANDING (QS) REFERENCE POSITION. THIS IS THE CHANGE IN ORIENTATION OF THE BONE-FIXED X-AXIS AND THE MARKER-FIXED X-AXIS WITH RESPECT TO QS. THESE ARE SHOWN FOR EACH OF THE TEST SUBJECTS, WITH THE AVERAGE, STANDARD DEVIATION AND RANGE STATED IN THE BOTTOM FOUR ROWS. THE MEAN FOR ALL CONDITIONS OF THE CALCANEUS AND NAVICULAR IS SHOWN TO BE LESS THAN ONE DEGREE WITH STANDARD DEVIATIONS AT APPROXIMATELY 0.5-1 DEGREES, EXCEPT FOR THE CALCANEUS AT HEEL STRIKE (HS). THE RANGE OF ALL OTHER VALUES IS 2-3 DEGREES WHEREAS AGAIN THE CALCANEUS AT HEEL STRIKE IS LESS THAN THE OTHER CONDITIONS.	130
TABLE 5.1. INTER-SEGMENTAL JOINT MEASURES AND LONGITUDINAL TORSION ANGLES. MEANS, STANDARD DEVIATIONS AND RANGES OF MOTION ARE GIVEN FOR EACH HINDFOOT, FOREFOOT, HALLUX MEDIAL LONGITUDINAL ARCH AND TORSION ANGLE MEASURES. POSITIVE VALUES MEAN SUPINATION FOR HINDFOOT (HIND), SUPINATION FOR FOREFOOT (FORE), PLANTAR-FLEXION FOR HALLUX (HAL) AND A RISING MEDIAL LONGITUDINAL ARCH (MLA). THE MEANS, STANDARD DEVIATIONS AND RANGES ARE TAKEN ACROSS THE STANCE PHASE OF RUNNING. A POSITIVE TORSION ANGLE MEANS THE HINDFOOT IS MORE PRONATED THAN THE FOREFOOT. SINCE THE	

TORSION ANGLE IS A DISCRETE MEASURE THE MINIMUM AND MAXIMUM VALUES ARE FOUND ACROSS THE 10 SUBJECTS.	160
TABLE 5.2. DIFFERENCE BETWEEN SHOED CONDITIONS AND BAREFOOT CONDITION. MAXIMUM MEAN DIFFERENCES AND TIMING OF MAXIMUM DURING STANCE PHASE ARE GIVEN TO COMPARE EACH OF THE THREE SHOE CONDITIONS WITH THE BAREFOOT CONDITION FOR EACH OF THE FOUR INTER-SEGMENTAL MEASURES. DIFFERENCES IN MEAN AND TIMING THAT ARE SIGNIFICANTLY DIFFERENT FROM 0.0 AT $P < 0.05$ ARE INDICATED WITH AN ASTERISK.	161
TABLE 5.3. DIFFERENCES BETWEEN THE SHOE CONDITIONS AND THE BAREFOOT CONDITION FOR EACH OF THE SUBJECTS IN THIS STUDY FOR EACH OF THE FOUR INTER-SEGMENTAL MEASURES. THE MINIMUM IMPORTANT DIFFERENCE (MID) WAS TAKEN AS GREATER THAN 5° FOR HF, FF AND HX AND AS 0.03 FOR MLA. CONDITIONS THAT WERE ABOVE THE MID BY 5° (0.03) OR MORE ARE INDICATED IN GRAY SHADING, THOSE BY 10° (0.054) OR MORE IN BLACK SHADING. CONDITIONS THAT WERE BELOW THE MID ARE IN WHITE.	163
TABLE 6.1. THE MAXIMUM MEAN DIFFERENCES (MMD) BETWEEN THE CUTTING TRIALS AND THE RUNNING TRIALS, THE TIMING OF THE MMD (TMMD), THE MINIMUM MEAN DIFFERENCES (MNMD) BETWEEN THESE SAME TRIALS AND THE TIMING OF MNMD (TMNMD) ARE LISTED. THE FOUR INTER-SEGMENTAL MOTIONS (HF-HINDFOOT, FF-FOREFOOT, HX - HALLUX, MLA - MEDIAL LONGITUDINAL ARCH) ARE SHOWN FOR BOTH THE BAREFOOT AND SHOED CONDITIONS. FOR EACH, THE MEANS AND STANDARD DEVIATIONS (SD) ARE REPORTED.	187
TABLE A1: PERCENTAGE OF MID TO MMD FOR EACH CONDITION.	213
TABLE B.1: THE AVERAGE NUMBER OF X-RAYS THAT ARE BEING EMITTED, A MEASURE OF THE CURRENT (mA) AND THE AVERAGE MEASURE OF THE ENERGY LEVELS OF THE X-RAYS (kV) FOR EACH SUBJECT.	214
TABLE C.1: RANGE OF MOTION (ROM) FOR EACH SUBJECT IN EACH CONDITION FOR THE HINDFOOT MOTION IN THE FRONTAL PLANE WITH RESPECT TO THE MIDFOOT. THE MEAN IS THE AVERAGE ACROSS THE GAIT CYCLE (+ = SUPINATION).	216
TABLE C2. RANGE OF MOTION (ROM) FOR EACH SUBJECT IN EACH CONDITION FOR THE FOREFOOT MOTION IN THE FRONTAL PLANE WITH RESPECT TO THE MIDFOOT. THE MEAN IS THE AVERAGE ACROSS THE GAIT CYCLE (+ = SUPINATION).	217
TABLE C3. RANGE OF MOTION (ROM) FOR EACH SUBJECT IN EACH CONDITION FOR THE DORSI/PLANTAR FLEXION OF THE HALLUX COMPONENT. THE MEAN IS THE AVERAGE ACROSS THE GAIT CYCLE (+ = PLANTARFLEXION).	218
TABLE C4. RANGE OF MOTION (ROM) FOR EACH SUBJECT IN EACH CONDITION FOR THE HEIGHT-TO-LENGTH RATIO OF THE MEDIAL LONGITUDINAL ARCH. THE MEAN IS THE AVERAGE ACROSS THE GAIT CYCLE (+ = RISING ARCH).	219
TABLE C5. MEAN DIFFERENCE AND THE PERCENTAGE OF THE GAIT CYCLE THAT THE MEAN DIFFERENCE OCCURRED AT FOR EACH SUBJECT IN EACH CONDITION FOR THE HINDFOOT MOTION IN THE FRONTAL PLANE WITH RESPECT TO THE MIDFOOT. THE MEAN IS THE AVERAGE ACROSS THE GAIT CYCLE. ..	220
TABLE C6. MEAN DIFFERENCE AND THE PERCENTAGE OF THE GAIT CYCLE THAT THE MEAN DIFFERENCE OCCURRED AT FOR EACH SUBJECT IN EACH CONDITION FOR THE FOREFOOT MOTION IN THE FRONTAL PLANE WITH RESPECT TO THE MIDFOOT. THE MEAN IS THE AVERAGE ACROSS THE GAIT CYCLE. ..	221
TABLE C7. RANGE OF MOTION (ROM) FOR EACH SUBJECT IN EACH CONDITION FOR THE DORSI/PLANTAR FLEXION OF THE HALLUX COMPONENT THE MEAN IS THE AVERAGE ACROSS THE GAIT CYCLE.	222
TABLE C8. RANGE OF MOTION (ROM) FOR EACH SUBJECT IN EACH CONDITION FOR THE HEIGHT-TO-LENGTH RATIO OF THE MEDIAL LONGITUDINAL ARCH. THE MEAN IS THE AVERAGE ACROSS THE GAIT CYCLE.	223
TABLE C9. TABLE 9 SHOWS THE MAXIMUM TORSIONAL ANGLES OF ALL 10 SUBJECTS WITH ONE STANDARD DEVIATION. THE MINIMUM AND MAXIMUM VALUES SHOW THE RANGE ACROSS THE SUBJECTS. THE OCCURRENCE OF THESE MAXIMUMS ALSO APPEAR IN THIS TABLE. THE LAST SECTION OF THE TABLE IS THE AVERAGE VALUES FOR THE MAXIMUM DIFFERENCE BETWEEN THE THREE SHOE CONDITIONS AND THE BAREFOOT CONDITION. BY EXAMINING THE MAXIMUM AND MINIMUM VALUES ALONG WITH THE STANDARD DEVIATION IT IS CLEAR THAT THERE IS A LARGE RANGE ACROSS SUBJECTS FOR ALL THREE MEASURES.	224
TABLE C.10. RANGE OF MOTION OF EACH SUBJECT WHILE WEARING EACH SHOE CONDITION AND IN BAREFOOT RUNNING.	225

Table of Figures

FIGURE 1.1. BONES OF THE LEFT FOOT MAKING UP THE HINDFOOT, OR REARFOOT, (CALCANEUS, TALUS), THE MIDFOOT (NAVICULAR, CUBOID, CUNEIFORMS), OR FOREFOOT (METATARSALS, PHALANGES) (REPRINTED WITH PERMISSION. "THIS ARTICLE WAS PUBLISHED IN LOGAN, SINGH, HUTCHINGS. MCMINN'S COLOR ATLAS OF FOOT AND ANKLE ANATOMY, THIRD EDITION. COPYRIGHT ELSEVIER, 2004.").....	3
FIGURE 1.2. IMAGE OF THE LEFT FOOT WITH FOCUS ON THE REARFOOT (CIRCLE) MADE UP OF THE CALCANEUS (1) AND THE TALUS (2). (REPRINTED WITH PERMISSION. "THIS ARTICLE WAS PUBLISHED IN LOGAN, SINGH, HUTCHINGS. MCMINN'S COLOR ATLAS OF FOOT AND ANKLE ANATOMY, THIRD EDITION. COPYRIGHT ELSEVIER, 2004.")	4
FIGURE 1.3. DESCRIPTION OF THE CORKSCREW MECHANISM OF THE RIGHT CALCANEUS. THE CALCANEUS TRANSLATES ANTERIORLY AND IN A CLOCKWISE DIRECTION AS THE FOOT SUPINATES. (REPRINTED WITH PERMISSION FROM SAMMARCO, JAMES G AND HOCKENBURY, ROSS TODD. "BIOMECHANICS OF THE FOOT AND ANKLE." BASIC BIOMECHANICS OF THE MUSCULOSKELETAL SYSTEM. ED. MARGARETA NORDIN AND VICTOR H. FRANKEL. MARYLAND: LIPPINCOTT WILLIAMS & WILKINS, 2001.)	5
FIGURE 1.4. THE AXIS OF THE SUBTALAR JOINT (CIRCLE). TOP: SAGITTAL VIEW, BOTTOM: TRANSVERSE VIEW. (REPRINTED WITH PERMISSION FROM SAMMARCO, JAMES G AND HOCKENBURY, ROSS TODD. "BIOMECHANICS OF THE FOOT AND ANKLE." BASIC BIOMECHANICS OF THE MUSCULOSKELETAL SYSTEM. ED. MARGARETA NORDIN AND VICTOR H. FRANKEL. MARYLAND: LIPPINCOTT WILLIAMS & WILKINS, 2001.)	5
FIGURE 1.5. IMAGE OF THE LEFT FOOT WITH FOCUS ON THE MIDFOOT COMPRISED OF THE NAVICULAR (3), CUBOID (7), MEDIAL CUNIFORM (4), INTERMEDIAL CUNIFORM (5), LATERAL CUNIFORM (6). (REPRINTED WITH PERMISSION. "THIS ARTICLE WAS PUBLISHED IN LOGAN, SINGH, HUTCHINGS. MCMINN'S COLOR ATLAS OF FOOT AND ANKLE ANATOMY, THIRD EDITION. COPYRIGHT ELSEVIER, 2004.").....	6
FIGURE 1.6. AXIS OF THE TRANSVERSE TARSAL JOINTS IN THE TWO POSITIONS EXPERIENCED DURING A NORMAL GAIT CYCLE. LEFT: POSITION OF THE AXIS DURING PRONATION AT THE BEGINNING OF THE STANCE PHASE. RIGHT: POSITION OF THE AXIS DURING SUPINATION AT THE END OF THE STANCE PHASE. (REPRINTED WITH PERMISSION FROM SAMMARCO, JAMES G AND HOCKENBURY, ROSS TODD. "BIOMECHANICS OF THE FOOT AND ANKLE." BASIC BIOMECHANICS OF THE MUSCULOSKELETAL SYSTEM. ED. MARGARETA NORDIN AND VICTOR H. FRANKEL. MARYLAND: LIPPINCOTT WILLIAMS & WILKINS, 2001.)	7
FIGURE 1.7. IMAGE OF THE LEFT FOOT WITH FOCUS ON THE FOREFOOT ENCOMPASSING THE FIRST TO FIFTH METATARSALS (8-12) AND THEIR PHALANGEALS (13-17). (REPRINTED WITH PERMISSION. "THIS ARTICLE WAS PUBLISHED IN LOGAN, SINGH, HUTCHINGS. MCMINN'S COLOR ATLAS OF FOOT AND ANKLE ANATOMY, THIRD EDITION. COPYRIGHT ELSEVIER, 2004.")	7
FIGURE 1.8. LOCATION OF THE LISFRANC'S JOINTS IN THE RIGHT FOREFOOT. (REPRINTED WITH PERMISSION FROM HECKMAN ET AL. 2009)	8
FIGURE 1.9. THE MEDIAL LONGITUDINAL ARCH IS LOCATED ON THE MEDIAL SIDE OF THE FOOT AND ENCOMPASSES THE CALCANEUS, NAVICULAR, MEDIAL CUNEIFORM AND THE FIRST METATARSAL. (REPRINTED WITH PERMISSION FROM HECKMAN ET AL. 2009)	9
FIGURE 1.10. DESCRIPTIONS OF MOVEMENTS IN EACH PLANE. DORSIFLEXION/ PLANTARFLEXION ARE IN THE SAGITTAL PLANE. ABDUCTION/ADDUCTION IS IN THE TRANSVERSE PLANE. EVERSION/INVERSION OR SUPINATION/PRONATION IS IN THE FRONTAL PLANE. (REPRINTED WITH PERMISSION FROM SAMMARCO, JAMES G AND HOCKENBURY, ROSS TODD. "BIOMECHANICS OF THE FOOT AND ANKLE." BASIC BIOMECHANICS OF THE MUSCULOSKELETAL SYSTEM. ED. MARGARETA NORDIN AND VICTOR H. FRANKEL. MARYLAND: LIPPINCOTT WILLIAMS & WILKINS, 2001.).....	10
FIGURE 1.11. LOCATION OF THE PLANTAR FASCIA ON THE PLANTAR ASPECT OF THE FOOT. (REPRINTED WITH PERMISSION FROM HECKMAN ET AL. 2009)	12
FIGURE 1.12. VISUAL EXPLANATION OF THE WINDLASS EFFECT USED TO RISE AND LOWER THE MEDIAL LONGITUDINAL ARCH. AS THE HALLUX DORSIFLEXES, AS SEEN IN THE BOTTOM PICTURE, THE	

PLANTAR FASCIA (REPRESENTED BY THE ROPE) CAUSES THE FIRST METATARSAL (REPRESENTED BY THE LONGER SEGMENT) AND THE NAVICULAR (REPRESENTED BY THE SHORTER SEGMENT) TO RISE. (REPRINTED WITH PERMISSION FROM HICKS ET AL. 1953)	12
FIGURE 1.13. LIGAMENTS OF THE FOOT. A. LATERAL LIGAMENTS OF THE FOOT FROM AN OBLIQUE DORSAL VIEW. B. MEDIAL LIGAMENTS OF THE FOOT. (REPRINTED WITH PERMISSION. "THIS ARTICLE WAS PUBLISHED IN LOGAN, SINGH, HUTCHINGS. McMINN'S COLOR ATLAS OF FOOT AND ANKLE ANATOMY, THIRD EDITION. COPYRIGHT ELSEVIER, 2004.").....	13
FIGURE 1.14. ELECTROMYOGRAPHY OF THE LOWER EXTREMITY MUSCLES DURING ONE GAIT CYCLE. PRETIBIAL MUSCLES ARE THE ANTERIOR MUSCLES OF THE LEG. TRICEPS ARE THE POSTERIOR MUSCLES OF THE LEG. INTRINSIC MUSCLES ARE THE MUSCLES THAT ORIGINATE AND INSERT IN THE FOOT. (REPRINTED WITH PERMISSION FROM NOVACHEK, TF, 1998).....	14
FIGURE 1.15. SUPERFICIAL DISSECTION OF THE RIGHT LOWER LEG AND FOOT, FROM THE MEDIAL SIDE. MUSCLES: 2-TIBIALIS POSTERIOR, 3-FLEXOR DIGITORUM LONGUS, 6-FLEXOR HALLUCIS LONGUS, 7-SOLEUS, 14- ABDUCTOR HALLUCIS, 16-TIBIALIS ANTERIOR, 17-EXTENSOR HALLUCIS LONGUS. (REPRINTED WITH PERMISSION. "THIS ARTICLE WAS PUBLISHED IN LOGAN, SINGH, HUTCHINGS. McMINN'S COLOR ATLAS OF FOOT AND ANKLE ANATOMY, THIRD EDITION. COPYRIGHT ELSEVIER, 2004.").....	17
FIGURE 1.16. SUPERFICIAL DISSECTION OF THE RIGHT LOWER LEG AND FOOT, FROM THE LATERAL SIDE. MUSCLES: 1-TIBIALIS ANTERIOR, 3-EXTENSOR DIGITORUM LONGUS, 4-PERONEUS BREVIS, 5-PERONEUS LONGUS, 7-SOLEUS, 16-EXTENSOR DIGITORUM BREVIS, 17-PERONEUS TERTIUS, 18- ABDUCTION DIGITI MINIMI, 20- EXTENSOR HALLUCIS LONGUS). (REPRINTED WITH PERMISSION. "THIS ARTICLE WAS PUBLISHED IN LOGAN, SINGH, HUTCHINGS. McMINN'S COLOR ATLAS OF FOOT AND ANKLE ANATOMY, THIRD EDITION. COPYRIGHT ELSEVIER, 2004.")	18
FIGURE 1.17. DEEP DORSUM OF THE RIGHT FOOT, FROM AN ANTERIOLATERAL VIEW POINT. MUSCLES: 1-TIBIALIS ANTERIOR, 2-EXTENSOR HALLUCIS LONGUS, 3-EXTENSOR DIGITORUM LONGUS, 5-PERONEUS BREVIS, 6-PERONEUS LONGUS, 18-EXTENSOR DIGITORUM BREVIS, 22-ABDUCTOR DIGITI MINIMI. (REPRINTED WITH PERMISSION. "THIS ARTICLE WAS PUBLISHED IN LOGAN, SINGH, HUTCHINGS. McMINN'S COLOR ATLAS OF FOOT AND ANKLE ANATOMY, THIRD EDITION. COPYRIGHT ELSEVIER, 2004.").....	19
FIGURE 1.18. DESCRIPTION OF THE GAIT CYCLE FOR WALKING (TOP) AND RUNNING (BOTTOM). WALKING HAS TWO PHASES: STANCE AND SWING. RUNNING HAS THREE PHASES: STANCE, FLOAT AND SWING. (REPRINTED WITH PERMISSION FROM SAMMARCO, JAMES G AND HOCKENBURY, ROSS TODD. "BIOMECHANICS OF THE FOOT AND ANKLE." BASIC BIOMECHANICS OF THE MUSCULOSKELETAL SYSTEM. ED. MARGARETA NORDIN AND VICTOR H. FRANKEL. MARYLAND: LIPPINCOTT WILLIAMS & WILKINS, 2001.)	20
FIGURE 1.19. LOCATION OF THE CENTER OF PRESSURE (COP) FOR A HEEL STRIKER (TOP) AND A MIDFOOT STRIKER (BOTTOM) FOR ONE GAIT CYCLE. (REPRINTED WITH PERMISSION FROM SAMMARCO, JAMES G AND HOCKENBURY, ROSS TODD. "BIOMECHANICS OF THE FOOT AND ANKLE." BASIC BIOMECHANICS OF THE MUSCULOSKELETAL SYSTEM. ED. MARGARETA NORDIN AND VICTOR H. FRANKEL. MARYLAND: LIPPINCOTT WILLIAMS & WILKINS, 2001.).....	22
FIGURE 1.20. AXIS OF THE TRANSVERSE TARSAL JOINTS. DURING PRONATION, THE SUBTALAR JOINT IS EVERTED UNLOCKING THE TALONAVICULAR AND CALCANEOCUBOID AXIS. SUPINATION HAS THE OPPOSITE EFFECT AND LOCKS THE TWO AXES. (REPRINTED WITH PERMISSION FROM SAMMARCO, JAMES G AND HOCKENBURY, ROSS TODD. "BIOMECHANICS OF THE FOOT AND ANKLE." BASIC BIOMECHANICS OF THE MUSCULOSKELETAL SYSTEM. ED. MARGARETA NORDIN AND VICTOR H. FRANKEL. MARYLAND: LIPPINCOTT WILLIAMS & WILKINS, 2001.)	24
FIGURE 1.21. HELEN HAYES MARKER SET UP WITH EMG ON A PATIENT IN WOBL (LEFT). MOTION ANALYSIS RECONSTRUCTION OF THE MARKERS IN REAL TIME (RIGHT).....	28
FIGURE 1.22. IMAGE OF DUAL C-ARM FLUOROSCOPES SET-UP FOR EVALUATING THE MEDIOLATERAL VIEW OF THE FOOT IN THE WOLF ORTHOPAEDIC BIOMECHANICS LABORATORY.	29
FIGURE 1.23: BONE PINS INSERTED INTO A SUBJECT'S FOOT FOR A WALKING STUDY CONDUCTED IN SWEDEN. (REPRINTED WITH PERMISSION ARNDT ET AL. 2007).....	32
FIGURE 1.24. DESCRIPTION OF ACHILLES TENDON ANGLE (BETA). TWO MARKERS ARE PLACED ON THE BISECTION OF THE CALCANEUS AND THE TIBIA. THE ANGLE BETWEEN THE TWO VECTORS, FORMED BY EACH MARKER SET, IS KNOWN AS ACHILLES' TENDON ANGLE. (REPRINTED WITH PERMISSION FROM NOVACHEK, TF, 1998)	35

FIGURE 1.25: A. TRIAD CLUSTER LOCATION FOR THE FIVE CLUSTER MARKERS OF THE JENKYN MODEL: HINDFOOT, MIDFOOT, MEDIAL FOREFOOT, LATERAL FOREFOOT AND HALLUX. B. TRIAD MARKER LOCATION OF UNDERLYING BONES: CALCANEUS, NAVICULAR, FIRST METATARSAL AND FIFTH METATARSAL. THE FOUR LETTER ABBREVIATION, WHICH DESCRIBES THE BONY LANDMARKS FOR THE DIGITIZATION PROCESS, CAN BE FOUND IN TABLE 2. (REPRINTED WITH PERMISSION FROM JENKYN ET AL. 2007)	44
FIGURE 1.26: LOCATION OF THE DIGITIZED LANDMARKS FOR THE JENKYN MODEL IS MARKED ON THE SUBJECT'S FOOT.....	47
FIGURE 1.27. MEASUREMENTS FROM THE JENKYN MODEL. A. HINDFOOT MOTION. ROTATION ABOUT THE 3-MIDFOOT AXIS (ANTERIOR/POSTERIOR) GIVES SUPINATION AND PRONATION. B. FOREFOOT TWIST ANGLE. MVH-MIH VECTOR IS PROJECTED ON THE PLANE ENCOMPASSING THE 1- AND 2- MIDFOOT AXIS (ADDUCTION/ABDUCTION, PLANTARFLEXION/DORSIFLEXION, RESPECTFULLY). C. HALLUX MOTION. SAGITTAL PLANE MOTION IS THE ANGLE OF THE HALLUX (H) WITH RESPECT TO THE FIRST METATARSAL. D. MEDIAL LONGITUDINAL ARCH MOTION. HEIGHT-TO-LENGTH RATIO IS CALCULATED BY THE SAME L-VECTOR USED IN THE HALLUX MOTION AND THE HEIGHT VECTOR WHICH IS PROJECTS PERPENDICULAR TO THE L-VECTOR TO THE NAVICULAR TUBEROSITY. (REPRINTED WITH PERMISSION FROM JENKYN ET AL, 2007)	50
FIGURE 1.28. THIS IS THE COMPLETE DIAGRAM OF THE MOTIONS CALCULATED THROUGHOUT THIS DISSERTATION. A. FRONTAL PLANE MOTION OF THE HINDFOOT. B. FOREFOOT TWIST. C. MEDIAL LONGITUDINAL ARCH HEIGHT-TO-LENGTH RATIO. D. HALLUX ANGLE IN THE SAGITTAL PLANE. (REPRINTED WITH PERMISSION FROM JENKYN ET AL., 2007)	51
FIGURE 1.29. CLUSTER MARKER SET PLACED ON THE FOOT USING FAUX LEATHER BASES, NYLON SCREWS AND CARBON FIBER RODS. THE RETRO-REFLECTIVE MARKERS' REFLECTION IS VISIBLE IN THE PHOTO.....	52
FIGURE 2.1: A,B) PLACEMENTS OF THE PASSIVE REFLECTIVE MARKERS ON THE SHOE AND THE MARKER TRIADS ON THE FOOT. ONLY THE RIGHT FOOT WAS INSTRUMENTED WITH THE MARKER TRIADS. TWO MARKERS WERE PLACED ON EACH SHOE, ONE ON THE TOE BOX AND ONE ON THE HEEL COUNTER. C) THE MARKER TRIAD CLUSTER ARE COMPRISED OF A NYLON NUT AND SCREW WITH CARBON FIBER WANDS PROTRUDING FROM THE HEAD OF THE SCREW AND ATTACHING TO RETRO-REFLECTIVE MARKERS.	71
FIGURE 2.2: THE DEFORMATION OF THE SHOE AT HEEL RISE IS MEASURED BY THE CHANGE IN THE LENGTH FROM THE TOE AND HEEL MARKERS BETWEEN THE HOLE CONDITIONS AND THE INTACT SHOE. THIS LENGTH SHOULD NOT DIFFER FROM THE INTACT LENGTH IF THE STRUCTURAL INTEGRITY OF THE SHOE WAS UNAFFECTED BY THE HOLES. THREE SHOE DESIGNS WERE STUDIED, NEUTRAL, STABILITY AND MOTION CONTROL (MC). AS EXPECTED, THE SMALLEST DEFORMATIONS WITH THE MOTION CONTROL SHOE, WHICH IS THE MOST SUPPORTIVE SHOE.....	76
FIGURE 2.3: DEFORMATION OF THE SHOE AT HEEL RISE WAS MEASURED BY THE CHANGE IN THE ANGLE BETWEEN THE HEEL-ANKLE-TOE MARKERS BETWEEN THE HOLE CONDITIONS AND THE INTACT SHOE. THIS ANGLE SHOULD NOT DIFFER FROM THE INTACT ANGLE IF THE SHOE WAS UNAFFECTED BY THE HOLES. THREE SHOE DESIGNS WERE STUDIED, NEUTRAL, STABILITY AND MOTION CONTROL. THE GREATEST CHANGE IN ANGLE WAS SEEN WITH THE LARGEST HOLE SIZE FOR THE CUSHIONING AND STABILITY SHOES. LITTLE DISRUPTION WAS SEEN IN THE MOTION CONTROL SHOE FOR ANY OF THE HOLE SIZES.	77
FIGURE 2.4: CHANGE IN HINDFOOT KINEMATICS WITH RESPECT TO THE MIDFOOT IN THE FRONTAL PLANE AT THE INSTANT OF HEEL RISE IN STANCE PHASE. THE ANGLE SHOULD NOT DIFFER FROM THE SMALLEST HOLE CONDITION (HOLE 1). THE MINIMUM IMPORTANT DIFFERENCE WAS CONSIDERED TO BE 5°. THREE SHOE DESIGNS WERE STUDIED, NEUTRAL, STABILITY AND MOTION CONTROL. THE MINIMUM IMPORTANT DIFFERENCE WAS SURPASSED FOR THE THIRD AND FOURTH HOLE SIZE OF THE MOTION CONTROL SHOE. LITTLE CHANGE WAS SEEN WITH BOTH THE CUSHIONING AND STABILITY SHOES FOR ALL SIZES OF HOLE.....	79
FIGURE 2.5: CHANGE IN FOREFOOT KINEMATICS WITH RESPECT TO THE MIDFOOT IN THE FRONTAL PLANE AT THE INSTANT OF HEEL RISE IN STANCE PHASE. THE ANGLE SHOULD NOT DIFFER FROM THE SMALLEST HOLE CONDITIONS (HOLE 1). THREE SHOE DESIGNS WERE STUDIED, NEUTRAL, STABILITY AND MOTION CONTROL. ALL MEAN DIFFERENCES WERE BELOW THE 5° DEFINED AS MINIMUM IMPORTANT DIFFERENCE.....	80

FIGURE 2.6: CHANGE IN THE BEHAVIOUR OF THE MEDIAL LONGITUDINAL ARCH (MLA) AT THE INSTANT OF HEEL RISE. THE MLA SHOULD NOT DIFFER FROM 0.0 IF THE SHOE WAS UNAFFECTED BY THE HOLES. LITTLE CHANGE WAS SEEN FOR THE NEUTRAL SHOE OR THE STABILITY SHOE FOR ANY HOLE SIZE. FOR THE MOTION CONTROL SHOE LARGE CHANGES IN ARCH BEHAVIOUR WERE SEEN FOR ALL HOLE CONDITIONS.	81
FIGURE 2.7: CHANGE IN HALLUX KINEMATICS WITH RESPECT TO THE MEDIAL FOREFOOT IN THE SAGITTAL PLANE AT THE INSTANT OF HEEL RISE. THE ANGLE SHOULD NOT DIFFER FROM THE SMALLEST HOLE CONDITIONS (HOLE 1). THE MINIMUM IMPORTANT DIFFERENCE WAS SURPASSED FOR ALL HOLE SIZES OF THE NEUTRAL SHOE. FOR THE OTHER TWO SHOE CONDITIONS ONLY THE FOURTH HOLE OF THE STABILITY SHOE SURPASSED THE MID.	82
FIGURE 2.8: RANGE OF MOTION OF THE HALLUX WITH RESPECT TO THE MEDIAL FOREFOOT FOR THE CUSHIONING SHOE CONDITION. THE SECOND HOLE HAS A SIMILAR PATTERN SHAPE TO THE THIRD AND FOURTH HOLE PATTERNS, BUT IS OFFSET BY A POSITIVE ANGLE. IT IS SPECULATED THAT THE OFFSET IS DUE TO AN UNINTENDED ROTATION OF A MARKER TRIAD WITH RESPECT TO ITS INITIAL POSITION AFTER REPLACING THE SHOE.	83
FIGURE 3.1: A) TRIAD MARKERS LOCATED ON THE FOOT FOR A BAREFOOT STATIC TRIAL. BONY LANDMARKS ARE WRITTEN IN PEN ON THE SUBJECT'S FOOT. B) AND C) HOLES CUT IN THE SHOE TO AFFIX MARKER TRIADS (A) TO THE FOOT.	95
FIGURE 3.2: BLACK BASE – FAUX LEATHER, BLUE – EPOXY, WHITE SCREW – NYLON, BLACK WANDS – CARBON FIBER.	96
FIGURE 3.3: NEUTRAL VALUES OF THE MEDIAL LONGITUDINAL ARCH HEIGHT-TO-LENGTH RATIO FOR 4 CONDITIONS OVER THE 10 SUBJECTS. THE SHOE CONDITIONS TEND TO RAISE THE MEDIAL LONGITUDINAL ARCH COMPARED TO THE BAREFOOT CONDITION.	100
FIGURE 3.4: NEUTRAL POSITIONS OF THE HALLUX IN THE SAGITTAL PLANE WITH RESPECT TO THE FIRST METATARSAL FOR 4 CONDITIONS OVER THE 10 SUBJECTS. A CLINICALLY SIGNIFICANT SHIFT TOWARDS INCREASE DORSI-FLEXION FOR MOST SHOE CONDITIONS FOR MOST SUBJECTS COMPARED TO THE BAREFOOT CONDITION IS VISIBLE.	101
FIGURE 3.5: NEUTRAL POSITIONS OF THE FOREFOOT WITH RESPECT TO MIDFOOT IN THE FRONTAL PLANE FOR 4 CONDITIONS OVER THE 10 SUBJECTS. THE FOREFOOT MOTION TRENDS TO INCREASE TOWARDS PRONATION FOR THE MOST SHOE CONDITIONS COMPARED TO THE BAREFOOT CONDITION.	101
FIGURE 3.6: NEUTRAL POSITIONS OF THE HINDFOOT WITH RESPECT TO MIDFOOT IN THE FRONTAL PLANE FOR 4 CONDITIONS OVER THE 10 SUBJECTS. THE HINDFOOT MOTION HAS THE MOST VARIABILITY ACROSS ALL SUBJECTS MAKING CONCLUSIONS DIFFICULT.	102
FIGURE 4.1. CUSTOM-BUILT MARKER TRIAD CLUSTERS VISIBLE TO BOTH THE FLUOROSCOPIC AND THE OPTICAL MOTION CAPTURE SYSTEMS. LATERAL (A) AND MEDIAL (B) VIEWS OF THE FOOT SHOW THE PLACEMENT OF THE MARKER TRIAD CLUSTERS IN THE LOCATIONS DESCRIBED BY JENKYN ET AL. (2007). THE BLUE LINES VISIBLE ON THE PLATFORM IN BOTH PHOTOS ARE THE OUT-OF-PLANE ORIENTATION REFERENCES IN 5 DEGREE INCREMENTS.	116
FIGURE 4.2. FLUOROSCOPIC IMAGE OF THE MIDFOOT AND HINDFOOT IN THE SAGITTAL VIEW. A) THE BONY LANDMARKS THAT WERE MANUALLY DIGITIZED TO DEFINE THE BONE-FIXED REFERENCE FRAMES ON THE NAVICULAR AND CALCANEUS ARE SHOWN AS WHITE DOTS (FOUR PER BONE). THE ORIENTATIONS OF THE BONE-FIXED X AND Y AXES ARE ALSO SHOWN. B) THE COORDINATE SYSTEMS FOR THE MARKER CLUSTERS AND THE BONES ARE SHOWN FOR THE NAVICULAR AND CALCANEUS BONES. THE DASHED LINES REPRESENT THE ORIGIN DISPLACEMENT LENGTH BETWEEN THE ASSOCIATED BONE AND MARKER SYSTEMS. THE β REPRESENTS THE SEGMENT ANGLE BETWEEN THE TWO SYSTEMS. ONLY β FOR THE CALCANEUS IS SHOWN.	120
FIGURE 4.3. FLUOROSCOPIC IMAGE OF THE GRID THAT WAS USED TO CALCULATE THE SCALE FACTOR TO TRANSFER FROM PIXELS TO MM. THERE IS 15 MM BETWEEN EACH HOLE SET.	123
FIGURE 4.4. CHANGE IN THE ORIGIN DISPLACEMENT LENGTH FROM THE TRUE LENGTH FOR THE CALCANEUS (SOLID LINE) AND THE NAVICULAR (DASHED LINE) WITH OUT-OF-PLANE ORIENTATION. THE DIFFERENCES BETWEEN THE TWO VALUES IN QUIET STANDING AT THE ZERO-DEGREE REFERENCE POSITION AND ± 5 -DEGREES OUT-OF-PLANE POSITIONS WERE LESS THAN 10.0 ± 8.5 MM. THE OUT-OF-PLANE ERRORS IN ORIGIN DISPLACEMENT LENGTH FOR OUT-OF-PLANE ORIENTATIONS GREATER THAN 5-DEGREES WERE CONSIDERED UNACCEPTABLY LARGE.	125

- FIGURE 4.5. CHANGE IN THE SEGMENT ANGLE FOR THE TRUE ANGLE FOR THE CALCANEUS (SOLID LINE) AND THE NAVICULAR (DASH LINE). THE DIFFERENCES BETWEEN THE TWO VALUES IN QUIET STANDING AT THE ZERO-DEGREE REFERENCE POSITION AND ± 5 -DEGREES OUT-OF-PLANE POSITIONS WERE LESS THAN $0.69 \pm 0.55^\circ$. ERRORS FOR OUT-OF-PLANE ORIENTATIONS GREATER THAN 5-DEGREES WERE CONSIDERED UNACCEPTABLE..... 125
- FIGURE 4.6. CHANGE IN THE APPARENT LENGTH OF THE CALCANEUS (SOLID LINE) AND THE NAVICULAR (DASHED LINE) BONES FROM TRUE LENGTH. THE DIFFERENCES BETWEEN THE TWO VALUES IN QUIET STANDING AT THE ZERO-DEGREE REFERENCE POSITION AND ± 5 -DEGREES OUT-OF-PLANE POSITIONS WERE LESS THAN 2.37 ± 2.90 MM..... 126
- FIGURE 5.1. A) LOCATION OF THE MARKER TRIAD CLUSTERS ON THE FOOT. THE BASE OF THE CLUSTER REMAINS AFFIXED TO THE FOOT THROUGHOUT THE TEST PROTOCOL WHILE THE WAND AND MARKER PORTION IS REMOVED TO ALLOW FOR SHOE CHANGES. B) THE THREE SHOE TYPES TESTED ARE THE CONTROL (NIKE FREE TRAINER 7.0, LEFT), THE CONTROL SHOE WITH A FOREFOOT CARBON PLATE ATTACHED TO THE MIDSOLE (MIDDLE), AND THE CONTROL SHOE WITH A FULL LENGTH CARBON PLATE ATTACHED TO THE MIDSOLE (RIGHT). ALL SHOES HAVE FIVE HOLES CUT IN THE UPPER AT THE HEEL COUNTER ON THE LATERAL SIDE, THE TOE BOX ABOVE THE HALLUX, ALONG THE MEDIAL AND LATERAL SIDES ABOVE THE FIRST AND FIFTH METATARSALS AND ON THE MEDIAL SIDE ABOVE THE NAVICULAR TUBEROSITY. C) EXAMPLE OF THE ANATOMICAL LANDMARKS THAT ARE DIGITIZED AT THE BEGINNING OF THE TEST SESSION. THE LANDMARKS FORM THE ANATOMICAL CO-ORDINATE SYSTEMS FOR THE DYNAMIC TRIALS. THIS IS FURTHER EXPLAINED IN JENKYN ET AL.²⁰ 148
- FIGURE 5.2. HINDFOOT MOTION IN THE FRONTAL PLANE WITH RESPECT TO THE MIDFOOT FOR THE BAREFOOT (GRAY TRIANGLES = BARE) AND THE THREE SHOE CONDITIONS (BLACK LINE = CO, DASHED LINE= FF, GRAY LINE= LF). FOR ALL FOUR CONDITIONS THE HINDFOOT IS SUPINATED AT HEELSTRIKE AND THEN PRONATES UNTIL 30-50% OF THE STANCE PHASE, WHEN IT BEGINS TO SUPINATE AGAIN. THE HIGHEST PEAK PRONATION IS OBSERVED FOR THE FF CONDITION, WHILE THE FL CONDITION APPEARS TO HINDER THE FOOT'S ABILITY TO RE-SUPINATION AFTER MIDSTANCE. THE CO CONDITION AND THE BAREFOOT CONDITION TEND TO PRODUCE SIMILAR MOVEMENT PATTERNS. 155
- FIGURE 5.3. FOREFOOT TWIST IN THE FRONTAL PLANE WITH RESPECT TO THE MIDFOOT FOR THE BAREFOOT (GRAY TRIANGLES = BARE) AND THE THREE SHOE CONDITIONS (BLACK LINE= CO, DASHED LINE= FF, GRAY LINE= LF). THE MOTION OF THE FOREFOOT IS LIMITED IN RANGE AND TENDS TO MIMIC THE HINDFOOT MOTION. THE FOREFOOT MOTION REMAINS CLOSE TO ITS NEUTRAL POSITION THROUGHOUT THE STANCE PHASE, WHICH HAS BEEN SHOWN TO OCCUR DURING RUNNING²⁵. THE FL AND FF CONDITIONS SHOWED SIMILAR MOTIONS, AND THE CO AND BARE WERE ALSO SIMILAR. 156
- FIGURE 5.4. LONGITUDINAL TORSION ANGLE IN THE FRONTAL PLANE, WHICH IS DEFINED AS THE FOREFOOT MOTION MINUS THE HINDFOOT MOTION. THIS IS SHOWN FOR THE BAREFOOT (GRAY TRIANGLES = BARE) AND THE THREE SHOE CONDITIONS (BLACK LINE = CO, DASHED LINE= FF, GRAY LINE= LF). THERE IS A LARGE NEGATIVE TORSION ANGLE FROM HEEL STRIKE UNTIL MIDSTANCE FOR THE FL CONDITION, WHEREAS THE FF CONDITION HAS A LARGE POSITIVE TORSION ANGLE FROM 20-70% OF THE STANCE PHASE. THE BAREFOOT CONDITION AND THE CO CONDITION TEND TO REMAIN AROUND 3 DEGREES UNTIL APPROXIMATELY 60% OF THE GAIT CYCLE WHERE IT BEGINS TO POSITIVELY INCREASE UNTIL IT REACHES A MAXIMUM AT HEEL STRIKE..... 157
- FIGURE 5.5. HALLUX MOTION IN THE SAGITTAL PLANE WITH RESPECT TO THE FIRST METATARSAL FOR THE BAREFOOT (GRAY TRIANGLES = BARE) AND THE THREE SHOE CONDITIONS (BLACK LINE= CO, DASHED LINE= FF, GRAY LINE = LF). THE MOTION OF THE HALLUX DURING THE SHOE CONDITIONS IS DIFFERENT FROM THE BAREFOOT CONDITION WITH THE BAREFOOT CONDITION TENDING TO REDUCE THE RANGE OF DORSI-FLEXION AND PLANTARFLEXION. THE FF CONDITION APPEARS TO INCREASE THE DORSI-FLEXION COMPARED TO THE CO CONDITION. THE FL CONDITION REDUCED DORSI-FLEXION COMPARED TO THE OTHER CONDITIONS. 158
- FIGURE 5.6. HEIGHT-TO-LENGTH RATIO OF MEDIAL LONGITUDINAL ARCH FOR THE BAREFOOT (GRAY TRIANGLES = BARE) AND THE THREE SHOE CONDITIONS (BLACK LINE= CO, DASHED LINE= FF, GRAY LINE = LF). FOREFOOT FRONTAL PLANE MOTION APPEARS TO FOLLOW THE DROPPING OF THE MEDIAL LONGITUDINAL ARCH²⁶. THE ARCH DROPS IN THE BEGINNING OF THE STANCE PHASE AND RISES IN THE SECOND HALF. THE BAREFOOT CONDITION AND THE CO CONDITION TENDED TO BE

SIMILAR. THE OTHER TWO CONDITIONS, FL AND FF, WERE ALSO SIMILAR BUT BEGIN WITH THE ARCH IN A LOWER POSITION AT HEEL-STRIKE. 159

FIGURE 6.1. PLACEMENT SITE DESCRIPTIONS (RIGHT) FOR THE FIVE MARKER CLUSTERS SEEN ON THE SUBJECT (LEFT). EACH SEGMENT OF THE FOOT MODEL HAD A TRIAD CLUSTER. ONLY THE RIGHT LEG AND FOOT KINEMATICS WERE STUDIED WITH THE MULTI-SEGMENT FOOT MODEL..... 181

FIGURE 6.2. FOUR INTER-SEGMENT MOTIONS ARE REPORTED: A) HINDFOOT MOTION IN THE FRONTAL PLANE WITH RESPECT TO THE MIDFOOT SEGMENT (SUPINATION, POSITIVE), B) FOREFOOT SUPINATION-PRONATION IN THE FRONTAL PLANE WITH RESPECT TO THE MIDFOOT SEGMENT (SUPINATION; POSITIVE), C) THE HALLUX ANGLE IN THE SAGITTAL PLANE WITH RESPECT TO THE FIRST METATARSAL (PLANTARFLEXION, POSITIVE), D) THE HEIGHT-TO-LENGTH RATIO OF THE MEDIAL LONGITUDINAL ARCH (RISING OF THE ARCH, POSITIVE). THE NEUTRAL OR ZERO POSITION FOR EACH MOTION WAS DEFINED DURING QUIET, DOUBLE SUPPORT STANDING. (REPRINTED WITH PERMISSION FROM JENKYN ET AL. 2007). 183

FIGURE 6.3. SUBJECT MOTION PATHS FOR THE A) LEVEL WALKING AND B) MEDIALY-DIRECTED, ANTICIPATED CUTTING TURNS, SHOWING THE SEQUENCE OF FOOTFALLS APPROACHING AND LEAVING THE FORCEPLATE. 185

FIGURE 6.4 BAREFOOT KINEMATIC CURVES OF THE AVERAGED INTER-SEGMENTAL JOINT MOTIONS DURING BAREFOOT RUNNING (DASHED LINE) AND CUTTING (SOLID LINE). FOUR MOTIONS ARE SHOWN: A) HINDFOOT MOTION WITH RESPECT TO THE MIDFOOT IN THE FRONTAL PLANE, B) FOREFOOT MOTION WITH RESPECT TO THE MIDFOOT IN THE FRONTAL PLANE, C) HALLUX MOTION IN THE SAGITTAL PLANE WITH RESPECT TO THE FIRST METATARSAL, AND D) MEDIAL LONGITUDINAL ARCH HEIGHT-TO-LENGTH RATIO. THE HORIZONTAL AXIS IS NORMALIZED TO 100% STANCE PHASE. THE HINDFOOT IS THE MOST DIFFERENT BETWEEN TASKS, WITH THE INTER-SEGMENTAL MOTIONS SIGNIFICANTLY DIFFERENT IN THE FIRST AND LAST 40% OF STANCE PHASE. FOR THE FOREFOOT, THE CUTTING TRIALS SHOW MORE VARIABILITY THAN THE RUNNING TRIALS. HOWEVER, THE RANGE OF MOTION FOR BOTH TASKS IS SMALL AND THE FOREFOOT KINEMATICS ARE SIMILAR BETWEEN TASKS. THE HALLUX MOTION IS THE LEAST VARIABLE AND YET SHOWS THE GREATEST DIFFERENCE BETWEEN THE CUTTING AND RUNNING TASKS. THE KINEMATIC CURVES SHOW SIMILAR PATTERNS IN BOTH TASKS, BUT THEY APPEAR TO BE OUT OF PHASE BY ABOUT 20% OF THE STANCE. THE MEDIAL LONGITUDINAL ARCH (MLA) MOTION DURING CUTTING APPEARS TO BE OUT OF PHASE BY 40% COMPARED TO DURING RUNNING. 190

FIGURE 6.5 SHOED KINEMATIC CURVES OF THE AVERAGED INTER-SEGMENTAL JOINT MOTIONS DURING SHOED RUNNING (DASHED LINE) AND CUTTING (SOLID LINE). FOUR MOTIONS ARE SHOWN: A) HINDFOOT MOTION WITH RESPECT TO THE MIDFOOT IN THE FRONTAL PLANE, B) FOREFOOT MOTION WITH RESPECT TO THE MIDFOOT IN THE FRONTAL PLANE, C) HALLUX MOTION IN THE SAGITTAL PLANE WITH RESPECT TO THE FIRST METATARSAL, AND D) MEDIAL LONGITUDINAL ARCH HEIGHT-TO-LENGTH RATIO. THE HORIZONTAL AXIS IS NORMALIZED TO 100% STANCE PHASE. THE HINDFOOT SHOWS THE LARGEST VARIABILITY OF ALL THE INTER-SEGMENTAL JOINT MOTIONS, PARTICULARLY FOR THE RUNNING TASK. SIMILAR TO THE BAREFOOT CONDITION IN FIGURE 4.4 THE HINDFOOT DURING CUTTING IS CONSISTENTLY DIFFERENT FROM THAT DURING RUNNING FOR THE FIRST AND LAST 40% OF STANCE. DURING BOTH THE RUNNING TASK AND THE CUTTING TASK THE FOREFOOT REMAINED CLOSE TO ITS NEUTRAL POSITION. HALLUX MOTION WAS SIMILAR TO THE BAREFOOT CONDITION AS SEEN IN FIGURE 4.4. THE HALLUX MOTION IS THE LEAST VARIABLE AND YET SHOWS THE GREATEST DIFFERENCE BETWEEN THE CUTTING AND RUNNING TASKS, WHICH HAVE A SIMILAR PATTERN BUT APPEAR TO BE OUT OF PHASE BY 20% OF STANCE. MEDIAL LONGITUDINAL ARCH MOTION DURING CUTTING APPEARS TO BE OPPOSITE THAT DURING RUNNING. 191

FIGURE B.1: DUAL C-ARM FLUOROSCOPE SET UP FOR CURRENT STUDY. A. MATLAB FIGURE REPRESENTATION OF THE ANGLE OF PROJECTION. B. PHOTO OF FLUOROSCOPE SET-UP..... 215

FIGURE C1 THE RANGE OF MOTION (ROM) OF THE HINDFOOT WITH RESPECT TO THE MIDFOOT IN THE FRONTAL PLANE FOR EACH SUBJECT (X-AXIS) IN EACH OF THE FOUR CONDITIONS (CO – RED LINES, FF – SOLID YELLOW, FL – BLUE LINES, BARE – BLUE DOTS). THE MEAN IS THE AVERAGE ACROSS THE GAIT CYCLE. 226

FIGURE C2: THE RANGE OF MOTION (ROM) OF THE FOREFOOT WITH RESPECT TO THE MIDFOOT IN THE FRONTAL PLANE FOR EACH SUBJECT (X-AXIS) IN EACH OF THE FOUR CONDITIONS (CO – RED LINES, FF – SOLID YELLOW, FL – BLUE LINES, BARE – BLUE DOTS). THE MEAN IS THE AVERAGE ACROSS THE GAIT. 226

FIGURE C3: THE RANGE OF MOTION (ROM) OF THE HALLUX WITH RESPECT TO THE FIRST METATARSAL IN THE SAGITTAL PLANE FOR EACH SUBJECT (X-AXIS) IN EACH OF THE FOUR CONDITIONS (CO – RED LINES, FF – SOLID YELLOW, FL – BLUE LINES, BARE – BLUE DOTS). THE MEAN IS THE AVERAGE ACROSS THE GAIT CYCLE..... 227

FIGURE C4: THE RANGE OF MOTION (ROM) OF THE MEDIAL LONGITUDINAL ARCH (HEIGHT-TO-LENGTH RATIO) FOR EACH SUBJECT (X-AXIS) IN EACH OF THE FOUR CONDITIONS (CO – RED LINES, FF – SOLID YELLOW, FL – BLUE LINES, BARE – BLUE DOTS). THE MEAN IS THE AVERAGE ACROSS THE GAIT CYCLE. 227

List of Appendices

APPENDIX A	212
8.1 Minimum important difference, including the calculation of a value for the Medial Longitudinal Arch	212
APPENDIX B	214
8.2 Support for Fluoroscopy Study (chapter 4).....	214
APPENDIX C	216
8.3 Support for Longitudinal Torsional Study (chapter 6)	216
APPENDIX D	228
8.4 Calculation of Torsional Stiffness and Bending Stiffness (chapter 6) .	228
8.4.1 Torsional Stiffness.....	228
8.4.2 Forefoot Stiffness.....	228
APPENDIX E	229
8.5 Permission Wiley-Blackwell.....	229
8.5.1 Permission from Elsevier.....	230
APPENDIX F - CODE	232
8.6 Deformation of the shoe	232
8.7 Soft tissue error translation and rotation.....	243
8.7.1 Sub-Function.....	245
APPENDIX G – ETHICS	247

List of Abbreviations and Symbols

3D	Three Dimensional
ANOVA	Analysis of Variance
Bare	Barefoot condition
Cal	Calcaneus
CAST	Calibrated Anatomical System Technique
CO	Control condition (Nike Frees)
COP	Center of Pressure
EMG	Electromyography
FF	Nike Frees with an added horizontal forefoot carbon plate
Fif	Fifth metatarsal
Fir	First metatarsal
FL	Nike Frees with a full-length carbon plate
FFlex	Resistance of a shoe to bend at the metatarsal break in the sagittal plane
Forefoot	Forefoot twist with respect to the midfoot in the frontal plane
Hal	Hallux
Hallux	Hallux angle in the sagittal plane with respect to the first metatarsal
HF	Hindfoot condition
HH	Helen Hayes
Hindfoot	Hindfoot with respect to the midfoot in the frontal plane
HS	Heel Strike
IBRSA	Image Based Roentgen Stereophotogrammetry Analysis
ITCL	Interosseous Talocalcaneal Ligament
LTS	Longitudinal Torsional Stress
MLA	Medial Longitudinal Arch
MLArch	Height-to-length ratio of the medial longitudinal arch
MMD	Maximum Mean Difference
MNMD	Minimum Mean Difference
MRI	Magnetic Resonance Imaging
MS	Midstance
MSKFM	Multi-Segment Kinematic Foot Model
MTP	Metatarsophalangeal
Nav	Navicular
NSRL	Nike Sport Research Lab
QS	Quiet Standing
ROM	Range of Motion
RSA	Roentgen Stereophotogrammetry
STA	Skin Tissue Artifact
TMMD	Time to the Maximum Mean Difference
TMNMD	Time to the Minimum Mean Difference
TO	Toeoff

WOBL Wolf Orthopaedic Biomechanics Laboratory
WOQIL Wolf Orthopaedic Qualitative Imaging Laboratory

Conditions

CO Control condition (Nike Frees)
FF Nike Frees with an added horizontal forefoot carbon plate
FL Nike Frees with a full-length carbon plate
Forefoot Forefoot twist with respect to the midfoot in the frontal plane
Hallux Hallux angle in the sagittal plane with respect to the first metatarsal
Hindfoot Hindfoot with respect to the midfoot in the frontal plane
MLArch Height-to-length ratio of the medial longitudinal arch

1 Chapter 1: Anatomy Overview of the Foot and Review of Foot Kinematic Research

Chapter 1 is an introduction to the anatomical features and functional biomechanics necessary to comprehend the methodology and results for the following study chapters, as well as a summary of foot kinematic research. The anatomical features and functional biomechanics focus on the foot, since it is the area of interest for this dissertation. Following this section, previously used technology and methods for analyzing foot kinematics during gait, as well as currently employed methodologies such as multi-segment foot models, are discussed. The objective of this dissertation is to develop a method to analyze kinematic changes of the foot in running shoes which will hopefully lead to research that will reduce running related injuries. These injuries and their predictors are discussed next in this section as the clinical relevance of this dissertation. In the last few pages of the chapter, the dissertation objective and the chapter outline are described.

1.1 Anatomical Overview of the Foot

The foot (Figure 1.1) has many functions including load bearing, shock absorption, protection, leverage, and balance. During gait, the foot is the first segment to contact the ground and therefore must be able to quickly adapt to its surroundings. However, in the second phase of the gait cycle the foot must be able to remain rigid for the forward propulsion of the body over the foot. Maintaining a normal gait pattern is important for injury prevention of the foot, as well as for injury prevention in other segments and joints in the kinetic chain as they are influenced by the motion of the foot.

The foot is a very complex structure comprised of 28 bones; including the sesamoids, 31 joints, and numerous muscles, tendons and ligaments. The medial side of the foot contains the medial longitudinal arch, which is comprised of the talus, navicular, first cuneiform and the first metatarsal. Other bones of the medial side are the second and third cuneiforms, metatarsals, and phalange bones¹. The lateral side of the foot is constructed of the calcaneus, the cuboid, the fourth and fifth metatarsal and their phalange joints¹. It contains the lateral arch, which is involved in weight-bearing during running and walking².

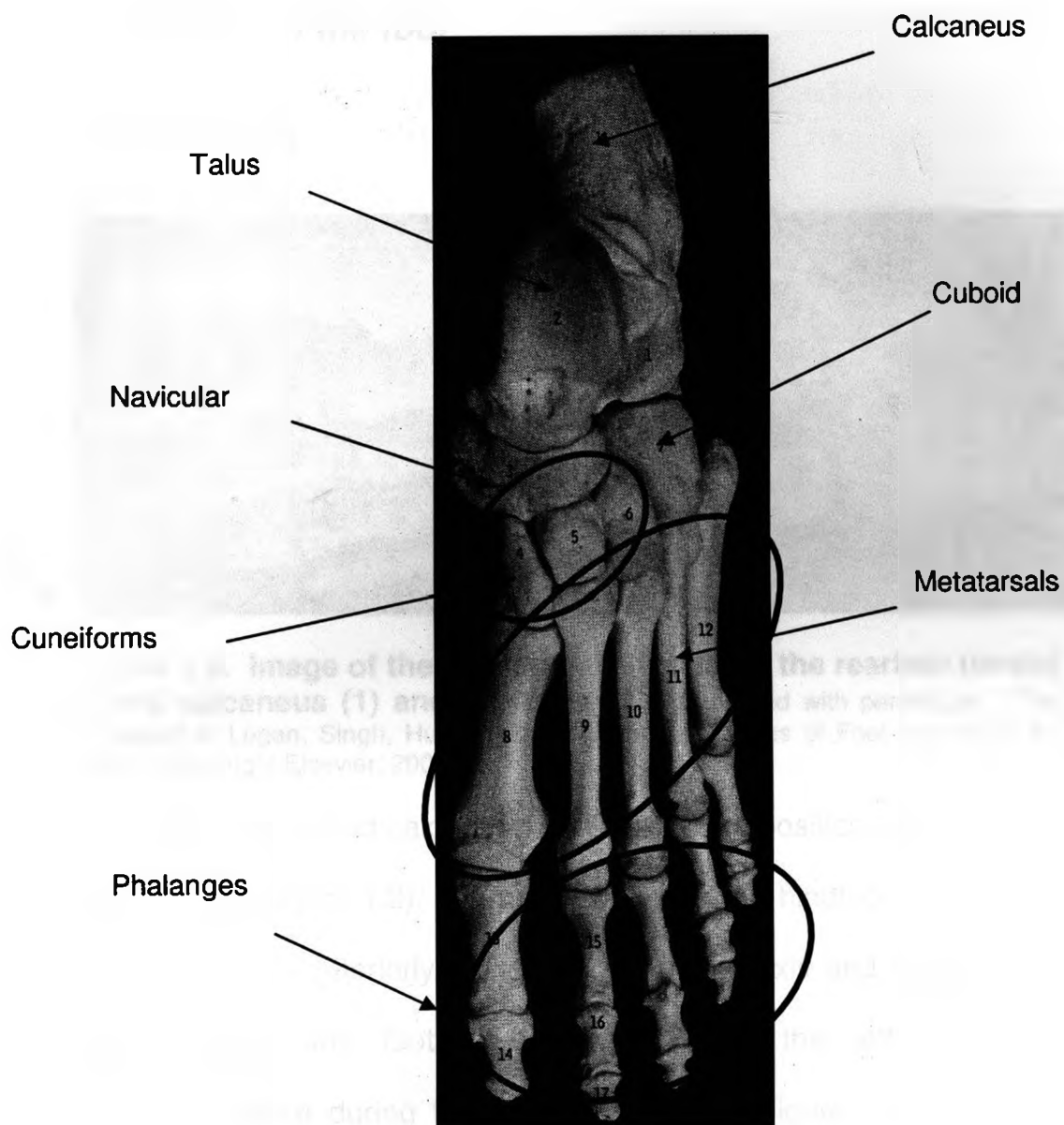


Figure 1.1. Bones of the left foot making up the hindfoot, or rearfoot, (calcaneus, talus), the midfoot (navicular, cuboid, cuneiforms), or forefoot (metatarsals, phalanges) (Reprinted with permission. "This article was published in Logan, Singh, Hutchings. McMinn's Color Atlas of Foot and Ankle Anatomy, third edition. Copyright Elsevier, 2004.")

1.2 *Bones of the foot*

1.2.1 Rearfoot

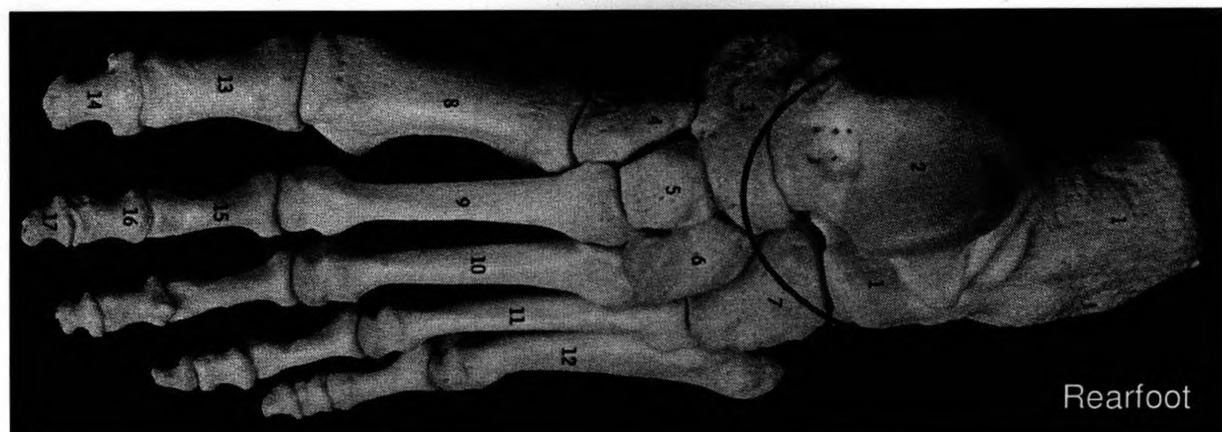


Figure 1.2. Image of the left foot with focus on the rearfoot (circle) made up of the calcaneus (1) and the talus (2). (Reprinted with permission. "This article was published in Logan, Singh, Hutchings. McMinn's Color Atlas of Foot and Ankle Anatomy, third edition. Copyright Elsevier, 2004.")

The lateral positioned calcaneus and the medial position talus form the bones of the rearfoot (Figure 1.2), often referred to as the hindfoot. The right calcaneus bone translates anteriorly along its longitudinal axis and rotates in a clockwise position when the foot is supinated, while the left calcaneous rotates counterclockwise during the same movement (Figure 1.3)¹. No muscles are directly attached to the talus, thus movement occurs when the muscles around it contract³.

There are two points of articulation between the two bones: the anterior (talocalcaneonavicular) articulation and the posterior (talocalcaneal) articulation. In a portion of the population, there is a third articulation between these two called the middle (talocalcaneonavicular) articulation¹. The functional joint encompassing these articulations is known as the subtalar joint. This joint is able

to move in the three principal planes due to the angulations in its orientation. The axis of the subtalar joint is 42° from the horizontal and 16° medial from the mid-line (Figure 1.4)¹.

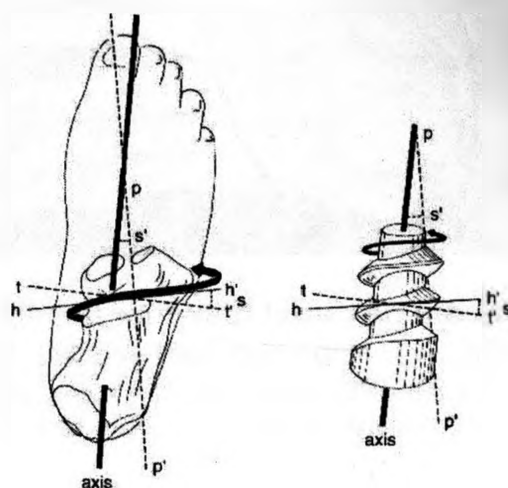


Figure 1.3. Description of the corkscrew mechanism of the right calcaneus. The calcaneus translates anteriorly and in a clockwise direction as the foot supinates. (Reprinted with permission from Sammarco, James G and Hockenbury, Ross Todd. "Biomechanics of the Foot and Ankle." Basic Biomechanics of the Musculoskeletal System. Ed. Margareta Nordin and Victor H. Frankel. Maryland: Lippincott Williams & Wilkins, 2001.)

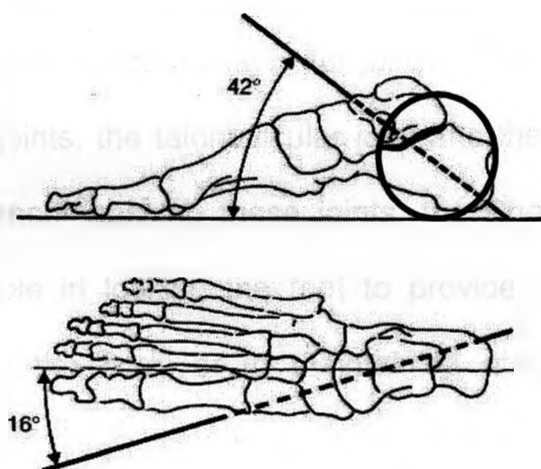


Figure 1.4. The axis of the subtalar joint (circle). Top: Sagittal View, Bottom: Transverse View. (Reprinted with permission from Sammarco, James G and Hockenbury, Ross Todd. "Biomechanics of the Foot and Ankle." Basic Biomechanics of the Musculoskeletal System. Ed. Margareta Nordin and Victor H. Frankel. Maryland: Lippincott Williams & Wilkins, 2001.)

1.2.2 Midfoot

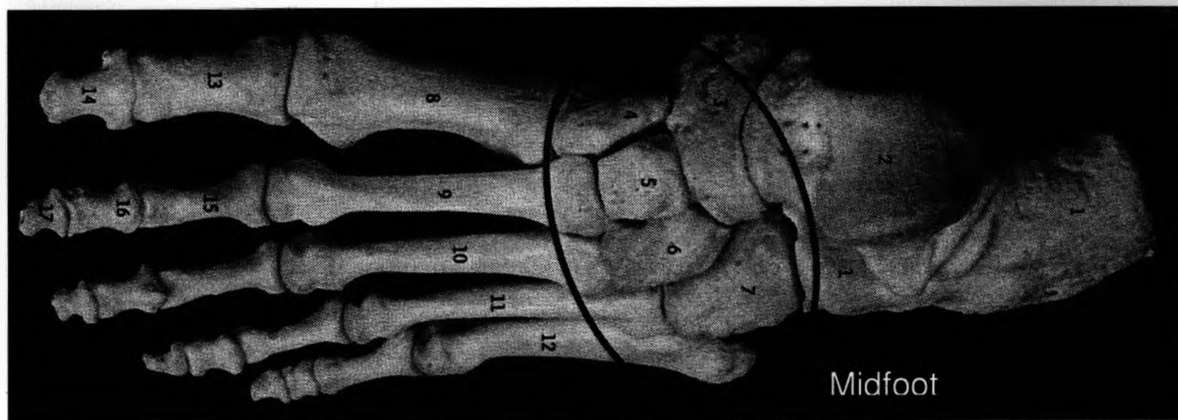


Figure 1.5. Image of the left foot with focus on the midfoot comprised of the navicular (3), cuboid (7), medial cunifform (4), intermedial cunifform (5), lateral cunifform (6). (Reprinted with permission. "This article was published in Logan, Singh, Hutchings. McMinn's Color Atlas of Foot and Ankle Anatomy, third edition. Copyright Elsevier, 2004.")

The midfoot segment of the foot (Figure 1.5), also known as the tarsus, consists of the navicular, the cuboid, and the medial, inter-medial and lateral cunifforms². The bones of this section of the foot create the talonavicular joint, the calcaneocuboid joint and the cunifonaviclar joints. The transverse tarsal joints include two of these joints, the talonavicular joint and the calcaneocuboid joint¹. The functional joint encompassing these joints, the Chopart joint (Figure 1.6), plays an important role in locking the foot to provide a rigid support for the forward propulsion of the body or to maintaining a flexible foot capable of adjusting to uneven surfaces². The exact details of this function can be found in section 1.6.2 on joint biomechanics.

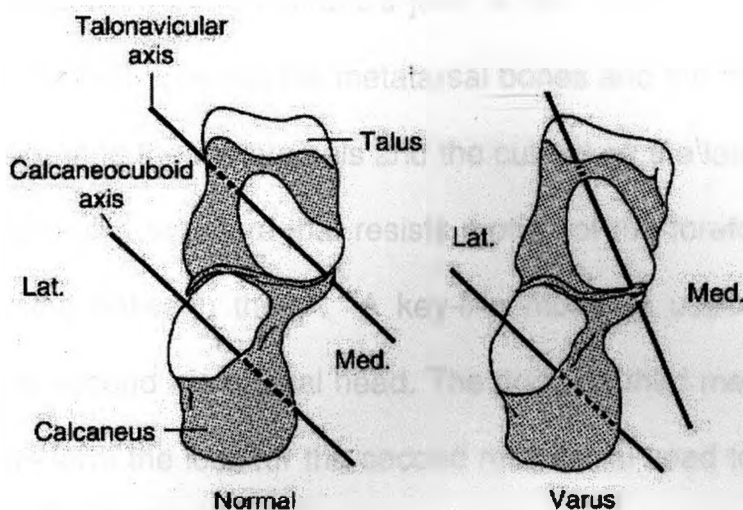


Figure 1.6. Axis of the transverse tarsal joints in the two positions experienced during a normal gait cycle. Left: Position of the axis during pronation at the beginning of the stance phase. Right: Position of the axis during supination at the end of the stance phase. (Reprinted with permission from Sammarco, James G and Hockenbury, Ross Todd. "Biomechanics of the Foot and Ankle." Basic Biomechanics of the Musculoskeletal System. Ed. Margareta Nordin and Victor H. Frankel. Maryland: Lippincott Williams & Wilkins, 2001.)

1.2.3 Forefoot

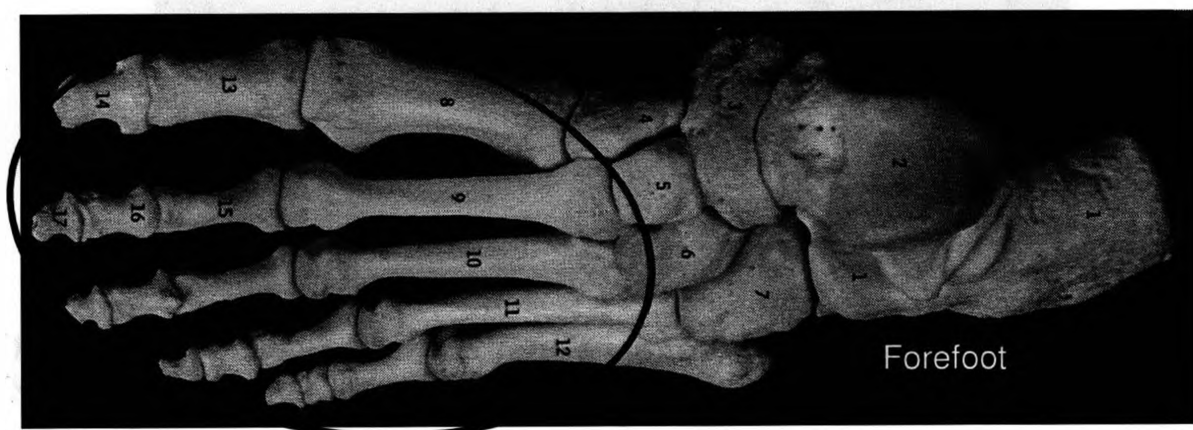


Figure 1.7. Image of the left foot with focus on the forefoot encompassing the first to fifth metatarsals (8-12) and their phalangeals (13-17). (Reprinted with permission. "This article was published in Logan, Singh, Hutchings. McMinn's Color Atlas of Foot and Ankle Anatomy, third edition. Copyright Elsevier, 2004.")

The tarsometatarsal joints, the Lisfranc joints (Figure 1.8), and the interphalangeal joints are constructed by the metatarsals and the phalanges in

the forefoot, respectively. The Lisfranc's joint is the articulation running medial-laterally across the foot between the metatarsal bones and the medial cuneiforms on the medial side and the metatarsals and the cuboid on the lateral side¹. These joints form an arch-like structure that resists motion of the forefoot allowing only minimal movement between them². A key-like model is used to describe the placement of the second metatarsal head. The first and third metatarsal, and the three cuneiforms form the lock for the second metatarsal head to fit into, thereby limiting the movement of the second metatarsal². The articulations of the distal and proximal phalangeals are the interphalangeal joints.

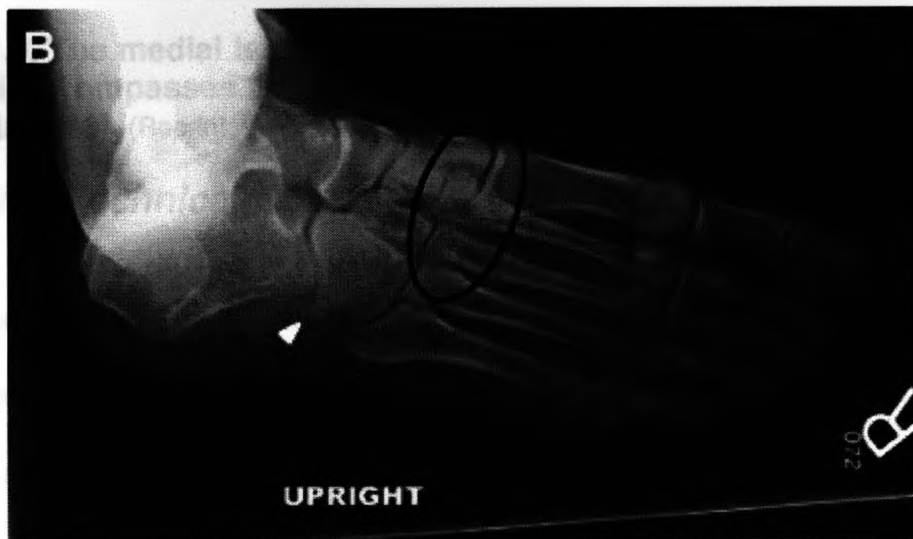


Figure 1.8. Location of the Lisfranc's joints in the right forefoot. (Reprinted with permission from Heckman et al. 2009)

1.2.4 Medial Longitudinal Arch

The medial longitudinal arch is located on the medial side of the foot and encompasses the calcaneus, talus, navicular and the first ray. These bones work together with the plantar fascia to create a windlass effect, which is explained in detail in section 1.4.1 on the plantar fascia². The rising or lowering of the arch

provides stability or mobility, respectively, depending on the foot function during the gait cycle.



Figure 1.9. The medial longitudinal arch is located on the medial side of the foot and encompasses the calcaneus, navicular, medial cuneiform and the first metatarsal. (Reprinted with permission from Heckman et al. 2009)

1.3 *Brief Technical Note*

Confusion often arises when discussing the position and movements of the foot since there is no consensus across researchers for the descriptions of the foot motions and positions. For the purpose of this paper, adduction and abduction will occur in the transverse plane, and flexion and extension will occur in the sagittal plane (Figure 1.10). Often, eversion and inversion is used to describe the position in the frontal plane; however pronation and supination are used interchangeably in research. Clinically, pronation and supintation are often terms used to describe the motion of the foot in all three planes. When the sole of the foot is pointing laterally, the foot is pronated. This motion is a combination of abduction, eversion and extension². The opposite is achieved when the sole of

the foot is facing medially. This is known as supination and is a combination of adduction, inversion and flexion². Since the foot model used in this study (described in Section 1.8.3) calculates forefoot twist, this will be classified as either supination or pronation in the frontal plane, and will be considered a movement as opposed to a position. To maintain uniformity, the motion of the hindfoot will also be considered pronation and supination in the frontal plane. For consistency this is how the motion will be described throughout this dissertation since this is how Jenkyn and Nicol^{4, 5} describe their model, which is the model used in this dissertation.

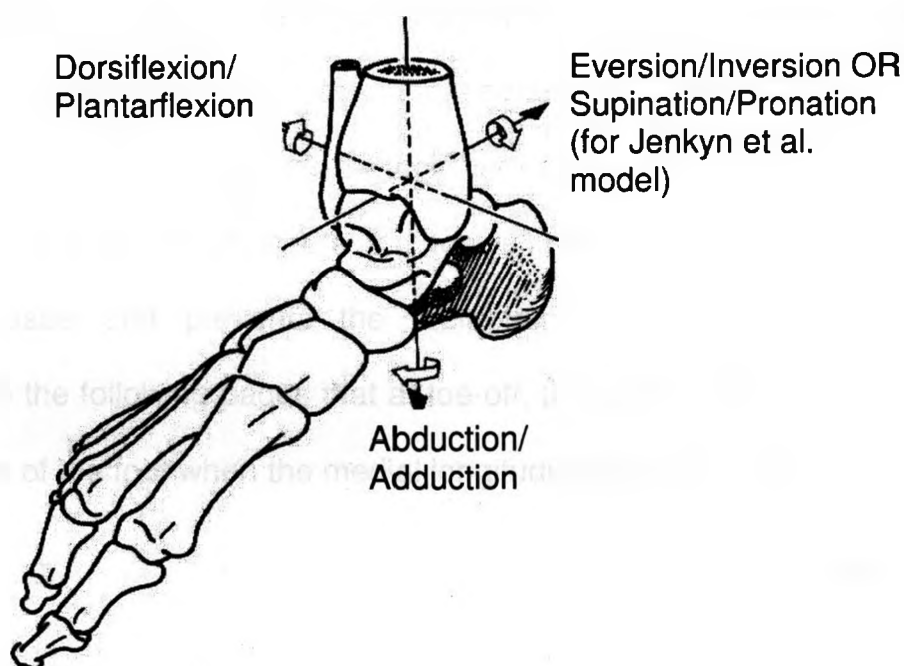


Figure 1.10. Descriptions of movements in each plane. Dorsiflexion/ plantarflexion are in the sagittal plane. Abduction/Adduction is in the transverse plane. Eversion/Inversion or Supination/Pronation is in the frontal plane. (Reprinted with permission from Sammarco, James G and Hockenbury, Ross Todd. "Biomechanics of the Foot and Ankle." Basic Biomechanics of the Musculoskeletal System. Ed. Margareta Nordin and Victor H. Frankel. Maryland: Lippincott Williams & Wilkins, 2001.)

1.4 Ligaments

1.4.1 Plantar Fascia

The plantar fascia (Figure 1.11) is found on the planar surface and is often described as the most important ligament in the foot². This ligament originates on the medial tuberosity of the calcaneus and inserts at the metatarsophalangeal joint, thereby crossing many foot joints¹. It also attaches the skin of the heel and forefoot to underlying bony and ligamentous structures².

The plantar fascia is also the main static stabilizer of the medial longitudinal arch through the windlass effect (Figure 1.12)¹. As the first phalanx is dorsiflexed, the two points of insertion, one on the calcaneus and one on the metatarsophalangeal, are brought closer together causing the arch to rise³. This can be seen in gait at toe-off where the toe is maximally dorsiflexed, which tightens the tissue and prevents the arch from collapsing¹. It will be demonstrated in the following pages that at toe-off, the foot is supinated which is often the motion of the foot when the medial longitudinal arch is raised².



Figure 1.11. Location of the plantar fascia on the plantar aspect of the foot.
(Reprinted with permission from Heckman et al. 2009)

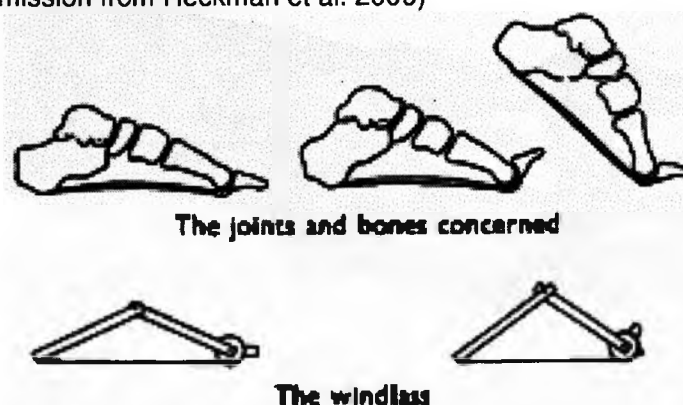


Figure 1.12. Visual explanation of the Windlass effect used to rise and lower the medial longitudinal arch. As the hallux dorsiflexes, as seen in the bottom picture, the plantar fascia (represented by the rope) causes the first metatarsal (represented by the longer segment) and the navicular (represented by the shorter segment) to rise. (Reprinted with permission from Hicks et al. 1953)

1.4.2 Intrinsic ligaments

Due to the vast number of articulations of the foot, there are numerous ligaments within the foot, which act as passive stabilizers. The majority are found on the dorsal aspect of the foot, however some plantar ligaments do exist¹. The interosseous talocalcaneal ligament (ITCL) connects the talus to the calcaneus,

along with the anterior talocalcaneal ligament (Figure 1.13.7), posterior talocalcaneal ligament, medial talocalcaneal ligament, and lateral talocalcaneal ligament¹. The ITCL is considered one of the most substantial and important ligaments in the foot. The most significant ligament in the forefoot is the Lisfranc ligament, which connects the second metatarsal head to the inter-medial cuneiform for added stability to this important and complex joint². The rest of the ligaments can be seen in Figure 1.13.

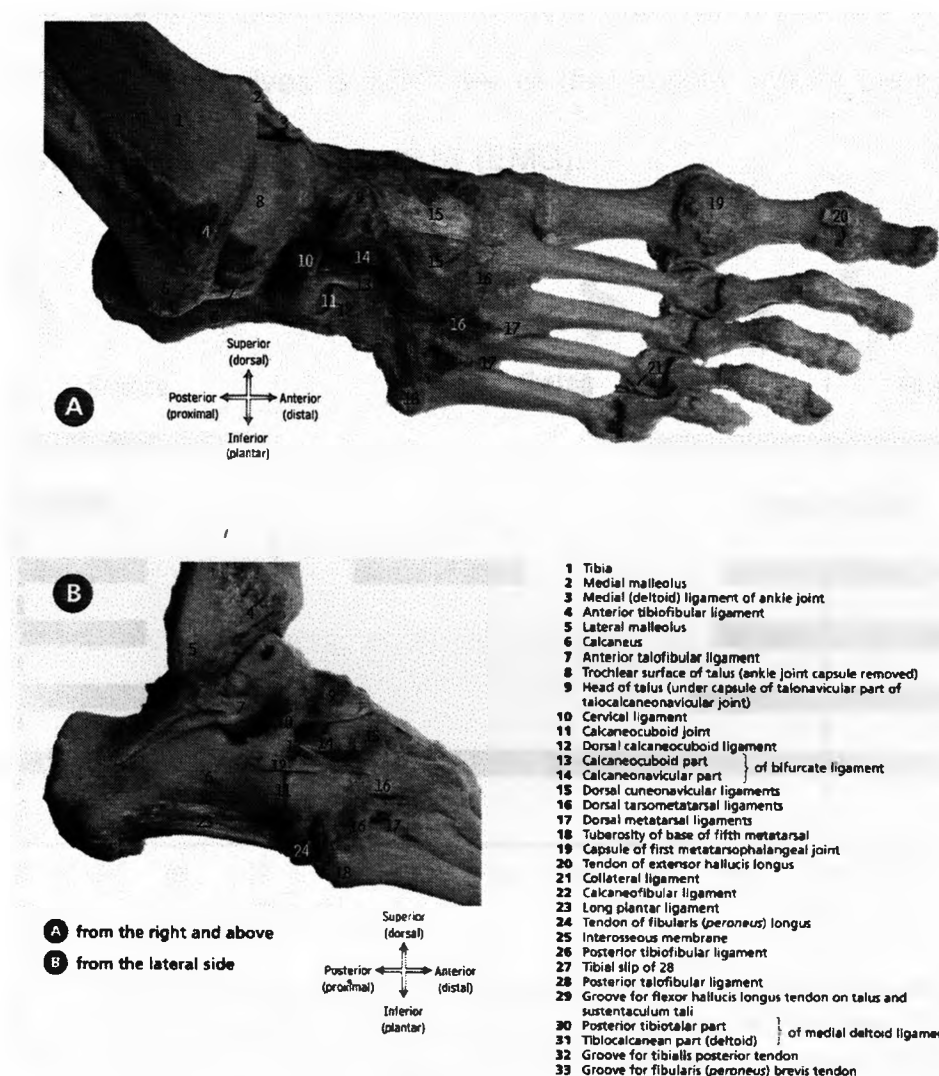


Figure 1.13. Ligaments of the foot. A. Lateral ligaments of the foot from an oblique dorsal view. B. Medial ligaments of the foot. (Reprinted with permission. "This article was published in Logan, Singh, Hutchings. McMinn's Color Atlas of Foot and Ankle Anatomy, third edition. Copyright Elsevier, 2004.")

1.5 Muscles and Tendons

The extrinsic muscles originate in the leg and insert in the foot, whereas the intrinsic muscles originate and insert in the foot. The 12 extrinsic muscles of the foot can be classified as either plantarflexors or dorsiflexors, and as evertors or invertors. These muscles are also classified as pretibial which are the anterior muscles (for example, tibialis anterior), calf muscles which are the posterior muscles (for example, gastrocnemius), or foot muscles which are the intrinsic muscles. Figure 1.14 gives a summary of the muscle activity during the gait cycle measured from electromyography (EMG).

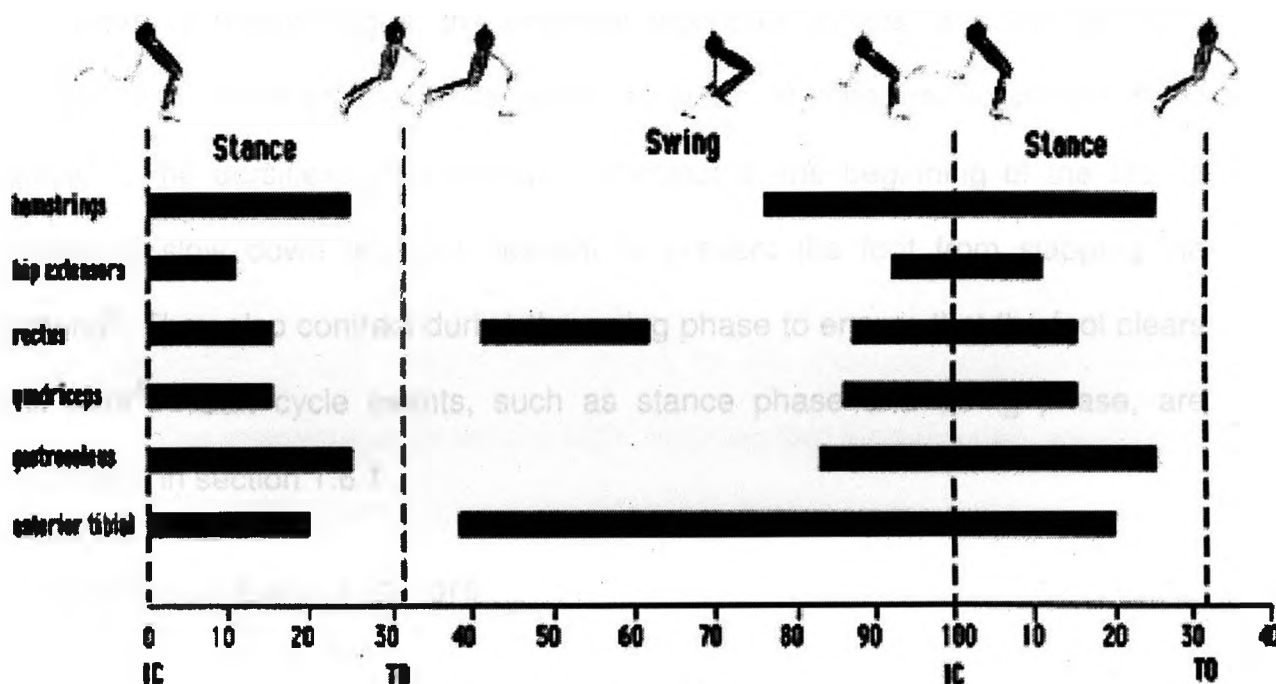


Figure 1.14. Electromyography of the lower extremity muscles during one gait cycle. Pretibial muscles are the anterior muscles of the leg. Triceps are the posterior muscles of the leg. Intrinsic muscles are the muscles that originate and insert in the foot. (Reprinted with permission from Novacheck, TF, 1998)

1.5.1 Plantarflexors and Dorsiflexors

A large group of muscles contract to cause the foot-ankle complex to plantarflex (Figure 1.15-1.17). These muscles include the gastrocnemius, the soleus, the peroneus longus, the peroneus brevis, the tibialis posterior, the flexor hallucis longus, and the flexor digitorum longus⁶. Contraction occurs in the middle of the stance phase to slow the forward motion of the tibia over the foot³. Much of the work of the plantarflexors is done by the soleus in conjunction with the gastrocnemius⁶.

The principal dorsiflexors (Figure 1.15-1.17) of the foot are the tibialis anterior, the extensor hallucis longus, the extensor digitorum longus, and the peroneus tertius⁶. The tibialis anterior is described as the most important dorsiflexor of the ankle¹. The dorsiflexors eccentrically contract at the beginning of the stance phase to slow down the foot descent to prevent the foot from slapping the ground⁶. They also contract during the swing phase to ensure that the foot clears the floor⁶. Gait cycle events, such as stance phase and swing phase, are described in section 1.6.1.

1.5.2 Invertors and Evertors

The main invertors (Figure 1.15-1.17) are the tibialis posterior, the tibialis anterior, the extensor hallucis longus, the flexor digitorum longus and the flexor hallucis longus⁶. These muscles insert on the medial side of the foot allowing them the correct line of action to invert the foot. The primary invertor is the

tibialis posterior, which is the main dynamic stabilizer of the medial longitudinal arch¹.

The evertor muscles (Figure 1.15-1.17) originate in the lower leg and attach on the lateral side of the leg. The principle everters are the peroneus longus, the peroneus brevis, the peroneus tertius and the extensor digitorum⁶. The primary evertors are the peroneus longus, whose function in gait is to depress the first metatarsal head, and the peroneus brevis, which acts to stabilize the forefoot laterally, in other words to resist inversion^{1, 6}.

1.5.3 Intrinsic muscles of the foot

The intrinsic muscles include the lumbricals and the interossei (Figure 1.15 - 1.17)¹. Located between the metatarsals, these muscles produce plantarflexion of the middle phalangeal joints of the foot, an important event for the propulsion phase of walking. The lumbricals comprise four muscles that originate from the flexor digitorum longus tendon and insert to the extensor digitorum longus tendon². The interossei muscles are eight muscles that form the deepest intrinsic muscle layer. The main intrinsic muscles are the abductor hallucis, adductor hallucis, flexor digitorum brevis, flexor hallucis brevis and the abductor digiti quinti, whose function is to support the toes at the metatarsophalangeal joint and the medial longitudinal arch². The other important intrinsic muscles' primary function is the motion of the great toe, the first phalanx¹.

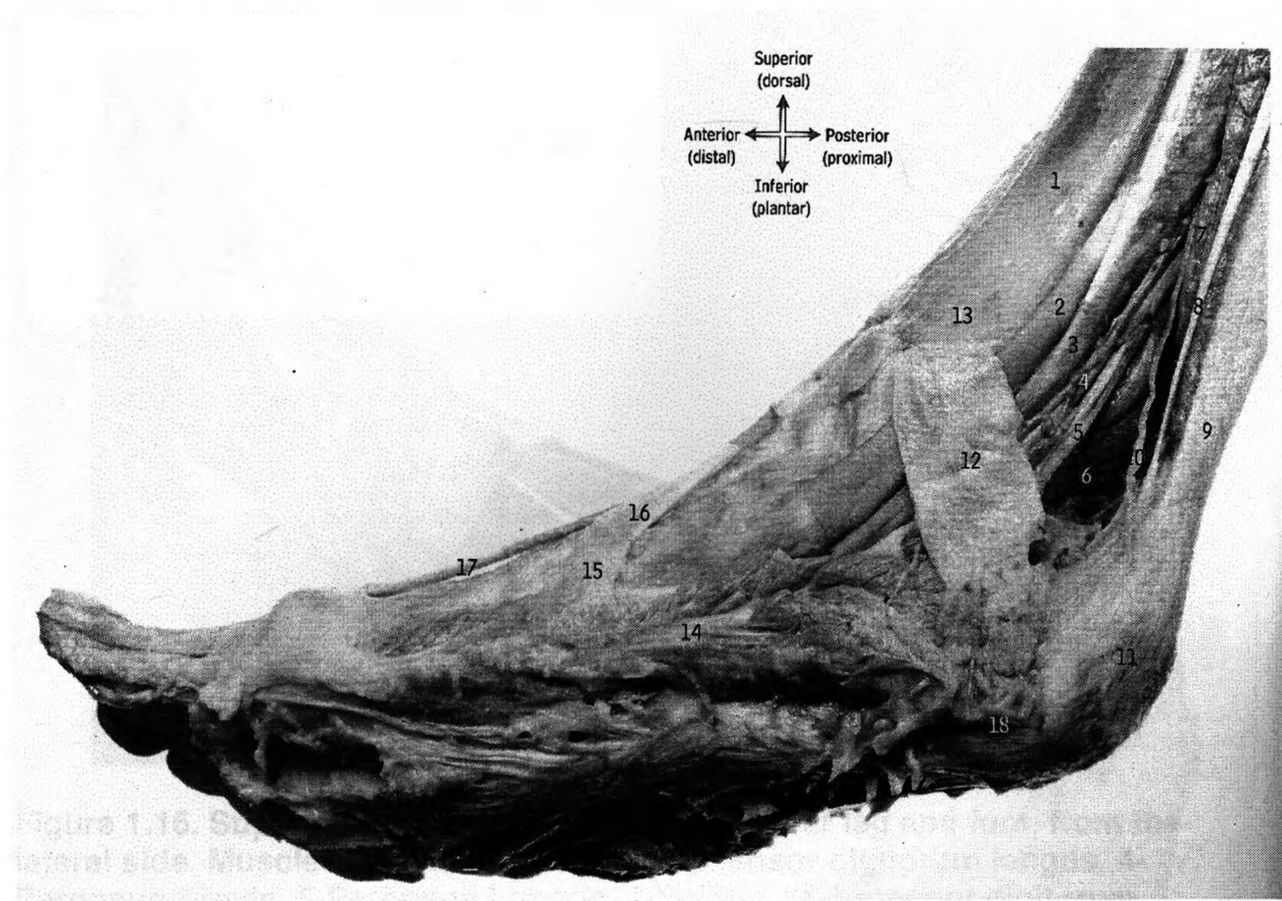


Figure 1.15. Superficial dissection of the right lower leg and foot, from the medial side. Muscles: 2-tibialis posterior, 3-Flexor digitorum longus, 6-Flexor hallucis longus, 7-Soleus, 14- Abductor hallucis, 16-Tibialis anterior, 17-Extensor hallucis longus. (Reprinted with permission. "This article was published in Logan, Singh, Hutchings. McMinn's Color Atlas of Foot and Ankle Anatomy, third edition. Copyright Elsevier, 2004.")

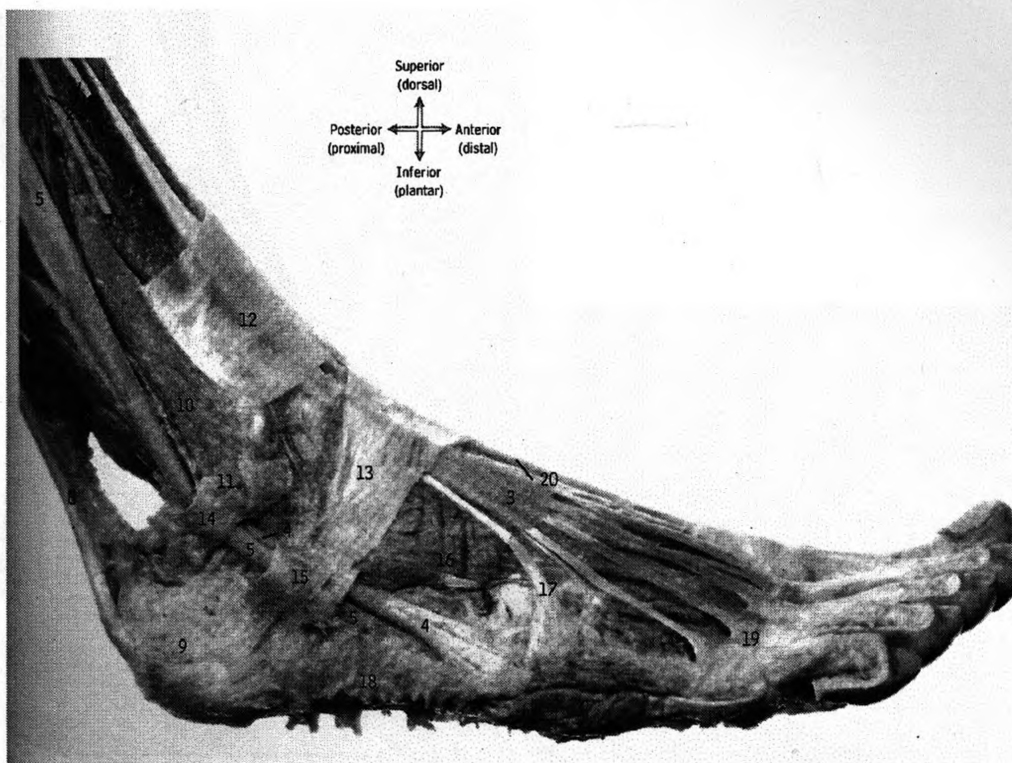


Figure 1.16. Superficial dissection of the right lower leg and foot, from the lateral side. Muscles: 1-tibialis anterior, 3-Extensor digitorum longus, 4-Peroneus Brevis, 5-Peroneus Longus, 7-Soleus, 16-Extensor digitorum brevis, 17 –Peroneus tertius, 18 – Abduction digiti minimi, 20 – Extensor hallucis longus). (Reprinted with permission. "This article was published in Logan, Singh, Hutchings. McMinn's Color Atlas of Foot and Ankle Anatomy, third edition. Copyright Elsevier, 2004.")



Figure 1.17. Deep dorsum of the right foot, from an anteriolateral view point. Muscles: 1-Tibialis anterior, 2-Extensor hallucis longus, 3-Extensor digitorum longus, 5-Peroneus brevis, 6-Peroneus longus, 18-Extensor digitorum brevis, 22-Abductor digiti minimi. (Reprinted with permission. "This article was published in Logan, Singh, Hutchings. McMinn's Color Atlas of Foot and Ankle Anatomy, third edition. Copyright Elsevier, 2004.")

1.6 Functional Biomechanics

1.6.1 Gait Cycle

The gait pattern of walking and running is commonly discussed by describing the events in one complete gait cycle. One gait cycle is classified from one initial contact of either the right or left foot to the following initial contact of the same foot³. Heel strike is commonly identified as the initial point of contact of the foot with the ground since most runners, at a jogging pace, are heel runners⁶ (see Figure 1.18, this figure will be discussed throughout this section). During the stance phase, which is when the foot is in contact with the ground, there are three different rockers, or pivot points, during a normal gait cycle⁶.

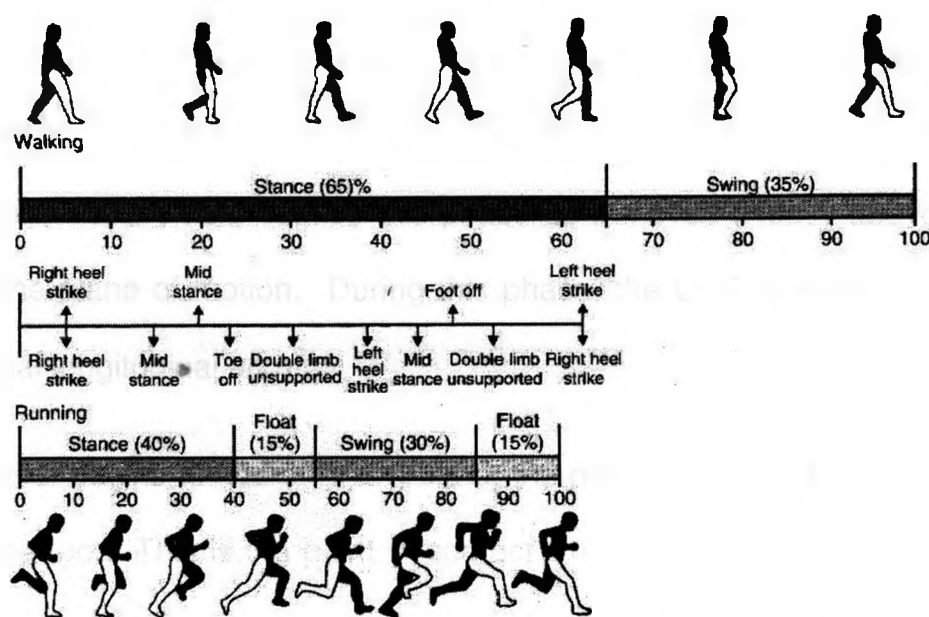


Figure 1.18. Description of the gait cycle for walking (top) and running (bottom). Walking has two phases: stance and swing. Running has three phases: stance, float and swing. (Reprinted with permission from Sammarco, James G and Hockenbury, Ross Todd. "Biomechanics of the Foot and Ankle." Basic Biomechanics of the Musculoskeletal System. Ed. Margareta Nordin and Victor H. Frankel. Maryland: Lippincott Williams & Wilkins, 2001.)

At the beginning of the gait cycle, which coincides with the heel strike, the initial rocker of the foot and ankle is the heel (since only heel strikers were used in all study chapters initial contact will be considered heel strike for this dissertation). After this initial contact, the foot rapidly plantarflexes but is controlled by the eccentric contraction of the tibialis anterior and other pretibial muscles⁶. A passive eversion moment also accompanies this plantarflexion moment as a consequence of the lateral contact of the foot with the ground³. Again the passive moment is controlled by active muscle moments of the invertors⁶. During this phase, the center of pressure (COP) is located under the heel (Figure 1.19)².

The ankle then becomes the rocker as the momentum of the swing leg moves the body forward as it is controlled by the active muscle moments. At this point the stationary foot becomes loaded. This phase is known as midstance, and occurs when the arches of the foot flex and flatten from the loading of the foot². The location of the tibia defines this phase as it moves directly above the ankle joint in the plane of motion. During this phase, the COP is under the middle of the medial longitudinal arch².

As the heel begins to rise off the ground, the pivot point, or rocker, becomes the ball of the foot. This is the point of contact when the foot pushes off the floor to propel the body forward. Heel rise, or push-off, occurs when the heel comes off the ground and the COP shifts to under the ball of the foot². The COP continues to move anteriorly until it is directly under the toes. Toe-off occurs at the end of the phase when the toe(s) lifts off the ground² ending the stance phase of the gait cycle.

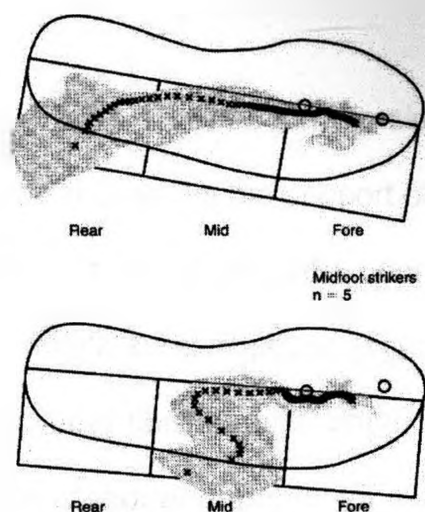


Figure 1.19. Location of the center of pressure (COP) for a heel striker (top) and a midfoot striker (bottom) for one gait cycle. (Reprinted with permission from Sammarco, James G and Hockenbury, Ross Todd. "Biomechanics of the Foot and Ankle." Basic Biomechanics of the Musculoskeletal System. Ed. Margareta Nordin and Victor H. Frankel. Maryland: Lippincott Williams & Wilkins, 2001.)

The gait cycle for walking can be split into two phases: the stance phase and the swing phase (Figure 1.18, top). The stance phase, which begins at heel strike and ends at toe-off, is described above using its three rockers³. During the stance phase there are two phases of double support, which is when both feet are in contact with the ground. These occur at the beginning and end of the stance phase surrounding a period of single support, where only one leg is in contact with the ground⁷. The second phase, known as the swing phase, begins at toe-off and ends at the second heel strike of the initial foot³. The foot in question is off the ground, swinging forward, hence the term swing phase. Movement is assisted by the forward swing of the leg driving the center of gravity forward on the supporting leg, which is supported by muscles contractions⁶.

Muscles, particularly the dorsiflexors, ensure that the foot clears the ground during this phase⁶.

The gait cycle for running (Figure 1.18, bottom) is similar to that of walking but has two main differences; there is no double support phase, and there is a period of floating, which occurs when there is no pedal contact with the ground⁷. The running cycle starts with a single support phase (stance), is followed by a float phase, then a swing phase, and finishes with another period of floating⁷. The timeline for the running cycle is shorter than that for the walking cycle as depicted in Figure 1.18⁷.

1.6.2 Locking mechanism of the foot during gait

One can divide the motion of the foot further by describing the motion of the subtalar joint and the transverse tarsal joint. At landing, there is a very brief moment where the subtalar joint inverts as the foot supinates. The foot then pronates while the subtalar joint everts from heel strike to flat foot². As this pronation occurs, the axes of the talonavicular joint and the calcaneocuboid joint are parallel and unlocked; consequently the midfoot is free to move (Figure 1.20)². This allows a flexible foot the ability to adjust to an uneven ground surface, and also attenuate the shock produced as the foot contacts the ground. From midstance to push-off, the foot becomes a rigid lever to assist the forward propulsion of the body. The transverse tarsal joint axes becomes congruent which locks the foot joints in place restricting the movement of the foot². This is accomplished when the subtalar joint is in inversion, or the foot is supinated².

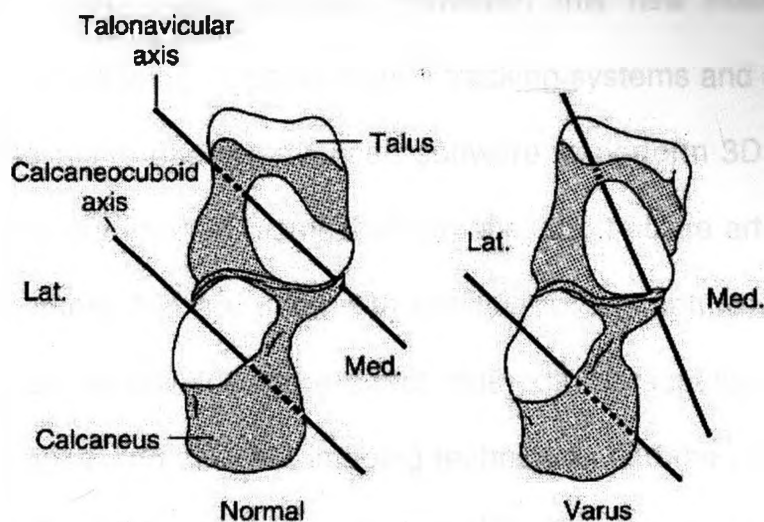


Figure 1.20. Axis of the transverse tarsal joints. During pronation, the subtalar joint is everted unlocking the talonavicular and calcaneocuboid axis. Supination has the opposite effect and locks the two axes. (Reprinted with permission from Sammarco, James G and Hockenbury, Ross Todd. "Biomechanics of the Foot and Ankle." Basic Biomechanics of the Musculoskeletal System. Ed. Margareta Nordin and Victor H. Frankel. Maryland: Lippincott Williams & Wilkins, 2001.)

1.6.3 Forefoot movement during Gait

Stabilization of the forefoot in the last half of the stance phase is important as a rigid forefoot needs to receive the load of the body during push-off when the forefoot is the rocker⁶. Intrinsic and extrinsic muscles, that insert into the distal section of the foot at the metatarsophalangeal joint, are responsible for stabilizing the hallux and the medial longitudinal arch².

1.7 Methods for Measuring Kinematics of the Foot during gait

In biomechanical research different methodologies and equipment are used to measure the kinematics of the foot bones. One of the first methods involved 2D film analysis; however research has shown that caution should be exercised when performing 2D analyses⁸. With technological advances 2D video analysis

was replaced by 3D video analysis; however, this new method demanded significant post-processing. Optical motion tracking systems and electromagnetic tracking devices make use of advanced software to perform 3D motion capture and are currently common in biomechanics labs. Soft tissue artifact (STA) from surface skin markers that are used with optical motion capture systems has led many researchers to develop more direct methods for visualizing the motion of the foot bones, including different imaging techniques and the use of intracortical pins with optical motion capturing systems⁹⁻¹². The following sections briefly explore these different techniques.

1.7.1 Optical Motion Analysis Systems

Optical motion capturing systems record the motion of surface skin markers located on specific landmarks of the body using sophisticated cameras with embedded software. The markers can be either passive (retro-reflective) or active (blinking lights). Passive retro-reflective marker triads were developed and are used in this dissertation for all five studies. Irrespective of the marker type, the cameras use the reflections from the markers to calculate the triangulated position of the markers in the lab space. Three collinear markers are then used to define a segment co-ordinate frame which can then be used to calculate joint angles, velocities and accelerations, as well as joint moments if the system is synchronized with a force plate. These systems can capture kinematics with up to six degrees of freedom in real time at a rate of up to 500 Hz. For a more complete clinical interpretation of the movement, three anatomical landmarks per segment, which can be virtual markers in the segment co-ordinate frame, can

be used to calculate an anatomical references frame which can then be used to calculate the above mentioned measures, including joint angles. This increases the clinical relevance of the results.

Most passive systems use visible red light or infrared light emitted from the cameras to detect the retro-reflective markers. Passive systems eliminate the use of wires during the analysis allowing subjects to maintain their natural gait patterns.

The advantages of optical motion capture systems are their high accuracy and high resolution, often to 1mm-2mm, and less than 1 degree. However, this accuracy does depend on the quality of the cameras and markers used, as well as the marker placement on the subject¹³. A limitation of this system is that a marker can only be reconstructed if it is visible to a minimum of two cameras. Another main disadvantage of this technology is that skin markers produce soft tissue artifact, which is the error associated with the assumption that the markers are capturing the movement of the bones and not the movement of the soft tissue¹⁴. Other techniques, such as fluoroscopy and intracortical pins are considered insensitive to soft tissue artifact error^{14, 15}. These methods are discussed later in this section.

In most clinical biomechanics labs, the data analysis for optical motion capture systems is performed using the manufacturers' software. In the Wolf Orthopaedic Biomechanics Laboratory (WOBL) the tracking and filtering software used is EVaRT 4.2 and the analysis software is OrthTraks (Motion Analysis

Corporation, Santa Rosa, CA). When performing standard gait analysis, WOBL uses the modified Helen Hayes marker system¹⁶, adding a scapula marker to decipher the left from the right, with a Motion Analysis Optical Tracking system (EvaRT 5.04, Eagle HiRes cameras, Motion Analysis Corp., Santa Rosa, CA). The Helen Hayes marker set (Figure 1.21) consists of 21 passive reflective markers used to calculate segmental movements of the entire body. The markers for the standard Helen Hayes model are attached with double sided adhesive discs over the following landmarks: both shoulders, both elbows, both wrists, both superior iliac spines, the sacrum, both lateral knees, both lateral ankles, both toes of the shoes, both heels of the shoes, left and right thigh wand (mid lateral thigh), and left and right shank wand (mid lateral shank)¹⁶. The markers are connected to produce segments. The foot segment is created by the toe and heel markers, treating the foot as a rigid segment. This is a major disadvantage when conducting foot research since no information on the articulations of the various foot bones including information on the hindfoot, midfoot, or forefoot, can be obtained.

Advances in foot modeling have allowed researchers the ability to use optical motion capture systems to analyze the foot. These new models are discussed in section 2.2.3. Imaging is another method used to calculate the motion between segments of the foot since the bones can be directly visualized.

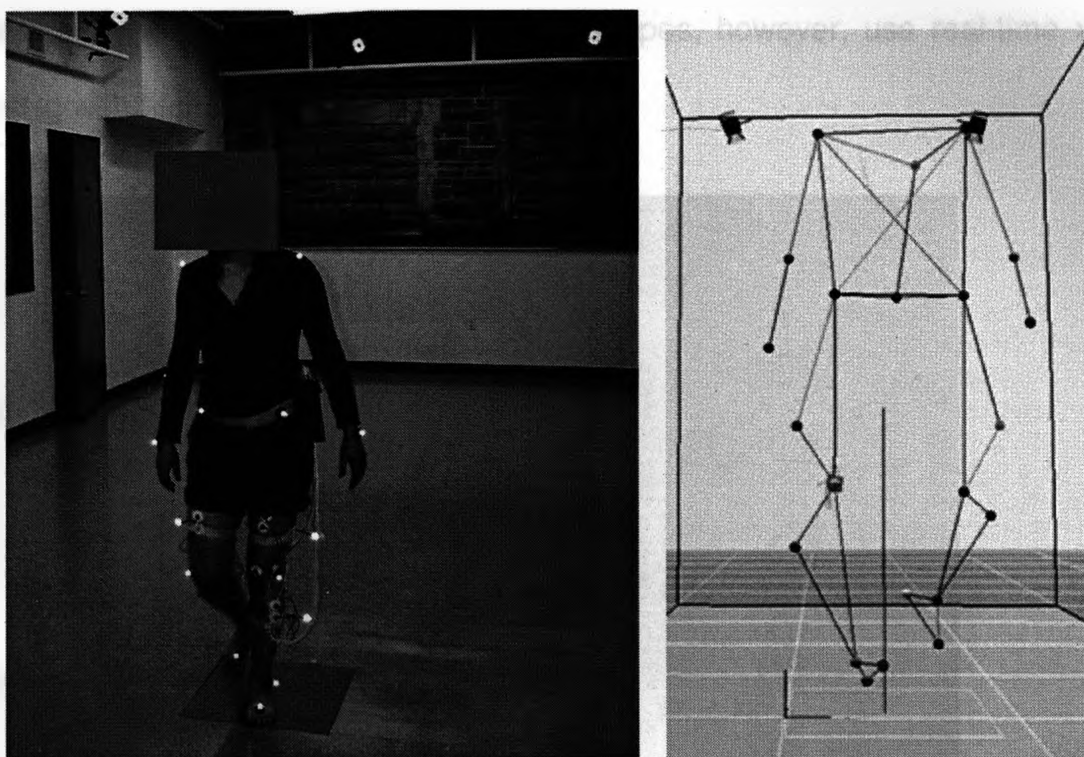


Figure 1.21. Helen Hayes Marker set up with EMG on a patient in WOBL (left). Motion Analysis reconstruction of the markers in real time (right).

1.7.2 Fluoroscopy

Fluoroscopy is an imaging technique used in hospitals during procedures such as gastrointestinal examinations, and peripheral vascular and cardiac angiography, where a physician must view internal organs and bones. In Orthopaedic medicine, fluoroscopes are commonly used to assist in setting fractures¹⁷. This eliminates the need for open surgery by reducing displaced and multipartite fractures by surpassing the tissue and viewing the bones directly¹⁸.

Figure 1.22 shows a typical fluoroscope with a 22.86 cm (9 inch) field of view. The image intensifier is the distinguishing feature of a fluoroscope. Many of the other components, including the x-ray tube, filters, and collimation, are similarly

found in x-ray imaging machines. Fluoroscopes, however, use real-time x-ray viewing with high temporal resolution¹⁷

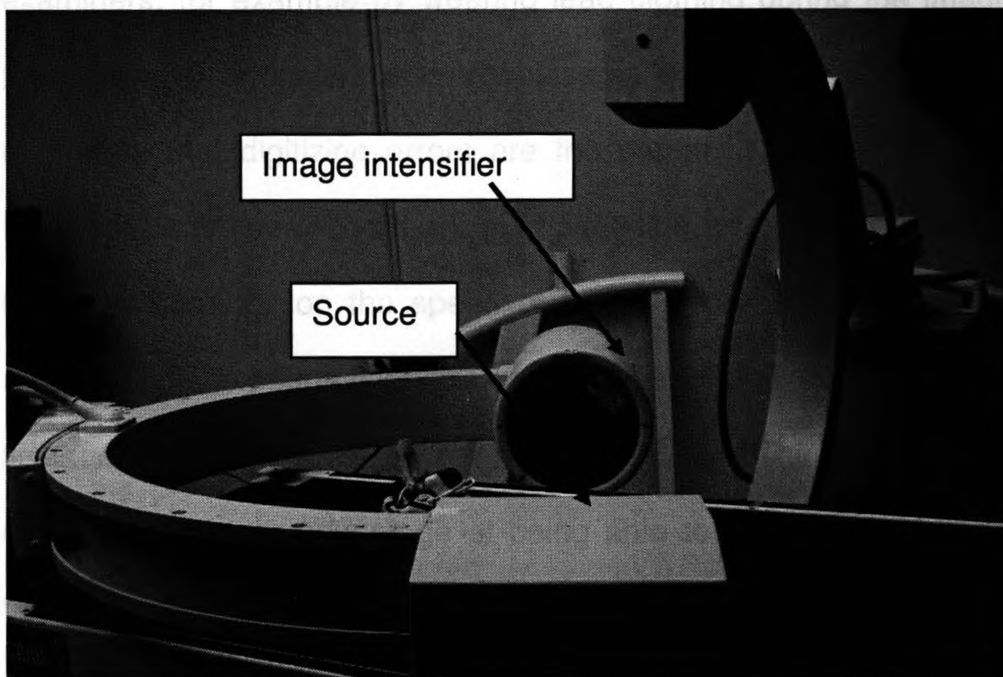


Figure 1.22. Image of dual C-arm fluoroscopes set-up for evaluating the mediolateral view of the foot in the Wolf Orthopaedic Biomechanics Laboratory.

Fluoroscopes can produce up to 18,000 images in a 10 minute session; in order for their dose to be safe, they therefore must produce usable images with relatively few x-ray photons¹⁷. The fluoroscopes' high quality image intensifier allows this to be achieved. Other methods used to reduce the dose received by the patients are the use of heavy x-ray beam filtration, the aggressive use of low frame rate pulsed fluoroscopy and the reduction of the number of radiographic images captured¹⁷.

A disadvantage of fluoroscopy is its limited field of view. This is particularly a problem with a 9-inch field of view machine since most patients' feet do not fit in

a single image. Radiation exposure is also a disadvantage, however, this can be reduced if the proper steps are taken to ensure the safety of the patients and the examiners, for example by wearing lead clothing during the imaging session¹⁹. Measurement errors are also troublesome when using fluoroscopy. Wearing et al.²⁰ state that digitizing errors are the primary source of errors in evaluating fluoroscopic images. There are also distortion errors for which the magnitude of the error depends on the speed of the subject's movement and the temporal resolution of the image intensifier²⁰. However, many of these errors fall within the limits of digitizing error or can be corrected. These disadvantages do not outweigh the clear advantage of being able to observe the bones directly, and therefore several researchers are now using this technology.

Direct tracking of the skeletal movement is possible with this technique, thereby eliminating soft tissue artifact errors²⁰. Roentgen stereophotogrammetry (RSA), is a method that tracks radiopaque tantalum markers (diameter 0.8–1.0 mm) which are operatively inserted into the bone and are visible on fluoroscopic images²¹. Although this technique has been used since the 1980s²²⁻²⁵, more researchers are exploring its potential for biomechanical research by investigating image based RSA (IBRSA)²⁶⁻²⁹. IBRSA uses MRI or CT scans with fluoroscopy to develop 3D models of the foot and ankle. It is speculated that as the fluoroscopy field of view increases so will the use of this technology, since it is a non-invasive method that allows the direct visualization of the bones.

1.7.3 Other Methods

2D video analysis uses a camera to record a subject's movement in the plane perpendicular to the given camera. Multiple cameras allow the research to view multiple planes (for example sagittal and frontal) but only one plane can be analyzed at a time. Qualitative observations can be made across planes only. Data analysis can be difficult as cameras must be perpendicular to the plane of motion for the specific calculation. For example, if calculating the knee flexion angle during running, the camera must be perpendicular to the flexion/extension axis of the knee. One advantage of the 2D analysis system is that it is portable and so remains useful for on-field analysis and clinical testing. However, 2D video analysis is becoming less common in research as the technology of the 3D optical motion capture system continues to improve. Although three-dimensional (3D) video analysis is possible, the tedious post-processing makes this option less favorable. The post-hoc 3D analysis transforms the two-dimensional data into three-dimensional marker coordinates; however the data must first be digitized and even with technological advances in software this task remains cumbersome.

Intracortical pins with retro-reflective markers attached to the ends can also be used instead of skin markers to track the movement of the bones using optical motion capture systems (see Figure 1.23). This is not common in North America since most ethics boards will not approve this invasive method. Patient's bones are drilled and bone pins, with retro-reflective markers attached to the ends, are positioned directly into bones to directly track their movements³⁰. The advantage

of this method is that it eliminates soft tissue artifact by surpassing the tissue and collects the true motion of the bones. This method is often considered the gold standard in biomechanics since the markers are affixed directly to the bones and the sampling frequency of the optical motion capture system allows for a dynamic activity to be analyzed. However, whether or not a subject maintains a normal foot gait pattern has yet to be proven. Insertion of the intracortical pins requires a local anesthetic and the drilling of subject's bones³⁰. Data collection is normally within two hours of the surgery, which is within the active time frame of the anesthetic³⁰. Another disadvantage of intracortical pins is that shoes cannot be changed during a single test session, which limits testing to barefoot or a single shoe analysis.

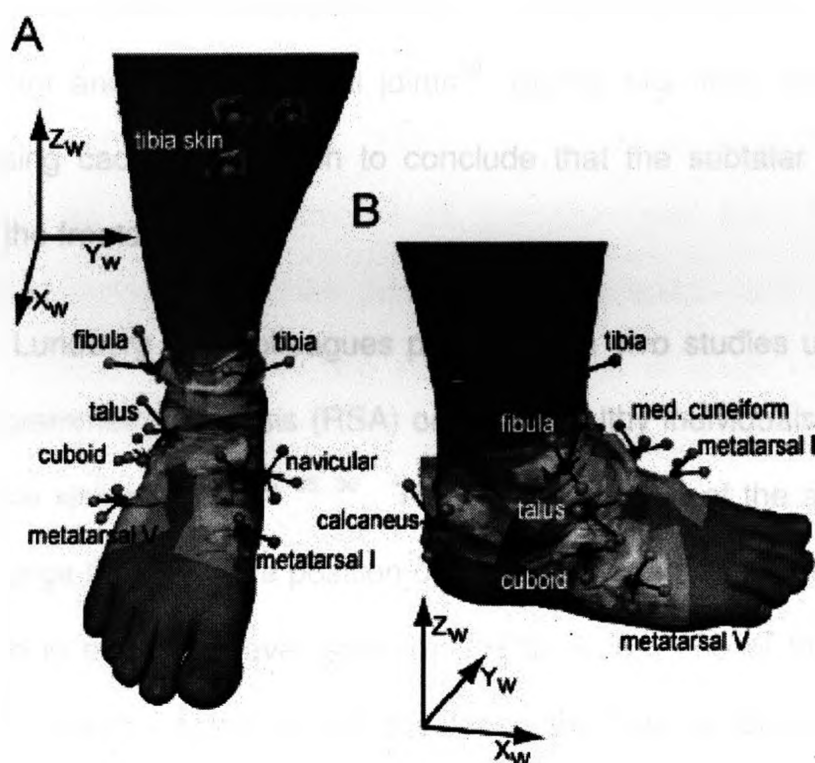


Figure 1.23: Bone pins inserted into a subject's foot for a walking study conducted in Sweden. (Reprinted with permission Arndt et al. 2007)

1.8 Previous Research Methods

1.8.1 Foot Kinematics during Gait

Foot biomechanics is a fairly new research discipline relative to other sciences. Although foot research began early in the 20th century, the kinematics of the foot joints were often unstudied due to the limitations of contemporary technology³¹. Cadaver research was initially used to investigate the mechanics of the foot; including the different axis of rotation of each of the major functional joints (subtalar, midtarsal and metatarsophalgenal) and the coupling effect of the hindfoot, midfoot and forefoot³²⁻³⁴. Much of this early research can still be found in biomechanics text books². "The mechanics of the foot I. The joints" published in 1953 is an extensive investigation into the movement of the subtalar joint, Chopart's Joint and the metatarsal joints³². During this time, Inman was also influential using cadaver research to conclude that the subtalar joint primarily functions in the frontal plane³⁴.

Years later, Lundberg and colleagues performed in vivo studies using roentgen stereophotogrammetric analysis (RSA) on eight healthy individuals to investigate foot and ankle kinematics^{22, 25, 35, 36}. The axis of rotation of the ankle joint was shown to change based on the position of the foot and the rotation of the leg²⁵, as demonstrated in earlier cadaver studies³². This is just one of the many result obtained from these studies, which developed the leading biomedical theories about the foot. This was a rare study since research ethics boards do not permit

radiopaque tantalum markers to be injected into healthy subjects in most countries of the world.

For this reason, a more less invasive method was developed that examined the motion of the hindfoot in the frontal plane using high-speed cinematography³¹. Two markers located on the bisection of the lower one third of the tibia and two markers located on the bisection of the calcaneus were digitized for each of the collected frames (Figure 1.24)³¹. The marker sets formed two vectors, the angle found between these two vectors was termed the Achilles Tendon Angle or the Rearfoot Angle. Although this method gave insight into the motion of the rearfoot, it only examined the combined motion of the subtalar joint and the talocrural joint. A more useful clinical model would examine each of these joints separately. Additionally, the majority of this research used 2D video analysis.

The research using this method fueled the excess pronation theory which suggests that an abnormal amount of pronation can lead to injury^{31, 37}. Researchers examined foot-strike position, peak eversion and peak eversion velocity attempting to discover the normal ranges of each measurement³¹. Excessive pronation was established as a risk of injury to all joints along the kinetic chain and an important element in shoe design. Using the Achilles' angle method, researchers explored different shoe parameters throughout the 1980s and early 1990s³⁸⁻⁴⁷. This research influenced the current categorization of running shoes: stability, motion control and neutral cushioning shoe³¹.

Soft tissue artifact (STA) error is of great concern with the Achilles' angle motion since the calcaneus markers are located on the shoe increasing the layers between markers and the actual bones⁴⁵. Studies concluded that this error was too large and holes needed to be cut into the shoe to adequately calculate the motion of the rearfoot^{38, 41}. These techniques improved the soft tissue artifact error by placing the markers directly on the foot, however, the protocol still dictated that the markers on the calcaneus be located directly over the Achilles' tendon. Therefore, the Achilles' tendon movement could directly influence the markers movement.

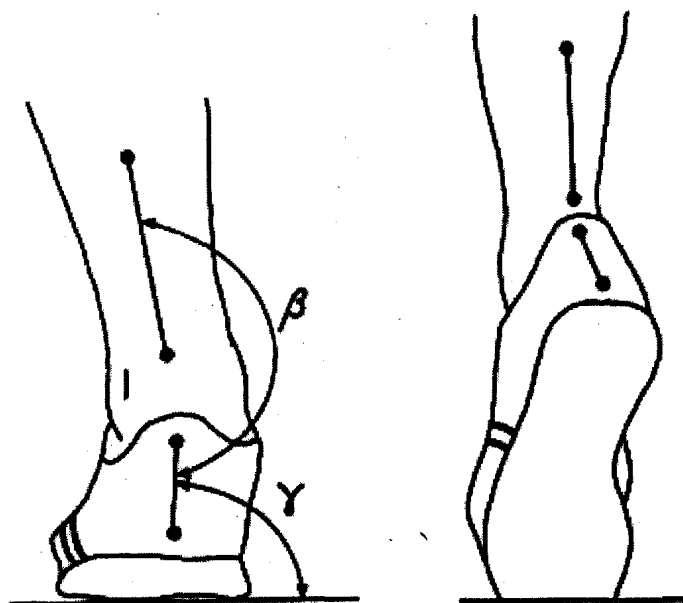


Figure 1.24. Description of Achilles tendon angle (Beta). Two markers are placed on the bisection of the calcaneus and the tibia. The angle between the two vectors, formed by each marker set, is known as Achilles' tendon angle. (Reprinted with permission from Novacheck, TF, 1998)

With technical advances, the use of three-dimensional motion capture systems became the gold standard and examination of the 6 degrees of freedom of the foot joints distal to the subtalar joint became possible. Although much of the

research still focused on rearfoot motion, information on the movement in the sagittal and transverse planes also became available⁴⁸⁻⁵¹. Researchers also measured the navicular height as a measure of the motion of the arch, both statically and dynamically^{52, 53}, as well as the movement of the forefoot^{48, 54}.

Recently, multi-segment foot models have been developed that calculate the movement of foot segments distal to the subtalar joint^{5, 55-59}. These models are discussed in more detail in Section 1.8.2.

Until the turn of the century, much of the data of such research was collected with skin markers attached to subjects for detection by the optical tracking system. In the late 1990s, researchers in Sweden introduced studies using intracortical pins to demonstrate that soft tissue artifact is an error in gait analysis^{12, 60}, especially present in foot kinematic studies. Since the introduction of intracortical pins, these researchers have published multiple studies describing the kinematics of most foot joints during walking and most recently running^{9, 10, 30, 61}. They generally use technical reference frames and not anatomic reference frames, consequently conclusions of the absolute motion in the anatomical planes are difficult. However, this research represented an important advancement in foot kinematics.

1.8.2 Foot Models

A kinematic multi-segment model is a collection of well identified rigid bodies, known as segments, which articulate at clearly defined anatomical joints or functional joints. The models discussed in this section were developed to

examine the kinematics of the foot and not its kinetics. Of the few models that were developed to explore both kinematics and kinetics of the foot, only the kinematic aspect of these models will be discussed. The emphasis of this section is the investigation of the clinical usefulness of the models.

Early modeling was performed on cadavers in the early 1950s until the late 1970s³². Inman used cadavers to investigate the motion of the forefoot with respect to the hindfoot³. His early discoveries maintain important parts of today's theories on foot mobility.

Currently, the most frequently used model was developed by Kadaba et al.¹⁶ and is commonly known as the Helen Hayes model. Twenty-one markers form the marker set, however only two markers are located on each foot: one on the heel and a second between the 2nd and 3rd metatarsal head, which functions as the distal foot marker¹⁶. A vector between the ankle center and the distal foot marker is used to calculate the orientation of the foot, which is the only foot measurement calculated with this model. Consequently, the foot is modeled as a rigid segment providing no information on the hindfoot, midfoot or forefoot. This remains the clinical standard despite the inability of the model to capture useful foot kinematics⁵.

Since the development of the Helen Hayes model, many researchers have attempted to develop clinically useful models to examine foot kinematics^{55-57, 59, 62-72}. Many of the earlier foot models focused on the subtalar joint and joints proximal to the subtalar joint, as was also observe in gait

research^{63, 69, 70, 72}. Although during this time, Scott et al.⁶⁷ developed an eight segmented foot model with a rigid mid-foot (navicular, cuboid, three cuneiforms, and 2nd metatarsal). The other segments comprised single bones: the talus, the calcaneus, the first metatarsal, the third metatarsal, the fourth metatarsal, the fifth metatarsal and the tibia. The data collection and the post analysis become very cumbersome as the number of segments increase, thus limiting the usefulness of the model in a clinical gait laboratory. A threshold exists for the number of useful segments employed in a clinical foot model and is dependent somewhat on the technology available in the laboratory in which the model is being used. For the studies in this dissertation which will be conducted at the Wolf Orthopaedic Biomechanics Laboratory and the Nike Sport Research Laboratory, four to five segments is considered an acceptable number.

A model developed in 1996 by Kidder et al.⁵⁵ consisted of joints distal to the subtalar joint and included the following four segments: 1) the tibia (tibia and fibula), 2) the hindfoot (calcaneus, talus and navicular), 3) the forefoot (cuboid, cuneiforms and metatarsals), and 4) the hallux (proximal phalange)⁵⁵. Clinical usefulness was attempted by using the Euler method for describing relative foot and ankle orientation. However, the use of radiographs to index the reflective markers and the underlying bones make this model less than desirable as a standard clinical model. Another setback of this model is that with only one subject tested it is difficult to generalize the findings, making it difficult to use this model clinically without conducting initial validation studies.

The model of Leardini et al.⁵⁹ uses the Calibrated Anatomical System Technique (CAST) to determine the anatomical landmarks which are used to calculate the desired foot kinematics. The method was presented in Cappozzo et al.⁷³ who attempted to standardize anatomical frame definitions and determinates of the lower limb bones. The CAST system uses a "pointer" with two markers attached which are a known distance to the end point. A static trial for each of the bony landmarks is obtained while the researcher points to the bony landmark with the pointer while the surface markers are affixed to the foot. These static trials are used to calculate the position of the bony landmark with respect to the segmental (marker) co-ordinate system so that these "virtual bony landmarks" can be recreated during the dynamic trials without having to have a physical marker at their locations. Anatomic reference frames can then be calculated from the bony landmarks during the dynamic trials. Leardini et al.⁵⁹ use this method to locate the bony landmarks with respect to the foot markers to calculate anatomic reference frames. Joint rotations using anatomical reference frames of the following five segments were calculated: 1) the tibia/fibula, 2) the calcaneus, 3) the mid-foot, 4) the first metatarsal, and 5) the hallux⁵⁹. Measurements in all three anatomical frames were taken with respect to the proximal segment of the segment of interest⁵⁹. By using anatomic reference frames, the researchers have developed a model that uses anatomical terminology to communicate the findings, bridging the gap between researchers and clinicians. This model can be used in clinical setting since it uses a non-invasive approach with only five segments and uses clinically relevant terminology by incorporating the CAST

method to identify anatomical landmarks. A potential limiting factor of this model is its use of metallic clamps to affix the markers to the foot in order to decrease soft tissue artefact⁵⁹. It remains unknown whether these clamps affect the gait pattern of the subjects. Another important limiting factor is the fact that the lateral forefoot was ignored.

As model development continued into the late 1990s and early 2000s, some models continued to increase the number of segments used to eight or nine^{62, 66, 71} and others focused again primarily on the rearfoot⁶⁵. Although these models may be beneficial in a research lab and produce valuable information on the kinematics of the foot, their use in a clinical gait laboratory is limited.

In 1998, Carson et al.⁶⁴ introduced a four segment foot model, now known as the Oxford Foot Model. The tibia, the hindfoot (calcaneus and talus), the forefoot (five metatarsals) and the hallux segments formed the model. The midfoot was considered a mechanism for transmitting motion between the forefoot and the hindfoot⁶⁴. There are no inter-segmental constraints in this model and therefore all six degrees of freedom between a pair of segments can be calculated. Similar to the Leardini model, all measurements are calculated using anatomic planes⁵⁹. This group later tested the model for reliability, including inter-subject, inter-tester and inter-session during walking⁵⁸. Results from a small sample size (n=2) showed that most segmental reliability was good. This model has recently been implemented in the VICON motion capture system (VICON, Oxford, UK). This is a very respected model, however, the combination of the lateral and medial forefoot as one rigid section does not allow for any motion of the transverse arch

to be collected. This can be important for pathological assessments since it is important to understand how the first ray and fifth ray move independent from each other.

Another model with a practical number of segments was presented in a publication by Hunt et al.⁵⁶ and studied healthy males walking and focused on the hindfoot, the forefoot and the medial longitudinal arch. Describing forefoot twisting with respect to the rearfoot was an objective of this model, while another was to explore the movement of the medial longitudinal arch under dynamic conditions. The MLarch in the Jenkyn model (explained in the next section) uses the same anatomical landmarks; however the MLarch is normalized to a subject's mean whereas the Jenkyn model uses a height/length ratio. From this study, Hunt et al.⁵⁶ concluded that the midfoot is an important segment for normal foot function during the stance phase of walking, and suggested that more researcher focus on this area since it is often overlooked. This conclusion was drawn from the large amount of forefoot motion found in all three planes of motion with respect to the hindfoot, as well as the large contribution of the forefoot to the overall foot motion⁵⁶. They also discuss the importance of inter-bone motion. The disadvantage of this model is that they referenced the forefoot motion with respect to the hindfoot motion; it is a combination of the motion of all the bones between the hindfoot and the metatarsals.

The main objective of a recent paper by Simon et al.⁶⁸ was to create a model that could measure joint motion in a patient with normal feet and maintain the same protocol for subjects with pathological feet. They accomplished this by using

functional angles of the midfoot and forefoot to examine the motion of the functional segments⁶⁸. The model used relative motion via projection angles to examine the motion of the foot using a more descriptive method thought to be more appropriate for clinical use.

1.8.3 Multi-Segment Foot Model

The focus of this dissertation is to develop a method to test shoe conditions in a clinical setting, therefore it is imperative that the model employed be clinically useful. This means that it should calculate joint angles with respect to anatomical reference frames and have minimal segments to simplify the post-processing and interpretation.

The multi-segment foot model used in this dissertation separates the foot into five segments: the hallux, the lateral forefoot (fifth metatarsal), the medial forefoot (first metatarsal), the midfoot (navicular, cuboid, three cuneiforms) and the hindfoot (calcaneus) (Figure 1.25)^{4, 5}. This is a simplified version of the Jenkyn model since the subtalar joint and talocrual joint are not included, thereby simplifying the analysis while still supplementing the field with knowledge that is currently unavailable. As mentioned above, biomechanics of the foot joints proximal to and including the subtalar joint have been extensively studied. The Jenkyn model has been shown to correlate well with other models, including the models discussed in the previous section, and to produce the expected foot joint movement patterns during gait^{4, 5}. A recent study explored the possible functional units and acceptable rigid segments of the foot for gait analysis¹⁰. The

authors established the following four segments from calculating the movement of intracortical pins placed in seven foot bones: calcaneus, navicular-cuboid, medial cuneiform-first metatarsal, fifth metatarsal. Although there appears to be a difference in the segment location for the cuneiforms, the midfoot marker for the model developed by Jenkyn et al. is located on the navicular. The cuneiform is a floating bone between the midfoot and the first metatarsal bone.

This simplified Jenkyn model⁵ uses markers placed on five segments in locations that decrease the amount of soft tissue found between the marker and the bone (see Table 1.1 for description). For example, the calcaneal marker triad is placed laterally to avoid the Achilles' tendon but posteriorly to avoid the peroneals' tendons. The markers consist of triad clusters of retro-reflective markers which are used to calculate the following six degrees of freedom: translation and rotation in the frontal plane, in the sagittal plane and in the transverse plane.

Table 1.1: Placement site descriptions for the eight marker clusters on the right leg and foot. Each segment has a single cluster except the lower leg and the midfoot segments which had two clusters (reprinted with permission from Jenkyn et al., 2007)

Segment	Cluster Placement
Hindfoot	Postero-lateral calcaneus, lateral to Achilles tendon
Midfoot	Dorso-medial foot over the navicular tuberosity
Medial Forefoot	Medial-dorsal foot over midshaft of first metatarsal
Lateral Forefoot	Lateral-dorsal foot over midshaft of fifth metatarsal
Hallux	Dorsal over the proximal phalangeal of the hallux

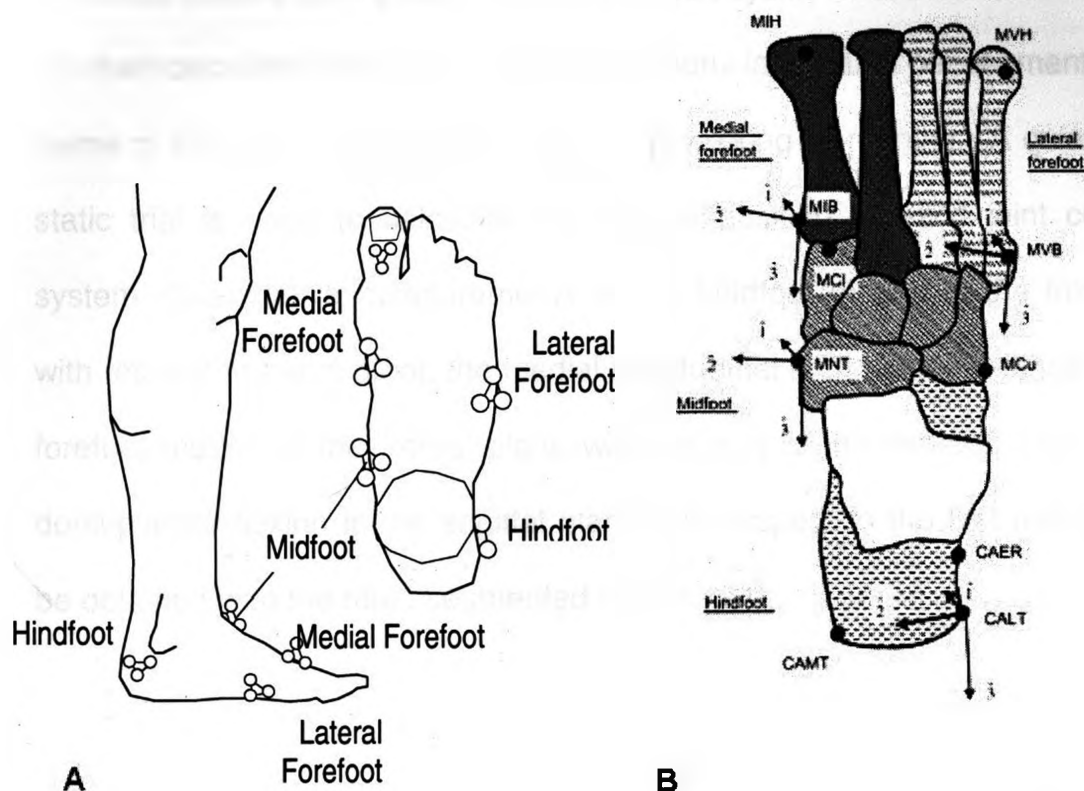


Figure 1.25: A. Triad cluster location for the five cluster markers of the Jenkyn model: hindfoot, midfoot, medial forefoot, lateral forefoot and hallux. B. Triad marker location of underlying bones: calcaneus, navicular, first metatarsal and fifth metatarsal. The four letter abbreviation, which describes the bony landmarks for the digitization process, can be found in Table 2. (Reprinted with permission from Jenkyn et al. 2007)

The CAST system was employed where at least three bony landmarks per segment were digitized using a stylus with three markers attached collinearly but at varying distance to the end-point and to each other. The clusters were affixed to the foot prior to the commencement of the digitization. These digitization trials, with the subject standing with their feet at hip width and in quiet standing, are used to obtain the reference points of sixteen different bony landmarks with respect to the clusters⁵ (see Table 1.2 for a full description and Figure 1.26 for a visual). Segmental reference frames were then calculated and the virtual anatomic landmarks could be re-calculated with respect to the segmental

reference frames during each frame of the gait cycle. Anatomic reference frames are then calculated from each of the three bony landmarks per segment for every frame of the gait cycle while the subject is walking or running. A quiet-standing static trial is used to calculate the neutral position of each joint co-ordinate system. Quantitative measurements of the hindfoot motion in the frontal plane with respect to the midfoot, the medial longitudinal arch height-to-length ratio, the forefoot motion in the frontal plane with respect to the midfoot, and the hallux dorsi-plantar flexion in the sagittal plane with respect to the first metatarsal can be obtained with the multi-segmented foot model⁵.

Table 1.2: The following is a full description of the bony landmark locations used to calculate the anatomical reference frames used in this dissertation. It is adapted from the Jenkyn et al. model. this includes the ankle complex and subtalar joint. (Reprinted with permission from Jenkyn et al., 2007)

Segment	Tracked landmarks
Hindfoot	CAER: eminentia retrotrochlearis (greatest lateral elevation)
	CALT: lateral tuberosity (lateral to Achilles tendon attachment)
	CAMT: medial tuberosity (medial to Achilles tendon attachment)
Midfoot	MCI: first cuneiform (distal dorsal crest)
	MNT: navicular tuberosity (most medial point)
	MCU: cuboid (lateral dorsal edge at joint with calcaneus)
Medial forefoot	MIH: first metatarsal head (most dorsal point)
	MIB: first metatarsal base (most dorsal point)
Lateral forefoot	MVH: fifth metatarsal head (most dorsal point)
	MVB: fifth metatarsal base (most dorsal point)
Ankle JCS	LMM: medial malleolus (most medial point) defined on the lower leg segment
	LLM: lateral malleolus (most lateral point) defined on the lower leg segment
Hallux	DH: most distal point of the hallux (and the foot)
	LPH: lateral head of the interphalangeal
	MPH: medial head of the interphalangeal

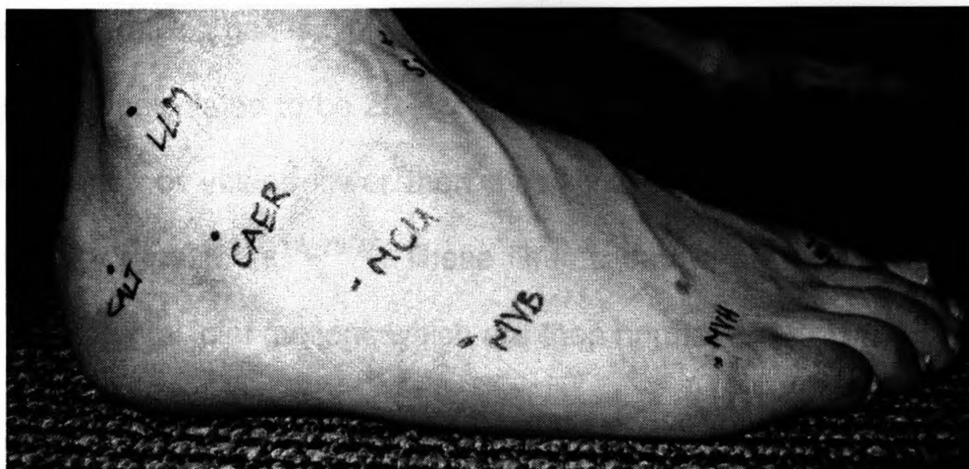


Figure 1.26: Location of the digitized landmarks for the Jenkyn model is marked on the subject's foot.

Before the inter-segmental joint motions are calculated all marker trajectory are filtered using causal-anti causal 0-lag 4th order Butterworth filter. This filter climate a phase shift in the data due to the filtering processes. The filter is run first in positive time at half of the cutoff frequency and getting a finite lag in the causal or positive time direction. Next the data are run through the filter backwards or in negative time (anti-casual direction) which obtains a lag in the negative time direction which cancels out the positive lag. The cutoff frequency has been shown, by experience, to correlate with stride frequency by six times.⁷⁴

For example, walking gait is typically 1 Hz so the cutoff frequency is 6Hz⁷⁴. For running this is calculated to be 20 Hz. These values for the walking and running cutoff frequency or values lower than these values stated here are commonly used by other researcher^{12, 75-77}. These filtered data are then used to calculate the inter-segmental joint motions which are then normalized to 100% stance time.

The three-dimensional motion of the hindfoot with respect to the midfoot is calculated with traditional Euler angles. The sequence is y-z-x: plantarflexion/dorsiflexion (sagittal plane), abduction/adduction (transverse plane), supination/pronation (frontal plane). An anatomical coordinate system is calculated from the quiet-standing trial and used as the neutral position for all subsequent calculations. The rotation of the coordinate system in the frontal plane (x-axis) is obtained for every dynamic frame throughout the stance phase. This produces the clinically relevant motion of pronation/supination of the hindfoot with respect to the midfoot (See Figure 1.27A and Figure 1.28A).

The motion of the forefoot is a combination of both the lateral and medial forefoot segments motion with respect to the midfoot. This allows for the pronation/supination movement to be calculated which is important when analyzing the foot's ability to lock and unlock to form an adaptable or rigid foot⁵. A vector created from the head of the fifth metatarsal to the head of the first metatarsal is projected onto the frontal plane of the midfoot segment axis. The angle is calculated from the mediolateral axis of the midfoot to the projected vector (See Figure 1.27B and Figure 1.28B). The calculated angle is known as the forefoot twist.

The movement of the medial longitudinal arch is reported by the arch height-to-length ratio. The arch length is found by determining the magnitude of the vector between the medial posterior aspect of the calcaneus (CAMT) and the first metatarsal head (MIH) (See Figure 1.27D and Figure 1.28C). The height vector is calculated by projecting a perpendicular line from the length vector superiorly to the navicular tuberosity (MNT). A decreasing height-to-length ratio implies that the arch is collapsing as found in forefoot pronation. Alternatively, an increasing height-to-length ratio implies a supinate position with a raising arch.

Analysis of the hallux segment was added to the Jenkyn model to complete the segments of the foot⁷⁸ (see Figure 1.27C and Figure 1.28D). The hallux angle is calculated as the dorsi-plantarflexion movement of the hallux relative to the first metatarsal. The hallux vector is calculated from the anatomical landmarks of the distal hallux and the proximal hallux, while the first metatarsal is represented by a vector from the first metatarsal head to the first metatarsal base. The angle between these two vectors in the sagittal plane is known as the hallux angle.

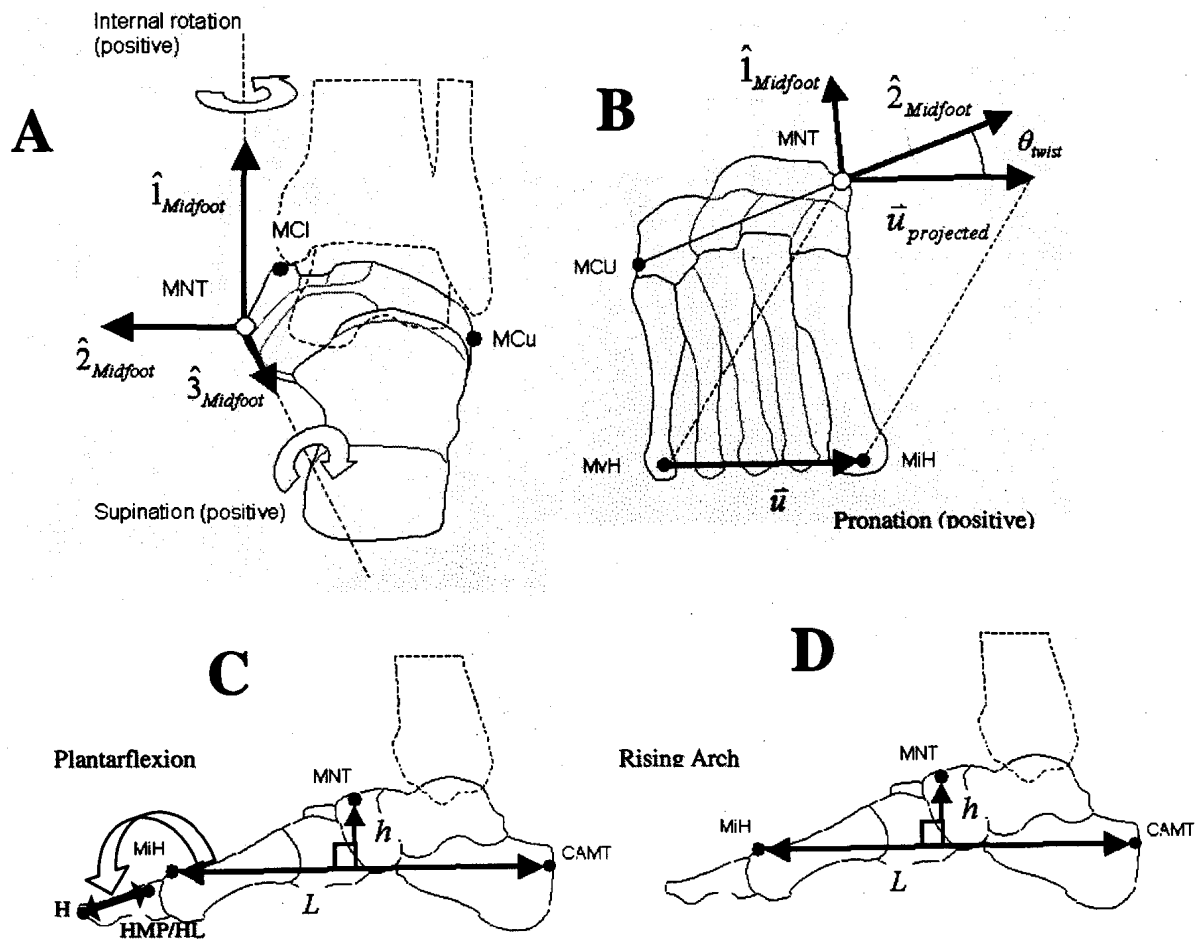


Figure 1.27. Measurements from the Jenkyn model. A. Hindfoot motion. Rotation about the 3-midfoot axis (anterior/posterior) gives supination and pronation. B. Forefoot twist angle. MvH-MiH vector is projected on the plane encompassing the 1- and 2- midfoot axis (adduction/abduction, plantarflexion/dorsiflexion, respectively). C. Hallux motion. Sagittal plane motion is the angle of the hallux (H) with respect to the first metatarsal. D. Medial Longitudinal Arch motion. Height-to-length ratio is calculated by the same L-vector used in the hallux motion and the height vector which projects perpendicular to the L-vector to the navicular tuberosity. (Reprinted with permission from Jenkyn et al, 2007)

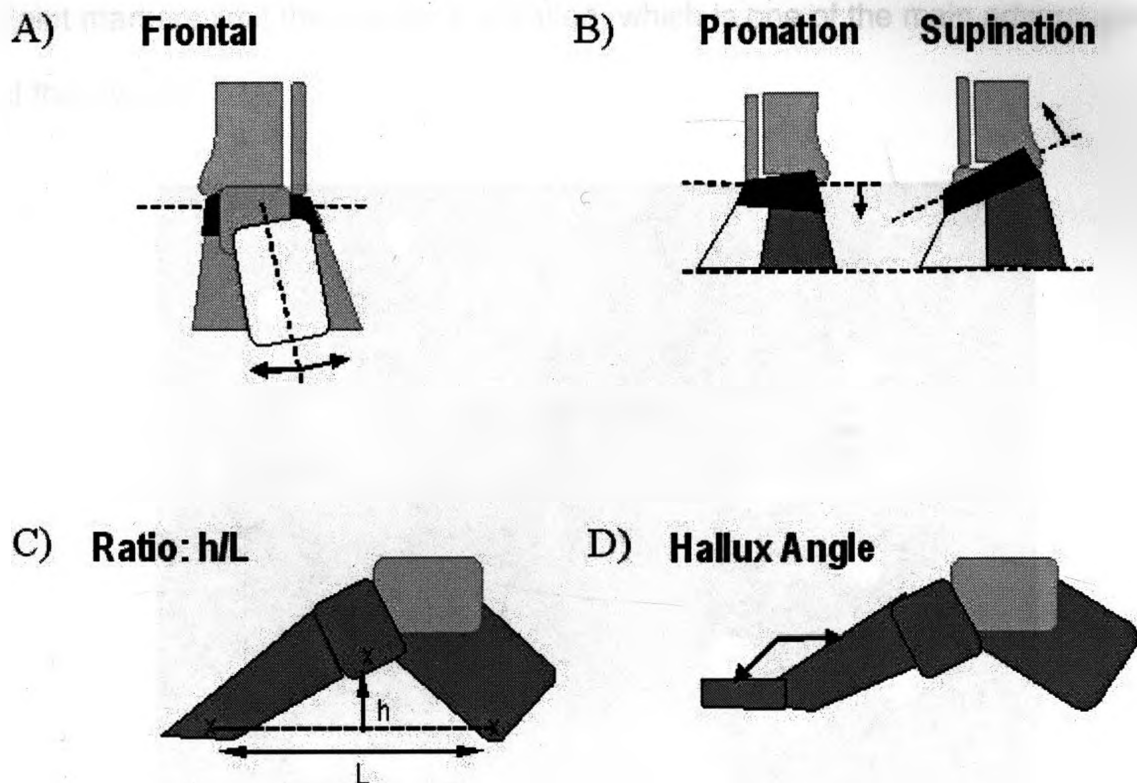


Figure 1.28. This is the complete diagram of the motions calculated throughout this dissertation. **A. Frontal plane motion of the hindfoot. B. Forefoot twist. C. Medial longitudinal arch height-to-length ratio. D. Hallux angle in the sagittal plane.** (Reprinted with permission from Jenkyn et al., 2007)

The cluster marker system for this model is made up of triad clusters attached to bases via carbon-fiber wands (see Figure 1.29). Each marker is an 8 mm delrin or wood ball covered with reflective tape, (3M, Minneapolis, MN). Only one triad cluster is needed to represent each rigid segment by describing all six degrees of freedom for the segment. One of the main benefits of this system is that only one palpable area is needed. The point marker system, which is the second of the marker systems, uses three individual markers to represent each rigid segment. A triad cluster is still needed on the hallux since this segment is too small to place the necessary three point markers needed to describe its six degrees of freedom.

Point markers limit the marker's vibration, which is one of the main advantages of this system.

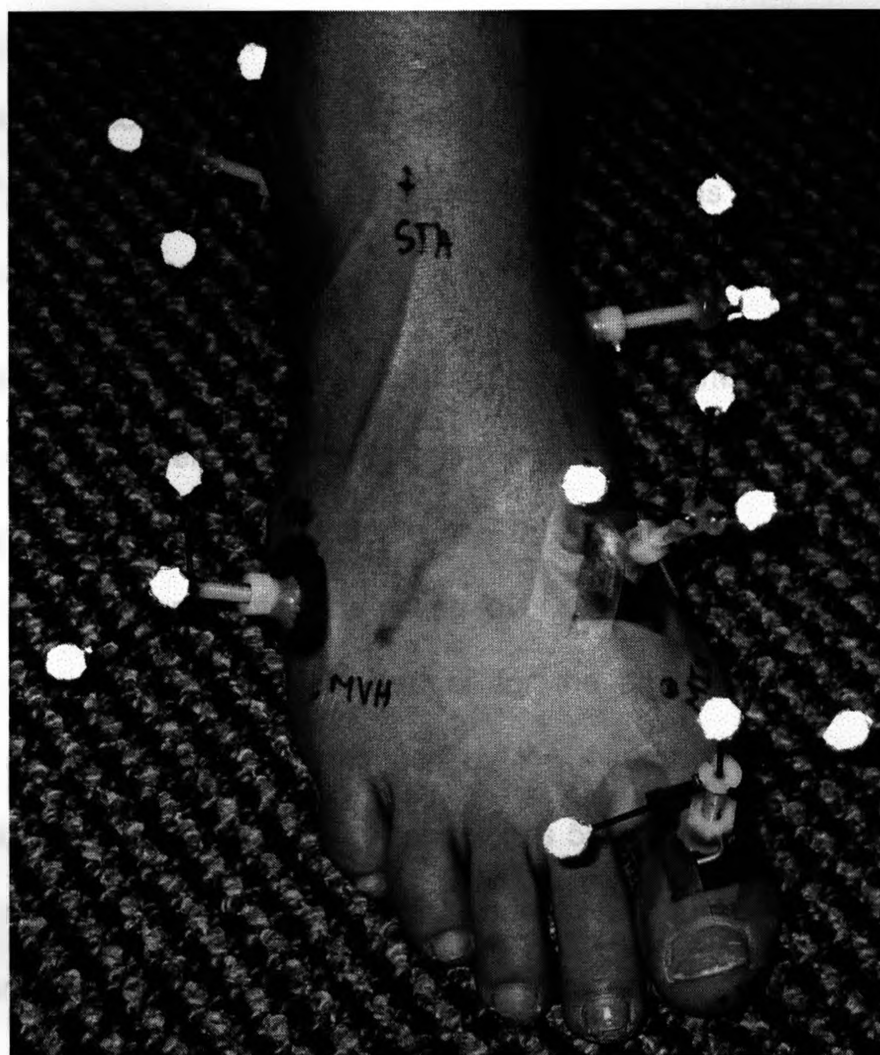


Figure 1.29. Cluster marker set placed on the foot using faux leather bases, nylon screws and carbon fiber rods. The retro-reflective markers' reflection is visible in the photo.

For the purposes of this dissertation, triad clusters will be used for all five studies. The majority of the studies conducted involve a shod condition thereby limiting the use of point markers. Cluster markers require less material to be removed from the test shoe's, which better maintains the shoes functional integrity.

1.9 Clinical Relevance

Men and women of all ages and skill levels enjoy the sport of running. It is currently considered one of the most popular fitness activities. The popularity of marathons has considerably increased in western societies in the last two decades⁷⁹. In 2004, an estimated 30 million Americans participated in long-distance running⁸⁰.

This large population of runners continuously stress their bodies as ground reaction forces between two to ten times their body weight are being generated with every foot strike. For example, a 70-Kg marathon runner sustains an average of 2800 tonnes of force acting over the three lower extremity joints during his/her marathon⁸⁰. The danger for the athlete is not simply in the immense amount of force experienced by the joints but also in its repetition. Lutter⁸¹ calculated that the average runner has 5000 foot strikes per hour. This repetitive motion means that runners are more likely to suffer overuse injuries rather than traumatic injuries. Lutter⁸¹ continues to explain that this repetitive motion can cause an insignificant biomechanical abnormality to become significant to the point of causing an athlete to have to cease running. He also notes that the biomechanical abnormality, not just the symptoms, must be diagnosed and treated in order to prevent the return of the symptoms⁸¹.

Running injuries can be caused by a single factor, such as a biomechanical abnormality, however they are most commonly caused by a combination of factors. The anatomy of the runner might make him or her more susceptible to

certain injuries. Some runners are simply more biomechanically efficient than others; however, the injuries are normally multi-factorial. Another contributor to running injuries includes the increasing of the mileage or the training duration too quickly^{81, 82}. The body, in particular the foot, is very effective at adapting to changes, however a common running approach is that of "too much too soon". The runner will increase the mileage, intensity or duration too quickly and the body will not be able to keep up with this increased demand. Running injuries are caused 60% of the time by training errors⁸³, such as those listed above. MacKenzie, Clement et al.⁸⁴ also identify training surfaces, a lack of flexibility and strength, the stage of growth and development of the runner, abnormal biomechanical features, as well as footwear, as possible contributors to injury.

Many of the studies conducted for this dissertation have involved barefoot or shod walking, running, or cutting. Today, it is common for clinicians to prescribe a specific type of running shoe after assessing one's foot and gait pattern. The patient will often perform a series of tests including a walking test, a squat test, maybe even a running test⁸⁵. The clinician may examine the old shoes of the individual and ask about any acute or chronic injuries⁸⁶. The clinician will then place the patient in a foot type category and prescribe a specific shoe type based on the patient's foot type⁸⁵

The three major foot types include pronators, neutral, and supinators. Three different types of running shoes attempt to maneuver the foot into a more supinated position and aid in shock absorption, in an attempt to decrease injuries. Motion control shoes have medial posts and dual density support to

prevent the foot from excessive pronation. Stability shoes have less medial support but still provide support against pronation while offering some additional cushioning. Over-supinators are prescribed neutral cushioning shoes since they need less motion control design characteristics and more cushioning which are the characteristics of neutral cushioning shoes.

Designing shoes to fit these categories is the common thought process behind running shoe design; however minimal comparison research studies have been conducted. A recent review article concluded that no such research has been conducted to provide evidence to the prescription of running shoes⁸⁷. However, some studies have compared kinetic variable differences between motion control shoes and stability shoes or neutral shoes^{86, 88, 89}. One study examined plantar pressure at the beginning and end of a 1.5 km race and found that there was no change in those wearing motion control shoes, however those wearing neutral cushioning shoes experienced an increase in plantar pressure by the end of the race⁸⁸. Another study showed that two different neutral cushioning shoes were able to decrease plantar pressure in cavus feet, as compared to motion control shoes⁸⁹. Much more research is necessary to assess how the foot adapts and is manipulated by the different shoe types. Additionally, these results should be discussed with reference to injury incidences and not simply biomechanical changes.

The studies conducted in this dissertation attempt to develop a method for testing the alteration of the joint angles of the foot in different shoes. This will hopefully lead to research that will assist in decreasing overuse running injuries caused by

both athletic shoes and everyday shoes, as well as providing evidence to the prescription of stability, neutral and motion control shoes. Insight into the movement of the foot bones may also help reduce injury or improve the treatment of other joints of the body. During stance phase, the lower extremity is in a closed kinetic chain activity, therefore looking at how the foot moves and how it influences other joints in the body could reduce the overuse incidence rates of athletic injury. The method developed here can be used with the standard Helen Hayes model to evaluate the kinematics of the entire body. Future research should also include a kinetic foot model.

1.10 Thesis Objective and Chapter Overview

The primary objective of this dissertation is to develop a method to analyze the relative motion of the bones of the foot within an athletic shoe, or while barefoot, during a variety of activities. The secondary objective is to apply this method in clinical studies to investigate the effect on foot kinematics due to modifications in the midsole properties of an athletic trainer shoe or during different movements. In all five studies, the multi-segment foot model developed by Jenkyn and Nicol⁴ (2007) is used to conduct a kinematic analysis of the hindfoot, which is calculated independent of the subtalar joint, as well a kinematic analysis for the medial forefoot, the lateral forefoot, the medial longitudinal arch and the hallux. An optical motion capture system is employed in all of the studies to measure the triangulated positions of the surface markers affixed to the foot. One of the

studies also uses fluoroscopy to assess the soft tissue artifact error of the optical motion system and skin-mounted marker clusters.

The sport of interest for this dissertation is running; however, the multi-segment foot model and method developed will be applicable to a variety of sports shoes. Running is the focus since, as noted above in section 1.9 the incidence of running injuries is high in the population of recreational and competitive runners. It is speculated that this population will benefit from this research since running shoes have been identified as a possible contributor to injuries while also being prescribed as a treatment.

1.10.1 Outline

The first section of chapter one was a review of the anatomy and functional biomechanics of the foot during the gait cycle. Also discussed were the different methods used in calculating foot kinematics. A brief overview of the gait research methods used in the past were given with a focus on foot kinematics and multi-segment foot models, including the foot model used in the studies of this dissertation. The common methods used in the five study chapters, for example the joint angle calculations, CAST method, filtering technique, etc were also introduced. Finally, the objective of the dissertation was presented followed by this outline of the chapters.

The first research study, chapter 2, introduces a method for validating the size of holes that can be cut into a shoe without compromising its structural integrity. These holes are required when using a multi-segment foot model with optical

motion capture. Holes must be cut into the shoe to create holes to affix the marker set directly to the foot while a subject is wearing a shoe. The size of the holes must be also be validated to ensure that the holes are large enough to be visible by the cameras of the optical tracking system.

A second study, chapter 3, investigates how the use of a single static trial, compared to pre-condition static trials, may change the interpretation of a dynamic gait study. The advantages and disadvantages of each method are discussed in this chapter, including the clinical relevance of the two methods. Static trials are collected for four different shoe conditions to analyze if the neutral positions for the joint co-ordinate systems are affected by a perturbation. A perturbation, such as footwear or orthotics, has an implication for the joint angle calculations during the dynamic trials, since the static trial is used to calculate the neutral position for these trials.

The third study, chapter 4, examines the soft tissue artifact error of two rigid segments, hindfoot and midfoot, of the multi-segment foot model developed by Jenkyn et al (2007)⁵. Landmarks on the bones and markers, which are visible on the fluoroscopy image, are used to calculate co-ordinate systems for the marker cluster and the underlying bone for each segment during quasi-static simulated gait positions. The translational and rotational components are calculated based on the movement of the triad clusters co-ordinate system relative to the particular bone segment co-ordinate system.

The first of two clinical studies is explained in chapter 5. This study examines the effect of Longitudinal Torsional Stiffness (LTS) and Forefoot Flexion (FFlex) on the same joint angles calculated in the neutral position study described in chapter 4. Joint angles during barefoot running are compared to joint angles during running in three distinct shoe conditions: a Nike Free Trainer 7.0, this same Nike Free shoe with a forefoot carbon plate, and again the same Nike Free trainer with a full length carbon plates. LTS and FFlex appear not to dramatically change the kinematic pattern of the foot; however trends were observed. For example, it appears that the foot moves similarly in the control shoe, Nike Free Trainer shoe, when compared to barefoot.

This last study, chapter 6, is a pilot study that retains the same procedure as that outlined in chapter 5. However, the motion of the foot during medial cutting movements is compared to that while running. This study provides insight into how the foot reacts to a directional change as opposed to running in a straight line, which is studied in chapter 5.

A brief discussion is included in chapter 7, which is the final chapter of this dissertation. Foot research is in its infancy; however the researchers that originally developed certain theories regarding how the foot behaves and how it is injured are beginning to question several widely held theories. This discussion examines how the theories, specifically those related to excessive pronation, came to be and why researchers are starting to question them. A few new hypotheses on the factors that produce a running injury are also discussed.

1.11 References

1. Riegger, C. L. Anatomy of the ankle and foot. *Phys Ther* 68, 1802-14 (1988).
2. Nordin, M. & Frankel, V. *Basic Biomechanics of the Musculoskeletal System* (ed. Leger, D.) (Lippincott Williams & Wilkins, Baltimore, Maryland, 2001).
3. Sarrafian, S. K. *Anatomy of the Foot and Ankle: Descriptive, Topographic, Functional* (2nd edition) (J.B. Lippincott Company, Philadelphia 1993).
4. Jenkyn, T. R., Anas, K. & Nichol, A. Foot segment kinematics during normal walking using a multisegment model of the foot and ankle complex. *J Biomech Eng* 131, 034504 (2009).
5. Jenkyn, T. R. & Nicol, A. C. A multi-segment kinematic model of the foot with a novel definition of forefoot motion for use in clinical gait analysis during walking. *J Biomech* 40, 3271-8 (2007).
6. Perry, J. *Gait analysis: normal and pathological function* (Slack, Inc, Thorofare, NJ, USA, 1992).
7. Dugan, S. A. & Bhat, K. P. Biomechanics and analysis of running gait. *Phys Med Rehabil Clin N Am* 16, 603-21 (2005).
8. McClay, I. & Manal, K. The influence of foot abduction on differences between two-dimensional and three-dimensional rearfoot motion. *Foot Ankle Int* 19, 26-31 (1998).
9. Arndt, A., Westblad, P., Winson, I., Hashimoto, T. & Lundberg, A. Ankle and subtalar kinematics measured with intracortical pins during the stance phase of walking. *Foot Ankle Int* 25, 357-64 (2004).
10. Wolf, P. et al. Functional units of the human foot. *Gait Posture* (2008).
11. Reinschmidt, C. et al. Tibiofemoral and tibiocalcaneal motion during walking: external vs. skeletal markers. *Gait and Posture* 6, 98-109 (October 1997).
12. Reinschmidt, C., van Den Bogert, A. J., Murphy, N., Lundberg, A. & Nigg, B. M. Tibiocalcaneal motion during running, measured with external and bone markers. *Clin Biomech* (Bristol, Avon) 12, 8-16 (1997).
13. Schwartz, M. H., Trost, J. P. & Wervey, R. A. Measurement and management of errors in quantitative gait data. *Gait Posture* 20, 196-203 (2004).
14. Stagni, R., Fantozzi, S., Cappello, A. & Leardini, A. Quantification of soft tissue artefact in motion analysis by combining 3D fluoroscopy and stereophotogrammetry: a study on two subjects. *Clin Biomech* (Bristol, Avon) 20, 320-9 (2005).

15. Alexander, E. J. & Andriacchi, T. P. Correcting for deformation in skin-based marker systems. *J Biomech* 34, 355-61 (2001).
16. Kadaba, M. P. et al. Repeatability of kinematic, kinetic, and electromyographic data in normal adult gait. *J Orthop Res* 7, 849-60 (1989).
17. Bushberg, F., Seibert, F. & Leidholdt, G. B., G. Fluoroscopy (Lippincott Williams & Wilkins, 2002).
18. Perlman, P. R., Dubois, P. & Siskind, V. Validating the process of taking lateral foot x-rays. *J Am Podiatr Med Assoc* 86, 317-21 (1996).
19. Fantozzi, S. et al. Fluoroscopic and gait analysis of the functional performance in stair ascent of two total knee replacement designs. *Gait Posture* 17, 225-34 (2003).
20. Wearing, S. C. et al. Sagittal movement of the medial longitudinal arch is unchanged in plantar fasciitis. *Med Sci Sports Exerc* 36, 1761-7 (2004).
21. de Bruin, P. W. et al. Image-based RSA: Roentgen stereophotogrammetric analysis based on 2D-3D image registration. *J Biomech* 41, 155-64 (2008).
22. Lundberg, A., Goldie, I., Kalin, B. & Selvik, G. Kinematics of the ankle/foot complex: plantarflexion and dorsiflexion. *Foot Ankle* 9, 194-200 (1989).
23. Selvik, G. Roentgen stereophotogrammetric analysis. *Acta Radiol* 31, 113-26 (1990).
24. Selvik, G., Alberius, P. & Fahlman, M. Roentgen stereophotogrammetry for analysis of cranial growth. *Am J Orthod* 89, 315-25 (1986).
25. Lundberg, A. Kinematics of the ankle and foot. In vivo roentgen stereophotogrammetry. *Acta Orthop Scand Suppl* 233, 1-24 (1989).
26. Valstar, E. R., de Jong, F. W., Vrooman, H. A., Rozing, P. M. & Reiber, J. H. Model-based Roentgen stereophotogrammetry of orthopaedic implants. *J Biomech* 34, 715-22 (2001).
27. Valstar, E. R. et al. Guidelines for standardization of radiostereometry (RSA) of implants. *Acta Orthop* 76, 563-72 (2005).
28. Valstar, E. R., Vrooman, H. A., Toksvig-Larsen, S., Ryd, L. & Nelissen, R. G. Digital automated RSA compared to manually operated RSA. *J Biomech* 33, 1593-9 (2000).
29. Kaptein, B. L., Valstar, E. R., Stoel, B. C., Rozing, P. M. & Reiber, J. H. A new type of model-based Roentgen stereophotogrammetric analysis for solving the occluded marker problem. *J Biomech* 38, 2330-4 (2005).
30. Arndt, A. et al. Intrinsic foot kinematics measured in vivo during the stance phase of slow running. *J Biomech* 40, 2672-8 (2007).
31. McClay, I. The evolution of the study of the mechanics of running. Relationship to injury. *J Am Podiatr Med Assoc* 90, 133-48 (2000).

32. Hicks, J. H. The mechanics of the foot. I. The joints. *J Anat* 87, 345-57 (1953).
33. Manter, J. Movements of the subtalar and transverse tarsal joints. *The Anatomical record* 80, 397 (1941).
34. Inman, V. T., Ralston, H. J. & Todd, F. *Human Walking* (Williams and Wilkins, Baltimore, 1981).
35. Lundberg, A., Svensson, O. K., Bylund, C., Goldie, I. & Selvik, G. Kinematics of the ankle/foot complex--Part 2: Pronation and supination. *Foot Ankle* 9, 248-53 (1989).
36. Lundberg, A., Svensson, O. K., Bylund, C. & Selvik, G. Kinematics of the ankle/foot complex--Part 3: Influence of leg rotation. *Foot Ankle* 9, 304-9 (1989).
37. Nigg, B. M. The role of impact forces and foot pronation: a new paradigm. *Clin J Sport Med* 11, 2-9 (2001).
38. Stacoff, A., Reinschmidt, C. & Stussi, E. The movement of the heel within a running shoe. *Med Sci Sports Exerc* 24, 695-701 (1992).
39. Stacoff, A., Steger, J. & Stussi, E. [Control of the rear foot in lateral movements in sports]. *Sportverletz Sportschaden* 7, 22-9 (1993).
40. Stacoff, A., Steger, J., Stussi, E. & Reinschmidt, C. Lateral stability in sideward cutting movements. *Med Sci Sports Exerc* 28, 350-8 (1996).
41. Reinschmidt, C., Stacoff, A. & Stussi, E. Heel movement within a court shoe. *Med Sci Sports Exerc* 24, 1390-5 (1992).
42. Nigg, B. M., De Boer, R. W. & Fisher, V. A kinematic comparison of overground and treadmill running. *Med Sci Sports Exerc* 27, 98-105 (1995).
43. McPoil, T. G. & Cornwall, M. W. Relationship between three static angles of the rearfoot and the pattern of rearfoot motion during walking. *J Orthop Sports Phys Ther* 23, 370-5 (1996).
44. McPoil, T. & Cornwall, M. W. Relationship between neutral subtalar joint position and pattern of rearfoot motion during walking. *Foot Ankle Int* 15, 141-5 (1994).
45. Stacoff, A., Kalin, X. & Stussi, E. The effects of shoes on the torsion and rearfoot motion in running. *Med Sci Sports Exerc* 23, 482-90 (1991).
46. Clarke, T. E., Frederick, E. C. & Hamill, C. L. The effects of shoe design parameters on rearfoot control in running. *Med Sci Sports Exerc* 15, 376-81 (1983).
47. Johanson, M. A., Donatelli, R., Wooden, M. J., Andrew, P. D. & Cummings, G. S. Effects of three different posting methods on controlling abnormal subtalar pronation. *Phys Ther* 74, 149-58; discussion 158-61 (1994).

48. Cornwall, M. W. & McPoil, T. G. Three-dimensional movement of the foot during the stance phase of walking. *J Am Podiatr Med Assoc* 89, 56-66 (1999).
49. Areblad, M., Nigg, B. M., Ekstrand, J., Olsson, K. O. & Ekstrom, H. Three-dimensional measurement of rearfoot motion during running. *J Biomech* 23, 933-40 (1990).
50. McClay, I. & Manal, K. A comparison of three-dimensional lower extremity kinematics during running between excessive pronators and normals. *Clin Biomech (Bristol, Avon)* 13, 195-203 (1998).
51. McClay, I. & Manal, K. Three-dimensional kinetic analysis of running: significance of secondary planes of motion. *Med Sci Sports Exerc* 31, 1629-37 (1999).
52. Nigg, B. M., Cole, G. K. & Nachbauer, W. Effects of arch height of the foot on angular motion of the lower extremities in running. *J Biomech* 26, 909-16 (1993).
53. McPoil, T. G. & Cornwall, M. W. The relationship between static lower extremity measurements and rearfoot motion during walking. *J Orthop Sports Phys Ther* 24, 309-14 (1996).
54. Hopson, M. M., McPoil, T. G. & Cornwall, M. W. Motion of the first metatarsophalangeal joint. Reliability and validity of four measurement techniques. *J Am Podiatr Med Assoc* 85, 198-204 (1995).
55. Kidder, S. M., Abuzzahab, F. S., Jr., Harris, G. F. & Johnson, J. E. A system for the analysis of foot and ankle kinematics during gait. *IEEE Trans Rehabil Eng* 4, 25-32 (1996).
56. Hunt, A. E., Smith, R. M., Torode, M. & Keenan, A. M. Inter-segment foot motion and ground reaction forces over the stance phase of walking. *Clin Biomech (Bristol, Avon)* 16, 592-600 (2001).
57. Rattanaprasert, U., Smith, R., Sullivan, M. & Gilleard, W. Three-dimensional kinematics of the forefoot, rearfoot, and leg without the function of tibialis posterior in comparison with normals during stance phase of walking. *Clin Biomech (Bristol, Avon)* 14, 14-23 (1999).
58. Carson, M. C., Harrington, M. E., Thompson, N., O'Connor, J. J. & Theologis, T. N. Kinematic analysis of a multi-segment foot model for research and clinical applications: a repeatability analysis. *J Biomech* 34, 1299-307 (2001).
59. Leardini, A., Benedetti, M. G., Catani, F., Simoncini, L. & Giannini, S. An anatomically based protocol for the description of foot segment kinematics during gait. *Clin Biomech (Bristol, Avon)* 14, 528-36 (1999).
60. Nester, C. et al. Foot kinematics during walking measured using bone and surface mounted markers. *J Biomech* 40, 3412-23 (2007).

61. Lundgren, P. et al. Invasive in vivo measurement of rear-, mid- and forefoot motion during walking. *Gait Posture* (2007).
62. MacWilliams, B. A., Cowley, M. & Nicholson, D. E. Foot kinematics and kinetics during adolescent gait. *Gait Posture* 17, 214-24 (2003).
63. van den Bogert, A. J., Smith, G. D. & Nigg, B. M. In vivo determination of the anatomical axes of the ankle joint complex: an optimization approach. *J Biomech* 27, 1477-88 (1994).
64. Carson, M. C., Harrington, M., Thompson, N. & Theologis, T. N. A Four Segment In Vivo Foot Model for Clinical Gait Analysis. *Gait and Posture* 8, 73 (1998).
65. Kaufman, K. R., Morrow, D., Hansen, D. & Kitaoka, H. B. Technique for Measurement of Foot and Ankle Kinematics. *Gait and Posture* 18, S20 (2003).
66. Hwang, S. J., Choi, H. S. & Kim, Y. H. Motion analysis based on a multi-segment foot model in normal walking. *Conf Proc IEEE Eng Med Biol Soc* 7, 5104-6 (2004).
67. Scott, S. H. & Winter, D. A. Biomechanical model of the human foot: kinematics and kinetics during the stance phase of walking. *J Biomech* 26, 1091-1104 (1993).
68. Simon, J. et al. The Heidelberg foot measurement method: development, description and assessment. *Gait Posture* 23, 411-24 (2006).
69. Scott, S. H. & Winter, D. A. Talocrural and talocalcaneal joint kinematics and kinetics during the stance phase of walking. *J Biomech* 24, 743-52 (1991).
70. Kepple, T. M., Stanhope, S. J., Lohmann, K. N. & Roman, N. L. A video-based technique for measuring ankle-subtalar motion during stance. *J Biomed Eng* 12, 273-80 (1990).
71. Cowley, M. S., MacWilliams, B. A. & Meek, S. A Multi-Segment Kinematics and Kinetic Foot Model for Clinical Decision Making. *Gait and Posture* 13, 297 (2001).
72. Moseley, L., Smith, R., Hunt, A. & Gant, R. Three-dimensional kinematics of the rearfoot during the stance phase of walking in normal young adult males. *Clin Biomech (Bristol, Avon)* 11, 39-45 (1996).
73. Cappozzo, A., Catani, F., Croce, U. D. & Leardini, A. Position and orientation in space of bones during movement: anatomical frame definition and determination. *Clin Biomech (Bristol, Avon)* 10, 171-178 (1995).
74. Kirtley, C. in *Clinical Gait Analysis: theory and practice* (ed. Kirtley, C.) 45 (Elsevier, Philadelphia, 2006).

75. Mundermann, A., Nigg, B. M., Humble, R. N. & Stefanyshyn, D. J. Orthotic comfort is related to kinematics, kinetics, and EMG in recreational runners. *Med Sci Sports Exerc* 35, 1710-9 (2003).
76. Cheze, L. Comparison of different calculations of three-dimensional joint kinematics from video-based system data. *J Biomech* 33, 1695-9 (2000).
77. Eslami, M., Begon, M., Farahpour, N. & Allard, P. Forefoot-rearfoot coupling patterns and tibial internal rotation during stance phase of barefoot versus shod running. *Clinical Biomechanics* 22, 74-80 (2007).
78. Anas, K. & Jenkyn, T. R. in ISB XXth Congress - ASB 29th Annual Meeting (Cleveland, Ohio, 2005).
79. Lucia, A. et al. Short-term effects of marathon running: no evidence of cardiac dysfunction. *Med Sci Sports Exerc* 31, 1414-21 (1999).
80. Hohmann, E., Wortler, K. & Imhoff, A. MR Imaging of the Hip and knee Before and After Marathon Running. *The American Journal of Sports Medicine* 32, 55-59 (2004).
81. Lutter, L. Injuries in the runner and jogger. *Minn Med* 63, 45-51 (1980).
82. Barr, K. P. & Harrast, M. A. Evidence-based treatment of foot and ankle injuries in runners. *Phys Med Rehabil Clin N Am* 16, 779-99 (2005).
83. Gellman, R. & Burns, S. Walking aches and running pains. Injuries of the foot and ankle. *Prim Care* 23, 263-80 (1996).
84. McKenzie, D. C., Clement, D. B. & Taunton, J. E. Running shoes, orthotics, and injuries. *Sports Med* 2, 334-47 (1985).
85. Yamashita, M. H. Evaluation and selection of shoe wear and orthoses for the runner. *Phys Med Rehabil Clin N Am* 16, 801-29 (2005).
86. Butler, R., Hamil, J. & Davis, I. Effect of footwear on high and low arched runners' mechanics during a prolonged run. *Gait and Posture* 26, 219-225 (2006).
87. Richards, C. E., Magin, P. J. & Callister, R. Is your prescription of distance running shoes evidence based? *Br J Sports Med* (2008).
88. Cheung, R. T. & Ng, G. Y. Influence of different footwear on force of landing during running. *Phys Ther* 88, 620-8 (2008).
89. Wegener, C., Burns, J. & Penkala, S. Effect of neutral-cushioned running shoes on plantar pressure loading and comfort in athletes with cavus feet: a crossover randomized controlled trial. *Am J Sports Med* 36, 2139-46 (2008).

Chapter 2 – Validation of Holes for Examining Kinematics of the Foot Using a Multi-Segment Foot Model

If the effect of a shoe design parameter on the motion of the foot is being assessed, then marker triads need to be affixed to the foot while the subject is wearing the study shoe. When the protocol calls for a multiple shoe comparison, this is even more difficult since the markers must remain in the same location and orientation throughout testing, including shoe changes. Holes in the shoes are considered to be the best option; however, the size of the hole could change the functional design of the shoe if important components of the shoe are disrupted. This study provides a method for validating holes cut in the shoe for standard gait analysis conducted using the triad cluster from the multi-segment foot model described in Jenkyn et al. Using this method, future studies will be able to test shoes without disrupting their intended function.

This chapter will be submitted for publication as an original paper to the Journal of Biomechanical Engineering.

Shultz, R – developed experiment, analyzed all results and wrote the paper

Jenkyn, TR – senior author - helped design the protocol and helped analyze the results

2 Abstract

Methodology restrictions limit research on foot motion within running shoes, leading to studies examining the motion of the joints proximal to the hindfoot. Other joints are avoided because a multi-segmented foot model is necessary for calculations. This makes holes in the shoe a necessity. The holes need to be large enough for the reflective markers of an optical tracking system to be undisturbed by the edge of the hole but small enough not to change the structural integrity of the shoe. The objective of this study was to develop a method for testing hole sizes in running shoes to achieve the previously mentioned goals. Holes were cut in the shoes at locations that placed the hole above the navicular, the calcaneus, the first metatarsal, the fifth metatarsal and the hallux for the three different types of running shoes. The hole locations corresponded to the marker positions used for the multi-segment foot model developed by Jenkyn and Nicol¹ (2007). The model separates the foot into five segments to calculate four different inter-segmented motions of 1) hindfoot motion with respect to the midfoot in the frontal plane, 2) forefoot twist with respect to the midfoot in the frontal plane, 3) the height-to-length ratio of the medial longitudinal arch and 4) the hallux angle with respect to the first metatarsal in the sagittal plane. A single subject walked along the runway in the lab in each of the three shoes for 10 trials for each hole size and each shoe. Hole sizes were increased after each set of 10 walking trials was completed. Results show that a 2.5 cm diameter hole maintains the shoe integrity and the foot movement within the shoe. Future research should conduct this study on more subjects and shoe types since it is assumed that the hole size effect is dependent on both these factors.

2.1 Introduction

Research has shown that 50-70% of runners will experience a running-related injury requiring medical attention over their running career². It is commonly believed that designing running shoes for specific foot types helps decrease running-related injuries since these injuries are thought to be caused by excessive motion within the foot. Athletes wearing inappropriate footwear for their specific foot type are therefore at greater risk of injury²⁻⁷. The proper choice of shoes could help a runner to prevent these injuries from occurring^{2, 7}.

To aid in the design of running shoes, researchers need a quantitative method to measure the relative motion of the foot within a shoe. One promising method uses passive reflective markers attached to the dorsum of the foot and optical motion capture to track the motion of segments within the foot. Some studies have used custom-made shoes or sandals to allow markers affixed to the foot to be visible to the optical system^{8, 9}.

However, such a setup is not capable of assessing common running shoes with a more complete upper. This requires "holes" be cut in the upper, making the foot visible to the optical system. But hole dimensions are limited to ensure that the integrity of the shoe is not compromised. Several studies have used holes in the shoes^{5, 7, 10-13}. Of these, only a few stated that a validation of hole size was conducted^{7, 10, 11} and published the hole sizes^{10, 11, 13}. One study completely removed the back of the shoe (a 5 cm portion) and replaced it with translucent urethane film. The modified shoe was considered "reasonably stable"¹³. Bulter et al.⁷ used a materials testing machine to examine shoe integrity after two holes

had been cut into the heel counter. This study found a 10% reduction in heel counter stiffness.

Many of these studies examined only the alignment of the rearfoot^{5, 10-12}. Stacoff et al.¹⁰, using the protocol of Nigg et al.¹⁴, studied whether tracking markers on the shoe were an adequate representation of heel motion. Hole size was validated and found that foot pronation/supination was unchanged for dimensions smaller than 2.1 cm by 1.7 cm¹⁰. They also demonstrated that shoe markers do not adequately represent heel motion¹⁰. A similar study examining lateral cutting movements¹¹ also concluded that shoe markers were not adequate to represent rearfoot motion and that markers should be placed directly on the skin¹¹.

The objective of this study is to quantify the influence of hole size on the structural integrity of the shoe being tested and on the kinematics of the foot within the shoe. Two sets of markers were used simultaneously, one set on the shoe to measure shoe deformation and one set on the foot to measure foot kinematics. It was hypothesized that oval holes smaller than 1.5cm x 2 cm would have no significant influence on the deformation of the shoe or the kinematics of the foot in the shoe during level walking. Holes, greater than this size, would tend to decrease the stiffness of the shoe. Three different shoe designs were examined: a stability shoe, a cushioning shoe and a motion control shoe. It was further hypothesized that the foot kinematics would differ in nature within the different shoe designs since the motion control shoe was designed to support the foot to a greater extent than the other two shoe designs.

2.2 Methods

2.2.1 Subject and equipment

A single subject (24 year old female; height 174.5 cm; mass 74.1 kg) volunteered for this study. This subject had no on-going symptoms from a previous foot or ankle injury, no significant foot or ankle injuries at the time of the study, no obvious lower extremity malalignment and did not regularly wear orthotics. Written consent was given and the proposal was approved by the institution's Research Ethics Board. Three designs of running shoe were tested: a cushioning design (Saucony Myth), a motion control design (Saucony Triump) and a stability design (Saucony Omid MC 5). All shoes were women's size 7.

The gait laboratory was equipped with an eight-camera, real-time optical motion capture system (Eagle HiRes cameras, EvaRT system, Motion Analysis Corp., Santa Rosa, CA). Kinematic data were collected at 60 Hz. Twenty-two passive reflective markers were attached to the subject's skin with double-sided tape in a modified Helen Hayes configuration (i.e. one extra marker placed on the right scapula identified front from back). Two (14mm) point markers were affixed to each shoe on the dorsal toe box and on the posterior heel counter (Figure 2.1, easy to view on the left foot) to measure the overall deformation during walking. Walking was chosen as the study activity since this was the first study of this nature using this model and marker set-up. The author wanted to ensure the method was feasible and the results reasonable before moving on to the more intensive activity of running, where it was expected that the foot segment ranges of motion would increase and require larger holes.

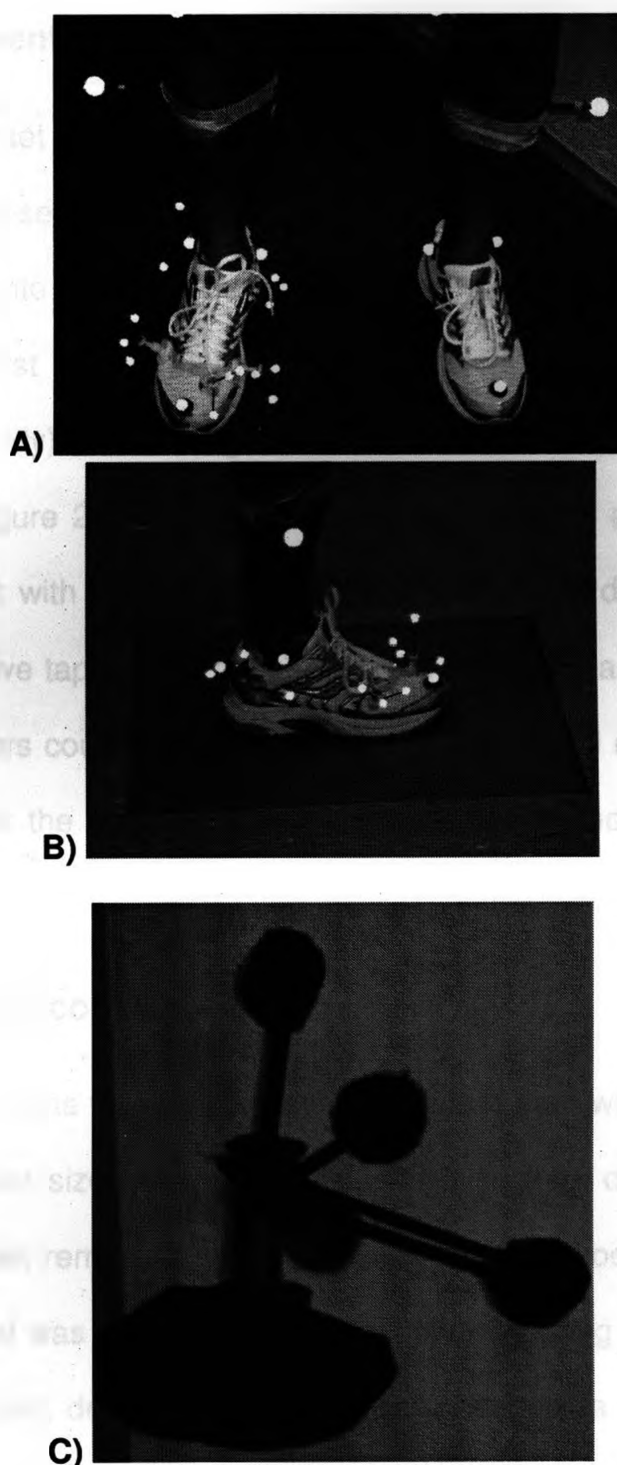


Figure 2.1: A,B) Placements of the passive reflective markers on the shoe and the marker triads on the foot. Only the right foot was instrumented with the marker triads. Two markers were placed on each shoe, one on the toe box and one on the heel counter. C) The marker triad cluster are comprised of a nylon nut and screw with carbon fiber wands protruding from the head of the screw and attaching to retro-reflective markers.

2.2.2 Multi-segment foot model marker set

A second marker set was attached to the foot directly. The configuration was based on the multi-segment foot model of Jenkyn and Nicol¹, which functionally divides the foot into five segments: hindfoot (calcaneous), midfoot (tarsus), medial forefoot (first metatarsal), lateral forefoot (fifth metatarsal), and hallux (added for this study). Each segment was tracked independently with a triad marker cluster (Figure 2.1c). The triad base consisted of a threaded base that affixed to the foot with double-sided tape. Three 8mm diameter Delrin balls, wrapped in reflective tape, were attached to the base with a nut and carbon-fiber stalks. The markers could be removed from the base and replaced in the same orientation, so that the base could remain attached to the foot throughout the testing protocol.

2.2.3 Testing protocol

The three shoe designs were each tested intact and then with a set of four holes cut into them. Four sizes of hole were tested with their dimensions becoming progressively larger, removing more material from the shoe uppers (Table 2.1). An initial static trial was collected with the subject wearing intact running shoes and standing in quiet, double support standing. Four extra markers were added for this trial only on the medial aspects of the knees and ankles, to establish segment-fixed axis directions and the joint centers. These were removed for the dynamic trials to follow. For all dynamic trials, the subject walked along an 8m walkway at a self-selected pace. Ten repetitions were collected for each of the

three shoe designs, for a total of 30 dynamic trials per intact or hole condition. When each intact shoe was placed on the subject, the shoelaces were marked with a pen to ensure the same tension when retied for subsequent trials.

Following the intact trials, sixteen barefoot trials with marker triads attached were collected to establish anatomic joint coordinate systems of the foot segments using the CAST method^{1, 15}. The subject stood in quiet standing while a barefoot static trial was collected to establish the neutral position for the foot marker set. The first (smallest) set of holes was cut into the right shoes of the cushioning, motion control and stability shoes. Each hole was an oval shape, with a prescribed long axis and short axis (Table 2.1). The triad markers were removed from their bases and the test shoe placed on the foot and the laces tightened. Then the markers were replaced so that they appeared through the holes (Figure 2.1).

In all, four hole sizes were tested on each shoe type (Holes 1 to 4, Table 2.1), with each test condition progressing from smallest to largest size hole. Since material was permanently removed with each hole condition, it was not possible to randomize the hole dimensions on a single shoe. However, for each hole size, the order of testing of each shoe design was randomized. No hole dimension exceeded 4 cm.

Table 2.1: Dimensions of the four hole sizes tested. Each hole was an oval with the long and short axis dimensions. Since material was permanently cut from the shoe to make the holes, the hole conditions progressed from smallest to largest size. It was not possible to randomize the hole sizes.

Condition	Long Axis [cm]	Short Axis [cm]
Intact	0	0
Hole 1	2.3	1.9
Hole 2	2.7	2.2
Hole 3	3.1	2.5
Hole 4	3.5	2.8

2.2.4 Shoe deformation analysis

The trajectory of each marker was filtered using a 4th order Butterworth smoothing filter with zero-lag (cutoff of 6Hz). The deformation of the shoe was quantified with two measures: the length from the toe to the heel markers and the angle between the heel-ankle-toe markers. These were calculated with custom-written software (MatLab, MathWorks, Natick, MA, USA). The values of these two measures were taken at the instant of heel rise in stance phase, defined as the first sample when the vertical coordinate of the heel marker increased after midstance. The average mean differences were calculated from the average of the six repetitions from each condition minus the six repetitions from the intact condition. If the shoe did not respond differently when holes were cut in it compared to the intact shoe, then this difference should be zero.

2.2.5 Foot kinematic analysis

The calculations of inter-segmental joint angles of the foot were calculated according to Jenkyn and Nicol¹ and were implemented in custom-written software (MatLab, MathWorks, Natick, MA, USA). The neutral position (i.e. zero point for each joint position) was defined using the initial barefoot static, quiet standing trial. Four inter-segmental measures were examined: the hindfoot angle with respect to the midfoot in the frontal plane, the forefoot angle with respect to the midfoot in the frontal plane, the height-to-length ratio of the medial longitudinal arch, and the hallux angle with respect to the medial forefoot in the sagittal plane¹. Means were calculated for the six repetitions of each condition and values were taken at the instant of heel rise in stance phase. Since there could not be an intact condition collected for the foot kinematics, each hole size condition was compared to the smallest hole size condition (Hole 1). An average mean difference for each set of trial means was then calculated. A minimum important difference (MID) of 5° was used for evaluation of the data¹⁶ (see Appendix A for justification for MID).

2.3 Results

Overall, for each of the three designs of running shoe, the deformation of the shoe and the kinematics of the foot were not dramatically altered for a hole size of less than about 2.7 cm x 2.2 cm (Hole 2). The two measures evaluating shoe deformation are shown in Figures 2.2 and 2.3. The length between the toe and heel markers at the instant of heel rise (Figure 2.2) is compared for each of the

holes sizes with the intact shoe for the three shoe designs: cushioning, stability and motion control.

The smallest deformations were with the motion control shoe. Figure 2.3 shows the angle between the heel, ankle and toe markers at heel rise. The greatest change in angle was seen with the largest hole size for both the cushioning and stability shoes. Little disruption was seen in the motion control shoe for any of the hole sizes.

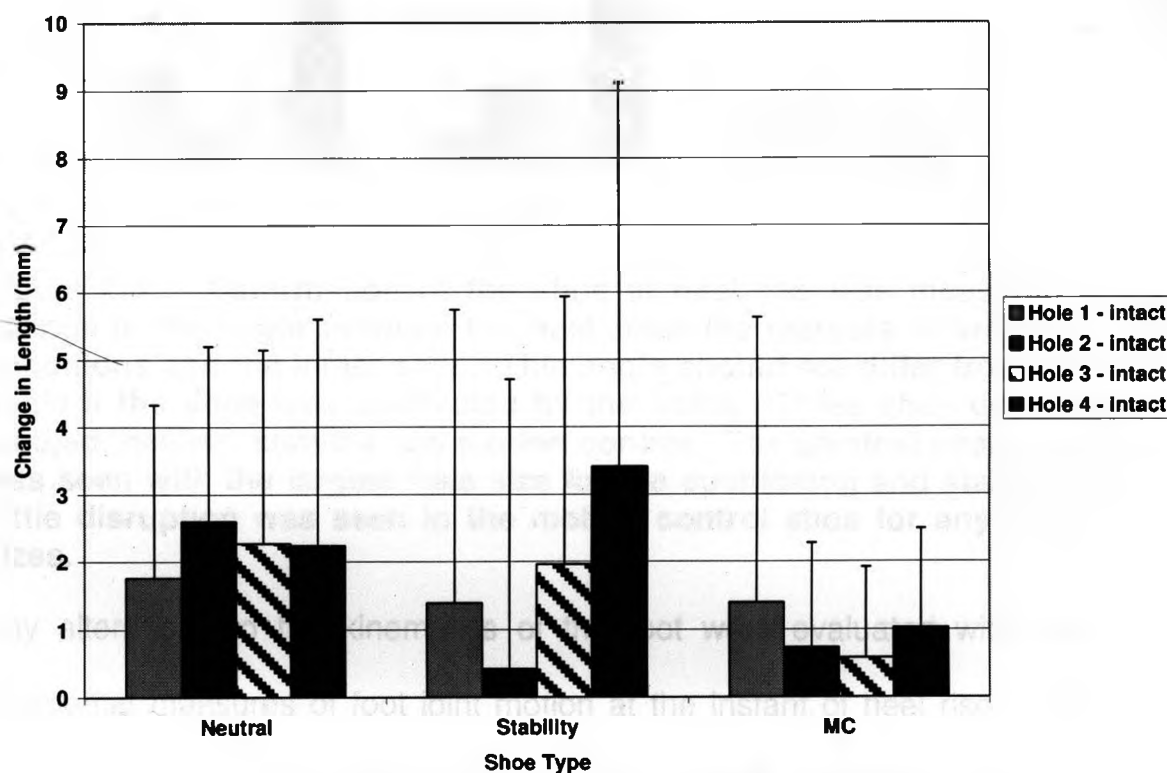


Figure 2.2: The deformation of the shoe at heel rise is measured by the change in the length from the toe and heel markers between the hole conditions and the intact shoe. This length should not differ from the intact length if the structural integrity of the shoe was unaffected by the holes. Three shoe designs were studied, neutral, stability and motion control (MC). As expected, the smallest deformations with the motion control shoe, which is the most supportive shoe.

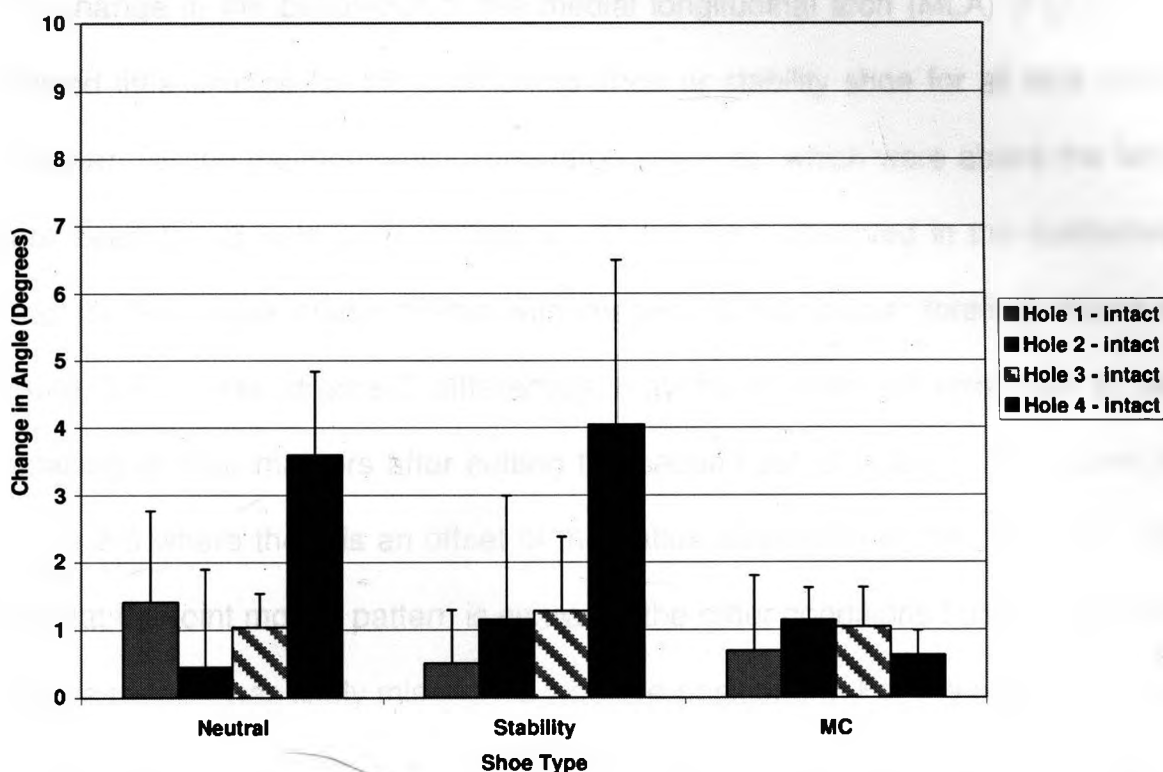


Figure 2.3: Deformation of the shoe at heel rise was measured by the change in the angle between the heel-ankle-toe markers between the hole conditions and the intact shoe. This angle should not differ from the intact angle if the shoe was unaffected by the holes. Three shoe designs were studied, neutral, stability and motion control. The greatest change in angle was seen with the largest hole size for the cushioning and stability shoes. Little disruption was seen in the motion control shoe for any of the hole sizes.

Any alterations to the kinematics of the foot were evaluated with four inter-segmental measures of foot joint motion at the instant of heel rise. These are plotted in Figures 2.4 through 2.7. The change in frontal plane hindfoot kinematics with respect to the midfoot is shown in Figure 2.4. The third and fourth holes sizes of the motion control shoe surpass the minimum important difference. Little change was seen with either the cushioning shoe or the stability shoe for any size hole. For the forefoot motion with respect to the midfoot in the frontal plane (Figure 2.5) all mean differences were below the 5° threshold.

The change in the behaviour of the medial longitudinal arch (MLA) (Figure 2.6) showed little change for the cushioning shoe or stability shoe for all hole sizes. However, for the motion control shoe large changes, which were above the MID, were seen for all hole size conditions. This is also observed in the cushioning shoe for the hallux plane motion with respect to the medial forefoot shown in Figure 2.7. These dramatic differences may have been an error due to the replacing of triad markers after cutting the second set of holes. This is seen in Figure 2.8 where there is an offset of the hallux joint angle of the first hole. The fact that the joint motion pattern is similar to the other conditions but offset implies that the marker was likely misaligned when re-positioned. For the other two shoe conditions only the fourth hole of the stability shoe surpasses the MID.

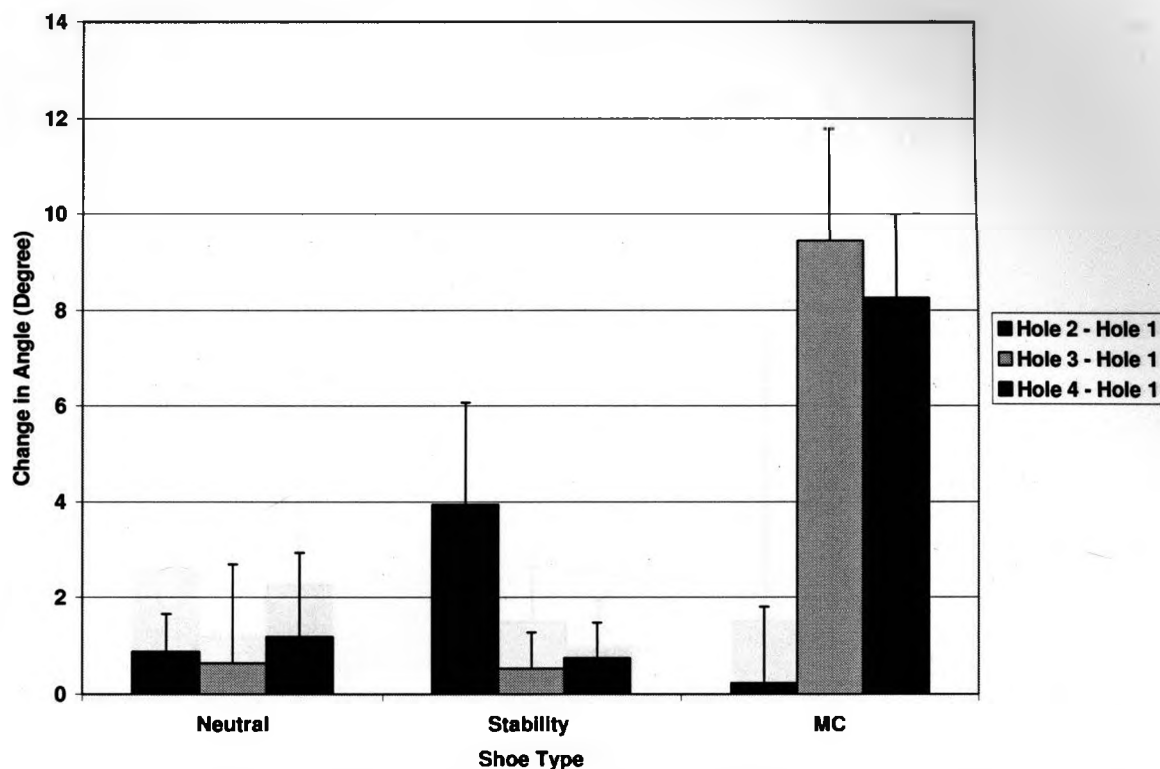


Figure 2.4: Change in hindfoot kinematics with respect to the midfoot in the frontal plane at the instant of heel rise in stance phase. The angle should not differ from the smallest hole condition (Hole 1). The minimum important difference was considered to be 5°. Three shoe designs were studied, neutral, stability and motion control. The minimum important difference was surpassed for the third and fourth hole size of the motion control shoe. Little change was seen with both the cushioning and stability shoes for all sizes of hole.

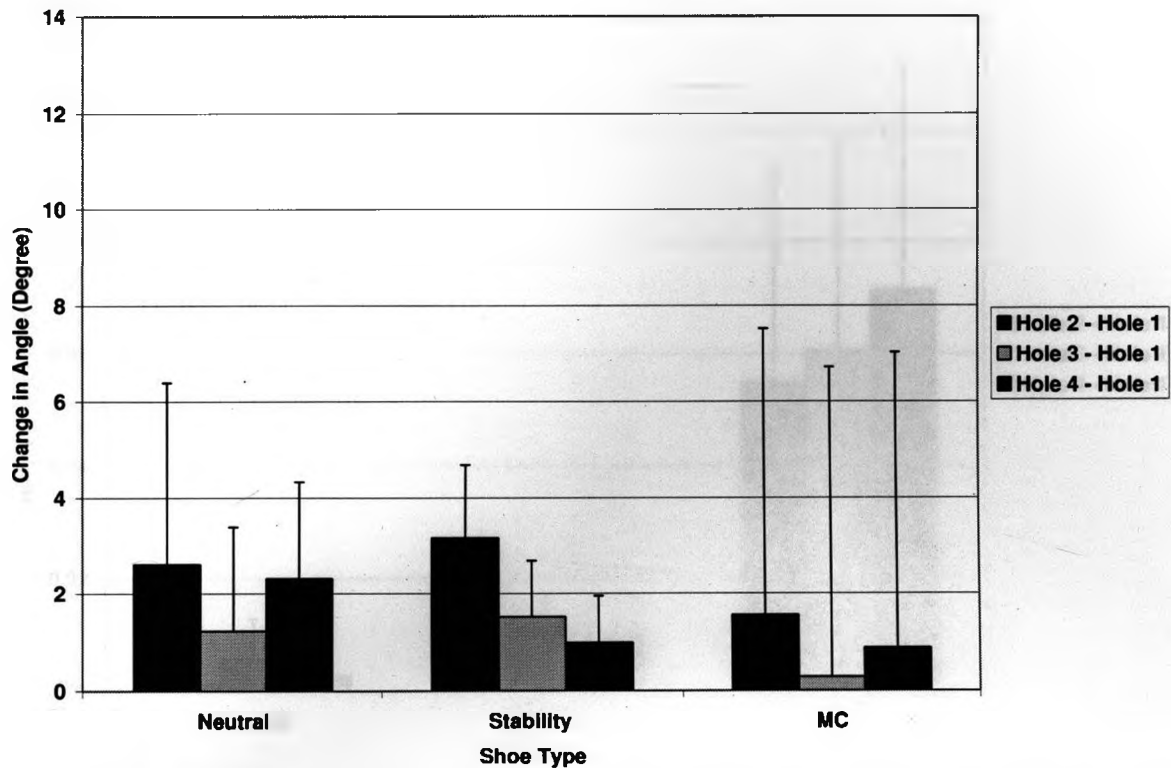


Figure 2.5: Change in forefoot kinematics with respect to the midfoot in the frontal plane at the instant of heel rise in stance phase. The angle should not differ from the smallest hole conditions (Hole 1). Three shoe designs were studied, neutral, stability and motion control. All mean differences were below the 5° defined as minimum important difference.

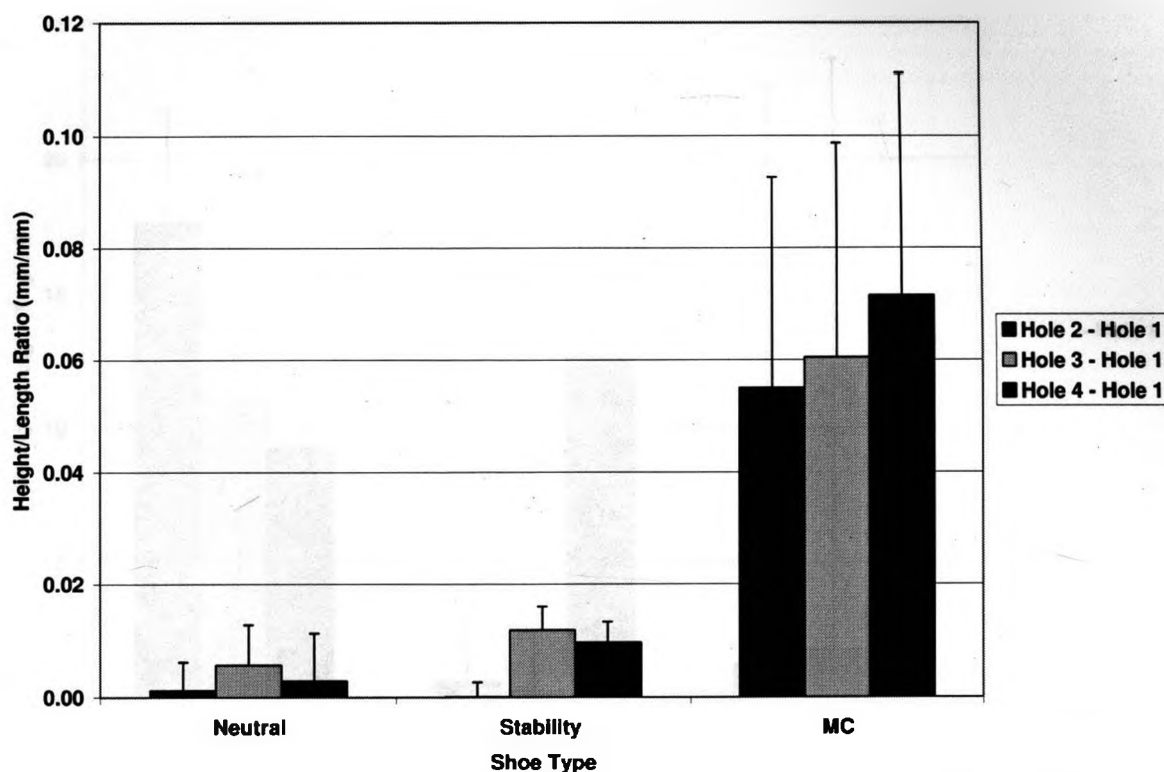


Figure 2.6: Change in the behaviour of the medial longitudinal arch (MLA) at the instant of heel rise. The MLA should not differ from 0.0 if the shoe was unaffected by the holes. Little change was seen for the neutral shoe or the stability shoe for any hole size. For the motion control shoe large changes in arch behaviour were seen for all hole conditions.

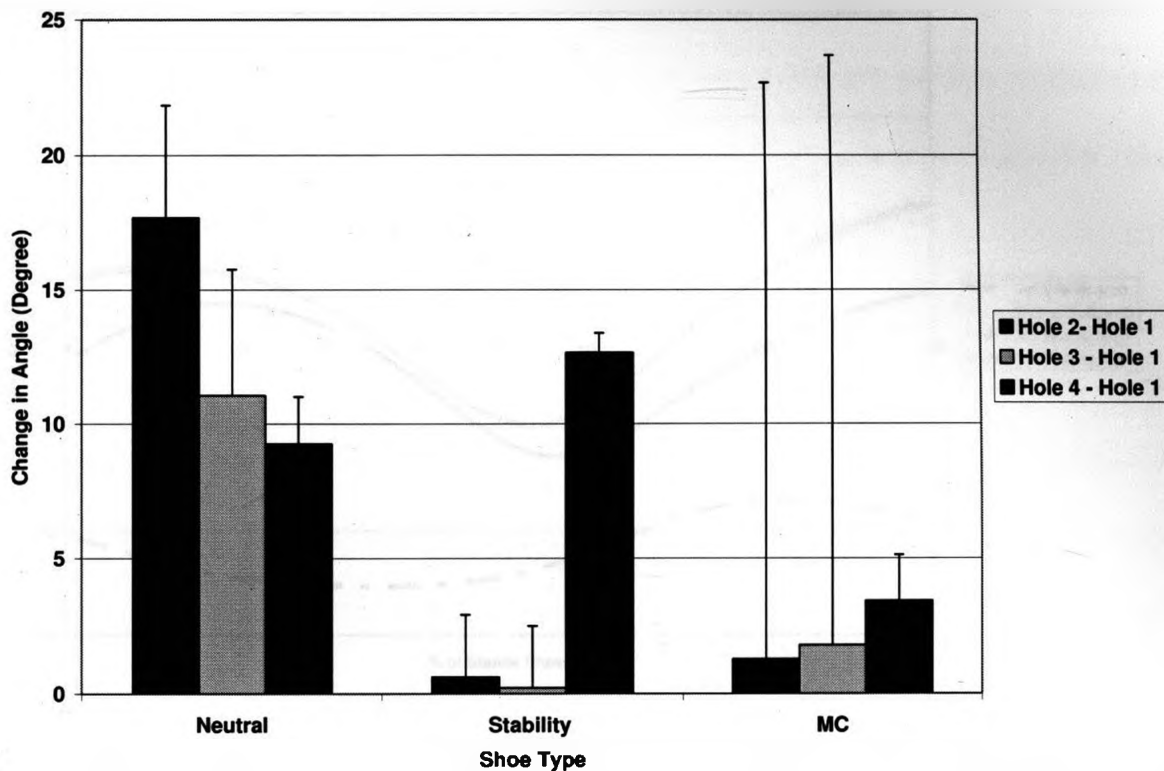


Figure 2.7: Change in hallux kinematics with respect to the medial forefoot in the sagittal plane at the instant of heel rise. The angle should not differ from the smallest hole conditions (Hole 1). The minimum important difference was surpassed for all hole sizes of the neutral shoe. For the other two shoe conditions only the fourth hole of the stability shoe surpassed the MID.

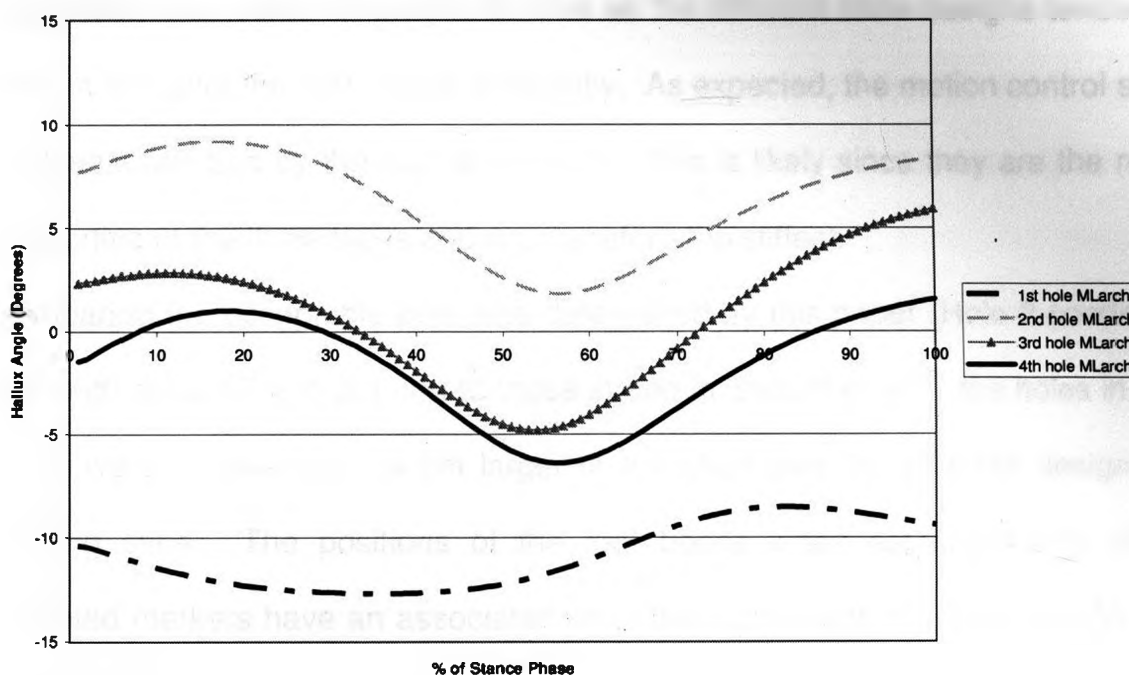


Figure 2.8: Range of motion of the hallux with respect to the medial forefoot for the cushioning shoe condition. The second hole has a similar pattern shape to the third and fourth hole patterns, but is offset by a positive angle. It is speculated that the offset is due to an unintended rotation of a marker triad with respect to its initial position after replacing the shoe.

2.4 Discussion

The objective of this study was to determine whether holes could be cut into a running shoe upper without significantly compromising its structural integrity or changing the kinematics of the foot within the shoe. If so, then this method of optical motion capture used with a multi-segment foot model would be a valid and non-invasive clinical method to examine the influence of footwear design on foot kinematics. This study demonstrates that properly sized holes cut can ensure that the shoe functions as if it were intact and that foot motion is unaffected by the loss of material. The validated hole size (Hole 2 condition, oval with axes 2.7 and 2.3 cm) was larger than what had been hypothesized. The secondary

hypothesis was demonstrated to be true as the different shoe designs tended to deform and alter the foot motion differently. As expected, the motion control shoe was least affected by the loss of material. This is likely since they are the most supportive of the three types and are therefore the stiffest.

Comparing the acceptable hole size determined by this paper (Hole 2 condition, oval with axes 2.7 and 2.3 cm) to those stated in Stacoff et al.¹⁰, the holes in this study were on average 0.4 cm larger in the short axis for all three designs of running shoe. The positions of the foot bones when estimated with shoe-mounted markers have an associated error that varies with the shoe design and more specifically with the heel counter rigidity¹⁷. It is speculated that the our larger acceptable hole size was due to the diameter of the marker stem, brand of shoe (Saucony) and the shoe design, rather than the method used to cut or to validate the holes. Stacoff et al. only cut holes in the heel counter for two point markers, whereas in this study holes were cut in four locations in addition to the heel counter. While one would have expected to observe a decrease in acceptable hole size, in this study compared to Stacoff et al.¹⁰, since five holes were cut in the shoes in this study, compared to two holes in the Stacoff study, the opposite was found to be true. The four holes cut outside of the heel counter region likely had little effect on the function of the shoe since they were cut in the nylon sections of the shoes and not in the support structures. The greater hole size in this study can then be attributed to cutting only a single hole in the heel counter region as opposed to two holes as in the Stacoff study.

A possible limitation of this validation study is that only one subject was tested, using only one shoe per design and only one shoe brand. Further studies could investigate other shoe brands, since this may alter the maximum acceptable hole size. It is speculated that the size limit depends on both the design and brand of shoe, as well as range of foot motion being studied. This last factor is dependent on activity being performed (i.e. running versus walking).

One of the challenges with this testing protocol was the need to remove and replace shoes without changing the positions and orientations of the marker triads with respect to the underlying bones of the foot. This was accomplished by designing the reflective markers removable from their base; the base could remain affixed to the foot throughout the testing protocol. Several prototype triad clusters were tried before a successful design was settled on (Figure 2.1c). The marker triad bases and removable markers were initially quite fragile. They were easily damaged during removal and replacement of the shoes, and during the walking tasks performed by the subject. The marker orientation was clearly identified before detaching the clusters from the bases to allow the reflective markers to be reattached and positioned exactly the same way each time. The base of the triad was a thin plastic oval no thicker than a sport sock that athletes would normally wear. Following this study, the authors added a locking screw to the markers to ensure that the markers were robustly reattached in the correct orientation for future studies. The base of the triads was also changed to a faux leather oval patch that remained no thicker than a sports sock. The leather is

affixed to the skin (after shaving if necessary) with medical adhesive spray (Medical Adhesive Spray, Hollister, Libertyville, IL).

Problems may be encountered in future research with this setup if the subjects were to run or perform cutting turns. During fast walking and running the rapid accelerations at heelstrike have been quantified at 5-15 times the acceleration due to gravity at the tibial level^{18, 19}. This could cause transient vibration of the triad cluster that would appear in the trajectories of the reflective markers. Care was taken to minimize any vibration of the triads by ensuring that each triad weighed less than 100g¹ and that the center of mass is as close to the base as possible.

In conclusion, this study validated a method to use optical motion capture and a multi-segment foot model¹ to quantify foot joint kinematics relative to the shoe during weight-bearing, dynamic activities. Further studies can now be conducted that examine foot kinematics during various shoed tasks and allow the simultaneous and independent tracking of shoe deformation. Other researchers have expressed concern that error in their studies arose due to shoe markers being inappropriate for tracking motion of the foot within the shoe. Skin markers are thought to be a far better indication of true bone motion in-vivo than shoe markers¹⁷, as demonstrated by Stacoff et al.¹⁰ and Reinschmidt et al.¹¹. However, the data obtained with skin-mounted markers on the foot must also be treated with caution. Although skin-mounted markers are better than shoe-mounted markers, Reinschmidt et al.¹⁷ demonstrated that invasive bone pin markers are the most representative of bone motion and that skin-mounted

markers have limits to their accuracy. Care has been taken in this study to develop a model that positioned the markers over bony landmarks, avoiding superficial ligaments and tendons that move the skin¹. In addition, by using anatomical landmarks to create anatomical coordinate systems, this method bridges the gap between the gait lab and clinical practice. Also, the clinical multi-segment foot model analyzes the hindfoot and forefoot simultaneously by calculating the joint's motion with respect to the midfoot.

The advantage of this method is that it is able to track the motion of the foot within various shoes and the shoes' deformation during a single session with the use of validated holes and custom triad clusters. This method should be used primarily for examining relative motion of the foot with respect to different shoes or barefoot.

2.5 References

1. Jenkyn, T. R. & Nicol, A. C. A multi-segment kinematic model of the foot with a novel definition of forefoot motion for use in clinical gait analysis during walking. *J Biomech* 40, 3271-8 (2007).
2. Nawoczenski, D. A., Saltzman, C. L. & Cook, T. M. The effect of foot structure on the three-dimensional kinematic coupling behavior of the leg and rear foot. *Phys Ther* 78, 404-16 (1998).
3. McKenzie, D. C., Clement, D. B. & Taunton, J. E. Running shoes, orthotics, and injuries. *Sports Med* 2, 334-47 (1985).
4. Shorten, M. R. The energetics of running and running shoes. *J Biomech* 26 Suppl 1, 41-51 (1993).
5. Stacoff, A., Kalin, X. & Stussi, E. The effects of shoes on the torsion and rearfoot motion in running. *Med Sci Sports Exerc* 23, 482-90 (1991).
6. James, S. L., Bates, B. T. & Osternig, L. R. Injuries to runners. *Am J Sports Med* 6, 40-50 (1978).

7. Butler, R., Hamill, J. & Davis, I. Effect of footwear on high and low arched runners' mechanics during a prolonged run. *Gait and Posture* 26, 219-225 (2006).
8. O'Connor, K. M. & Hamill, J. The role of selected extrinsic foot muscles during running. *Clinical Biomechanics* 19, 71-77 (2004).
9. Eslami, M., Begon, M., Farahpour, N. & Allard, P. Forefoot-rearfoot coupling patterns and tibial internal rotation during stance phase of barefoot versus shod running. *Clinical Biomechanics* 22, 74-80 (2007).
10. Stacoff, A., Reinschmidt, C. & Stussi, E. The movement of the heel within a running shoe. *Med Sci Sports Exerc* 24, 695-701 (1992).
11. Reinschmidt, C., Stacoff, A. & Stussi, E. Heel movement within a court shoe. *Med Sci Sports Exerc* 24, 1390-5 (1992).
12. Clarke, T. E., Frederick, E. C. & Hamill, C. L. The effects of shoe design parameters on rearfoot control in running. *Med Sci Sports Exerc* 15, 376-81 (1983).
13. Johanson, M. A., Donatelli, R., Wooden, M. J., Andrew, P. D. & Cummings, G. S. Effects of three different posting methods on controlling abnormal subtalar pronation. *Phys Ther* 74, 149-58; discussion 158-61 (1994).
14. Nigg, B. M., Eberle, G., Frey, D., Segesser, B. & Weber, B. Bewegungsanalyse für Schuhkorrekturen (Movement Analysis for Shoe Constructions). *Medita* 9, 160-163 (1977).
15. Cappozzo, A., Catani, F., Croce, U. D. & Leardini, A. Position and orientation in space of bones during movement: anatomical frame definition and determination. *Clin Biomech (Bristol, Avon)* 10, 171-178 (1995).
16. Nester, C. et al. Foot kinematics during walking measured using bone and surface mounted markers. *J Biomech* 40, 3412-23 (2007).
17. Reinschmidt, C., van Den Bogert, A. J., Murphy, N., Lundberg, A. & Nigg, B. M. Tibiocalcaneal motion during running, measured with external and bone markers. *Clin Biomech (Bristol, Avon)* 12, 8-16 (1997).
18. Voloshin, A. The influence of walking speed on dynamic loading on the human musculoskeletal system. *Med Sci Sports Exerc* 32, 1156-9 (2000).
19. Lafortune, M. A., Lake, M. J. & Hennig, E. Transfer function between tibial acceleration and ground reaction force. *J Biomech* 28, 113-7 (1995).

Chapter 3 – Effect of Neutral trial on Foot Kinematics

During gait analysis, a static trial is commonly used to establish the neutral position for the joints of interest. Using pre-condition static trials allows the range of motion to be compared between each condition. A single static trial for all conditions allows the differences in absolute angles to be compared between conditions. If a subject is approaching the joint's end-of-range then the absolute motion is clinically important not simply the range of motion. It has been suggested that this can induce stress on the soft tissue and bony constraints, which could lead to injury. This study examines whether separate static trials should be collected for each footwear condition in a test protocol that uses a multi-segment foot model. The previously mentioned multi-segment kinematic foot model is used to measure the absolute change in neutral position for three different shoe conditions and a barefoot condition for four inter-segmental positions of the foot.

This chapter will be submitted for publication as a technical note to the Journal of Clinical Biomechanics.

Shultz, R – developed experiment, analyzed all results and wrote the paper

Jenkyn, TR – senior author - helped design the protocol and helped analyze the results

3 Abstract

During gait analysis, a static trial is commonly used to establish the neutral position for the joints of interest. This study examines whether separate static trials should be collected for each footwear condition in a test protocol that uses a multi-segment foot model. A multi-segment kinematic foot model and optical motion analysis are used to measure the absolute change in neutral position for four inter-segmental positions of the foot: 1) hindfoot-to-midfoot in the frontal plane, 2) forefoot-to-midfoot in the frontal plane, 3) hallux-to-forefoot in the sagittal plane, and 4) the height-to-length ratio of the medial longitudinal arch. A barefoot condition was compared with three shoe conditions; Nike Frees with varying amounts of longitudinal torsional stiffness. A minimum important difference in the neutral position was found between shoe conditions across most subjects, despite a high variability in both within subjects and shoe conditions. The shoes tended to raise the arch and to dorsi-flex the hallux compared to barefoot condition. This study evaluates whether a single static trial or several per-condition static trials are more appropriate for establishing neutral positions during gait analyses that compare footwear conditions and concludes that it is conditionally dependent. Per-condition static trials allow the range of motion to be compared between each condition. A single static trial for all conditions allows the differences in absolute angles to be compared between conditions. Absolute motion is important clinically when determining whether or not a subject is

approaching a joint's end of range, since it has been suggested this can induce stress on the soft tissue and bony constraints and lead to injury.

3.1 Introduction

Optical motion analysis is a powerful technique for quantifying the effect of footwear and orthotics on gait in clinical and sport biomechanics. Usually, a series of dynamic tasks (i.e. level walking or running) are collected after an initial static trial is collected in quiet standing¹⁻⁷. The static trial establishes the neutral position for the joints of interest or the zero point for joint-fixed coordinate systems^{5, 7-10}. However, error in interpretation of joint angles may arise when testing several footwear or orthotic conditions if a common neutral position from a single static trial is used for all conditions. For example, the shoe condition may change the absolute joint angle but not the joint range of motion. If the researcher was unaware of this effect, then the conclusions drawn from the study about the pathological joint motion could be incorrect.

It has been suggested that muscle patterning during running is predetermined¹⁰ with muscles adapting subtly to different footwear geometries at the foot¹¹. O'Connor et al.¹² tried to test this theory, and although not convinced with the results from their study, did demonstrate that muscle recruitment may not be altered by a perturbation at the foot. A perturbation can be described as a disturbance, for example from a shoe or orthotic, that may influence the motion of the foot and cause it to adapt to its presence. This group speculated that a complex relationship between foot perturbation and neuromuscular response perhaps exists. Another explanation may be that the foot is a structurally redundant system with many possible strategies for obtaining the gross measurements measured with simple foot models¹⁰. With a more complex foot

model, capable of tracking individual segments, the differences in foot positioning from different foot perturbations may become apparent. These would likely appear as differences in segmental joint neutral positions between footwear conditions or perturbations. It may be that during a dynamic task the ranges of motion (ROM) of joints of the foot or lower limb, common variables in gait analysis¹³, remain constant despite a change of footwear. But the absolute magnitudes of joint angles are indeed changed with the perturbation, possibly placing the joint closer to its end range and consequentially at risk of injury. If per-condition static trials were to be used to define each joint neutral position, then it would appear as if the perturbation had no effect on the foot joints and valuable clinically relevant information could be missed. This could be avoided by using a common, static trial to calculate the absolute joint angles.

This study compares separate neutral positions calculated from quiet standing static trials collected for each footwear condition in a test protocol. A multi-segment kinematic foot model and optical motion capture¹⁴⁻¹⁶ are used to measure the absolute change in neutral position for four inter-segmental positions of the foot during quiet standing: the hindfoot angle with respect to the midfoot in the frontal plane, the forefoot angle with respect to the midfoot in the frontal plane, the height-to-length ratio of the medial longitudinal arch, and the hallux angle with respect to the medial forefoot in the sagittal plane. It is hypothesized that the neutral position will be significantly different between the barefoot and shoe conditions. Differences between the three shoe conditions may also be seen.

3.2 Methods and Procedures

3.2.1 Subjects

Ten active male subjects volunteered for the study (average age 30 ± 5 years; average height 172.0 ± 0.4 cm; average mass 70 ± 7 kg). Subjects had no ongoing symptoms from a previous foot or ankle injury, no significant foot or ankle injuries at the time of the study, no obvious lower extremity malalignment and did not wear orthotics. Consent was attained from the relevant ethics committees at the research lab where the study was conducted at the authors' university.

3.2.2 Gait Analysis and Data Collection

The study was conducted at the Nike Sport Research Laboratory (NSRL, Beaverton, OR). The laboratory is equipped with an eight-camera, three-dimensional (3D) optical motion capture system (EvaRT 5.04, Eagle HiRes cameras, Motion Analysis Corp., Santa Rosa, CA). Kinematic data were sampled at 240 Hz in a 3m x 1.5 m x 1m capture volume.

The foot-ankle complex was analysed using a multi-segment kinematic foot model that tracks individual foot segments via skin-mounted marker cluster triads, one per segment. For this study, the foot was functionally divided into five segments; hindfoot (calcaneous), midfoot (tarsals), lateral and medial forefoot (metatarsals divided between the 2nd and 3rd rays) and the hallux. A full description of the multi-segment foot model can be found in Jenkyn and Nicol¹⁴. Four inter-segmental motions were tracked throughout stance phase: the hindfoot with respect to the midfoot in the frontal plane (hindfoot), the forefoot twist with

respect to the midfoot in the frontal plane (forefoot), the hallux angle in the sagittal plane with respect to the first metatarsal (hallux) and the height-to-length ratio of the medial longitudinal arch (MLA).

Three sets of size 9 Nike Free 7.0 trainers (Nike, Inc, Beaverton, OR) were pre-cut with five 'holes' each (holes of ~2.5 cm diameter) so that the skin-mounted triad clusters could be tracked by the optical motion capture system (Figure 3.1).

The hole diameters were the maximum that would not sacrifice the structural integrity of the shoe. This was validated in a separate pilot study on the same model of shoes used in this study, Nike Free Trainers 7.0, using the validation method outlined in Chapter 2. The same hole size was found to be valid for the Nike Frees as was found to be valid for the three Saucony shoes in Chapter 2, except this time a circle hole 2.5cm in diameter was cut into the shoes since the shoes were leather and easier to punch out than the nylon Saucony shoes.

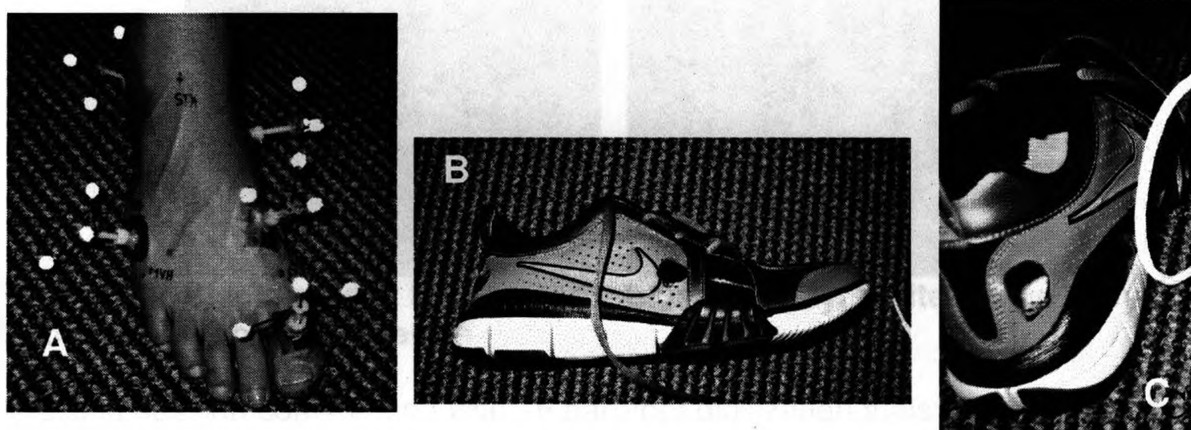


Figure 3.1: A) Triad Markers located on the foot for a barefoot static trial. Bony landmarks are written in pen on the subject's foot. B) and C) holes cut in the shoe to affix marker triads (A) to the foot.

The marker cluster triads were designed so that the reflective markers could be detached from their base, which remained affixed to the skin of the foot throughout the testing protocol. This allowed shoes to be changed between test conditions without changing the locations of the triad bases. After a new shoe was placed on the foot, the reflective markers for each of the five triads were replaced with the same orientation as that of the previous shoe and all the initial digitization trials. The stem of the triad cluster consisted of a nylon screw with three carbon-fibre wands protruding from the screw head and attached to wooden balls (8mm diameter) wrapped in reflective tape (3M, Minneapolis, MN). The base was a nylon nut epoxied to a faux leather patch and affixed to the foot with medical adhesive spray (Hollister Incorporated, Libertyville, IL) (Figure 3.2).

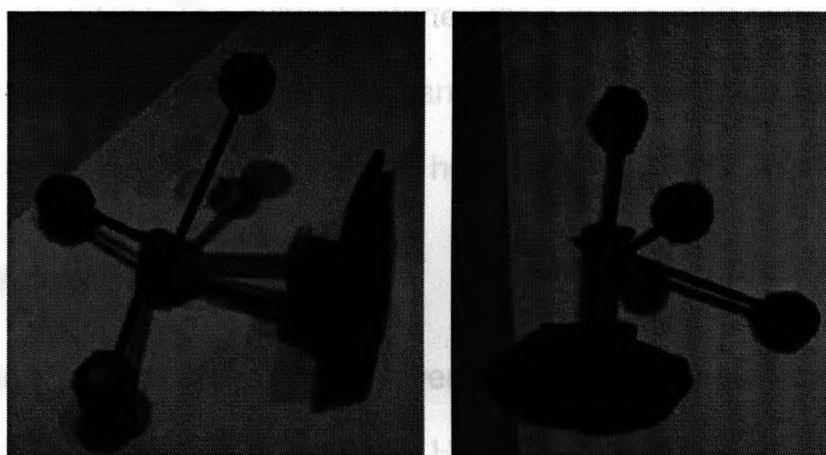


Figure 3.2: Black base – faux leather, blue – epoxy, white screw – nylon, black wands – carbon fiber.

A testing session commenced with 16 barefoot digitization trials where three bony landmarks per foot segment were located with an instrumented stylus¹⁴. The four testing conditions were: 1) barefoot, 2) in Nike Frees (control shoes, CO), 3) in Nike Frees with an added horizontal forefoot carbon plate (FF), and 4) in Nike Frees with a full-length carbon plate (FL). Conditions 2, 3 and 4 are the same

shoes, Nike Free Trainers 7.0 available commercially. However, carbon fiber plates have been added underneath the insole and glued to prevent slipping. Nike Frees are designed to mimic barefoot walking and so have a relatively flexible sole with little support function such as posting or dual density midsoles. For the intact control shoe, the forefoot plate shoe and the full length plate shoe, the longitudinal stiffness was 88.0 N-m/degree, 78.2 N-m/degree and 130.6 N-m/degree, respectively. Testing was performed in the Mechanics and Materials lab at Nike and is outlined in detail in Appendix D. For each footwear condition, a separate neutral static trial in quiet standing was collected while the subject stood in the center of the capture volume with feet at shoulder width. Seven dynamic trials for each footwear condition were then collected where the subject ran at a 7 min/mile pace ($\pm 5\%$). The subjects started their run on a 50 m track 25 m from the force plate. Only the right foot was analyzed. The dynamic data were used for a separate study and is not presented here.

3.2.3 Data Analysis

Trajectory data for each of the markers were filtered using a 4th order Butterworth filter with zero lag (low pass cutoff at 20 Hz, see chapter one for explanation on cutoff frequency). The four inter-segmental joint measures were calculated in software implemented in MatLab (MathWorks, Inc, Natick, MA). For the static, quiet standing trials, the value for each inter-segmental motion was averaged over 0.5 seconds.

3.2.4 Statistical Analysis

To test the hypothesis that different footwear conditions had different neutral positions, a repeated measures analysis of variation (ANOVA) with 1 factor at 4 levels was performed on each of the four static measurements. The three shoe conditions (CO, FL, FF) and the barefoot condition were the levels. An average per condition neutral trial over the collected frames for each subject was used in the ANOVA. A Tukey test post-hoc test was used after the ANOVA to correct the level of significance to account for the fact that multiple comparisons had been made.

3.3 Results

The average joint positions and standard deviations for each of the four inter-segmental joints examined (MLarch, Hallux, Forefoot, Hindfoot) are shown in Table 3.1 for each of the four footwear conditions (Bare, CO, FF, FL). Statistically significant differences are indicated with an asterisk (*) at a significance level of $p=0.05$. The multiple comparison test showed that a statistically significant difference was found between the control shoe condition (CO) and the barefoot condition (Bare) for both the height-to-length ratio of the MLA (MLarch) and for the hallux (Table 3.1).

Table 3.1: Summary of neutral positions: The means and standard deviations (SD) for each of the footwear conditions across each of the four inter-segmental joints tested. Statistically significant difference between the control shoe (CO) condition and the barefoot condition (Bare) were found for the height-to-length medial longitudinal arch and the hallux angle at $p < 0.05$. Differences were found between the shoe conditions and the barefoot condition for the other two inter-segmental joints, but these were not significant.

	MLarch (ratio)		Hallux (deg)		Forefoot (deg)		Hindfoot (deg)	
	Mean	SD	Mean	SD	Mean	SD	Mean	SD
Bare	0.000*	0.001	-0.06*	0.16	-0.09	0.17	0.12	0.23
CO	0.028*	0.036	-8.85*	10.43	-3.92	4.95	0.26	2.49
FF	0.022	0.032	-3.26	12.32	-2.20	5.97	3.91	8.66
FL	0.008	0.018	-4.38	4.89	-1.80	3.52	1.21	5.04

The comparison of absolute neutral positions between footwear conditions is plotted in figures 3.3 through 3.6 for each of the four inter-segment joints. The neutral positions for each plot are averaged over 0.5 seconds of the static trial. These plots were then compared to a minimum important difference (MID) of 5 degree⁶. The neutral value of the height-to-length ratio of the medial longitudinal arch was consistent between subjects for the barefoot trial. There was also a consistent trend of the three shoe conditions raising the arch compared to the barefoot trial (Figure 3.3). The hallux neutral position was also consistent between subjects for barefoot, but tended to be more dorsi-flexed for the three shoe conditions, with differences above the minimum important difference (i.e. $>5^\circ$) being seen between shoe conditions (Figure 3.4). Forefoot twist in the

frontal plane with respect to the midfoot segment was consistent between subjects for the barefoot condition, but showed differences above the MID between the three test shoe conditions (Figure 3.5). Hindfoot motion in the frontal plane with respect to the midfoot was the most variable of all the joints measured, but differences above the MID were seen between the shoe conditions and the barefoot condition (Figure 3.6). A large variance was also observed across each of the subjects.

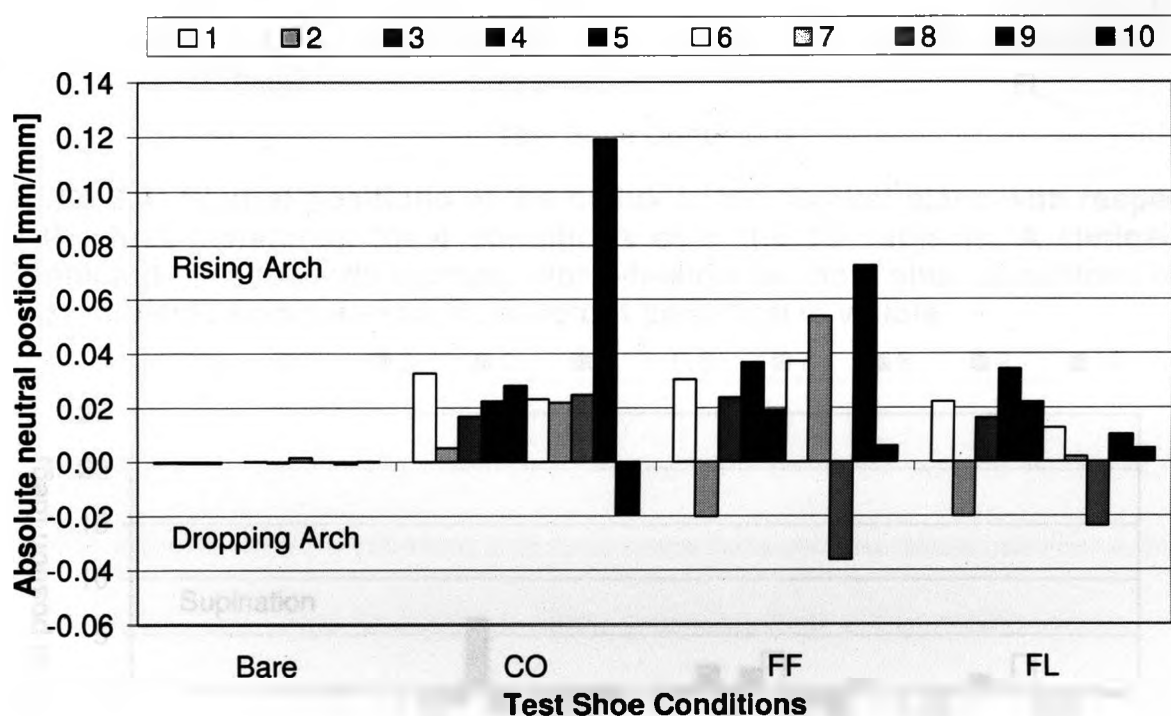


Figure 3.3: Neutral values of the medial longitudinal arch height-to-length ratio for 4 conditions over the 10 subjects. The shoe conditions tend to raise the medial longitudinal arch compared to the barefoot condition.

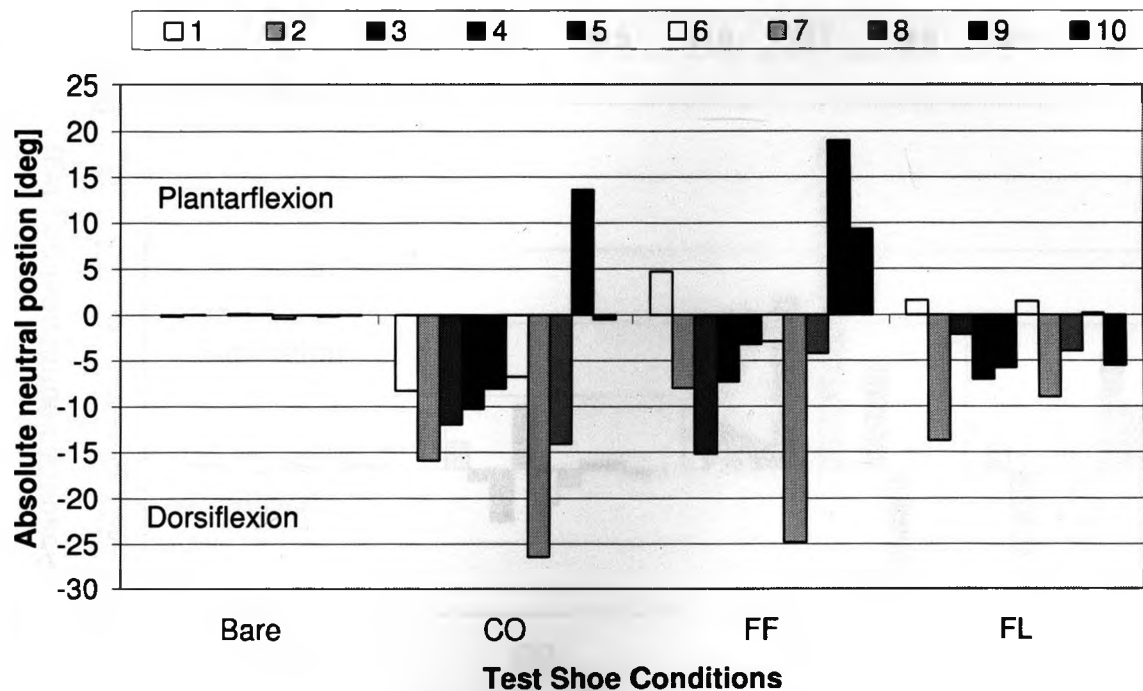


Figure 3.4: Neutral positions of the hallux in the sagittal plane with respect to the first metatarsal for 4 conditions over the 10 subjects. A clinically significant shift towards increase dorsi-flexion for most shoe conditions for most subjects compared to the barefoot condition is visible.

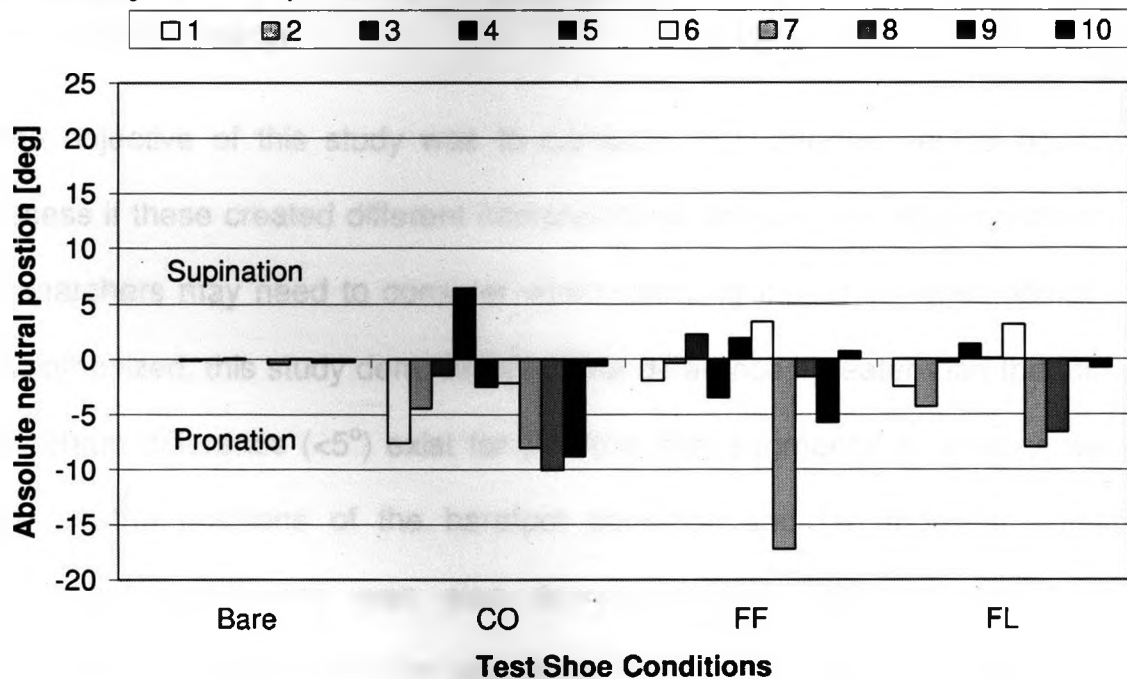


Figure 3.5: Neutral positions of the forefoot with respect to midfoot in the frontal plane for 4 conditions over the 10 subjects. The forefoot motion trends to increase towards pronation for the most shoe conditions compared to the barefoot condition.

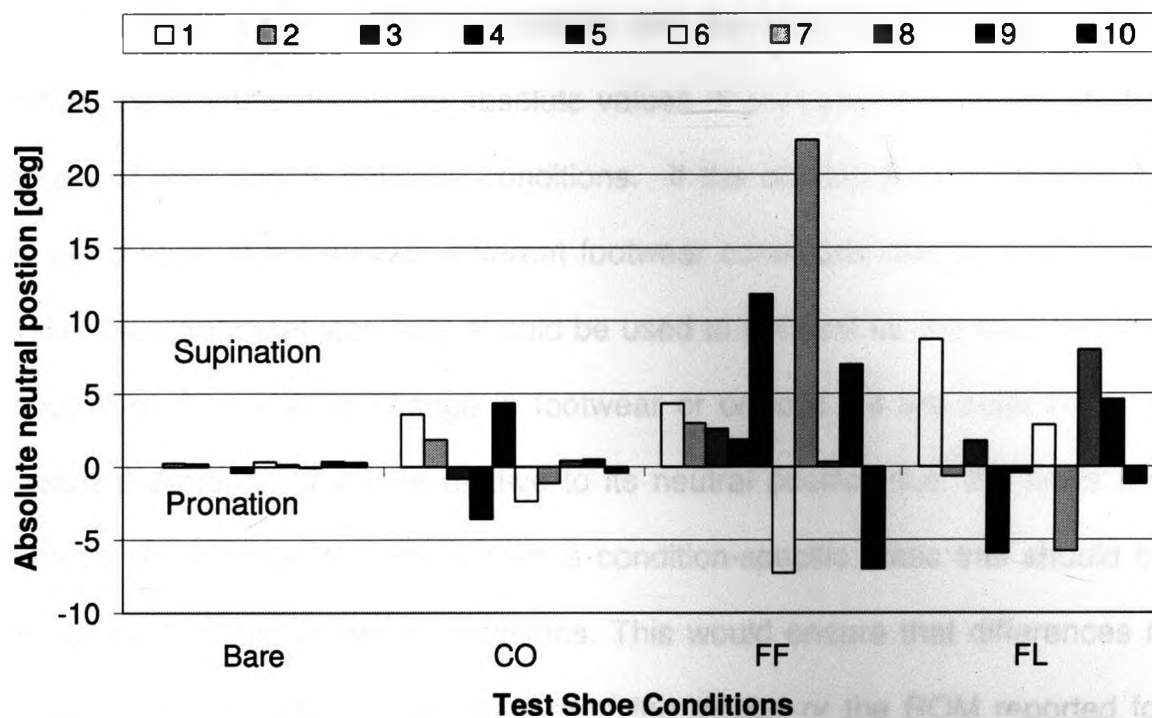


Figure 3.6: Neutral positions of the hindfoot with respect to midfoot in the frontal plane for 4 conditions over the 10 subjects. The hindfoot motion has the most variability across all subjects making conclusions difficult.

3.4 Discussion

The objective of this study was to compare four different neutral positions to assess if these created different interpretations between the shoe conditions that researchers may need to consider when planning their study methodology. As hypothesized, this study demonstrated that differences greater than the minimum important difference ($<5^\circ$) exist for the four inter-segmental kinematics between the neutral positions of the barefoot condition and the footwear conditions. Statistical significance was also demonstrated between two of the shoe conditions for two of the inter-segmental kinematics (bare compared to CO for Hallux and MLArch). Therefore care should be taken when establishing a research protocol that compares different footwear conditions. The condition-

specific differences in a neutral position can be important methodologically whether one is interested in the absolute values of joint angles or in the relative changes of joint angles between conditions. If the objective is to examine the absolute motion of a joint with different footwear conditions then a single static trial (i.e. barefoot quiet standing) should be used to account for the static change in neutral position due to change in footwear or orthotic. If the objective is to compare the motion of a joint relative to its neutral position (i.e. the limits and symmetry of its range of motion) then a condition-specific static trial should be used for each of the footwear conditions. This would ensure that differences in the static trials do not affect the pattern of the motion or the ROM reported for each condition. Examining the ROM of a particular foot joint with respect to the condition-specific neutral position may be important for examining the effects of a particular perturbation to the joint. As noted above, Stacoff et al.¹⁰ suggest that the foot may have a predetermined kinematic pattern that is maintained even when an intervention is introduced. Future research investigating these results is best done using a per-condition static trial. If a single common static trial was used in this case, then the absolute difference between the conditions, seen in comparing the static trials, could appear as a difference in the unchanged ROM.

However, potentially useful information may be lost when using condition-specific static trials. Quantifying the change in neutral position with different footwear, as obtained when using a single trial for determining the neutral position, may be important for identifying risks of injury. If during an activity, a subject moves past the active boundary of a joint's ROM and closer to the passive ROM boundary

the joint may be at risk of injury¹⁷. It has been suggested that as a joint moves close to the passive end range, the stress placed on surrounding tissue can cross the threshold for injury¹⁷. Accurately reporting the absolute joint position would be necessary to indicate whether the joint was moving toward the edge of its end of range during the dynamic tasks, and therefore at increased risk of soft tissue or bone injury. This would be missed if a condition-specific static trial were used. Table 3.2 is a summary of the strength and weaknesses of the single and per-condition static trials. As explained above each type of static trial can be beneficial or detrimental depending on the research question.

Table 3.2: Summary of strengths and weaknesses of single versus per-conditions static trials and neutral positions.

	Single neutral	Per-condition neutral
Strengths:	<p><u>Less variability in joint positions</u> -only one neutral trial is used, in this study it was the Barefoot condition which was the most consistent and least variable between subjects</p> <p><u>End-of-range information</u> -absolute joint positions can show whether a joint is close or exceeding its safe end-of-range -this could indicate a mechanism of injury or risk of injury during dynamic activities -end-of-range is often assessed statically in barefoot by clinicians, therefore using the barefoot neutral as the reference allows clinically significant joint positions to be identified</p>	<p><u>Joint symmetry information</u> -joint position measure with respect to a condition-specific neutral position indicates how symmetrically the ROM is around neutral -this is useful for footwear design and orthotic prescription</p> <p><u>Neutral position information</u> -the absolute positions of the condition-specific neutral positions are themselves of importance -footwear and orthotics will alter the neutral position of the foot joints, which is useful therapeutically and for improving performance</p>
Weaknesses:	<p><u>No joint symmetric information</u> -absolute joint positions are referred to the single, barefoot neutral -since the neutral position for each condition is not known, the symmetry of the ROM cannot be determined</p> <p><u>No neutral position information</u> -by only collecting a single neutral position, no static positioning information is known about the footwear or orthotic conditions</p>	<p><u>More variability in joint positions</u> -by using a neutral trial for each condition, the variability between subjects for the neutral position will be added to the relative joint positions reported -in this study, each of the footwear positions showed large variability</p> <p><u>No end-of-range information</u> -since joint positions are relative to condition-specific neutral, it is impossible to tell whether the joint is approaching or exceeding a dangerous limit</p>

This observation is relevant for researchers when developing their study methodology. Care should be taken when reviewing results from the literature regarding foot joint motion, footwear, range of motion and risk of injury. Further research on the end of joint range and how it affects different subjects will give more insight into the importance of establishing a proper static trial for each specific study objective.

The protocol here now needs to be expanded to dynamic trials. The change in ROM and the foot joint movement patterns need to be further investigated with a change in footwear using per-condition neutral trials, as well as an investigation using a common single neutral trial to assess the joint's proximity to end of range in different footwear conditions. However, techniques for measuring end of joint range are limited in the literature and should therefore also be further investigated.

3.5 References

1. Simon, J. et al. The Heidelberg foot measurement method: development, description and assessment. *Gait Posture* 23, 411-24 (2006).
2. Pohl, M. B., Messenger, N. & Buckley, J. G. Forefoot, rearfoot and shank coupling: effect of variations in speed and mode of gait. *Gait Posture* 25, 295-302 (2007).
3. McClay, I. & Manal, K. A comparison of three-dimensional lower extremity kinematics during running between excessive pronators and normals. *Clin Biomech (Bristol, Avon)* 13, 195-203 (1998).
4. MacLean, C., Davis, I. M. & Hamill, J. Influence of a custom foot orthotic intervention on lower extremity dynamics in healthy runners. *Clin Biomech (Bristol, Avon)* 21, 623-30 (2006).
5. Arndt, A. et al. Intrinsic foot kinematics measured in vivo during the stance phase of slow running. *J Biomech* 40, 2672-8 (2007).
6. Nester, C. et al. Foot kinematics during walking measured using bone and surface mounted markers. *J Biomech* 40, 3412-23 (2007).

7. Lundberg, A. Kinematics of the ankle and foot. In vivo roentgen stereophotogrammetry. *Acta Orthop Scand Suppl* 233, 1-24 (1989).
8. Hunt, A. E., Smith, R. M., Torode, M. & Keenan, A. M. Inter-segment foot motion and ground reaction forces over the stance phase of walking. *Clin Biomech (Bristol, Avon)* 16, 592-600 (2001).
9. Leardini, A., Benedetti, M. G., Catani, F., Simoncini, L. & Giannini, S. An anatomically based protocol for the description of foot segment kinematics during gait. *Clin Biomech (Bristol, Avon)* 14, 528-36 (1999).
10. Stacoff, A. et al. Effects of shoe sole construction on skeletal motion during running. *Med Sci Sports Exerc* 33, 311-9 (2001).
11. Nigg, B. M. & Wakeling, J. M. Impact forces and muscle tuning: a new paradigm. *Exerc Sport Sci Rev* 29, 37-41 (2001).
12. O'Connor, K. M., Price, T. B. & Hamill, J. Examination of extrinsic foot muscles during running using mfMRI and EMG. *J Electromyogr Kinesiol* 16, 522-30 (2006).
13. Hamill, J., Bates, B. T. & Holt, K. G. Timing of lower extremity joint actions during treadmill running. *Med Sci Sports Exerc* 24, 807-13 (1992).
14. Jenkyn, T. R. & Nicol, A. C. A multi-segment kinematic model of the foot with a novel definition of forefoot motion for use in clinical gait analysis during walking. *J Biomech* 40, 3271-8 (2007).
15. Jenkyn, T. R., Anas, K. & Nichol, A. Foot segment kinematics during normal walking using a multisegment model of the foot and ankle complex. *J Biomech Eng* 131, 034504 (2009).
16. Anas, K. & Jenkyn, T. R. in *ISB XXth Congress - ASB 29th Annual Meeting (Cleveland, Ohio, 2005)*.
17. Rodrigues, P., Tomasko, A. & Hamill, J. in *The Eighth Footwear Biomechanics Symposium, XXI Congress of the International Society of Biomechanics (Taipei, 2007)*.

Chapter 4 – Quantifying Skin Motion Error in Optical Tracking of a Multi-Segment Foot Model using Single-Plane Fluoroscopy

Optical gait analysis, as mentioned in Chapter 1, works by affixing reflective markers on the body that are visible to infrared or strobe cameras. It is common practice to discuss the movement of the underlying bones based on the marker movements. The error associated with this is called soft tissue artifact (STA) since it is the movement of the soft tissue that could make the marker move independent of the underlying bone. The study detailed in this chapter aims to assess the STA associated with the multi-segment foot model marker set used in subsequent chapters. A 2D Fluoroscope study investigates the STA of the calcaneus and the navicular. The results from this study should increase the confidence with which the joint kinematics measured with a multi-segment foot model and optical motion system are analyzed, since the magnitude and nature of the STA has been quantified.

This chapter will be submitted for publication as an original paper in Journal of Biomedical Engineering.

Shultz, R – developed experiment, analyzed all results and wrote the paper

Jenkyn, TR – senior author - helped design the protocol and helped analyze the results

4 Abstract

During a standard gait analysis, passive reflective or active markers are placed on the skin and used as landmarks for an optical motion capture system to track the body's three-dimensional motion. The trajectories of these skin-mounted markers are assumed to be an adequate representation of the underlying bone motions. However, it is generally accepted that some relative motion occurs between the bones and the skin-mounted markers. Soft tissue artifact (STA) is the error associated with the movement of the soft tissue with respect to the underlying bone. This study aims to quantify the STA associated with a novel multi-segment foot model developed by Jenkyn and Nichol (2007) to track joint kinematics between segments of the foot.

The model uses marker triad clusters on the hindfoot, midfoot, lateral forefoot, medial forefoot and hallux to track the six-degree-of-freedom segment kinematics during functional activities. To quantify the STA of the hindfoot and midfoot clusters, fluoroscopic images were collected on 27 subjects during four quasi-static positions, 1) quiet standing (non-weight bearing), 2) at heel strike (weight bearing) of walking stance phase, 3) at midstance (weight bearing) and 4) at toe-off (weight bearing). Further research will examine the STA associated with the other three clusters of the model.

To quantify STA, the translation and rotation of the cluster-fixed coordinate systems were calculated with respect to the bone-fixed coordinate systems in the sagittal plane. The average translational difference was from 5.90 ± 7.29 mm

(HeelStrike(HS)-Quite Standing (QS)) to 12.15 ± 0.25 mm (Toe Off (TO)-QS) for the calcaneus and -7.57 ± 7.58 mm (HS-QS) to -16.42 ± 16.68 mm (TO-QS) for the navicular. The average rotational differences were $0.13 \pm 2.23^\circ$ (HS-QS) to $0.24 \pm 0.48^\circ$ (MS-QS) and $-0.62 \pm 0.88^\circ$ (HS-QS) to $-0.73 \pm 0.70^\circ$ (TO-QS), for the calcaneus and navicular, respectively. The maximum translational STA found in this study (16mm for the navicular), is smaller than the STA reported in the literature for the thigh (up to 44mm) or the lower leg (up to 21mm), but is larger than the STA found for point markers affixed to the foot (4.3 mm). This is perhaps due to the use of marker triad clusters that consist of markers on wands attached to a base affixed to the foot, which would tend to increase the inertial and vibrational motions compared to simple point markers. Overall, this study quantifies that the soft tissue artifact of midfoot and hindfoot marker clusters are comparable with STA found in the literature.

4.1 Introduction

Optical motion analysis systems work by tracking passive reflective or active markers placed on the skin surface and triangulating their spatial position in three dimensions with great speed and accuracy. Marker trajectories are considered an adequate representation of the motion of the underlying bone for identification of subjects with gross pathologies compared to healthy individuals, despite the fact that there is relative motion between the tissues^{1,2}. Between the bone and the skin surface where the marker resides is soft tissue, including muscle and fat, which moves throughout any dynamic activity³. Soft tissue artifact (STA) is the error associated with the skin markers moving relative to the underlying bone due to inertial effects, skin deformation and sliding, and deformation due to muscle contraction^{2, 3}. STA is a detrimental error for gait analysis using optical methods with skin surface markers since the kinematics derived from any marker set will be incorrect⁴. Developing a general algorithm to correct for STA is difficult since STA is both a systematic and random error², is specific to the configuration of the marker set and marker locations⁵, and is dependent on the nature of the activity being performed^{2, 6}.

Studies quantifying the STA have primarily focused on the knee^{4, 6-9} with limited research focused on the ankle^{10, 11} and the foot¹². STA has also been shown to be joint specific¹³ due to different muscle, ligaments and fat dispersed between the bone and the marker. Therefore understanding the amount of STA at one joint or of one segment does not aid in the correction of another joint's kinematics.

Markers attached to inter-cortical pins drilled directly into the bone eliminates STA^{1, 11, 13, 14}, however, the effect of this invasive procedure on the gait pattern of the foot is still not well understood¹⁴. This technique, when simultaneously employed with skin mounted markers, has been used to quantify the STA in the knee^{1, 3, 6, 9, 13}. In these studies, the kinematics of the joint were calculated using both skin mounted markers and markers attached to the bone pins. The difference in kinematics measured between the two techniques was considered to arise from tissue movement. Using this method during walking, 73% of the kinematic data showed a greater than 5° difference between joint angles calculated with skin mounted and bone pin marker sets, with the greatest difference being at the navicular/cuboid segment with respect to the tibia¹. Also, calcaneal eversion/inversion was found to be overestimated by markers mounted to the shoe (rather than the skin) during running by 34.7% (4.6°)¹⁵.

The use of x-ray fluoroscopy instead of more invasive bone pins may be a better technique to compare skin mounted marker movement to the movement of the underlying bone. Fluoroscopy is a non-invasive procedure that allows direct visualization of bone motion with a low radiation dosage rate¹⁶. As a consequence, fluoroscopy is becoming a useful tool in foot biomechanics research. A group of studies by Lundberg et al. in the late 1980s, among others, used fluoroscopy to assess the kinematics of the ankle and foot¹⁶⁻²⁵. Fluoroscopes have been used to examine the changes in the calcaneal pitch, which is an indirect measure of the subtalar joint, during the stance phase of walking gait²⁵. Participants walked across a platform while fluoroscopic images

of the foot in the sagittal plane were captured at various points of the gait cycle²⁵. Difficulties arose when trying to find a consistent gait velocity that would allow the researchers to capture the desired frames. Other studies combined fluoroscopy with other imaging tools to examine the ankle joint complex and the foot^{23, 24}. Digital radiographic fluoroscopy with an optical contact pressure display method was used to develop and validate a foot model²⁴. Fluoroscopy data, skeletal dynamics and active muscle force loading was used to fit the model to six simulated gait positions, including heel strike, midstance, and toe-off. Another study used dual-orthogonal fluoroscopes and magnetic resonance imaging (MRI) techniques to investigate the ankle joint complex²³. Multiple weight bearing and non-weight bearing, static and quasi-static positions were captured. A three-dimensional model was developed using the MRI images and then, similar to Gefen et al.²⁴, the orthogonal fluoroscopic images were used to place the model in the desired positions. One foot study used fluoroscopy to test the rigidity of the clinically popular triangle foot model¹⁶. Using the actual bone movement obtained from the fluoroscope images to assess functional units based on foot rigidity, the authors proposed a new foot model for clinical practice with a hinge joint at the anterior talus and the metatarsophalangeal joint.

Recent studies have also used x-ray fluoroscopy to assess STA at the knee⁴ and simple static x-rays to examine STA at the foot¹². One study involved subjects in quiet standing for three weight bearing positions while two-dimensional roentgen photogrammetry captured images of point markers located on the medial malleolus, the navicular, the medial aspect of calcaneus and the base and head

of the fifth metatarsal and the first metatarsal¹². The error associated with the translational motion in the sagittal plane was calculated for these point markers and found to be 4.3mm¹².

The objective of this study is to use x-ray fluoroscopy to estimate the soft tissue artifact of the skin mounted marker set used with the multi-segment foot model developed by Jenkyn et al^{26, 27}. This model was developed as a clinical tool and incorporates a special marker set of four foot marker triad clusters that are placed on the skin adjacent to the calcaneus, the navicular, the first metatarsal and the fifth metatarsal. It is hypothesized that the greater distance from the foot of the reflective markers on the triad clusters, compared to single (point) markers placed directly on the skin, will increase the STA error arising from inertial effects. Nonetheless, the cluster markers are expected to possess less STA than the soft tissue artifact observed at other locations on the lower extremity.

4.2 Methods

4.2.1 Subjects

Twenty-seven participants volunteered for this study in the Wolf Orthopaedic Quantitative Imaging Laboratory (WOQIL) at the Fowler Kennedy Sport Medicine Clinic. All participants had no previous foot or ankle disorders or malalignment, and no foot or ankle injury in the previous six months prior to the study. Approval was attained from the relevant ethics committee at the authors' university. All participants gave informed written consent before testing began and were screened to ensure that he/she was not 1) pregnant, 2) exposed to

radiation as a part of his/her occupation or 3) had two or more X-ray procedures of any type due to injury or illness in the past 12 months.

4.2.2 Equipment

The WOQIL is equipped with a C-arm x-ray fluoroscope (SIREMOBIL Compact-L; Siemens Medical Solutions USA Inc., Malvern, PA) with a nine-inch image intensifier. Automatic contrast control was engaged, but the average exposure factors were 0.89 ± 0.11 mA and 56.9 ± 0.9 kVp over all the subjects. The complete imaging sequence of a testing session required a total of 60 seconds of x-ray exposure, which corresponded to a dosage of 4.2 mSv (at an approximate dose rate of 0.07 mSv/s). All fluoroscopic images were captured with a digital video capture device and accompanying software (DVD Xpress DX2; ADS Technologies, Cerritos, CA) and stored in digital format on a laboratory control PCs. Details of the equipment set up can be found in Dunk et al.²⁸.

The fluoroscope was positioned horizontally to achieve a sagittal plane view of the calcaneus and the navicular throughout the range of foot motion tested. Fluoroscopic data were collected at 60 interlaced frames per second.

Custom-made marker triad clusters were developed with lead beads (1mm diameter) placed in the center of Delrin balls (8mm diameter). The Delrin balls were covered with reflective tape (3M, Minneapolis, MN) and attached to carbon-fiber wands (Figure 4.1). These markers could then be recognizable to an optical motion capture system while the lead beads were visible under fluoroscopy. The three wands of each triad were affixed to plastic bases that were affixed to the skin of the foot with double-sided tape (3M, Minneapolis, MN).

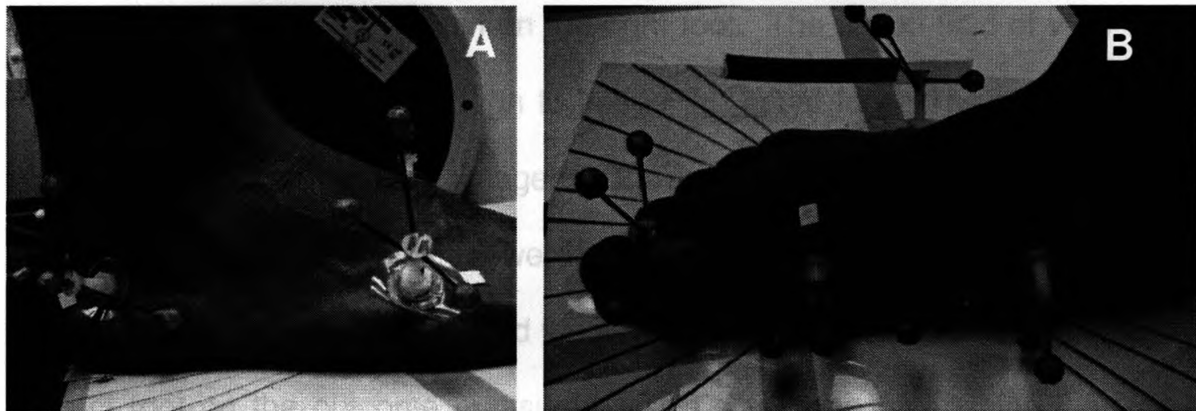


Figure 4.1. Custom-built marker triad clusters visible to both the fluoroscopic and the optical motion capture systems. Lateral (A) and medial (B) views of the foot show the placement of the marker triad clusters in the locations described by Jenkyn et al. (2007). The blue lines visible on the platform in both photos are the out-of-plane orientation references in 5 degree increments.

A platform was designed to position the subject's foot in the center of the fluoroscope's field of view. The platform was required since the C-arm of the fluoroscope could not be lowered to ground level. Blue lines were drawn on the platform in 5 degree increments of out-of-plane rotation, ranging from 30 degrees to -30 degrees with respect to the plane of the fluoroscope (see Figure 4.1). These lines ensured that the same plane of motion was used for each quasi-static condition and to calculate an average projection error due to out-of-plane rotation.

4.2.3 Testing Procedure

Leaded clothing was placed over the subject's upper and lower body, including a thyroid collar and protective eyewear so that only the feet were exposed to the x-ray beam. The marker triad clusters were attached to five locations on the foot, superficial to five bones (navicular, first metatarsal, fifth metatarsal, calcaneus

and first phalange of the hallux) on the right foot. The 9-inch field of view of the fluoroscope was not large enough to image the entire foot. Therefore, only the hindfoot and midfoot were imaged. Consequently, only the data from the navicular and calcaneus clusters were used in this study.

The first phase of testing quantified the influence of out-of-plane orientation of the subject foot on the outcome measures. This was done by imaging the foot at different orientation with respect to the fluoroscope, from -30 degrees to +30 degrees at 5-degree increments. The line connecting the second ray and the middle of the posterior calcaneus was aligned with each line drawn on the platform.

From the 13 orientations, the x-ray technologist then chose the orientation that had the best visualization of the navicular and calcaneus bones. The second phase of testing was then carried out at this orientation with respect to the fluoroscope. It turned out that testing for all trials of all 27 subjects was carried out between 5 degrees and -5 degrees, and most often at 0 degrees (i.e. parallel to the plane of the fluoroscope).

The second phase of testing consisted of capturing images of the calcaneus and navicular in four quasi-static positions, 1) quiet standing (non-weight bearing), 2) at heel strike (weight bearing), 3) at midstance (weight bearing) and 4) at toe-off (weight bearing). The subjects imitated one gait step per condition with their right foot and stopped at the appropriate point in stance phase for each condition for an image to be captured.

4.2.4 Analysis

The digital fluoroscopic images were saved as *.tif files (Adobe Illustrator; Adobe Systems Incorporated, San Jose, CA) and imported into custom-written software (Matlab; The MathWorks, Inc, Natick, MA). The center of each marker on the two triad clusters and eight bony landmarks were manually digitized. The specific targets on the images of each of the bones were digitized to obtain the x- and y-coordinates in the image frame of reference^{29, 30}. Table 4.1 describes the bony landmarks chosen to define the navicular and calcaneus and Figure 4.2A shows the points within the image.

Table 4.1. Location of the manually digitized landmarks for the navicular and the calcaneus.

Bony Landmark	Description
Navicular – 1	Anterior, superior corner (dorsal surface)
Navicular – 2	Posterior, superior corner (dorsal surface)
Navicular – 3	Anterior, inferior corner (navicular tuborsity)
Navicular – 4	Posterior, inferior corner (navicular tuborsity)
Calcaneus –1	Superior point of the articular surface for cuboid (anterior border of calcaneus)
Calcaneus –2	Inferior point of the articular surface for cuboid (anterior border of calcaneus at concave point formed by articular surface for cuboid and the anterior articular surface of the talus)
Calcaneus –3	Posterior, superior border of the posterior surface; the posterior border of the Achilles tendon attachment
Calcaneus –4	Posterior border of the inferior surface; the superior border of the plantar fascia attachment.

Two-dimensional coordinate systems were constructed for each of the two marker triad clusters and for the calcaneus and navicular bones. For the calcaneus bone-fixed coordinate systems, the x-axis was the bone's longitudinal axis defined as the unit vector formed from the midpoint of anterior pair of digitized bony landmarks to the midpoint of the posterior pair of bony landmarks (see Figure 4.2A). For the navicular bone-fixed coordinate system, the x-axis was defined as the unit vector from the midpoint of the superior pair of digitized bony landmarks to the midpoint of the inferior pair of bony landmarks (see Figure 2.4A).

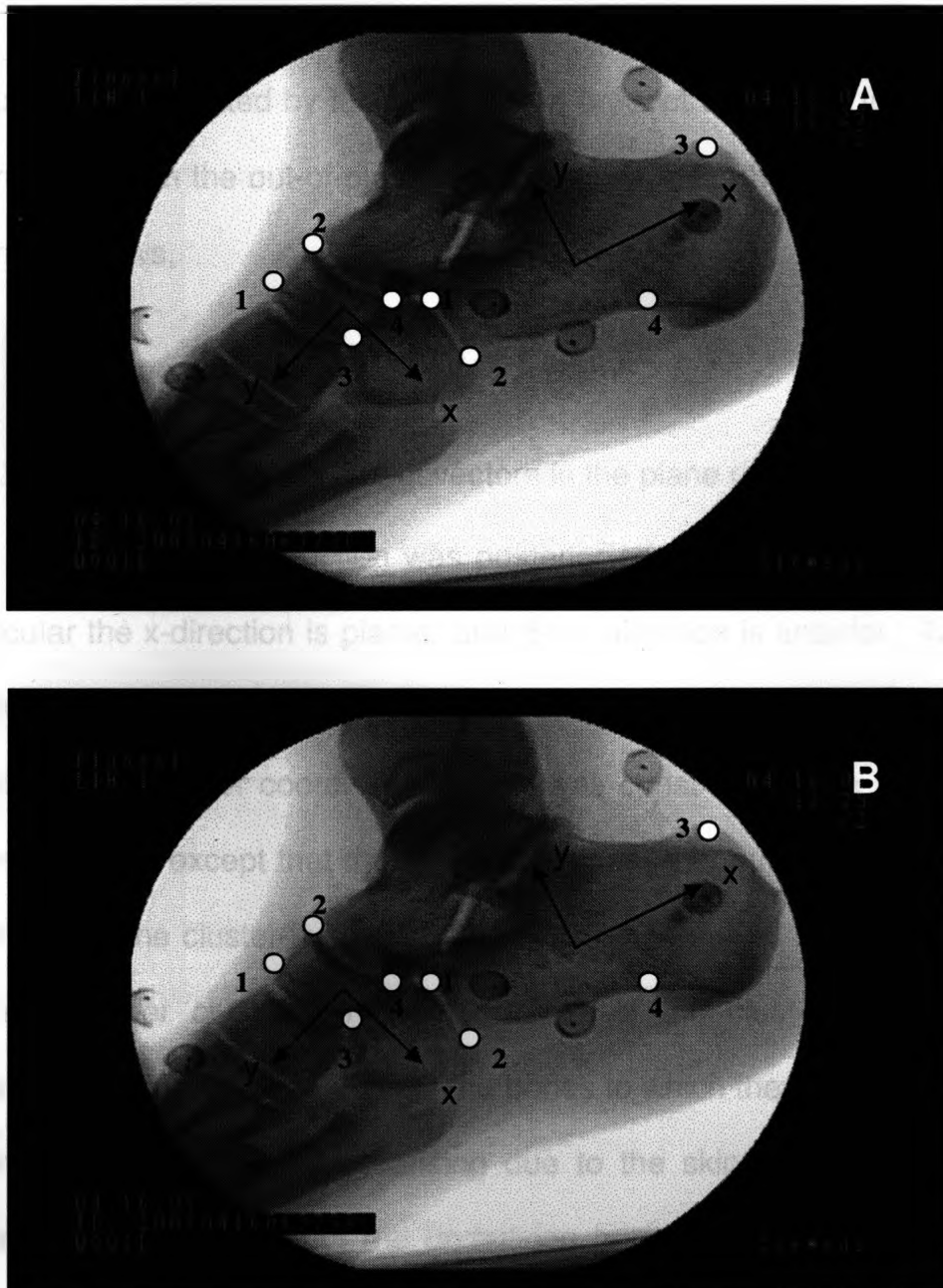


Figure 4.2. Fluoroscopic image of the midfoot and hindfoot in the sagittal view. A) The bony landmarks that were manually digitized to define the bone-fixed reference frames on the navicular and calcaneus are shown as white dots (four per bone). The orientations of the bone-fixed x and y axes are also shown. B) The coordinate systems for the marker clusters and the bones are shown for the navicular and calcaneus bones. The dashed lines represent the origin displacement length between the associated bone and marker systems. The β represents the segment angle between the two systems. Only β for the calcaneus is shown.

The y-axis was calculated by taking the cross product of the unit vector in the x-direction and that in the out-of-plane z-direction to obtain the unit vector in the y-direction as follows,

$$(\bar{y}, 0) = (\bar{x}, 0) \times (0, 0, -1) \text{ and } \hat{y} = \frac{\bar{y}}{\|\bar{y}\|} \quad \text{Eqns. 1, 2}$$

where \bar{x} and \bar{y} are two-dimensional vectors in the plane of the image.

For the calcaneus, the x-direction was posterior and the y-axis dorsal, while for the navicular the x-direction is plantar and the y-direction is anterior. The origins of the two bone-fixed systems were defined at the centroid of the four bony landmarks. The marker coordinate system was constructed in a similar way to the bone systems, except that the x-axis was defined from marker 1 to marker 2 on each triad. The cluster-fixed system origins were also at the centroids of the three markers per cluster. The orientations of the cluster-fixed coordinate systems were arbitrary with respect to the bones to which they were attached.

To quantify the amount of error arising due to the skin-mounted marker triad cluster moving with respect to the underlying bone, the distance between the cluster and bone-fixed system origins and the relative orientations of the two systems was calculated. With no skin motion error, the vector between the origins should be constant in magnitude. The magnitude, or 'origin displacement length' l , was found as follows (Figure 4.2B),

$$l = \left\| \bar{O}_{bone} - \bar{O}_{cluster} \right\| \quad \text{Eqn. 3}$$

where \bar{O}_{bone} is the bone-fixed origin and $\bar{O}_{cluster}$ is the cluster-fixed origin.

The relative orientation of the cluster-fixed and bone-fixed systems was defined by the 'segment angle' between the x-axes of each system. The segment angle was found as follows,

$$\theta = \arccos(\hat{x}_{bone} \cdot \hat{x}_{cluster}) \quad \text{Eqn. 4}$$

The origin displacement lengths and segment angles for the navicular and calcaneus in quiet standing (QS) were taken as the reference values. The lengths and segment angles at each of the three stance phase foot positions (heel strike, HS; midstance, MS; and toe-off, TO) were compared to the values in QS. In the absence of any skin motion error, the differences between the values at HS, MS and TO and the reference position QS should be zero.

For a subset of five subjects, the same bone-fixed and marker-fixed coordinate systems were constructed for each of the 5-degree interval positions ranging from 30 to -30 degrees out-of-plane with the subject in quiet standing. This was done to quantify any error arising from incorrect positioning (i.e. out-of-plane orientation) of the foot with respect to the fluoroscope. The same origin displacement length between bone-fixed and marker-fixed system origins was calculated for each position. The zero-degree foot position was taken to be the reference condition for this data series. If there was a perspective error that arises due to out-of-plane orientation affecting the origin displacement lengths and segment angles, then this could be quantified at each of the 5-degree out-of-plane intervals.

To test the intra-test repeatability of manual digitization of markers and bony landmarks, ten fluoroscopic images were blinded and digitized twice by the same investigator in random order. This was the same investigator who digitized all fluoroscope images in the current study. Root mean squared values were calculated using the formulas found in Gluer et al.³¹. Individual standard deviations were found using each set of images.

To ensure that the measurements made were true (i.e. in millimeters, mm) a grid was built to calculate the scale factor of mm per pixel (Figure 4.3). The distance between each set of holes was machined to be 15mm, accurate to 50 microns. The scale factor was determined to be 0.3 mm/pixels in each direction. All positions digitized from the images were multiplied by this scale factor to give true measurement in mm.

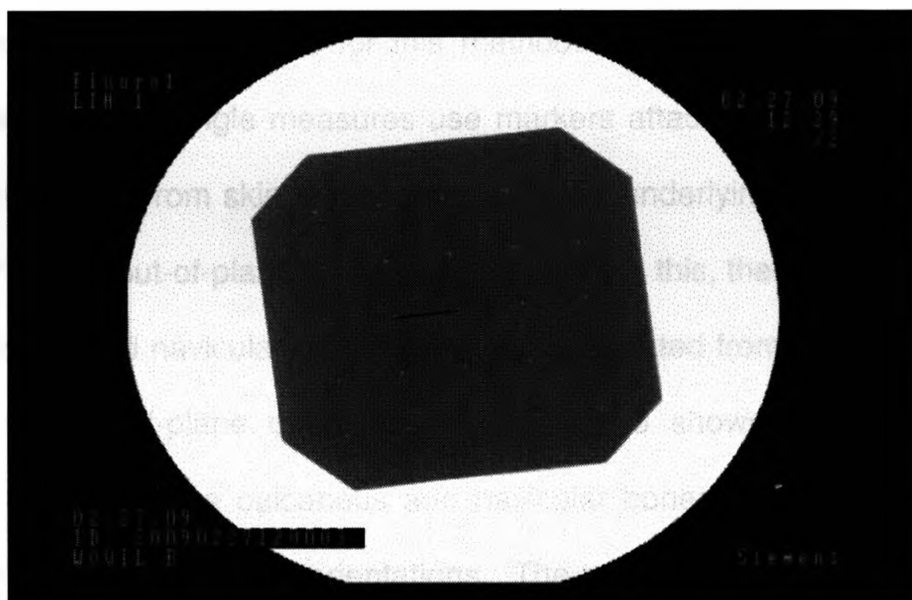


Figure 4.3. Fluoroscopic image of the grid that was used to calculate the scale factor to transfer from pixels to mm. There is 15 mm between each hole set.

4.3 Results

For the out-of-plane testing on a subset of five subjects, two subjects were eliminated due to lack of visibility of the markers in all the digital images. Figures 4.4 and 4.5 show the change in origin displacement length (Figure 4.4) and the segment angle (Figure 4.5) from their true values due to a changing out-of-plane orientation of the foot. The results on the remaining subjects showed that between and including -5-degrees to 5-degrees out-of-plane orientation the projection errors were less than $10.0 \pm 8.5\text{mm}$ (for navicular marker) and $7.6 \pm 2.2\text{mm}$ (for calcaneal marker) for the origin displacement length and less than $0.69 \pm 0.55^\circ$ (for navicular marker) and $0.1 \pm 0.18^\circ$ (for calcaneal marker) for the segment angle. Errors arising from orientations of more than 5 degrees were considered unacceptably large. All the data for this study were collected within the range of -5 to 5-degrees out-of-plane, so these values can be taken as the linear and angular accuracies for this method. Since the origin displacement length and segment angle measures use markers attached to the skin, some of the error will arise from skin motion relative to the underlying bones, and will not be purely due to out-of-plane projection. To address this, the apparent lengths of the calcaneus and navicular bones were also calculated from bony landmarks at each of the out-of-plane orientations. Figure 4.6 shows the change in the apparent lengths of the calcaneus and navicular bones, along their long axes, due to changing out-of-plane orientations. The maximum change in bone length from their true lengths was $1.4 \pm 1.2\text{mm}$ for the calcaneus and $2.3 \pm 2.9\text{mm}$ for the navicular.

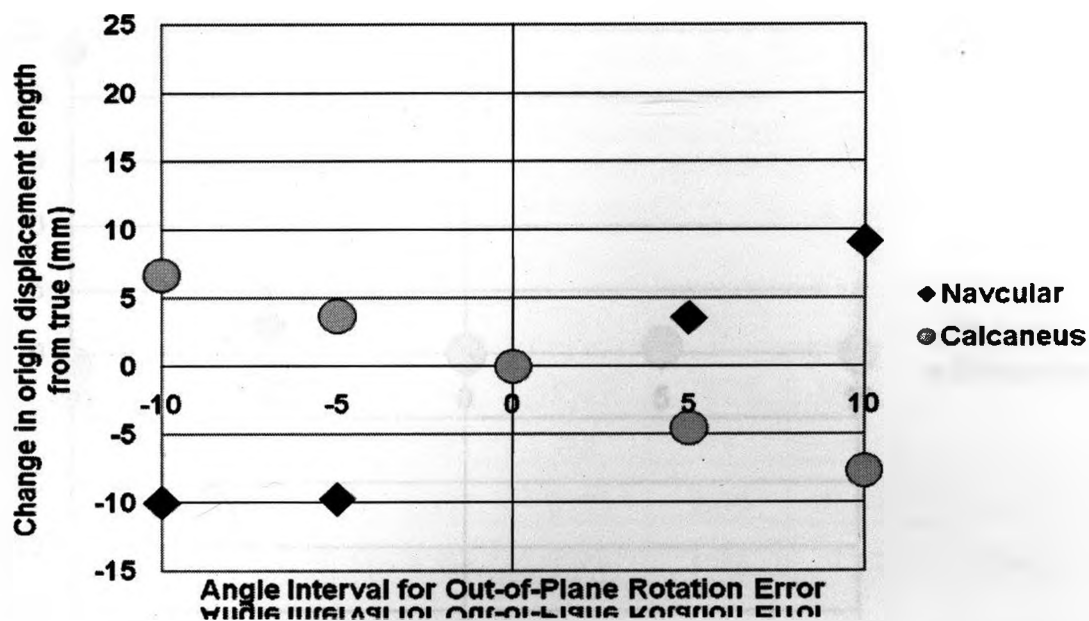


Figure 4.4. Change in the origin displacement length from the true length for the calcaneus (solid line) and the navicular (dashed line) with out-of-plane orientation. The differences between the two values in quiet standing at the zero-degree reference position and ± 5 -degrees out-of-plane positions were less than 10.0 ± 8.5 mm. The out-of-plane errors in origin displacement length for out-of-plane orientations greater than 5-degrees were considered unacceptably large.

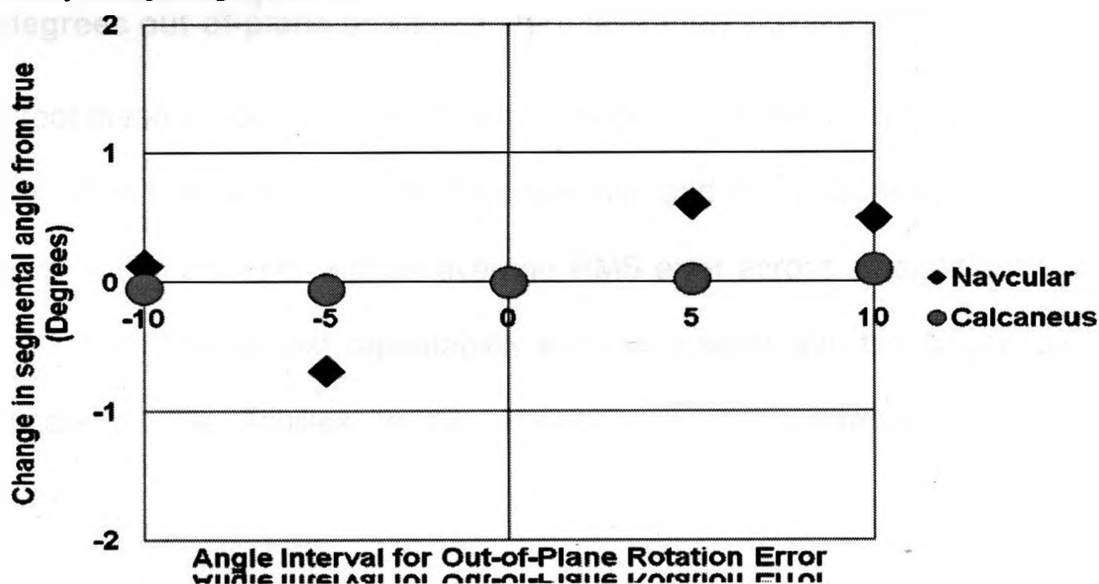


Figure 4.5. Change in the segment angle for the true angle for the calcaneus (solid line) and the navicular (dash line). The differences between the two values in quiet standing at the zero-degree reference position and ± 5 -degrees out-of-plane positions were less than $0.69 \pm 0.55^\circ$. Errors for out-of-plane orientations greater than 5-degrees were considered unacceptable.

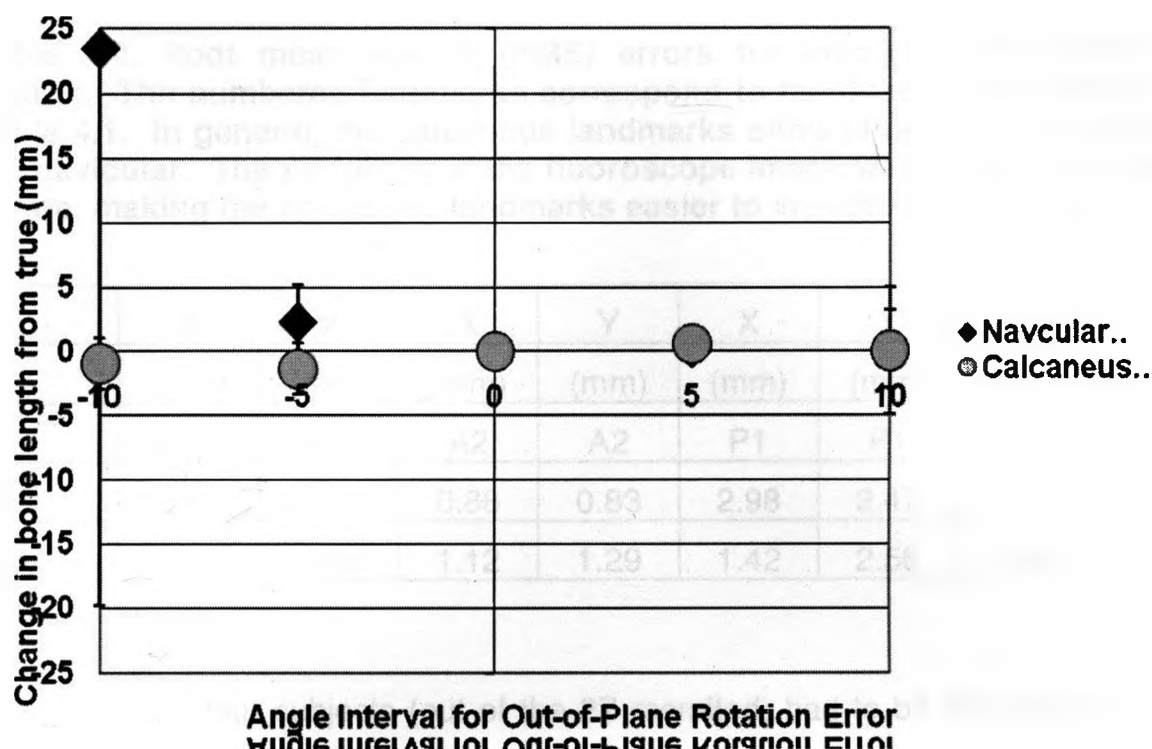


Figure 4.6. Change in the apparent length of the calcaneus (solid line) and the navicular (dashed line) bones from true length. The differences between the two values in quiet standing at the zero-degree reference position and ± 5 -degrees out-of-plane positions were less than 2.37 ± 2.90 mm.

The root mean squared errors (shown in Table 4.2) for the intra-rater repeatability testing show that all eight points (four navicular and four calcaneal) were digitized at worst within 2.7 mm, with an average RMS error across all eight points being 1.3 ± 0.7 mm. The largest repeatability error was seen with the calcaneus bony landmark 3, the Achilles tendon insertion on the posterior aspect of the calcaneus.

Table 4.2. Root mean square (RMS) errors for intra-rater repeatability testing. The numbered landmarks correspond to the descriptions listed in Table 4.1. In general, the calcaneus landmarks showed better results than the navicular. The periphery of the fluoroscope image was clearer than the centre, making the calcaneus landmarks easier to visualize and digitize.

	X	Y	X	Y	X	Y	X	Y
	(mm)	(mm)	(mm)	(mm)	(mm)	(mm)	(mm)	(mm)
	A1	A1	A2	A2	P1	P1	P2	P2
CAL	0.57	0.61	0.88	0.83	2.98	2.47	0.90	1.47
NAV	0.84	1.16	1.12	1.29	1.42	2.58	0.66	1.03

The data from four subjects (out of the 27 recruited) had to be discarded since lack of focus in the fluoroscopic images made the bony landmarks and marker beads undetectable. For the remaining 23 subjects, the complete analysis was applied. Table 4.3 lists the differences in origin displacement lengths for the heel strike (HS), midstance (MS) and toe-off (TO) conditions with respect to quiet standing (QS) for the calcaneus and navicular for each of the 23 subjects analyzed. For the calcaneus at HS the average difference for the origin displacement length compared to QS was 5.90 ± 7.29 mm. The difference was 6.46 ± 7.76 mm for the MS condition and -12.15 ± 0.25 mm for TO. For the navicular the average differences in origin displacement length with respect to QS were -7.57 ± 7.58 mm, -7.61 ± 7.61 mm and -16.42 ± 16.68 mm for HS, MS and TO respectively.

Table 4.3. The difference in origin displacement length between the stance phase instances of heel strike (HS), mid-stance (MS) and toe-off (TO) with respect to the quiet standing (QS) reference position. This is the change in distance between the origin of the bone-fixed coordinate system and the marker-fixed coordinate system with respect to QS. These are shown for each of the test subjects, with the average, standard deviation and range stated in the bottom four rows. The largest differences for both the calcaneus and the navicular were seen at toe-off (TO).

Subject	Calcaneus (mm)			Navicular (mm)		
	HS	MS	TO	HS	MS	TO
1	4.48	4.53	-11.96	-7.37	-7.43	10.51
2	4.70	7.63	-12.13	-7.74	-7.78	28.08
3	8.56	1.81	-11.74	-7.72	-7.44	5.97
4	14.79	13.36	-12.11	-7.66	-7.72	9.29
5	1.64	-1.49	-12.27	-7.73	-7.44	7.73
6	8.30	15.47	-12.21	-7.85	-7.71	7.02
7	11.05	8.23	-11.90	-7.48	-7.70	20.99
8	-10.01	-3.14	-12.43	-7.37	-7.86	17.53
9	12.81	-0.48	-12.32	-7.75	-7.68	1.49
10	7.45	10.92	-11.86	-7.46	-7.38	0.90
11	11.92	10.99	-12.24	-7.60	-7.86	28.98
12	-2.66	-0.31	-12.49	-7.69	-7.68	22.81
13	-7.69	-7.45	-12.42	-7.81	-7.88	11.83
14	-8.58	-9.12	-12.04	-7.59	-7.58	8.28
15	2.64	1.99	-11.59	-7.01	-7.15	37.68
16	8.25	10.08	-11.93	-7.00	-7.34	30.48
17	4.72	9.34	-12.35	-7.72	-7.80	7.51
18	11.12	13.64	-12.17	-7.28	-7.56	14.38
19	8.08	5.47	-12.37	-7.89	-7.79	12.40
20	14.89	14.85	-12.39	-7.82	-7.78	22.08
21	4.76	6.71	-12.23	-7.65	-7.68	26.08
22	14.34	20.97	-11.88	-7.04	-7.20	16.21
23	10.18	14.55	-12.48	-7.89	-7.51	29.33
Average	5.90	6.46	-12.15	-7.57	-7.61	16.42
Standard Deviation	7.29	7.76	0.25	-7.58	-7.61	16.68
Max	14.89	20.97	-11.59	-7.00	-7.15	37.68
Min	-10.01	-9.12	-12.49	-7.89	-7.88	0.90

Table 4.4 lists the differences in segment angle for the HS, MS and TO stance phase instances with respect to the QS condition for each of the test subjects. It also shows average, standard deviation and range of values for the calcaneus and navicular bone. All three stance phase instances (HS, MS and TO) for both the calcaneus and navicular bones saw less than 1° change in angular orientation with respect to QS. For the calcaneus the differences were $0.13 \pm 2.23^\circ$ for the HS, $0.24 \pm 0.48^\circ$ for the MS, and $0.17 \pm 0.56^\circ$ for the TO, and for the navicular these values were $-0.62 \pm 0.88^\circ$, $-0.62 \pm 0.91^\circ$, $-0.73 \pm 0.70^\circ$, for the HS, MS and TO, respectively.

Table 4.4. The difference in segment angle between the stance phase instances of heel strike (HS), mid-stance (MS) and toe-off (TO) with respect to the quiet standing (QS) reference position. This is the change in orientation of the bone-fixed x-axis and the marker-fixed x-axis with respect to QS. These are shown for each of the test subjects, with the average, standard deviation and range stated in the bottom four rows. The mean for all conditions of the calcaneus and navicular is shown to be less than one degree with standard deviations at approximately 0.5-1 degrees, except for the calcaneus at heel strike (HS). The range of all other values is 2-3 degrees whereas again the calcaneus at heel strike is less than the other conditions.

Subject	Calcaneus (degrees)			Navicular (degrees)		
	HS	MS	TO	HS	MS	TO
1	0.03	-0.04	-0.03	0.83	0.05	-0.16
2	0.00	-0.01	-0.12	-1.30	-1.18	-1.31
3	0.10	-0.04	0.00	0.04	-1.10	-0.19
4	-0.07	0.02	0.07	-1.71	-0.92	-1.12
5	-0.06	0.12	-0.12	-0.85	-1.16	-0.17
6	0.29	0.95	0.08	0.36	-1.53	-1.09
7	0.13	-0.08	0.20	-1.43	-0.33	-1.05
8	-0.06	-0.10	-0.08	-0.05	0.04	-1.57
9	0.43	0.49	0.46	-1.18	-1.21	-0.97
10	0.30	0.33	0.12	-1.13	-0.24	0.02
11	0.07	0.10	0.16	0.03	-0.72	-1.57
12	-0.01	-0.12	-0.04	-0.48	-1.02	-0.97
13	0.06	0.07	0.00	-1.74	-1.40	-1.64
14	-0.01	-0.05	-0.13	-1.63	-0.69	-0.64
15	0.13	0.23	0.17	-1.45	1.25	0.79
16	0.11	0.30	0.23	0.58	1.27	0.17
17	0.28	0.38	0.29	-1.30	-1.11	-1.39
18	0.23	0.40	0.06	0.06	0.34	-0.57
19	0.09	0.21	0.11	-1.43	-1.67	-1.34
20	0.41	0.01	0.03	-0.77	-1.45	-1.31
21	-0.12	-0.06	-0.13	-1.01	-0.87	-0.97
22	0.33	0.35	0.03	0.13	1.16	0.63
23	0.22	2.09	2.64	1.13	-1.67	-0.42
Average	0.13	0.24	0.17	-0.62	-0.62	-0.73
Standard Deviation	0.16	0.48	0.56	0.88	0.91	0.70
Max	0.43	2.09	2.64	1.13	1.27	0.79
Min	-0.12	-0.12	-0.13	-1.74	-1.67	-1.64

4.4 Discussion

This study aimed to estimate the soft tissue artifact (STA) occurring between the calcaneus and navicular bones, and the marker triad cluster positioned on the skin superficial to these bones. The toe-off position of the foot was shown to have the highest average STA error, of 16.42 ± 16.68 mm for the navicular and 12.15 ± 0.25 mm for the calcaneus, compared to the other positions during stance phase that experienced approximately half the error.

The muscle contraction patterns that occur at toe-off may explain the increased STA found in this position compared to quiet-standing since the muscles adjacent to the attachment sites of the marker triads are suspected to act differently at toe-off compared to quiet-standing. The calcaneal marker cluster was placed on the lateral side of the hindfoot, close to the sheathes of the peroneus longus and the peroneus brevis that pass posterior to the lateral malleolus. These tendons act to depress the first metatarsal head and elevate the fifth metatarsal base throughout the stance phase, except at toe-off³². The navicular marker was also placed near tendons on the medial side of the foot. The tibialis anterior inserts near where the navicular marker cluster was affixed. This muscle tends to concentrically contract around toe-off in anticipation of the need to help the foot clear the floor during the swing phase³³. This muscle also tends to eccentrically contract from heelstrike to midstance³³ resulting in a different positioning of the navicular cluster at toe-off. Another tendon that may effect the navicular cluster toe-off position differently than the other two positions is the adductor hallucis, an interosseus muscle that stabilizes the forefoot during toe-off only³². Muscle

contraction has been shown to be an element of STA error and is suspected to be a changing parameter between the foot positions in this study².

The translational results of the current study (6.46 – 16.72 mm) are larger than the results obtained in the Tranberg et al study¹² (4.3mm) that examined the STA on point markers at similar locations¹². This is likely due to a difference in methodology, including the type of markers used. The increased inertia of the cluster compared to a point marker, due its larger size and weight, make clusters susceptible to greater movement relative to the bone. The marker clusters also protrude out from the skin of the foot more than point markers due to their wand design. This would tend to increase the moment of inertia of the cluster compared to point markers, resulting in more vibration of larger magnitude experienced by the marker cluster. Differences may also exist due to digitization error. Both of these studies used manual digitization but by different methods. Therefore different intra-rater repeatability makes comparisons difficult between the two studies.

The intra-repeatability of this study was shown to be good with root mean square (RMS) values of between 0.57mm - 2.98mm for the calcaneus and 0.66mm – 2.58mm for the navicular. Examining all eight points, the navicular was less repeatable than the calcaneus. It is speculated that the periphery of the fluoroscope image was clearer than the centre, making the calcaneus landmarks easier to visualize and digitize.

Like Tranberg et al¹², the main limitation of the calcaneus and navicular segmental calculations was that a two-dimensional assessment was conducted

for a three-dimensional problem. An attempt was made to incorporate the rotational component of the marker triads (β – difference in the x-axis of the marker co-ordinate system with respect to the bony co-ordinate system) within the plane of motion. However, this may not have been adequate, especially for the calcaneus which is known to have a corkscrew movement pattern with respect to the tibia during the gait cycle³². Frontal plane movement in the calcaneus and the navicular with respect to the talus during slow running has been calculated with bone pins to be as high as 8.3° and 13.5°, respectively¹⁴.

Another limitation to the current study was that subjects were in quasi-static positions as opposed to performing dynamic movement. This was due to the limitation of the sampling frequency of the fluoroscopes that would have led to significant blurring of the images. Inertial effects on the marker clusters and the anatomy and the magnitude of muscle contractions are suspected to increase with dynamic movement. This would most likely tend to increase the STA found at the marker cluster locations.

The limited field of view of the fluoroscope caused additional limitations in this study since only the navicular and calcaneus bones could be simultaneously captured perpendicular to the plane of motion. This eliminated the hallux, the first metatarsal, and the fifth metatarsal bones from the study due to projection errors. These three other bones had been captured with a second fluoroscope oriented at a 75° angle from the horizontal plane (see Appendix B), which was not entirely perpendicular to the direction of motion of the bones. However, when the images were examined it was concluded that too much movement occurred out-of-plane

to reliably analyze the STA of these bones. Future two-dimensional studies could use a jig for the foot to be placed on, similar to the one found in the Tranburg et al¹².

Many of the limitations that occurred in the current study can be eliminated with the use of an image-based Rotrogen photostereometric analysis (IBRSA) method, which is a true three-dimensional tracking technique that is currently being implemented in the WOQIL³⁴. This technique reconstructs the six-degree-of-freedom motion of the bones by fitting a mathematical bone surface model to the two fluoroscopic images. This removes the out-of-plane projection errors as well as manual digitization errors since direct registration of the bone model to the images would be used instead. The true rotational and translational STA errors could then be detected with this technique³⁵.

As hypothesized, the translational errors on the foot were lower than the STA observed at the knee or thigh, which have been shown to be as high as 31mm⁴. Skin markers compared to bone pins in the tibia have also been shown to differ by up to 23mm in the anterior-posterior direction². The smaller STA results of the current study are attributed to the smaller range of motion of the foot and the smaller mass of soft tissue in the foot.

Bone pins have also been used in the foot to examine STA. Studies examining the difference between bone pins and surface markers generally calculate the joint angles using each marker set and then compute the mean difference between joint angles^{1, 13}. Talocalcaneal joint rotation difference between bone pins and surface markers in inversion/eversion have been shown to have a RMS

error of 2.1^{011} . Comparison of the current results to these studies is difficult due to differing methodology and marker locations. But they do imply that the rotational errors of significantly less than 1° in this study could be an underestimation of the true three-dimensional rotational STA.

In conclusion, this study demonstrates that there is soft tissue artifact for the navicular and calcaneal bones and associated triad marker clusters. It appears that the error is maximum in the toe-off position for both the calcaneus and the navicular when assessed using quasi-static positions. It is suspected that during normal gait the rapid accelerations that accompany heel strike would tend to add to the initial effects of the markers clusters. Future studies should use a true three-dimensional analysis of each of five marker triad clusters during dynamic movement to fully capture the STA error associated with the multi-segment foot model.

4.5 References

1. Nester, C. et al. Foot kinematics during walking measured using bone and surface mounted markers. *J Biomech* 40, 3412-23 (2007).
2. Leardini, A., Chiari, L., Della Croce, U. & Cappozzo, A. Human movement analysis using stereophotogrammetry. Part 3. Soft tissue artifact assessment and compensation. *Gait Posture* 21, 212-25 (2005).
3. Manal, K., McClay, I., Stanhope, S., Richards, J. & Galinat, B. Comparison of surface mounted markers and attachment methods in estimating tibial rotations during walking: an in vivo study. *Gait Posture* 11, 38-45 (2000).
4. Stagni, R., Fantozzi, S., Cappello, A. & Leardini, A. Quantification of soft tissue artefact in motion analysis by combining 3D fluoroscopy and stereophotogrammetry: a study on two subjects. *Clin Biomech (Bristol, Avon)* 20, 320-9 (2005).
5. Cappozzo, A., Cappello, A., Della Croce, U. & Pensalfini, F. Surface-marker cluster design criteria for 3-D bone movement reconstruction. *IEEE Trans Biomed Eng* 44, 1165-74 (1997).

6. Reinschmidt, C., van den Bogert, A. J., Nigg, B. M., Lundberg, A. & Murphy, N. Effect of skin movement on the analysis of skeletal knee joint motion during running. *J Biomech* 30, 729-32 (1997).
7. Alexander, E. J. & Andriacchi, T. P. Correcting for deformation in skin-based marker systems. *J Biomech* 34, 355-61 (2001).
8. Fantozzi, S. et al. Fluoroscopic and gait analysis of the functional performance in stair ascent of two total knee replacement designs. *Gait Posture* 17, 225-34 (2003).
9. Benoit, D. L. et al. Effect of skin movement artifact on knee kinematics during gait and cutting motions measured in vivo. *Gait Posture* 24, 152-64 (2006).
10. Westblad, P., Hashimoto, T., Winson, I., Lundberg, A. & Arndt, A. Differences in ankle-joint complex motion during the stance phase of walking as measured by superficial and bone-anchored markers. *Foot Ankle Int* 23, 856-63 (2002).
11. Arndt, A., Westblad, P., Winson, I., Hashimoto, T. & Lundberg, A. Ankle and subtalar kinematics measured with intracortical pins during the stance phase of walking. *Foot Ankle Int* 25, 357-64 (2004).
12. Tranberg, R. & Karlsson, D. The relative skin movement of the foot: a 2-D roentgen photogrammetry study. *Clin Biomech (Bristol, Avon)* 13, 71-76 (1998).
13. Reinschmidt, C., van Den Bogert, A. J., Murphy, N., Lundberg, A. & Nigg, B. M. Tibiocalcaneal motion during running, measured with external and bone markers. *Clin Biomech (Bristol, Avon)* 12, 8-16 (1997).
14. Arndt, A. et al. Intrinsic foot kinematics measured in vivo during the stance phase of slow running. *J Biomech* 40, 2672-8 (2007).
15. Reinschmidt, C. et al. Tibiofemoral and tibiocalcaneal motion during walking: external vs. skeletal markers. *Gait and Posture* 6, 98-109 (October 1997).
16. Wrbaskic, N. & Dowling, J. J. An investigation into the deformable characteristics of the human foot using fluoroscopic imaging. *Clin Biomech (Bristol, Avon)* 22, 230-8 (2007).
17. Lundberg, A. Kinematics of the ankle and foot. In vivo roentgen stereophotogrammetry. *Acta Orthop Scand Suppl* 233, 1-24 (1989).
18. Lundberg, A., Goldie, I., Kalin, B. & Selvik, G. Kinematics of the ankle/foot complex: plantarflexion and dorsiflexion. *Foot Ankle* 9, 194-200 (1989).
19. Lundberg, A., Svensson, O. K., Bylund, C., Goldie, I. & Selvik, G. Kinematics of the ankle/foot complex--Part 2: Pronation and supination. *Foot Ankle* 9, 248-53 (1989).

20. Lundberg, A., Svensson, O. K., Bylund, C. & Selvik, G. Kinematics of the ankle/foot complex--Part 3: Influence of leg rotation. *Foot Ankle* 9, 304-9 (1989).
21. Komistek, R. D., Stiehl, J. B., Buechel, F. F., Northcut, E. J. & Hajner, M. E. A determination of ankle kinematics using fluoroscopy. *Foot Ankle Int* 21, 343-50 (2000).
22. Wearing, S. C. et al. Sagittal movement of the medial longitudinal arch is unchanged in plantar fasciitis. *Med Sci Sports Exerc* 36, 1761-7 (2004).
23. de Asla, R. J., Wan, L., Rubash, H. E. & Li, G. Six DOF In Vivo Kinematics of the Ankle JOint COmplex? Applicaition of a COmbined Dual-Orthogonal Fluoroscopic and Magnetic Resonance Imaging Technique *Journal of Orthopaedic Research* 24, 1019-27 (2006).
24. Gefen, A., Megido-Ravid, M., Itzchak, Y. & Arcan, M. Biomechanical analysis of the three-dimensional foot structure during gait: a basic tool for clinical applications. *Journal of biomechanical Engineering* 122, 630-9 (2000).
25. Perlman, P. R., Siskind, V., Jorgensen, A., Wearing, S. & Squires, S. Changes in the calcaneal pitch during stance phase of gait. A fluoroscopic analysis. *J Am Podiatr Med Assoc* 86, 322-6 (1996).
26. Jenkyn, T. R. & Nicol, A. C. A multi-segment kinematic model of the foot with a novel definition of forefoot motion for use in clinical gait analysis during walking. *J Biomech* 40, 3271-8 (2007).
27. Jenkyn, T. R., Anas, K. & Nichol, A. Foot segment kinematics during normal walking using a multisegment model of the foot and ankle complex. *J Biomech Eng* 131, 034504 (2009).
28. Dunk, N. M., Kedgley, A. E., Jenkyn, T. R. & Callaghan, J. P. Evidence of a pelvis-driven flexion pattern: are the joints of the lower lumbar spine fully flexed in seated postures? *Clin Biomech (Bristol, Avon)* 24, 164-8 (2009).
29. Suzuki, J., Tanaka, Y., Takaoka, T., Kadono, K. & Takakura, Y. Axial radiographic evaluation in hallux valgus: evaluation of the transverse arch in the forefoot. *J Orthop Sci* 9, 446-51 (2004).
30. Komeda, T. et al. Evaluation of the longitudinal arch of the foot with hallux valgus using a newly developed two-dimensional coordinate system. *Journal of orthopaedic science* 6, 110-118 (2001).
31. Gluer, C. C. et al. Accurate assessment of precision errors: how to measure the reproducibility of bone densitometry techniques. *Osteoporos Int* 5, 262-70 (1995).
32. Nordin, M. & Frankel, V. *Basic Biomechanics of the Musculoskeletal System* (ed. Leger, D.) (Lippincott Williams & Wilkins, Baltimore, Maryland, 2001).

33. Perry, J. Gait analysis: normal and pathological function (Slack, Inc, Thorofare, NJ, USA, 1992).
34. Baker, R. Gait analysis methods in rehabilitation. J Neuroeng Rehabil 3, 4 (2006).
35. Li, G., Wuerz, T. H. & DeFrate, L. E. Feasibility of using orthogonal fluoroscopic images to measure in vivo joint kinematics. J Biomech Eng 126, 314-8 (2004).

Chapter 5 – Effect of Longitudinal Torsion and Forefoot Flexion of Running Shoes on Foot Kinematics

Chapter 5 investigates the effect of longitudinal torsion on foot kinematics during running. Foot joint angles are calculated while the subject runs in three different shoe conditions and in barefeet. The multi-segment foot model discussed in previous chapters is used in this investigation as well. This study is the first of two in vivo studies that consider the results from the previous studies. Two of the three types of shoes used in this study were run through the validation study (Chapter 2) to ensure that the integrity of the shoes was maintained throughout the current study. The validation study needed to be re-conducted at Nike since in the original study the subject walked at a self-selected pace wearing three different types of Saucony shoes; however for this study the subjects ran at a 7 min/mile pace in variations of the Nike Frees. The marker set employed in this chapter is the same set that was tested in Chapter 4, where it was concluded that soft tissue artifact is an issue. The base of the markers was changed to leather instead of plastic; however this is not expected to change the outcome or to improve the initial study. Since this study examines the difference between running and cutting, the range of motion with respect to the foot and not the absolute motion was obtained. For this reason, a neutral study for each condition was used to investigate the the range of motion for each inter-segmental joint.

This chapter will be submitted for publication as an original paper in Journal of Biomechanics.

Shultz, R – developed experiment, analyzed all results and wrote the paper

Jenkyn, TR – senior author - helped design the protocol and helped analyze the results

5 Abstract

Longitudinal torsion stiffness (LTS) is the resistance of a running shoe to torsional loading about its long axis. Another shoe property is forefoot flexion (FFlex) stiffness which is the resistance of a shoe to bend in the sagittal plane at the metatarsal break. It is speculated that altering the stiffnesses may also affect foot kinematics. The objective of this study is to explore the effect of LTS on the foot joint kinematics in the frontal plane and to explore the effect of FFlex on the foot joint kinematics in the sagittal plane during running. Ten male subjects ran at a 7 min/mile pace in three different training shoes as well as barefoot while an optical motion capture system tracked marker triad clusters affixed to the right foot. The three trainers varied in torsional stiffness due to carbon-fibre plates of different lengths glued to the midsole. A multi-segment foot model was used with optical motion capture to track four inter-segmental motions: 1) the hindfoot with respect to the midfoot in the frontal plane, 2) the forefoot twist with respect to the midfoot in the frontal plane, 3) the hallux angle in the sagittal plane with respect to the first metatarsal, and 4) the height-to-length ratio of the medial longitudinal arch. A repeated measures ANOVA with 1 factor at 3 levels was run across the difference of each shoe condition compared to the barefoot condition. Only the differences between the hindfoot motion of the two shoes with similar stiffness (Nike Free, Nike Free with a forefoot carbon fibre plate) was found to be statistically significant. However, when compared to barefoot, the maximum differences for each shoe condition were greater than the MID (5°) for most subjects in the hindfoot motion and the hallux motion. Differences were also

found in the forefoot twist motion and the medial longitudinal arch, but to a lesser degree. These results imply that the shoe conditions affect the inter-segmental joints in a similar way, which was found to be different from the barefoot condition. The Nike Free shoe did tend to mimic the barefoot condition more than the other two modified shoes.

5.1 Introduction

Altering the properties of a shoe's sole to optimize its performance is a well-established pursuit for shoe manufacturers. However, the advantages of some of these changes are still being debated.¹⁻⁷ Research in this area is controversial since certain parameters have been shown in one study to affect foot kinematics while other studies have shown no significant influence⁸. One study that examined 36 different shoe property combinations found that softer midsoles allowed significantly more rearfoot movement⁵. In another study, similar midsole material modifications were found to have no effect on peak acceleration and time to acceleration, however these outcomes were found to be greater when subjects ran in shoes than when they remained barefoot⁶. Changes in the amount of midsole flare were not found to influence the kinematics of the tibio calcaneal rotations substantially², but were found to increase peak pronation and the total rearfoot movement⁵.

Longitudinal torsion stiffness (LTS) is the property of a running shoe that quantifies its resistance to torsion along its long axis⁹. It was first introduced as a feature of an innovative running shoe that had the ability to decouple the motions of the hindfoot and the forefoot¹⁰. It has been speculated that altering the LTS should affect foot kinematics in the frontal plane.

Much of the early research on shoe torsion was conducted using two-dimensional (2D) film analyses with reflective markers placed either on the foot or the shoe⁹⁻¹¹. This methodology has been shown to have large projection errors⁹ and high soft tissue artifact errors, but the general trends of the results are still relevant to

the design of running shoes^{12, 13}. It was demonstrated that, compared to barefoot, the shoed conditions decreased torsion of the foot while significantly increasing the foot pronation¹⁰. This was assumed to be the result of both the shoe being stiffer than the barefoot condition and the shoe preventing midfoot motion within the foot. Allowing motion in the transverse tarsal joint is suspected to decrease this pronation by increasing the torsion angle of the foot, which is defined as the hindfoot angle in the frontal plane minus the forefoot angle in the frontal plane¹⁰.

Another shoe property is forefoot flexion (FFlex), which is the ability of a shoe to bend at the metatarsal break in the sagittal plane. A recent study concluded that a change in dorsi-flexion and metatarsal flexion can affect the muscle recruitment patterns and reorganize the motor patterns¹⁴.

Very few studies were found in the literature that used more recent technologies to investigate the change in foot kinematics due to a change in the LTS or FFlex of a running shoe. Stefanyshyn and his colleagues have recently investigated the metatarsophalangeal joint (MTP) and the effect of LTS and FFlex stiffness (called longitudinal bending stiffness and midsole bending stiffness, respectively)^{1, 3, 4, 15}. Outcome measures from these studies focused on kinetics, running economy, and comfort, but not on the kinematics. An example of only a single representative subject was given to demonstrate the effect of LTS and forefoot bending stiffness on the metatarsal kinematics^{3, 4}, however there was no other mention of kinematic data during running in the paper. This study focused on maximum jump height performance and discovered that as the bending

stiffness of the shoe increased, a large decrease in MTP joint dorsi-flexion was observed³. The same trend was observed for running in the single subject example. Change in motion of the MTP joint with respect to LTS and FFlex has been examined but the effect of these shoe properties on the remainder of the foot is still unknown.

This study aims to explore the effect of LTS and FFlex on the kinematics of multiple foot segments. Barefoot running was chosen as the control. However there is limited research on foot kinematics for joints distal to the subtalar joint during barefoot running that can be used as a comparison. Recently, invasive bone pins have been used to examine the foot's inter-segmental motion during slow running¹⁶⁻¹⁸. The usefulness of this method is seriously limited since bone pins cannot feasibly be used in clinical studies and several shoed conditions cannot be tested in one continuous session. Another obstacle in foot research is the lack of standards for foot joint co-ordinate systems (i.e. such as International Society of Biomechanics, ISB) which makes comparison across studies and during clinical exams difficult¹⁷. Additionally, research on the foot joints distal to the subtalar joint has been avoided because of the difficulty in placing the reflective markers directly on the foot while a subject is wearing running shoes¹⁹.

A novel multi-segment foot model using passive reflective marker triads is used in the current study to evaluate the inter-segmental motion of the hindfoot, medial and lateral forefoot, medial longitudinal arch and the hallux. The model uses the midfoot as the segment of reference for the kinematics of the hindfoot and the

forefoot²⁰. The description of the model can be found in Jenkyn and Nicol²⁰ and Jenkyn, Anas et al.^{20, 21}

The primary objective of this study is to use a multi-segment foot model to explore how foot kinematics are influenced with a set of Nike Free trainers that have different longitudinal torsion and forefoot flexion stiffnesses. Three shoe conditions are tested as well as the barefoot condition while the subject is running. Four inter-segmental motions are measured: hindfoot in the frontal plane, forefoot in the frontal plane, height-to-length ratio of the medial longitudinal arch and hallux in the sagittal plane. A fifth measure is calculated from the hindfoot and forefoot measures; this is the 'torsion angle' in the frontal plane. It is hypothesized that an increased shoe stiffness will decrease the range of motion of the hallux segment as seen in a previous study^{3, 14}. A flexible shoe may allow for the foot to 'roll through' the stance phase of gait (in the sagittal plane) as the subject runs, whereas a stiff shoe may act as a rigid lever causing a foot slap to occur during early stance¹⁰. This would tend to affect the motions of the hindfoot, forefoot and medial longitudinal arch. The pronation of the foot as a whole has already been shown to be proportional to the longitudinal torsion stiffness of the shoe as the torsional angle decreases¹⁰, but it is hypothesized that this will also be seen in this study for the inter-segment foot joint angles.

A secondary objective of this study is to examine whether running with the unaltered Nike Free, the study shoe, mimics barefoot running. This is what the shoe was designed to do since barefoot running populations have been shown to have extremely low running-related injuries compared to more conventionally

shoed running populations²². If a participant has had adequate training with the Nike Free, it is speculated that their foot kinematics and kinetics would be similar to the kinematics and kinetics calculated during barefoot running.

5.2 Methods

5.2.1 Subjects

Ten active male subjects volunteered for the study (average age 30 ± 5 years; average height 172.0 ± 0.4 cm; average mass 70 ± 7 kg). The subjects were heelstrickers who ran a least 15 km a week and considered themselves 'runners'. The majority of them were regular subjects in the Nike Sport Research Lab and could consistently run a 7 min/mile pace for multiple trials. Subjects had no ongoing symptoms from previous foot or ankle injuries, no significant foot or ankle injuries at the time of the study, no obvious lower extremity malalignment and did not wear orthotics. Consent was attained from the relevant ethics committees at the research lab where the study was conducted and from the authors' university.

5.2.2 Experimental equipment

The study was conducted at the Nike Sport Research Laboratory (NSRL, Portland, Oregon). The laboratory is equipped with an eight-camera, real-time three-dimensional (3D) optical motion capture system (EvaRT 5.04, Eagle HiRes cameras, Motion Analysis Corp., Santa Rosa, CA) with an integrated floor-mounted forceplate (Kistler, Amherst, NY). Kinematic data were sampled at 240 Hz and kinetic data at 1200 Hz.

Three types of size 9 Nike Free 7.0 trainers (Nike, Inc, Beaverton, OR) were used in this study. The first shoe was unchanged from how it was manufactured and is considered the control shoe (CO). The second shoe was a modified version of the control shoe with a forefoot carbon-fiber plate (FF) placed directly below the insole and glued to the insole to prevent slippage. The third shoe had a full length carbon-fiber plate (FL) placed under the insole. All shoe modifications took place in the Sample Room at Nike (Nike Inc., Beaverton, Oregon). Three pairs of each type of shoe were used in the study.

Five 'holes' (holes of size ~2.5 cm in diameter) were pre-cut in each of the nine pairs of shoes. For the three pairs of each type of shoe, the location of the midfoot hole differed slightly. The location of the navicular tuberosity on each test subject determined which pair of shoes was used during testing. The holes allowed marker triad clusters to be attached to the skin of the foot and at the same time be visible to the optical motion capture system (Figure 5.1). The marker triads were located on the foot according to the multi-segment foot model described by Jenkyn and Nicol²⁰. The maximum size of the holes that could be cut in the shoe without sacrificing its structural integrity was validated in a separate pilot study. The pilot study used the hole validation method outlined in Chapter 2. It was suspected that the nature of the study activity would affect the valid hole size. However this appears not to be the case since a 2.5 cm diameter hole was found to be valid for both walking, cutting and running in four very different shoe types (Saucony – Neutral cushioning, stability, motion control, Nike – Frees). Only the Nike FL and the Nike CO shoe were analyzed using this

method since the CO and FF were shown to have similar stiffness. All three shoe types shoes were mechanically tested.



Figure 5.1. A) Location of the marker triad clusters on the foot. The base of the cluster remains affixed to the foot throughout the test protocol while the wand and marker portion is removed to allow for shoe changes. B) The three shoe types tested are the control (Nike Free trainer 7.0, left), the control shoe with a forefoot carbon plate attached to the midsole (middle), and the control shoe with a full length carbon plate attached to the midsole (right). All shoes have five holes cut in the upper at the heel counter on the lateral side, the toe box above the hallux, along the medial and lateral sides above the first and fifth metatarsals and on the medial side above the navicular tuberosity. C) Example of the anatomical landmarks that are digitized at the beginning of the test session. The landmarks form the anatomical co-ordinate systems for the dynamic trials. This is further explained in Jenkyn et al.²⁰

The longitudinal torsion stiffness (LTS) of the shoes along the axis running from the toe to the heel was measured both before and after the holes were cut in the shoe upper with a material testing machine (Instron, MA, USA). The LTS of the shoes with holes was within 5% of that for intact shoes further validating the hole size. For the intact control shoe, the forefoot plate shoe, and the full length plate shoe, the LTS were 88.0 N-m/degree, 78.2 N-m/degree and 130.6 N-m/degree, respectively. An in-house device also measured the forefoot stiffness in the sagittal plane of the same three shoes. This device measures the amount of force required to bend the shoe one degree at the forefoot break. These were found to be 0.85 N/degree, 0.28 N/degree and 0.20 N/degree, for the full length plate shoes, the forefoot plate shoes, and the control shoe, respectively. See appendix D for a more detailed description of these testing procedures.

Marker triad clusters were designed and built in-house so that the wand and reflective marker portion could be detached from their base, which remained affixed to the skin of the foot throughout the testing protocol. This allowed for subjects to change shoes between test conditions without altering the locations of the marker triads. The stem of the triad cluster consisted of a nylon screw with three carbon-fiber wands protruding from it to which were attached three wooden balls (8mm) wrapped in reflective tape (3M, Minneapolis, MN). The base was a nylon nut epoxyed to a faux leather base and affixed to the foot via medical adhesive spray (Hollister Medical Adhesive Spray, Hollister Incorporated, Libertyville, IL).

5.2.3 Multi-segment foot model

The foot complex was analyzed using a multi-segment kinematic foot model that tracked five foot segments and the inter-segmental motions between them via one marker triad cluster per segment. For this study, the foot was functionally divided into the hindfoot (calcaneous), midfoot (tarsals), lateral and medial forefoot (5th and 1st metatarsals respectively) and the hallux (both phalanges). An expanded description of this multi-segment kinematic foot model can be found in Jenkyn and Nicol²⁰ and in Jenkyn, Anas, et al.²¹.

Throughout one stance phase of the gait cycle, the three-dimensional trajectory of each marker on each cluster was triangulated with the optical motion capture system and used to calculate the inter-segment motions of each foot segment. The motions were reported as follows: the hindfoot with respect to the midfoot in the frontal plane (hindfoot), the forefoot twist (of both forefoot segments) with respect to the midfoot in the frontal plane (forefoot), the hallux angle in the sagittal plane with respect to the first metatarsal (hallux) and the height-to-length ratio of the medial longitudinal arch (MLA).

5.2.4 Procedure

The testing session began by locating the positions on the foot where the marker triad clusters could protrude through the holes correctly and the markers could be placed over the correct bony landmarks²⁰. The base of each triad cluster remained on the foot for the remainder of the testing session while the reflective markers were removed and replaced with each shoe change.

A barefoot static trial, which is used to calculate the neutral position for the barefoot condition, was collected while subjects stood in the center of the capture volume (2.0m x 1.0m x 1.5m) with feet hip-width apart. Next, a series of barefoot, quiet standing trials where 16 bony landmarks were digitized with an instrumented stylus as outlined by Jenkyn and Nicol²⁰ (see Figure 5.1c). The three anatomical landmarks per segment are described by the CAST system^{23, 24} and were used to establish the anatomical co-ordinate frames for each condition: 1) barefoot (bare), 2) Nike Free trainers control shoe (CO), 3) forefoot carbon-fiber plate (FF) and 4) full length carbon-fiber plate (FL). A per-condition static trial was collected and used as the neutral position for each condition. This method was used since the objective was to examine the range of motion of the foot while the subject was wearing the different shoes.

Seven dynamic trials were collected per condition while participants ran down an 50m runway at a 7 min/mile ($\pm 5\%$) pace. Timing gates were used to ensure that the participants reached the target speed during each trial. Subjects were requested to strike the force plate with their right foot while not concentrating on contacting it. The force plate data were used to indicate the timing of the heel strike and toe-off.

All subjects performed the barefoot running trials first to ensure that a minimum of seven good barefoot trials were collected for each subject, since disruption of the marker clusters was more likely to occur during a shoe change. After the barefoot condition, the three shoe conditions were tested in random order. Static, quiet standing trials were collected for each footwear condition before the

dynamic trials. The digitization trials were only repeated if the orientation of a marker cluster was disrupted during a shoe change.

5.2.5 Data and statistical analysis

Data were filtered using a low-pass 4th order Butterworth filter (cut-off frequency of 20 Hz, justification for this cut-off frequency can be found in chapter 1.8.3) with zero lag. Each dynamic trial was normalized in time to 100% of stance phase. The inter-segmental joint angles of the multi-segment foot model were calculated in custom-written software (MatLab; The MathWorks, Natick, MA) from the three-dimensional marker trajectories. The static trials collected for each footwear condition were used to establish the neutral position of the inter-segmental joints for the condition's dynamic trials. This allowed for the range of motion of each joint to be comparable between footwear conditions rather than the absolute joint range of motion. For each of the four inter-segment motions, an average mean difference between each shoe condition and the barefoot condition was calculated throughout stance phase. The maximum mean differences (MMD) for each inter-segmental motion for the three shoed conditions for all subjects were recorded. The timing of each MMD was also recorded (as a percentage of stance phase). The foot frontal plane torsion angle was calculated by subtracting the hindfoot motion in the frontal plane from the forefoot motion in the frontal plane throughout stance phase. The maximum torsion angle and its timing in all conditions were then calculated.

Statistical significance and the minimum important difference were evaluated. A repeated measures analysis of variance (ANOVA) with 1 factor at 3 levels was

performed for the maximum mean differences for each of the four inter-segmental motions and on the maximum torsion angle. The three mean differences of each shoe condition (CO, FL, FF) compared to barefoot running were the three levels of the ANOVA. A p-value of less than 0.05 was considered to be significant. The Tukey post-hoc test was used to correct for multiple comparisons. An average over the collected trials for each subject was used in the ANOVA. The minimum important difference was 5° for the inter-segmental joint angles and 0.03 for the medial longitudinal arch (mm/mm) (see Appendix A for a detailed explanation of this calculation).

5.3 Results

Figures 5.2-5.3 and 5.5-5.6 plot the inter-segmental joint motions for the hindfoot, forefoot, hallux and medial longitudinal arch respectively. Figure 5.4 plots the torsion angle. Each plot shows the barefoot condition (Bare) and the three shoe conditions (CO, FL, and FF). The first three figures (5.2, 5.3 and 5.4) show the motion of the foot in the frontal plane and the last two figures (5.5 and 5.6) show the motion of the foot in the sagittal plane. Each motion curve for each condition is averaged over the three best trials for all 10 subjects in the study. The timing of all curves is normalized to 100% stance phase of running, starting at initial contact (0%) and ending at toe-off (100%).

Comparing Figure 5.2 to 5.3, the hindfoot has a larger range of motion than the forefoot with respect to the midfoot. The torsion angle (Figure 5.4), which is the difference between the forefoot and hindfoot motions, is therefore primarily influenced by the motion of the hindfoot. The increased pronation of the FF

conditions seems to coincide with a positively increased torsion angle, whereas the increased supination of the FL condition coincides with a negatively increased torsion angle. In the frontal plane, the barefoot and control condition (CO) seem to move similarly with a minimal torsion angle during the first 60% of the stance phase, followed by an increase from heel rise until toe-off, where it reaches a maximum for all the conditions. The similar minimal torsional angle for the Bare and CO is likely due to the similar movement patterns of the hindfoot and forefoot as seen in Figures 5.2 and 5.3 until approximately heel rise where the hindfoot begins to pronate.

The hallux and medial longitudinal arch motions are plotted in the sagittal plane. Figure 5.5 demonstrates that the range of motion of the hallux during barefoot running is small compared to all three shoe conditions throughout the first 60% of stance phase. The three shoe conditions each produce a high plantarflexion peak at approximately 40% of the stance phase, whereas the hallux angle remains around zero at this point for the barefoot condition. The motion of the MLA (Figure 5.6) tends to split into two groups. The Nike Free control shoe (CO) tends to mimic barefoot walking and the FL and FF conditions were similar. However, overall the shape of MLA motion curves is similar across all conditions.

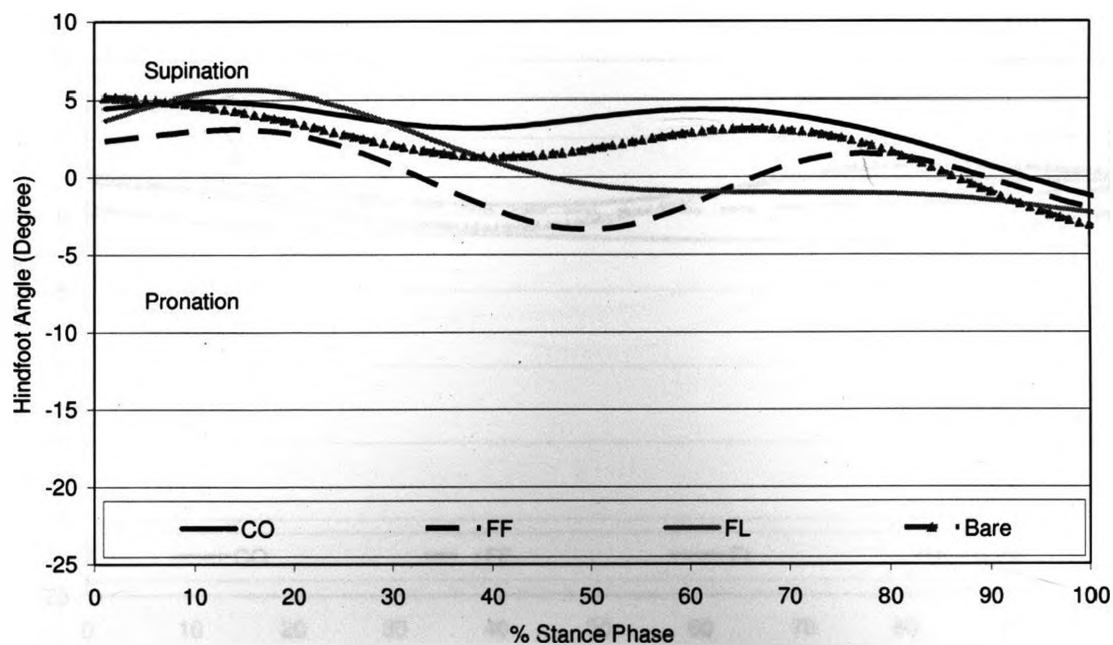


Figure 5.2. Hindfoot motion in the frontal plane with respect to the midfoot for the barefoot (gray triangles = Bare) and the three shoe conditions (black line = CO, dashed line= FF, gray line= LF). For all four conditions the hindfoot is supinated at heelstrike and then pronates until 30-50% of the stance phase, when it begins to supinate again. The highest peak pronation is observed for the FF condition, while the FL condition appears to hinder the foot's ability to re-supination after midstance. The CO condition and the barefoot condition tend to produce similar movement patterns.

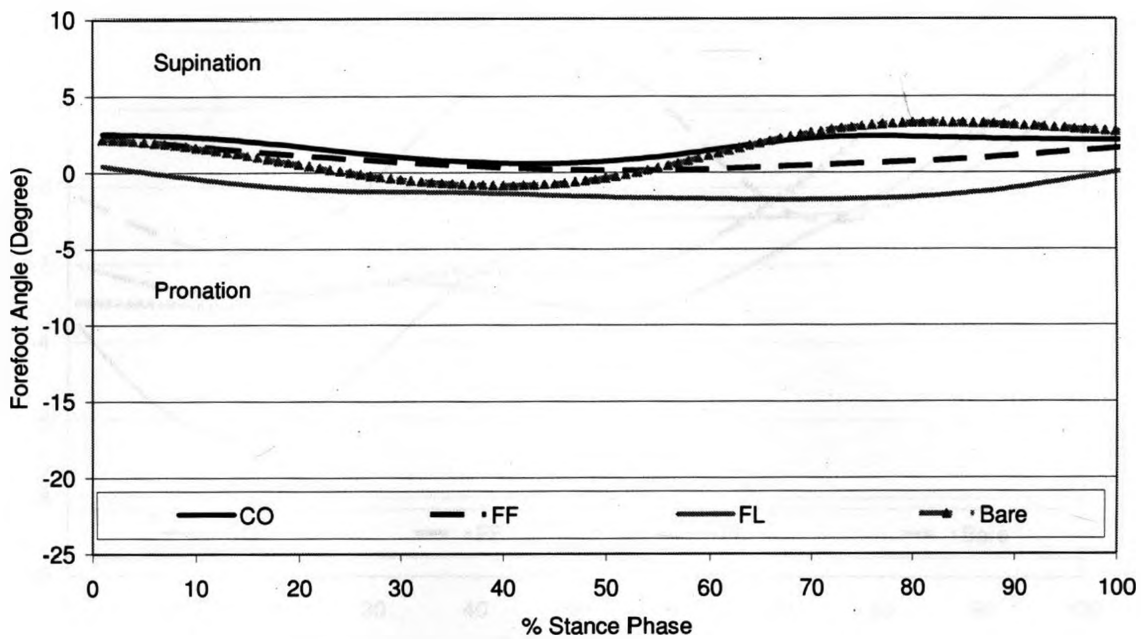


Figure 5.3. Forefoot twist in the frontal plane with respect to the midfoot for the barefoot (gray triangles = Bare) and the three shoe conditions (black line= CO, dashed line= FF, gray line= LF). The motion of the forefoot is limited in range and tends to mimic the hindfoot motion. The forefoot motion remains close to its neutral position throughout the stance phase, which has been shown to occur during running²⁵. The FL and FF conditions showed similar motions, and the CO and Bare were also similar.

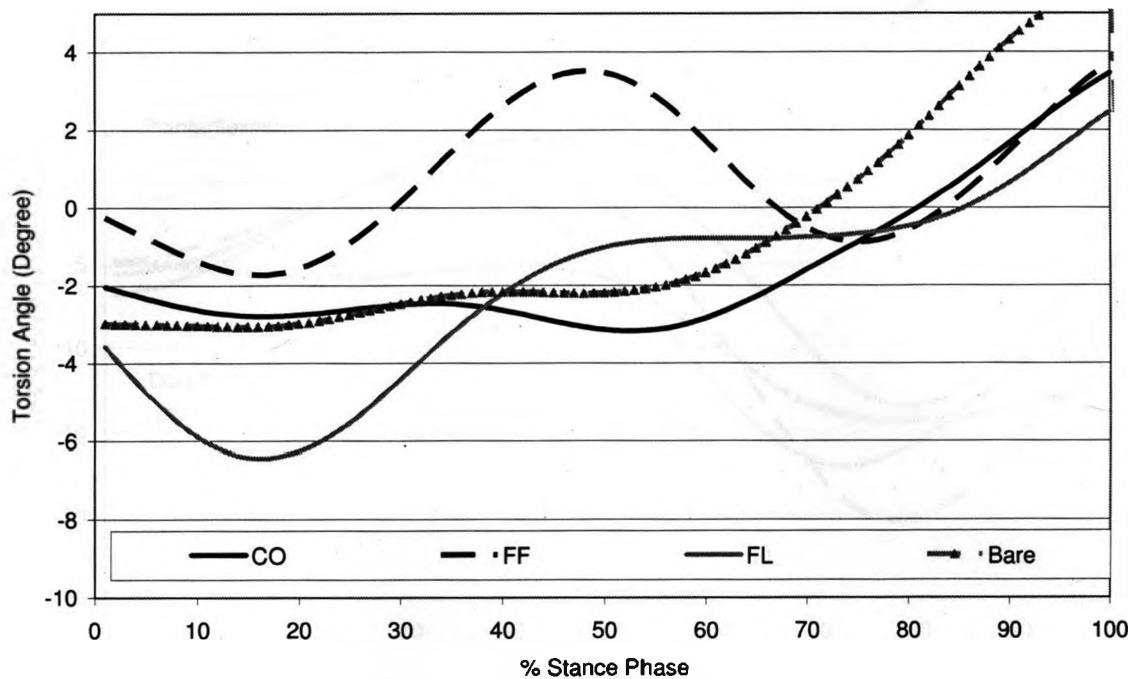


Figure 5.4. Longitudinal torsion angle in the frontal plane, which is defined as the forefoot motion minus the hindfoot motion. This is shown for the barefoot (gray triangles = Bare) and the three shoe conditions (black line = CO, dashed line= FF, gray line= LF). There is a large negative torsion angle from heel strike until midstance for the FL condition, whereas the FF condition has a large positive torsion angle from 20-70% of the stance phase. The barefoot condition and the CO condition tend to remain around 3 degrees until approximately 60% of the gait cycle where it begins to positively increase until it reaches a maximum at heel strike.

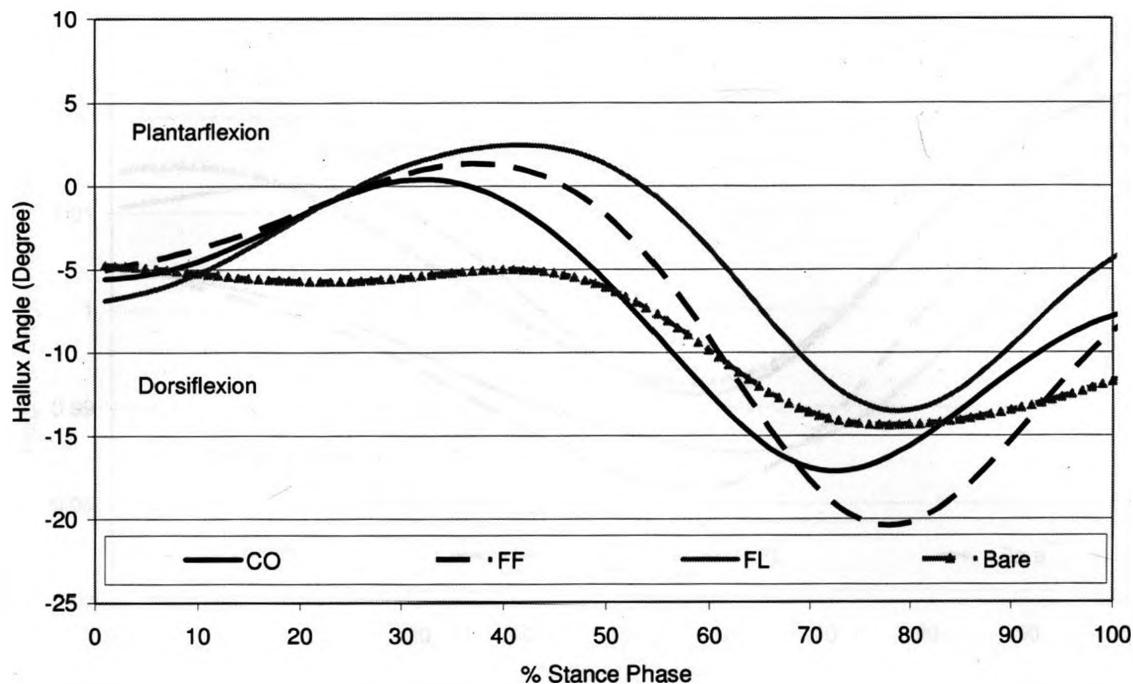


Figure 5.5. Hallux motion in the sagittal plane with respect to the first metatarsal for the barefoot (gray triangles = Bare) and the three shoe conditions (black line = CO, dashed line = FF, gray line = LF). The motion of the hallux during the shoe conditions is different from the barefoot condition with the barefoot condition tending to reduce the range of dorsiflexion and plantarflexion. The FF condition appears to increase the dorsiflexion compared to the CO condition. The FL condition reduced dorsiflexion compared to the other conditions.

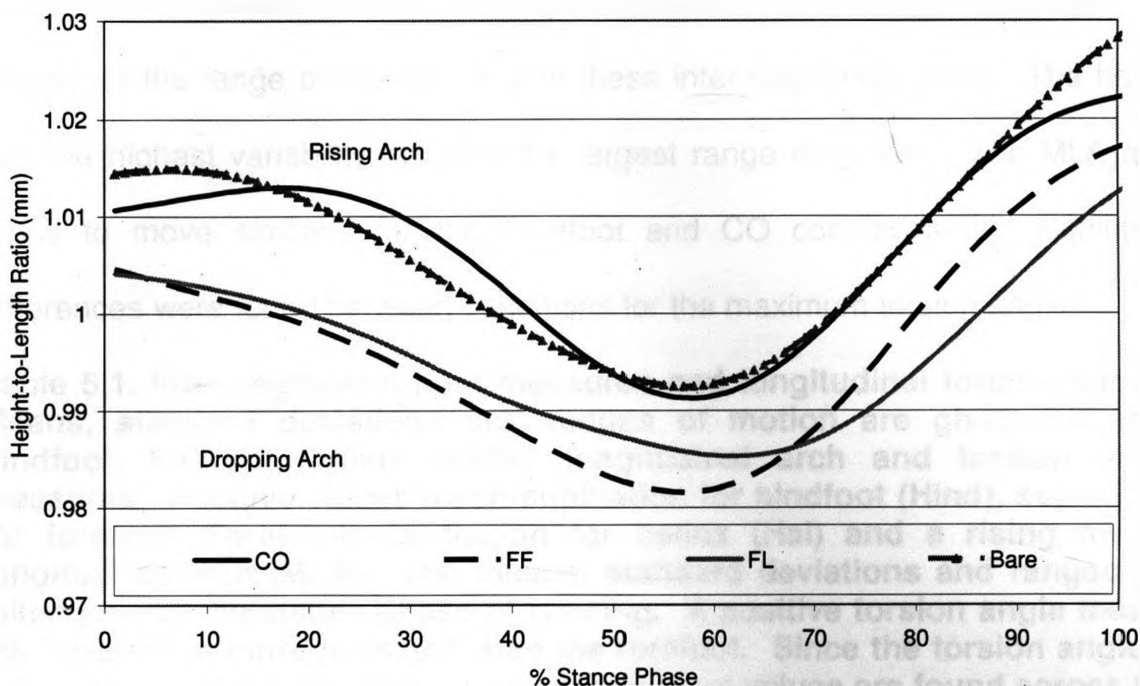


Figure 5.6. Height-to-length ratio of medial longitudinal arch for the barefoot (gray triangles = Bare) and the three shoe conditions (black line= CO, dashed line= FF, gray line = LF). Forefoot frontal plane motion appears to follow the dropping of the medial longitudinal arch²⁶. The arch drops in the beginning of the stance phase and rises in the second half. The barefoot condition and the CO condition tended to be similar. The other two conditions, FL and FF, were also similar but begin with the arch in a lower position at heel-strike.

The mean positions, standard deviations and ranges of motion of each of the four inter-segmental measures are listed in Table 5.1 for each of the barefoot and three shoed conditions. Also listed in the bottom row is the maximum torsion angle. Recall that positive values mean supination for the hindfoot (Hind) and the forefoot (Fore) motions, plantar-flexion for the hallux (Hal) and a rising medial longitudinal arch (MLA). Recall for the torsion angle that a positive value means the hindfoot is more pronated than the forefoot. Since this is a discrete measure, the minimum and maximum values given are across the 10 subjects. Table 5.1 indicates that the CO condition and the barefoot condition produce similar

hindfoot and forefoot motion, although the standard deviations are high with respect to the range of motion for both these inter-segmental joints. The hallux has the highest variability but also the largest range of motion. The MLA also tends to move similarly for the barefoot and CO conditions. No significant differences were found between conditions for the maximum torsion angle.

Table 5.1. Inter-segmental joint measures and longitudinal torsion angles. Means, standard deviations and ranges of motion are given for each hindfoot, forefoot, hallux medial longitudinal arch and torsion angle measures. Positive values mean supination for hindfoot (Hind), supination for forefoot (Fore), plantar-flexion for hallux (Hal) and a rising medial longitudinal arch (MLA). The means, standard deviations and ranges are taken across the stance phase of running. A positive torsion angle means the hindfoot is more pronated than the forefoot. Since the torsion angle is a discrete measure the minimum and maximum values are found across the 10 subjects.

	Bare		CO		FF		FL	
	Mean	(SD)	Mean	(SD)	Mean	(SD)	Mean	(SD)
	Max	Min	Max	Min	Max	Min	Max	Min
Hind (°)	2.0	2.0	3.3	1.6	0.1	2.1	1.0	2.7
	8.8	-5.6	9.2	-5.4	8.7	-7.9	9.7	-7.1
Fore (°)	1.3	1.5	1.7	0.7	0.8	0.6	1.1	0.6
	-5.5	2.1	-5.3	1.9	-4.9	2.0	-4.0	2.0
Hal (°)	-7.9	3.9	-6.7	5.7	-6.1	7.5	-4.0	5.2
	-1.2	-20.2	0.3	-18.2	1.9	-20.9	1.6	-16.4
MLA (ratio)	0.007	0.01	0.06	0.009	0.004	0.01	0.004	0.01
	0.03	-0.01	0.02	-0.01	0.02	-0.02	0.008	-0.02
Maximum Torsion Angle (N-m/deg)	-3.0	15.7	-0.04	16.8	-0.03	17.0	-0.3	18.5
	19.5	-26.6	31.1	-20.4	18.9	-33.2	26.4	-22.3

The differences between the three shoe conditions and the barefoot condition are listed in Table 5.3. The maximum mean differences and the timing of these maxima during stance phase are listed for each of the four inter-segmental measures. The largest maximum mean differences were found for the hallux segment with the hindfoot segment being the second largest. However, statistical significance was only found between the CO shoe and the FF shoe in the hindfoot condition for the maximum mean difference between the shoe condition and the barefoot condition ($p < 0.05$). There was no significant difference found for the timing of these maximum mean differences. This is probably due to the high variability seen in the timing of the maximum mean differences for all shoe conditions.

Table 5.2. Difference between shoed conditions and barefoot condition. Maximum mean differences and timing of maximum during stance phase are given to compare each of the three shoe conditions with the barefoot condition for each of the four inter-segmental measures. Differences in mean and timing that are significantly different from 0.0 at $p < 0.05$ are indicated with an asterisk.

	CO-Bare		FF-Bare		FL-Bare	
	Mean	(SD)	Mean	(SD)	Mean	(SD)
	Timing	(SD)	Timing	(SD)	Timing	(SD)
Hind (°)	8.4*	3.3	12.4*	6.7	12.2	3.2
	55.0	28.7	47.7	31.4	62.5	33.4
Fore (°)	6.0	3.6	7.3	6.5	7.4	2.8
	52.5	31.1	58.2	26.0	55.0	35.8
HX (°)	14.1	8.3	12.6	5.9	15.3	5.6
	52.2	39.1	56.6	34.5	67.6	34.2
MLA (ratio)	0.02	0.01	0.03	0.01	0.03	0.02
	78.4	27.1	53.9	35.9	88.6	15.7

There was great variability in the results between the 10 subjects in this study. For some subjects, there were minimal differences between shoe conditions for each of the inter-segmental measures. For others there were large differences between all shoe conditions and all joint measures. The remainders were a

mixture of the two. Table 5.3 illustrates the differences between each of the three shoe conditions with respect to the barefoot condition for each of the four inter-segmental motions, showing each subject individually. Differences greater than the minimum important difference (MID) (of greater than 5° for Hind, Fore, Hal, or 0.03 or greater for MLA) are indicated in gray. Differences greater than 10° (0.054 for MLA) are indicated in black. Differences that are not greater than the MID are in white.

Table 5.3. Differences between the shoe conditions and the barefoot condition for each of the subjects in this study for each of the four inter-segmental measures. The minimum important difference (MID) was taken as greater than 5° for HF, FF and HX and as 0.03 for MLA. Conditions that were above the MID by 5° (0.03) or more are indicated in gray shading, those by 10° (0.054) or more in black shading. Conditions that were below the MID are in white.

Subject	Shoe	Hind	Fore	Hal	MLA
1	CO-Bare	11.19	1.93	5.53	0.03
	FF-Bare	8.53	2.16	4.47	0.04
	FL-Bare	9.99	6.66	3.61	0.04
2	CO-Bare		13.88	19.65	
	FF-Bare	9.88	24.14	15.60	0.04
	FL-Bare	14.42	7.56	21.56	0.06
3	CO-Bare	9.89	6.21	14.61	0.01
	FF-Bare	10.15	4.90	10.64	0.02
	FL-Bare	9.26	4.74	22.15	0.01
4	CO-Bare	5.65	3.69	5.84	0.01
	FF-Bare	8.63	6.01	6.04	0.02
	FL-Bare	11.37	10.93	13.44	0.02
5	CO-Bare	8.28	3.55	15.11	0.02
	FF-Bare	10.26	2.61	14.49	0.03
	FL-Bare	8.41	2.14	10.34	0.03
6	CO-Bare	10.02	4.04	6.64	0.03
	FF-Bare	27.69	5.89	13.13	0.02
	FL-Bare	16.58	11.23	13.86	0.02

7	CO-Bare	3.98		24.33	
	FF-Bare		3.85	25.87	
	FL-Bare	13.01		23.73	0.06
8	CO-Bare	11.85	10.49	16.82	0.01
	FF-Bare	19.01	11.37	13.64	
	FL-Bare	12.23		17.60	
9	CO-Bare	3.23	3.95	4.55	0.01
	FF-Bare	4.41			0.02
	FL-Bare			11.61	0.01
10	CO-Bare	11.43		27.54	
	FF-Bare	16.10		12.39	
	FL-Bare	17.51			

5.4 Discussion

The objective of this study was to investigate the foot joint kinematics during running and how they are altered in three shoes with varying torsion and bending stiffnesses, compared to the barefoot condition, in the sagittal and frontal planes. The movement patterns for the inter-segmental motion appear to be consistent with previous research^{18,24}. (Figures 5.2 to 5.6). The control shoe and the barefoot conditions tended to produce similar movements in all inter-segmental joints, as hypothesized, with the exception of the hallux and torsion angles during stance phase. However, these trends were not statistically significant.

The motion of the foot in the frontal plane was examined by calculating the torsion angle (Figure 5.4) from the hindfoot motion (Figure 5.2) and forefoot motion (Figure 5.3) in this plane. The expected relationship between stiffness, torsional angle and pronation was shown to more complex than expected. The increased pronation during midstance of the hindfoot in the FF shoe condition tended to cause a larger positive torsion angle as the hindfoot and forefoot moved in the same direction. This shoe is also the shoe with the least longitudinal torsion stiffness. It appears that the greater flexibility of the rear section of the shoe tended to allow the hindfoot to move dramatically with respect to the midfoot and the rigid forefoot. However, the FL shoe condition, which is the torsionally stiffest shoe, seems to affect the foot as well. The increased supination of the hindfoot tends to create a larger negative torsion angle during the loading response and into midstance. It was expected that the FL shoe would cause the hindfoot and forefoot to move more as a unit and that there would be little rotation between the forefoot and the hindfoot. However, the larger torsion angle is due to the opposing rotation of the forefoot and the hindfoot.

The foot was also examined in the sagittal plane. The hallux motion and the medial longitudinal arch motion should be correlated in this plane due to the assumed presence of the windlass effect. This can be seen by examining the barefoot condition, as the heel rises and the hallux becomes dorsi-flexed, the MLA begins to rise. Earlier in stance phase when the hallux is in a more neutral position, the plantar fascia is not taut which allows the arch to drop as the foot is loaded. Examining the shoe conditions, it appears that this correlation between

hallux and MLA is disrupted. The arch continues to move in a similar pattern to the barefoot condition, especially the control shoe; however the hallux motion is much different. Upon further inspection one can see that the windlass effect is still somewhat present as the FF condition and the FL condition produce a hallux motion that remains more plantar-flexed and an arch motion that remains lower. The lower arch position may be due to rigidity of the midsole of the shoe allowing minimal motion of the forefoot and hindfoot which are in direct contact with the insole of the shoe. The bones forming the arch however are free to drop until they themselves reach the insole of the shoe. This of course would require a mobile foot. The FL shoe was shown to have a decreased dorsi-flexion when compared with the control shoe. As hypothesized, this stiffness in the forefoot appears to have limited the hallux ability to dorsi-flex. One study found that this has the ability to affect the muscle recruitment patterns and motor pattern which may explain some of the varied movement in the other inter-segmental joints¹⁴.

Statistical significance was only found for the hindfoot segment between two shoe conditions that have similar LTS and FFlex values (LTS: 78.0 Nm/degree for FF shoe and 88.0 Nm/degree for CO shoe; FFlex: 0.28 N/degree for FF shoe and 0.20 N/degree for CO shoe). It appears that changing the LTS and FFlex do not influence the inter-segmental foot kinematics measured in this study. Future research should investigate other parameters that might be more likely to change by the addition of the forefoot plate; for example, thickness and hardness of the midsole have been shown to influence foot kinematics¹⁰.

High inter-subject variability and unsystematic small shoe sole effects are common in shoe research^{2, 19, 27}. This type of data also make finding statistically significant differences difficult since a stronger within subject difference is needed between conditions. For this study, no strong conclusions based on statistical significance could be made due to the large inter-subject variability and the relatively small sample size. This is not unusual in foot research, since high variability across subjects exists even in bone pin studies where skin artifact errors are not present²⁸. A post-hoc power analysis showed that 40 subjects would be necessary to show a statistically significance between outcome effects of the size reported in this study (with $\alpha=0.05$, power = 0.80).

However, the lack of statistical significance across shoe conditions is not suspected to arise due to the lack of power. An inability for a perturbation to dramatically disrupt the foot kinematics has previously been shown¹¹. A possible explanation for the measured foot kinematics being uninfluenced by the midsole stiffness change is that the foot is speculated to be a structurally redundant system². A redundant system has multiple kinematic patterns with which to achieve the same kinematic solution. Multi-segment foot models calculate the angular articulation of a segment with regard to another segment, considered a functional unit or a rigid segment. A perturbation may change the position of the individual bones but the segment kinematics remain unchanged. Future research should attempt to 1) examine the functional units of this model and 2) try to measure the individual bony articulations within each segment under a perturbation.

The idea of a redundant system seems improbable since a recent study by Wolf et al.¹⁸ examines the movement of individual foot bones using invasive bone pins in seven different foot bones¹⁸. Functional units were designated from this research and support the definition of segments in the model used in this study. Future analysis should involve imaging technologies, such as fluoroscopy, to directly visualize the foot bones and give further insight into the effects of perturbations on foot kinematics. Currently, there are technical aspects that make using fluoroscopy difficult, such as the limited field of view of the imaging and the sample frequency limited to 30 frames per second^{29, 30}.

The second possible explanation for the non-significant results in this study is that the body uses muscle activation to maintain a preferred foot position for a given movement²⁷. Introducing an intervention causes the muscles to increase or decrease their activity to maintain the general kinematics and kinetics of the foot for a given movement²⁷. This theory is still under investigation, since research has focused on the kinetic partner theory related to impact forces and soft tissue damping³¹⁻³⁵. However, Roy et al. have already demonstrated that the muscle activity of certain extrinsic foot muscles was unaffected by a change in LTS⁴. Electromyography (EMG) and MRI data also appeared to show that no neuromuscular adaptation was observed when varus and valgus shoe perturbations were tested³⁶. Collecting kinetics and extrinsic muscle activation may give insight into this theory and the effects observed in this study. The fact that muscle activity was not collected in this study is a limitation. Although, it appears that LTS does not affect the measured foot kinematics, Stefanyshyn and

colleagues found that increasing the LTS of a shoe had physiological and mechanical advantages^{1, 3, 4}. The most recent study from this group concludes that LTS improves running economy but that the muscular activation patterns of the extrinsic foot muscles remain the same⁴. The underlying mechanism of these effects is still unknown.

Another limitation of this study is that participants were not split into groups according to two suspected dependent variables: foot type and foot muscle training. This is due to the small sample size. The individual subject gait curves for each inter-segment motion suggest that sub-groups may exist. It is speculated that these groups depend on foot type¹⁹ and the amount of muscle training the subject had due to the regular use of Nike Free shoes. It is speculated that participants with flexible, mobile feet may have been influenced more by changes in LTS than subjects with immobile feet. However, Figures 5.2 to 5.6 show that when wearing the control shoe and when barefoot, subjects appear to have similar average kinematics. Since the Nike Frees were developed to mimic barefoot running, the shoe appears to function as intended, however this is an average and so we cannot infer what is happening within each subject. It is unknown whether this is a trained effect, since the subject's use of Nike Free shoes or barefoot running is unknown.

Results from the current study did show that the majority of the mean differences between the shoe conditions and the barefoot condition were greater than the minimum important difference for the hindfoot and the hallux. It should be mentioned that the minimum important difference for this study was acquired

from a bone pin study where skin artifact error is not present³⁷. Since this multi-segment foot model uses skin-mounted marker clusters, it is susceptible to skin artifact error. However, statistically significant differences have previously been found in foot kinematics between shoed and barefoot conditions during running^{9, 10, 19} and during cutting¹¹ using skin-mounted markers. For running, the effect was present between the barefoot condition and the shoed conditions but not between the different shoed conditions⁹. Similar to Stacoff et al (1991), the differences were more extensive in the hindfoot. In a study by the same group on cutting turns, there were statistical significance between the stiffest shoes and barefoot, but not for less stiff shoes¹¹. It is possible that the shoes in the current study were not stiff enough to obtain a statistically significant difference between conditions.

In conclusion, clinicians and researchers should be aware of the large inter-subject variability that is present whenever assessing feet, since it appears that different patients may have different strategies during running for adapting to footwear perturbations. This study demonstrates that there were no statistically significant differences in foot kinematics between shoes with different longitudinal torsion stiffnesses or forefoot flexion stiffnesses. However, there appears to be an important difference between the shoed conditions and barefoot condition. Future research should attempt to distinguish between the two possible explanations for the non-significant shoe results; either the foot is acting as a redundant system to maintain a preferred loading pattern, or there is an adaptive muscle activation pattern that is influenced by the footwear conditions.

5.5 References

1. Stefanyshyn, D. & Fusco, C. Increased shoe bending stiffness increases sprint performance. *Sports Biomech* 3, 55-66 (2004).
2. Stacoff, A. et al. Effects of shoe sole construction on skeletal motion during running. *Med Sci Sports Exerc* 33, 311-9 (2001).
3. Stefanyshyn, D. J. & Nigg, B. M. Influence of midsole bending stiffness on joint energy and jump height performance. *Med Sci Sports Exerc* 32, 471-6 (2000).
4. Roy, J. P. & Stefanyshyn, D. J. Shoe midsole longitudinal bending stiffness and running economy, joint energy, and EMG. *Med Sci Sports Exerc* 38, 562-9 (2006).
5. Clarke, T. E., Frederick, E. C. & Hamill, C. L. The effects of shoe design parameters on rearfoot control in running. *Med Sci Sports Exerc* 15, 376-81 (1983).
6. McNair, P. J. & Marshall, R. N. Kinematic and kinetic parameters associated with running in different shoes. *Br J Sports Med* 28, 256-60 (1994).
7. Butler, R., Hamil, J. & Davis, I. Effect of footwear on high and low arched runners' mechanics during a prolonged run. *Gait and Posture* 26, 219-225 (2006).
8. Divert, C., Mornieux, G., Baur, H., Mayer, F. & Belli, A. Mechanical comparison of barefoot and shod running. *Int J Sports Med* 26, 593-8 (2005).
9. Stacoff, A., Kalin, X. & Stussi, E. The effects of shoes on the torsion and rearfoot motion in running. *Med Sci Sports Exerc* 23, 482-90 (1991).
10. Segesser, B., Stussi, E., von, A. S. M., Kalin, X. & Ackermann, R. [Torsion --a new concept in construction of sports shoes. Motion excursion of the foot in athletic stress--anatomical and biomechanical observations and their effects on construction of sports shoes]. *Sportverletz Sportschaden* 3, 167-82 (1989).
11. Stacoff, A., Steger, J., Stussi, E. & Reinschmidt, C. Lateral stability in sideward cutting movements. *Med Sci Sports Exerc* 28, 350-8 (1996).
12. Stacoff, A., Reinschmidt, C. & Stussi, E. The movement of the heel within a running shoe. *Med Sci Sports Exerc* 24, 695-701 (1992).
13. Reinschmidt, C., Stacoff, A. & Stussi, E. Heel movement within a court shoe. *Med Sci Sports Exerc* 24, 1390-5 (1992).
14. Bourgit, D., Millet, G. Y. & Fuchslocher, J. Influence of shoes increasing dorsiflexion and decreasing metatarsus flexion on lower limb muscular activity during fitness exercises, walking, and running. *J Strength Cond Res* 22, 966-73 (2008).

15. Miller, J. E., Nigg, B. M., Liu, W., Stefanyshyn, D. J. & Nurse, M. A. Influence of foot, leg and shoe characteristics on subjective comfort. *Foot Ankle Int* 21, 759-67 (2000).
16. Stacoff, A. et al. in XX ISB Congress (2007).
17. Arndt, A. et al. Intrinsic foot kinematics measured in vivo during the stance phase of slow running. *J Biomech* 40, 2672-8 (2007).
18. Wolf, P. et al. Functional units of the human foot. *Gait Posture* (2008).
19. Eslami, M., Begon, M., Farahpour, N. & Allard, P. Forefoot-rearfoot coupling patterns and tibial internal rotation during stance phase of barefoot versus shod running. *Clinical Biomechanics* 22, 74-80 (2007).
20. Jenkyn, T. R. & Nicol, A. C. A multi-segment kinematic model of the foot with a novel definition of forefoot motion for use in clinical gait analysis during walking. *J Biomech* 40, 3271-8 (2007).
21. Jenkyn, T. R., Anas, K. & Nichol, A. Foot segment kinematics during normal walking using a multisegment model of the foot and ankle complex. *J Biomech Eng* 131, 034504 (2009).
22. Robbins, S. & Hanna, A. Running-related injury prevention through barefoot adaptations. *Med Sci Sports Exerc* 19, 148-156 (1987).
23. Cappozzo, A., Catani, F., Croce, U. D. & Leardini, A. Position and orientation in space of bones during movement: anatomical frame definition and determination. *Clin Biomech (Bristol, Avon)* 10, 171-178 (1995).
24. Leardini, A., Benedetti, M. G., Catani, F., Simoncini, L. & Giannini, S. An anatomically based protocol for the description of foot segment kinematics during gait. *Clin Biomech (Bristol, Avon)* 14, 528-36 (1999).
25. Pohl, M. B., Messenger, N. & Buckley, J. G. Changes in foot and lower limb coupling due to systematic variations in step width. *Clin Biomech (Bristol, Avon)* 21, 175-83 (2006).
26. Hunt, A. E., Smith, R. M., Torode, M. & Keenan, A. M. Inter-segment foot motion and ground reaction forces over the stance phase of walking. *Clin Biomech (Bristol, Avon)* 16, 592-600 (2001).
27. Nigg, B. M. The role of impact forces and foot pronation: a new paradigm. *Clin J Sport Med* 11, 2-9 (2001).
28. Reinschmidt, C., van Den Bogert, A. J., Murphy, N., Lundberg, A. & Nigg, B. M. Tibiocalcaneal motion during running, measured with external and bone markers. *Clin Biomech (Bristol, Avon)* 12, 8-16 (1997).
29. Wearing, S. C. et al. Sagittal movement of the medial longitudinal arch is unchanged in plantar fasciitis. *Med Sci Sports Exerc* 36, 1761-7 (2004).
30. Perlman, P. R., Dubois, P. & Siskind, V. Validating the process of taking lateral foot x-rays. *J Am Podiatr Med Assoc* 86, 317-21 (1996).

31. Boyer, K. A. & Nigg, B. M. Changes in muscle activity in response to different impact forces affect soft tissue compartment mechanical properties. *J Biomech Eng* 129, 594-602 (2007).
32. Wakeling, J. M., Liphardt, A. M. & Nigg, B. M. Muscle activity reduces soft-tissue resonance at heel-strike during walking. *J Biomech* 36, 1761-9 (2003).
33. Wakeling, J. M., Nigg, B. M. & Rozitis, A. I. Muscle activity damps the soft tissue resonance that occurs in response to pulsed and continuous vibrations. *J Appl Physiol* 93, 1093-103 (2002).
34. Boyer, K. A. & Nigg, B. M. Muscle tuning during running: implications of an un-tuned landing. *J Biomech Eng* 128, 815-22 (2006).
35. Wakeling, J. M., Pascual, S. A. & Nigg, B. M. Altering muscle activity in the lower extremities by running with different shoes. *Med Sci Sports Exerc* 34, 1529-32 (2002).
36. O'Connor, K. M. & Hamil, J. The role of selected extrinsic foot muscles during running. *Clinical Biomechanics* 19, 71-77 (2004).
37. Nester, C. et al. Foot kinematics during walking measured using bone and surface mounted markers. *J Biomech* 40, 3412-23 (2007).

Chapter 6 – Kinematics of the Segments of the Foot during Level Running and Medial Cutting Turns using a Multi-segment Foot Model

Chapter 6 is a pilot study that examines the difference in foot joint kinematics during running in a straight line and performing an anticipated medial cut at a 60 degree angle. Three subjects performed the two tasks in the same Nike Free trainers that were validated and used in Chapter 5. No other studies were found that examined the difference in kinematics of foot joints distal to the subtalar joint during running and cutting. Methodological difficulties with this study, including the destruction of the markers during the cutting turn, were one of the suspected issues that discourage researchers from examining foot mechanics during cutting. Subjects were only able to cut at 70% effort for this reason.

This chapter will be submitted for publication as an original paper in *Gait & Posture*.

Shultz, R – developed experiment, analyzed all results and wrote the paper

Jenkyn, TR – senior author - helped design the protocol and helped analyze the results

6 Abstract

Optical motion analysis was used to quantify the three-dimensional kinematics of several foot segments during level running and medial cutting turns. A multi-segment model tracked the foot as five individual segments: hindfoot (calcaneus), midfoot (tarsus), medial forefoot (first metatarsal), lateral forefoot (fifth metatarsal), and the hallux. Four inter-segment motions are reported: 1) hindfoot-to-midfoot motion in the frontal plane, 2) forefoot twist with respect to the midfoot in the frontal plane, 3) medial longitudinal arch height-to-length ratio and 4) the hallux angle with respect to the medial forefoot in the sagittal plane. The neutral position for each motion was defined by per-condition static trials in quiet standing. Three male athletes performed two tasks: level running run (7 min/mile) and an anticipated medial cutting turn. Each was performed barefoot and in Nike Free training shoes.

Throughout stance phase, the hindfoot-to-midfoot motion, the forefoot-to-midfoot motion, and the hallux-to-first metatarsal motion, were shown to be greater than the minimum important difference ($>5^\circ$) between the medial cutting task and the running task for both the shoe condition and the barefoot condition. The hallux motion demonstrated the largest change in the barefoot condition occurring at approximately half of the stance phase while the hindfoot segment was the largest for the shoe condition occurring at approximately three quarters of the stance phase. The hindfoot was the most variable for the maximum mean difference (MMD). The forefoot motion was only slightly different compared to the other inter-segmental joint motions, which is likely due to the minimal range of

motion that was observed in the frontal plane for the forefoot during these tasks. The medial longitudinal arch (MLA) height-to-length ratio tended to show differences between the two tasks but again these appeared to be minimal. Future research which places the midfoot marker on the lateral side of the foot may improve the procedure and should investigate the trends found in this study with a larger subject size.

6.1 Introduction

Studies of the kinematics of the joints that make up the foot-ankle complex during level walking, to date, have primarily been limited to hindfoot motion with respect to the tibia^{1,2}. This is sufficient to characterize the movement of joints proximal to the subtalar joint and hindfoot, but does not give information about the more distal, and clinically important, foot joints during level walking^{3, 4}. With improvements in optical tracking accuracy have come investigations of foot joint kinematics more distal than the hindfoot, including the motion of the longitudinal arches and the metatarsophalangeal joints⁵⁻¹¹. Single plane fluoroscopy technology has also lead to studies of foot joint motion during level walking^{12, 13}. However, the most accurate description of three-dimensional foot joint kinematics comes from bone pin studies, which are not readily applicable in clinical practice due to their invasiveness¹⁴⁻¹⁷.

Despite these studies, there is still limited research on foot joint kinematics during other gait tasks, such as cutting turns and running. Studies examining the kinetics and muscle activation behaviour of the ankle-foot complex have pointed to the medial direction change as a common mechanism for lower extremity injuries, including sprain of the ankle lateral ligaments¹⁸⁻²⁴. It is speculated that understanding foot joint motions during this movement could lead to greater insight of the ankle joint kinematics and kinetics²⁵

Three studies have examined foot kinematics during cutting. These compared barefoot versus shoed conditions and focused on the effects of specific shoe and orthotic designs²⁶⁻²⁸. However, these studies only considered the forefoot,

hindfoot, ankle and lower extremity. Useful data were lost by treating the forefoot as a single segment and by not including a separate midfoot segment²⁹.

Only one study has examined multiple foot joint motions of joints distal to the subtalar joint during barefoot running³⁰. To overcome the methodological difficulty of measuring accurate kinematics of all the foot joints during running, this group used invasive bone pins to directly track the bone motions about several joints³⁰. However, the study reported their results in technical frames of reference as opposed to anatomical frames, which severely limits their clinical usefulness. Another group examined the metatarsophalangeal (MTP) joint during running, specifically how MTP joint extension correlated with running economy³¹ and foot sole position³².

What is missing from the literature is a comprehensive study of the three-dimensional kinematics of the foot joint during medial cutting turns and level running. This should be studied in both barefoot and shoed conditions since it is expected that the foot moves differently for each condition. The objective of this study was to compare several foot joint motions during level running and anticipated medial cutting turns. Foot joint kinematics were evaluated using a multi-segment kinematic foot model and an optical motion capture system, a modification of the method developed by Jenkyn and Nicol^{29, 33}. Four inter-segmental motions were examined: hindfoot (calcaneus) with respect to the midfoot (tarsus) in the frontal plane, twist of the forefoot with respect to the midfoot in the frontal plane, angle of the hallux (both phalanges) with respect to the medial forefoot (first metatarsal) in the sagittal plane, and the height-to-length

ratio of the medial longitudinal arch. Each measure was calculated throughout stance phase of both movement tasks in both a barefoot condition and a shoed condition. It was hypothesized that the four inter-segmental joint motion patterns during medial cutting turns would be spatially and temporally different from those during the running task due to the differing position of the tibia with respect to the foot and pathway of the body centre of mass.

6.2 Methods

6.2.1 Subjects

Three male subjects (age = 27 ± 7 years, weight = 69 ± 5 kg) volunteered for this study. None of the subjects had any gait abnormalities of neurological or orthopaedic nature, or any history of surgery or severe trauma to the lower leg or foot. Each subject was a heelstriker who ran at least 15 km per week and was considered a 'trained cutter' in the Nike Sport Research Laboratory (NSRL) database. A 'trained cutter' implies that the subject demonstrated to a Nike researcher that he could consistently cut at the same effort while planting on the forceplate. This study was part of a larger running study conducted at the NSRL on Nike Free Trainers. Three of the running subjects from the larger study returned to complete a cutting session on a different day. The same researcher performed the testing on all three subjects for both the running and cutting sessions.

6.2.2 Experimental equipment

The study was conducted at the Nike Sport Research Laboratory (Nike Inc., Beaverton, OR). The laboratory was equipped with an eight-camera, real-time optical motion capture system (EvaRT 5.04, Eagle HiRes cameras, Motion Analysis Corp., Santa Rosa, CA) with an integrated floor-mounted forceplate (Kistler, Amherst, NY). Kinematic data were sampled at 240 Hz and kinetic data at 1200 Hz.

Three sets of size 9 Nike Free 7.0 trainers were pre-cut with five round 'holes' (hole size ~2.5 cm diameter). The difference between the shoe sets was the navicular hole location, which changed by about 1.0 cm across shoe sets in the anterior/posterior direction. The location of each subject's navicular tuberosity determined which shoe set was used. Holes were needed so that marker triad clusters, attached to the skin of the foot, were visible to the optical motion capture system while a subject was wearing the shoe (Figure 4.1). The maximum size of the holes that could be cut into the shoe without sacrificing the shoe's structural integrity was validated in a separate pilot study on the same model of shoes as in this study (see chapter 2 for further details on this method). These are the same shoes that were used in Chapter 5 for the running study.

The marker triad clusters were designed so that the reflective markers could be detached from their base, which remained affixed to the skin of the foot throughout the protocol. This allowed changing of the shoe between test conditions to occur without disrupting the marker locations or orientations. The stem of the triad cluster consisted of a nylon screw with three carbon-fiber wands

protruding from the screw head. Wooden balls (8mm diameter) attached to the wands were wrapped in reflective tape (Figure 6.1). The base was a nylon nut epoxied to a faux leather base and affixed to the foot via medical adhesive spray (Hollister Medical Adhesive Spray, Hollister Incorporated, Libertyville, IL).



Segment	Cluster Placement
Hindfoot	Postero-lateral calcaneus, lateral to achilles tendon
Midfoot	Dorso-medial foot over the navicular tuberosity
Medial Forefoot	Medial-dorsal foot over midshaft of first metatarsal
Lateral Forefoot	Lateral-dorsal foot over midshaft of fifth metatarsal
Hallux	Dorsal foot over the distal phalange

Figure 6.1. Placement site descriptions (right) for the five marker clusters seen on the subject (left). Each segment of the foot model had a triad cluster. Only the right leg and foot kinematics were studied with the multi-segment foot model.

6.2.3 Multi-segment foot model

The foot was functionally divided into five segments; hindfoot (calcaneous), midfoot (tarsus), medial forefoot (first metatarsal), lateral forefoot (fifth metatarsal) and the hallux (both phalanges). One cluster triad tracked each segment and was placed on the foot according to Jenkyn and Nicol²⁹. Each cluster triad resolved the six degree-of-freedom position and orientation of the segment to

which it was attached. From this four inter-segmental motions were calculated throughout stance phase (Figure 6.2): A) the hindfoot with respect to the midfoot in the frontal plane, B) combined twisting of the two forefoot segments with respect to the midfoot in the frontal plane, C) the angle of the hallux in the sagittal plane with respect to the medial forefoot and D) the height-to-length ratio of the medial longitudinal arch (MLA).

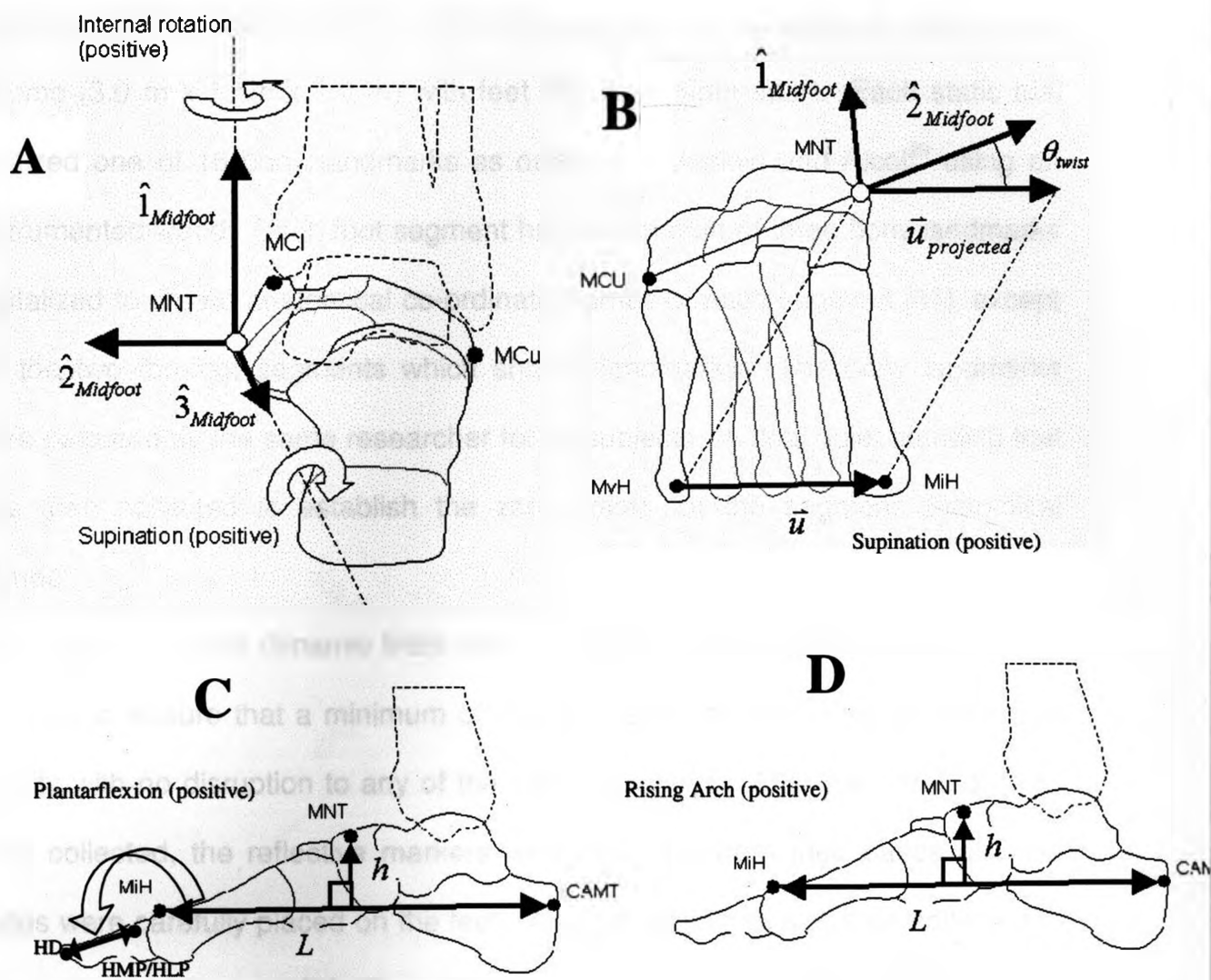


Figure 6.2. Four inter-segment motions are reported: A) hindfoot motion in the frontal plane with respect to the midfoot segment (supination, positive), B) forefoot supination-pronation in the frontal plane with respect to the midfoot segment (supination, positive), C) the hallux angle in the sagittal plane with respect to the first metatarsal (plantarflexion, positive), D) the height-to-length ratio of the medial longitudinal arch (rising of the arch, positive). The neutral or zero position for each motion was defined during quiet, double support standing. (Reprinted with permission from Jenkyn et al. 2007).

6.2.4 Experimental Protocol

Two testing sessions were conducted on separate days, first the running session and then the cutting turn session. Each testing session began with a series of

barefoot trials in quiet standing with the subject at the center of the capture volume (3.0 m x 1.5m x 1.0 m) with feet shoulder width apart. Each static trial digitized one of 16 bony landmarks as outlined in Jenkyn and Nicol²⁹ using an instrumented wand. Each foot segment had a minimum of three bony landmarks digitalized to create anatomical co-ordinate frames of each segment [31], except for the two forefoot segments which shared landmarks. The bony landmarks were palpated by the same researcher for all subjects. A final quiet standing trial was then collected to establish the zero points for the segment anatomical frames.

After digitization, the dynamic trials (either running or cutting) were performed in barefoot to ensure that a minimum of 7 good stance phases were collected per activity with no disruption to any of the marker clusters. After the barefoot trials were collected, the reflective markers were removed from their bases and the shoes were carefully placed on the feet. Another static trial was then collected in quiet standing to establish the shoed neutral positions (per-condition). The digitization trials were only repeated if a marker cluster had been disrupted from its original position during the placement of the shoe.

The two movement tasks tested were level running (at a 7 min/mile pace \pm 5%) and medially-directed, anticipated cutting turns. For the running trials, subjects were requested to strike the forceplate with their right foot without concentrating on contacting the plate (Figure 6.3A). For the medial cutting turns, subjects approached the forceplate at an angle of approximately 60 degrees to the direction of running and left at the same angle (Figure 6.3B). The subjects were

asked to cut at approximately 70% maximal effort. Preliminary data showed that at 100% maximal effort the navicular marker was damaged or rubbed the floor during the planting stage of the cut. Shear forces for each cutting trial were calculated from the floor-mounted forceplate and compared to a maximum barefoot cutting trial to ensure consistency across trials. Only right foot strikes were studied for both movements.

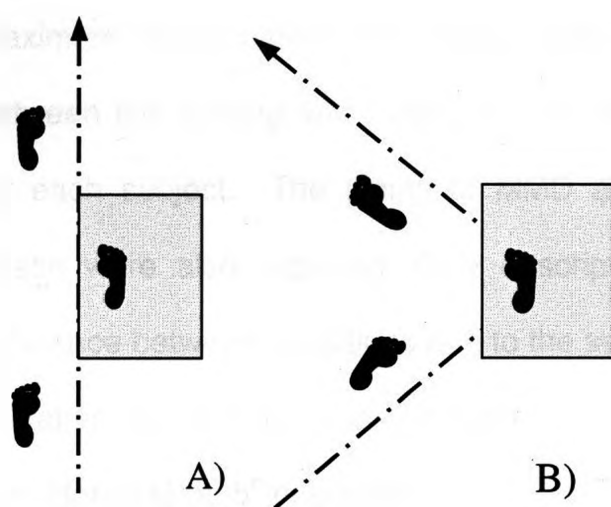


Figure 6.3. Subject motion paths for the A) level walking and B) medially-directed, anticipated cutting turns, showing the sequence of footfalls approaching and leaving the forceplate.

6.2.5 Data Reduction and Analysis

The trajectories from each of the cluster markers were individually filtered using a 4th order Butterworth filter with a low pass cut-off frequency of 20 Hz (justification for cutoff frequency can be found in chapter 1, section 1.8.3) that was dual passed to obtain zero-lag. Calculations of the inter-segmental positions of the multi-segment foot model were performed by custom-written software (Matlab, The Mathworks, Natick, MA). The inter-segmental positions from each static trial were averaged over 0.5 seconds to obtain the neutral positions. From the

dynamic trials, the hindfoot motion, the combined forefoot twist, the height-to-length ratio of MLA and the hallux angle were calculated throughout stance phase for five running and the five cutting trials each for barefoot and shoe conditions. The timing of trials was normalized to 100% stance phase (from heel strike to toe-off). The trials for each condition were averaged and standard deviations for each condition for each inter-segmental motion were calculated. Maximum mean differences (MMD) and minimum mean differences (MNMD) between the running and cutting curves were then calculated for each condition for each subject. The timing of MMD and MNMD as percentages of stance phase were also captured. Only descriptive statistics were used to examine difference between conditions due to the small sample size and the high standard deviation found in the foot kinematics^{17, 30}. A minimum important difference was considered to be 5° or greater¹⁷.

6.3 Results

Table 6.1 compares the cutting and running kinematic curves for each of the four inter-segmental motions in both the barefoot and shoed conditions. The measures listed are the maximum mean differences (MMD), the timing of the MMD (TMMD), the minimum mean differences (MNMD) and the timing of MNMD (TMNMD). For each of these measures the means and standard deviations (SD) are reported.

Table 6.1. The maximum mean differences (MMD) between the cutting trials and the running trials, the timing of the MMD (TMMD), the minimum mean differences (MNMD) between these same trials and the timing of MNMD (TMNMD) are listed. The four inter-segmental motions (HF-Hindfoot, FF-Forefoot, HX - Hallux, MLA - Medial Longitudinal Arch) are shown for both the barefoot and shod conditions. For each, the means and standard deviations (SD) are reported.

	Barefoot							
	MMD		TMMD		MNMD		TMNMD	
	Mean	SD	mean	SD	mean	SD	mean	SD
HF (deg)	17.3	6.6	97.0	4.0	2.4	4.1	38.7	27.0
FF (deg)	6.3	2.9	75.3	26.0	0.02	0.02	62.7	22.5
HX (deg)	19.0	4.3	51.0	45.5	0.1	0.1	41.3	16.9
MLA (ratio)	0.04	0.03	64.3	32.6	0.0004	0.0003	53.6	16.3
	Shoes							
	MMD		TMMD		MNMD		TMNMD	
	mean	SD	mean	SD	mean	SD	mean	SD
HF* (deg)	25.8	28.8	70.0	21.9	4.3	4.9	42.0	14.5
FF (deg)	8.7	3.9	38.7	18.2	2.5	4.0	49.8	17.6
HX (deg)	20.4	1.5	75.9	8.5	0.8	2.1	41.3	16.9
MLA (ratio)	0.09	0.13	39.4	5.7	0.04	0.11	64.0	14.0

**The data for subject 2 were removed from the hindfoot shoe condition since the triad cluster was offset during this trial*

This comparison shows that the hallux segment has the largest maximum mean difference for the barefoot condition (MMD = $19.0^{\circ} \pm 4.3$), whereas the hindfoot segment has the largest MMD for the shoe condition (MMD = $25.8^{\circ} \pm 28.8$).

These differences occur on average at $51.0\% \pm 45.5$ of the stance phase for the hallux segment for the barefoot condition and in late stance (TMMD = $70.0\% \pm 21.9$) for the hindfoot segment of for the shoed condition. However the barefoot condition for the hallux segment is highly variable with a standard deviation of 45.51% stance phase. The hindfoot segment also shows large variance for the maximum mean difference for both the barefoot and shoed conditions (MMD= $17.3^\circ \pm 6.61$,bare; MMD= $25.8^\circ \pm 28.8$, shoed), although it is smaller during the barefoot condition than during the shoe conditions. The maximum mean differences and variability between the forefoot motion and the motion of the arch were considered minimal compared to the other two joint motions. It should be noted that this difference tends to occur during the first half of stance phase during the shoed condition and during the second half of stance phase during the barefoot condition for both running and cutting (see Table 6.1).

The minimum mean differences show that during a portion of the cutting task, each of the inter-segmental motions tends to mimic their motions observed during running. However, the timing of the MNMD occurrence is inconsistent and the magnitude is often limited (see Table 6.1).

Figures 6.4 and 6.5 show the mean curves (averaged over the three subjects) for the four inter-segmental motions for the barefoot (Figure 6.4) and the shoed conditions (Figure 6.5). The hindfoot segment motions pattern during cutting is similar to that during running around midstance only (30-50% of stance phase) for both the shoed and barefoot conditions. The forefoot range of motion is small compared the hindfoot motion and hallux motion, and tends to remain around its

neutral position for both conditions and for both activities. The hallux motion during the cutting task appears to deviate from the running task with a similar kinematic pattern but out of phase by 20% of stance. The pattern of the hallux motion during these activities appears to be similar between tasks (Figure 6.4C and 6.5C). As seen in Figures 6.4D and 6.5D there is little difference between the medial longitudinal arch motion between the barefoot condition and the shoe condition. The minimum important difference for the medial longitudinal arch height-to-length ratio is considered to be 0.03 (refer to Appendix A for this calculation). However, qualitatively the patterns for the MLA kinematics during the cutting task appear opposite to that during the running task for the barefoot condition and out of phase by 40% of stance for the shoed conditions.

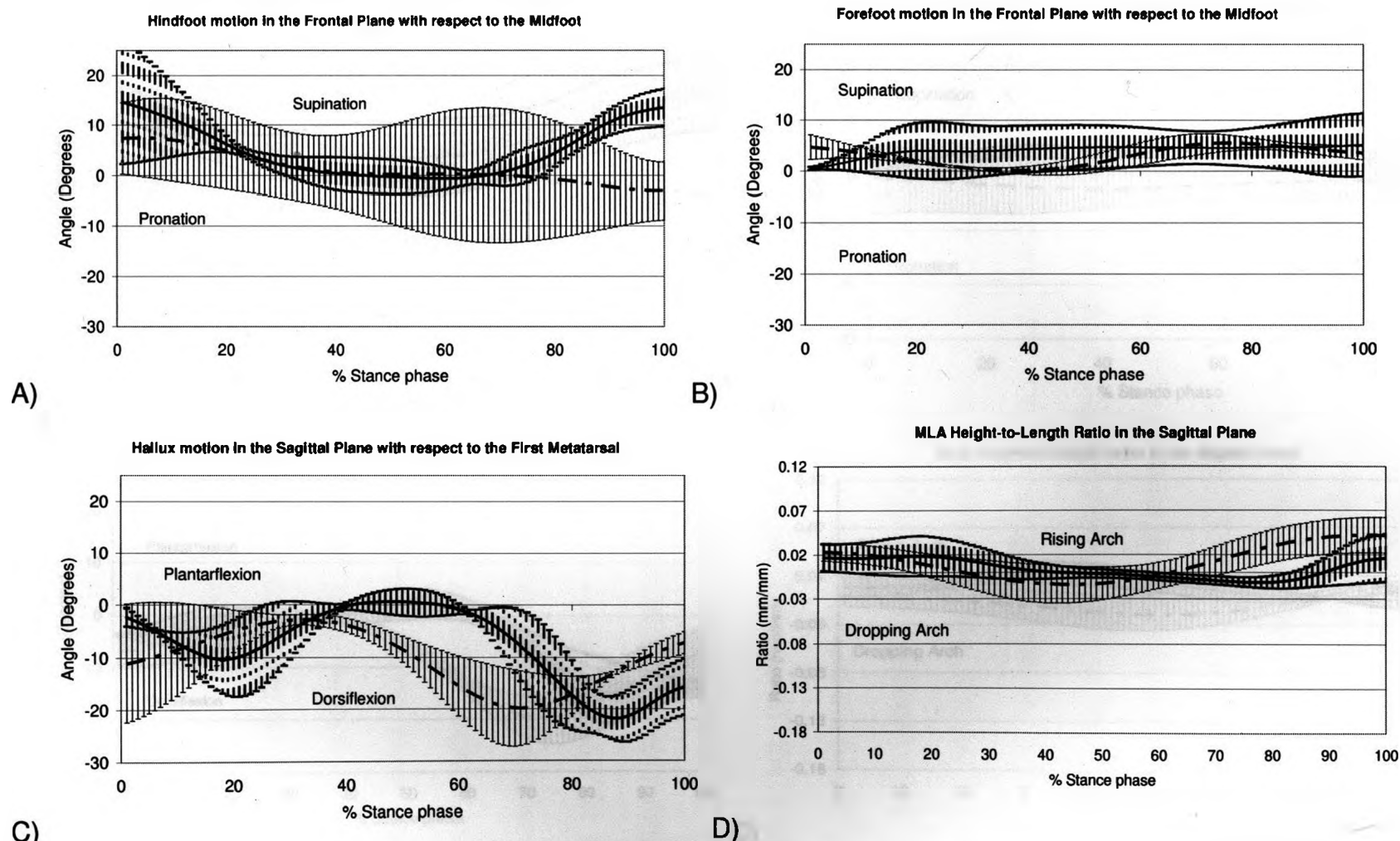


Figure 6.4 Barefoot kinematic curves of the averaged inter-segmental joint motions during barefoot running (dashed line) and cutting (solid line). Four motions are shown: A) hindfoot motion with respect to the midfoot in the frontal plane, B) forefoot motion with respect to the midfoot in the frontal plane, C) hallux motion in the sagittal plane with respect to the first metatarsal, and D) medial longitudinal arch height-to-length ratio. The horizontal axis is normalized to 100% stance phase. The hindfoot is the most different between tasks, with the inter-segmental motions significantly different in the first and last 40% of stance phase. For the forefoot, the cutting trials show more variability than the running trials. However, the range of motion for both tasks is small and the forefoot kinematics are similar between tasks. The hallux motion is the least variable and yet shows the greatest difference between the cutting and running tasks. The kinematic curves show similar patterns in both tasks, but they appear to be out of phase by about 20% of the stance. The medial longitudinal Arch (MLA) motion during cutting appears to be out of phase by 40% compared to during running.

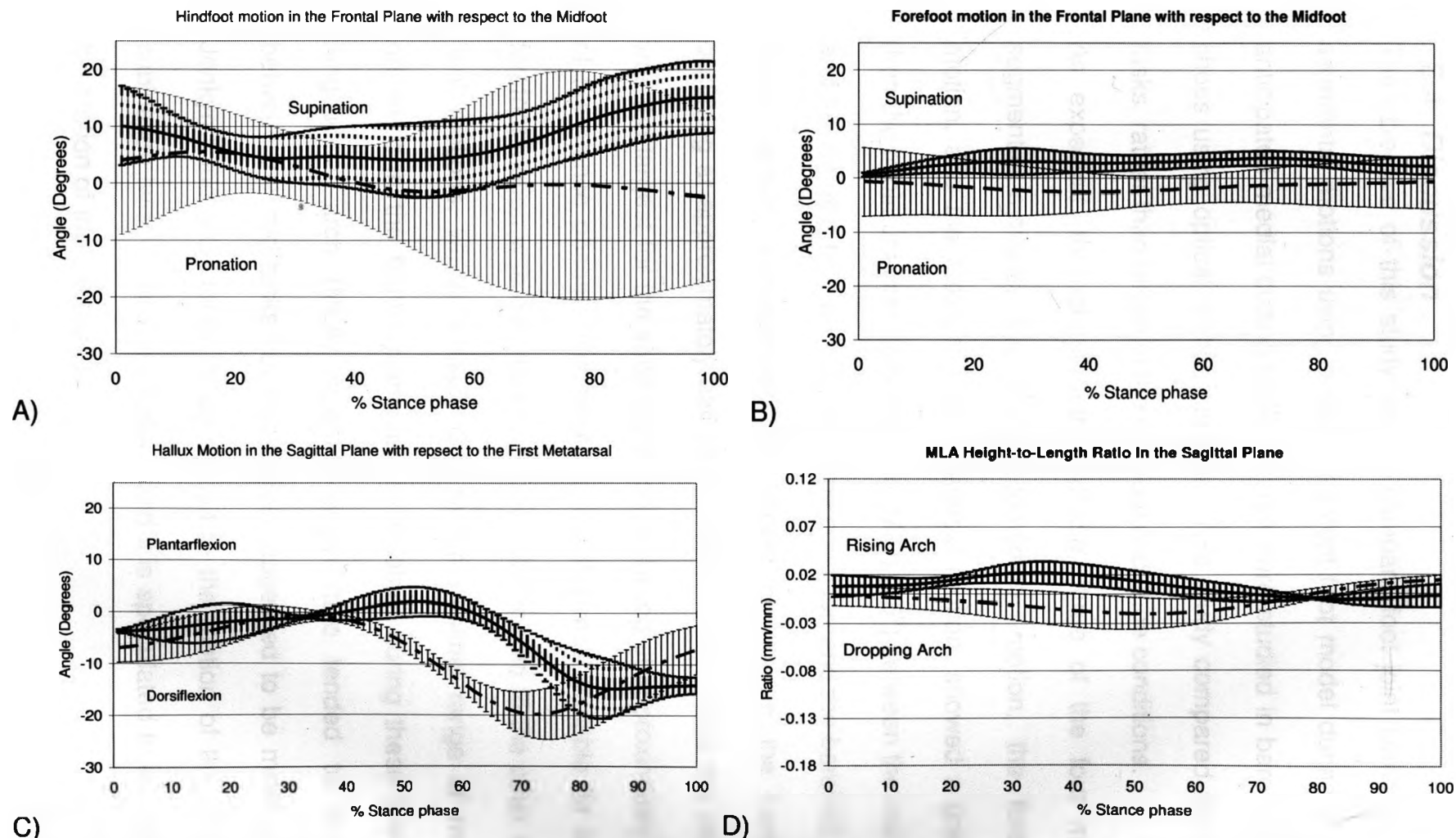


Figure 6.5 Shoed kinematic curves of the averaged inter-segmental joint motions during shoed running (dashed line) and cutting (solid line). Four motions are shown: a) hindfoot motion with respect to the midfoot in the frontal plane, b) forefoot motion with respect to the midfoot in the frontal plane, c) hallux motion in the sagittal plane with respect to the first metatarsal, and d) medial longitudinal arch height-to-length ratio. The horizontal axis is normalized to 100% stance phase. The hindfoot shows the largest variability of all the inter-segmental joint motions, particularly for the running task. Similar to the barefoot condition in Figure 4.4 the hindfoot during cutting is consistently different from that during running for the first and last 40% of stance. During both the running task and the cutting task the forefoot remained close to its neutral position. Hallux motion was similar to the barefoot condition as seen in Figure 4.4. The hallux motion is the least variable and yet shows the greatest difference between the cutting and running tasks, which have a similar pattern but appear to be out of phase by 20% of stance. Medial longitudinal arch motion during cutting appears to be opposite that during running.

6.4 Discussion

The objective of this study was to compare foot joint kinematics of four inter-segmental motions using a multi-segment foot model during level running and anticipated medial cutting turns. These were studied in barefoot and in running shoes using optical motion capture. This study compared the two movement tasks, rather than between the barefoot and shoe conditions.

As expected, throughout stance phase, three of the four measured inter-segmental motions, the hindfoot-to-midfoot motion, the forefoot-to-midfoot motion, and the hallux-to-first metatarsal motion, showed a greater difference than the minimum important distance (MID) ($>5^\circ$) between the medial cutting task and the running task for both the shoe condition and the barefoot condition. The hallux motion demonstrated the largest change in the barefoot condition occurring at approximately half of the stance phase while the hindfoot segment was the largest for the shoe condition occurring at approximately three quarters of the stance phase. The hindfoot was the most variable for the MID. The forefoot motion was only slightly different compared to the other inter-segmental joint motions, which is likely due to the minimal range of motion that was observed in the frontal plane for the forefoot during these tasks. The medial longitudinal arch (MLA) height-to-length ratio tended to show differences between the two tasks but again these appeared to be minimal. As noted by Jenkyn²⁹ the MLA tends to be related to the motion of the forefoot pronation-supination twist in the frontal plane and it is speculated to also be influenced by the motion of the calcaneus.

The differences between the cutting and running tasks were likely driven by the more medial positioning of the lower leg segment during a cutting turn relative to the foot during stance phase, as well as the pathway of the body center of mass. During level walking along a straight path, the tibia remains in the same vertical plane throughout stance phase. The center of mass also remains on a generally straight trajectory in the direction of motion. It appears that the adaptations of the foot to the medial lean of the leg and the change in the trunk position occurs in the hindfoot since there was minimal difference in the forefoot and MLarch motion pattern between the running task and cutting task. This may also be due to the instruction to cut at 70% maximum effort as it may have caused the subjects to maintain more of rigid forefoot during their cutting trials. The motion of the hallux in the sagittal plane was also limited by the floor which may explain why the pattern of motion in the sagittal plane during cutting is similar to that obtained during running. However, the hallux motion tended to be out of phase when compared between the cutting and running gait patterns, most likely a consequence of the increased push-off required at toe-off during a cutting movement. Overall, as hypothesized it appears that the four inter-segmental motions calculated during running and cutting are either spatially or temporally different. However, these differences may not be similar between the shoes and barefoot running and cutting, as seen in Figure 6.4 and 6.5, specifically the hindfoot and the medial longitudinal arch. Further research is need to compare across these conditions (shoes and barefoot) while subjects are running and cutting while wearing shoes or in barefeet.

A weakness of the current study is that unanticipated cutting turns were not examined. It is suspected that unanticipated direction changes would alter the joint motion during the cutting trials, as they have been shown to double the moments at the knee during unanticipated side stepping³⁴. A future study where the timing and direction of the cutting turn were unknown to the subject prior to each trial could test this hypothesis. Also, the subjects were asked to cut at only 70% maximum effort which is likely to decrease the range of motion of the foot during the cutting trials. Placing a marker cluster on the cuboid instead of the navicular would allow the subjects to cut at 100% maximum effort. However, this would be an adaptation to the multi-segment foot model used in this study that would need prior validation.

In this study, the high within-subject and between-subject variability seen could in part be due to a small sample size, and the skin motion error that is inherent with skin-mounted marker clusters and optical motion capture. Skin-mounted markers are known to move relative to the underlying bone which introduces errors into the measured kinematics, particularly in smaller distal segments such as those of the foot¹⁵. During running, the rapid deceleration of the foot at heel strike is speculated to cause inertial motions in the marker clusters³⁵ that are independent of the underlying bones. It has been noted in the literature that as a subject's pace increases from walking to running there appears to be an increase in the standard deviations of kinematic measures²⁹.

It is difficult to compare this study to previous foot kinematic studies due to the methodological differences. Using this multi-segment kinematic foot model, the

hindfoot and forefoot kinematics are calculated with respect to the midfoot. Previous studies often calculate hindfoot motion with respect to the tibia, which combines hindfoot motion with subtalar and ankle joint motions³⁶. Several studies have also used technical coordinate frames of reference whereas in this study anatomic frames were used^{17, 30}. As Arndt et al³⁰ mention, the lack of an International Society of Biomechanics (ISB) recommended joint coordinate system for the foot-ankle complex continues to make comparisons across studies difficult.

No other data were found examining the kinematics of joints distal to the subtalar joint during barefoot medial cutting movements. A few studies examined shoe kinematics or lower limb kinematics using two-dimensional film analysis, but these results can not be compared to the present study^{26, 27}. However, the gait curves of the stance phase for the hindfoot motion from this study and a study by Reinschmidt et al³⁷ show a similar gait pattern.

Although this study gives insight into how the foot joints react to a direction change compared to level running, further research is necessary to further characterize these results. Future studies focusing on joint motion during a directional change, such as a cutting turn, or during running, should examine a variety of running shoes worn and tested on a larger number of subjects. This study does provide evidence that the foot moves differently during running and cutting turns, which may influence not only the joints in the foot but also the other joints more proximal. This may be important when analyzing lower limb

biomechanical parameters and their influences on lower joint pathologies, including commonly occurring sports injuries.

6.5 References

1. Cornwall, M. W. & McPoil, T. G. Three-dimensional movement of the foot during the stance phase of walking. *J Am Podiatr Med Assoc* 89, 56-66 (1999).
2. Youberg, L. D., Cornwall, M. W., McPoil, T. G. & Hannon, P. R. The amount of rearfoot motion used during the stance phase of walking. *J Am Podiatr Med Assoc* 95, 376-82 (2005).
3. Perry, J. *Gait analysis: normal and pathological function* (Slack, Inc, Thorofare, NJ, USA, 1992).
4. Leardini, A., Benedetti, M. G., Catani, F., Simoncini, L. & Giannini, S. An anatomically based protocol for the description of foot segment kinematics during gait. *Clin Biomech (Bristol, Avon)* 14, 528-36 (1999).
5. Pohl, M. B., Messenger, N. & Buckley, J. G. Forefoot, rearfoot and shank coupling: effect of variations in speed and mode of gait. *Gait Posture* 25, 295-302 (2007).
6. Cornwall, M. W. & McPoil, T. G. Motion of the calcaneus, navicular, and first metatarsal during the stance phase of walking. *J Am Podiatr Med Assoc* 92, 67-76 (2002).
7. Pohl, M. B., Messenger, N. & Buckley, J. G. Changes in foot and lower limb coupling due to systematic variations in step width. *Clin Biomech (Bristol, Avon)* 21, 175-83 (2006).
8. Cornwall, M. W. & McPoil, T. G. Relative movement of the navicular bone during normal walking. *Foot Ankle Int* 20, 507-12 (1999).
9. Cornwall, M. W. et al. The influence of first ray mobility on forefoot plantar pressure and hindfoot kinematics during walking. *Foot Ankle Int* 27, 539-47 (2006).
10. Kappel-Bargas, A., Woolf, R. D., Cornwall, M. W. & McPoil, T. G. The windlass mechanism during normal walking and passive first metatarsalphalangeal joint extension. *Clin Biomech (Bristol, Avon)* 13, 190-194 (1998).
11. Reischl, S. F., Powers, C. M., Rao, S. & Perry, J. Relationship between foot pronation and rotation of the tibia and femur during walking. *Foot Ankle Int* 20, 513-20 (1999).
12. Wearing, S. C. et al. Sagittal movement of the medial longitudinal arch is unchanged in plantar fasciitis. *Med Sci Sports Exerc* 36, 1761-7 (2004).

13. Perlman, P. R., Dubois, P. & Siskind, V. Validating the process of taking lateral foot x-rays. *J Am Podiatr Med Assoc* 86, 317-21 (1996).
14. Westblad, P., Hashimoto, T., Winson, I., Lundberg, A. & Arndt, A. Differences in ankle-joint complex motion during the stance phase of walking as measured by superficial and bone-anchored markers. *Foot Ankle Int* 23, 856-63 (2002).
15. Reinschmidt, C. et al. Tibiofemoral and tibio-calcaneal motion during walking: external vs. skeletal markers. *Gait and Posture* 6, 98-109 (October 1997).
16. Arndt, A., Westblad, P., Winson, I., Hashimoto, T. & Lundberg, A. Ankle and subtalar kinematics measured with intracortical pins during the stance phase of walking. *Foot Ankle Int* 25, 357-64 (2004).
17. Nester, C. et al. Foot kinematics during walking measured using bone and surface mounted markers. *J Biomech* 40, 3412-23 (2007).
18. Hartsell, H. D. & Spaulding, S. J. Eccentric/concentric ratios at selected velocities for the invertor and evertor muscles of the chronically unstable ankle. *Br J Sports Med* 33, 255-8 (1999).
19. Nyska, M. et al. Dynamic force distribution during level walking under the feet of patients with chronic ankle instability. *Br J Sports Med* 37, 495-7 (2003).
20. Spaulding, S. J., Livingston, L. A. & Hartsell, H. D. The influence of external orthotic support on the adaptive gait characteristics of individuals with chronically unstable ankles. *Gait Posture* 17, 152-8 (2003).
21. Laughman, R. K., Carr, T. A., Chao, E. Y., Youdas, J. W. & Sim, F. H. Three-dimensional kinematics of the taped ankle before and after exercise. *Am J Sports Med* 8, 425-31 (1980).
22. Rand, M. K. & Ohtsuki, T. EMG analysis of lower limb muscles in humans during quick change in running directions. *Gait Posture* 12, 169-83 (2000).
23. Hase, K. & Stein, R. B. Turning strategies during human walking. *J Neurophysiol* 81, 2914-22 (1999).
24. Nieuwenhuijzen, P. H., Gruneberg, C. & Duysens, J. Mechanically induced ankle inversion during human walking and jumping. *J Neurosci Methods* 117, 133-40 (2002).
25. Jenkyn, T. in *Gait and Clinical Movement Society, 1st Annual Meeting* (Chattanooga, TN, USA, 2001).
26. Stacoff, A., Steger, J., Stussi, E. & Reinschmidt, C. Lateral stability in sideward cutting movements. *Med Sci Sports Exerc* 28, 350-8 (1996).
27. Stacoff, A., Steger, J. & Stussi, E. [Control of the rear foot in lateral movements in sports]. *Sportverletz Sportschaden* 7, 22-9 (1993).

28. Gudibanda, A. & Wang, Y. Effect of the ankle stabilizing orthosis on foot and ankle kinematics during cutting maneuvers. *Res Sports Med* 13, 111-26 (2005).
29. Jenkyn, T. R. & Nicol, A. C. A multi-segment kinematic model of the foot with a novel definition of forefoot motion for use in clinical gait analysis during walking. *J Biomech* 40, 3271-8 (2007).
30. Arndt, A. et al. Intrinsic foot kinematics measured in vivo during the stance phase of slow running. *J Biomech* 40, 2672-8 (2007).
31. Roy, J. P. & Stefanyshyn, D. J. Shoe midsole longitudinal bending stiffness and running economy, joint energy, and EMG. *Med Sci Sports Exerc* 38, 562-9 (2006).
32. Krell, J. B. & Stefanyshyn, D. J. The relationship between extension of the metatarsophalangeal joint and sprint time for 100 m Olympic athletes. *J Sports Sci* 24, 175-80 (2006).
33. Jenkyn, T. R., Anas, K. & Nichol, A. Foot segment kinematics during normal walking using a multisegment model of the foot and ankle complex. *J Biomech Eng* 131, 034504 (2009).
34. Besier, T. F., Lloyd, D. G., Ackland, T. R. & Cochrane, J. L. Anticipatory effects on knee joint loading during running and cutting maneuvers. *Med Sci Sports Exerc* 33, 1176-81 (2001).
35. Gillespie, K. A. & Dickey, J. P. Determination of the effectiveness of materials in attenuating high frequency shock during gait using filterbank analysis. *Clin Biomech (Bristol, Avon)* 18, 50-9 (2003).
36. Dugan, S. A. & Bhat, K. P. Biomechanics and analysis of running gait. *Phys Med Rehabil Clin N Am* 16, 603-21 (2005).
37. Reinschmidt, C., Stacoff, A. & Stussi, E. Heel movement within a court shoe. *Med Sci Sports Exerc* 24, 1390-5 (1992).

7 Chapter 7: Conclusion

The overall objective of this thesis was to develop a method to measure four inter-segmental joint motions of the foot using a multi-segment foot model during running in a variety of shoe modifications and different dynamic movements, such as running and cutting. Favourable results were found in most of the studies, with the exception of the rotation component of the soft tissue artifact. The results of the three methodological studies influenced the protocol for the two clinical studies, including the size of the window cut into the testing shoes, which type of neutral trial was used, and the error associated with using skin surface markers. Conclusions from the clinical tests demonstrate that the foot appears to have a method for adapting to foot perturbation or that the sensitivity of the system was not high enough to capture the true motion of the individual foot bones during running in different running shoe conditions. This was not the case for a change in direction, a cutting turn compared to level running, where the joint curve patterns of motion for the measured inter-segment joints for the cutting turn deviated from the running curves.

Past research has shown that soft tissue error decreases when the passive reflective markers are affixed directly to the foot via windows in the shoe as opposed to placing the markers on the shoe. In chapter 2, a method was developed to ensure that the structural integrity of the shoe and the joint motion patterns of the foot are maintained when these windows are cut into the shoe. The method analyzed the motion of the foot and the deformation of the shoe simultaneously, and determined the maximum window size that could be cut into a shoe to achieve the previously mentioned objectives. A window size of 2.5 cm provided adequate space for the markers to avoid rubbing against the shoe. It was observed that the foot motion deviated from the previous joint patterns for hole sizes above this size for the hindfoot, hallux and the medial longitudinal arch. As expected, the motion control shoe was the most affected by the holes, followed by the stability shoe and the neutral cushioning shoe. This window size

validation procedure should be conducted before the commencement of any research study that uses a multi-segment foot model to test the function of running shoes.

The method developed in chapter 2 was used to validate the hole sizes for the Nike Free trainers that were tested in chapters 5 and 6. Results of this testing revealed that a 2.5 cm hole size was appropriate for the Nike Free Trainers 7.0, which is similar to the hindfoot holes reported in Stacoff et al.¹ (1.7 x 2.4 cm). Future research should continue to test different brands and types of running shoes, since the studies conducted in this dissertation, along with the Stacoff study, tested three different shoe brands and four different shoe types (motion control, stability, neutral cushioning and Nike Free trainers) and found similar, validated hole sizes.

It is suspected that different brands and types of running shoes will also affect the neutral position of each of the inter-segmental joints, ultimately affecting their absolute motion during a dynamic task. As discussed in chapter 3, this is an important concept for researchers examining running-related injury mechanisms, specifically those researchers who are investigating the underlying mechanisms for the clinical effectiveness of orthotics and specifically designed running shoes for specific foot types. These devices are designed to alleviate pain and restore function. Static trials of ten participants were collected while the subjects stood in quiet-standing in three different shoe conditions and barefoot. The results showed that there were statistical differences between the shoe conditions and the differences were greater than the MID for the four inter-segmental joint motions. These differences in the neutral positions would not be observed in a dynamic test if a pre-condition static trial method is used, and consequently valuable data will be lost. The method of static trials is an important consideration when designing the methodology of a research study that examines the differences in kinematics across different shoe conditions. As shown in chapter three, there are strengths and weaknesses to both of these methods. The single neutral position produces less variability in the joint

positions and is able to investigate the end-of-range, but the researcher is unable to separate the neutral position from the ROM, meaning that no data on the neutral position is obtained, nor is information on the symmetry of the joint. The per-condition trial, on the other hand, produces information on the joint symmetry information by separating the neutral trial from the range of motion, which means that the researcher also obtains information on the neutral position. The disadvantage with this method is that there is more variability in the joint positions and no end-of-range information is available.

Throughout this dissertation, different hypotheses on how the foot adapts to a footwear perturbation have been discussed. These proposed hypotheses, include pre-determined muscle activation patterns, pre-determined kinematic foot patterns and also the idea that the foot is a redundant system. There is also the idea that there is an end-of-range or an active boundary for each structure of the body that when surpassed can increase an athlete's risk of injury. Knowing the absolute range of motion of the joint for each condition is important for investigating this hypothesis. The evaluation of all of these hypotheses is important and depends on the careful selection of per-condition neutral positions or a single neutral position for the study's methodology.

Another methodological consideration is the amount of soft tissue artifact the skin surface markers are susceptible to in the given marker locations on the foot. This is one of the most discussed errors of gait analysis. Chapter 5 attempted to calculate the rotational and translational components of the STA for the hindfoot and midfoot cluster markers used in this dissertation. These markers are located on the lateral calcaneus (hindfoot) and the navicular tuberosity (midfoot). The average translational differences were from 5.90 ± 7.29 mm (HS-QS) to 12.15 ± 0.25 mm (TO-QS) for the calcaneus and -7.57 ± 7.58 mm (HS-QS) to -16.42 ± 16.68 mm (TO-QS) for the navicular. The average rotational differences were $0.13 \pm 2.23^\circ$ (HS-QS) to $0.24 \pm 0.48^\circ$ (MS-QS) and $-0.62 \pm 0.88^\circ$ (HS-QS) to $-0.73 \pm 0.70^\circ$ (TO-QS), for the calcaneus and navicular, respectively. The hindfoot marker cluster better represented the motion of the calcaneus than the midfoot

marker cluster represented the motion of the navicular. However, both markers moved more relative to the underlying bone during the toe-off position than the heel strike or midstance position. This amount of STA is perhaps to be expected since it is higher than the STA found when point markers are used on the foot but less than the STA observed when skin markers are attached to the lower leg or thigh. It is suspected that the rotational component might not have been accurately measured since it was consistently lower than one degree which seems very low compared to other observed values in research. Further research using Roentgen stereophotogrammetry analysis (RSA) and 3D imaging technologies, including dual fluoroscopy, is suspected to better calculate this error. Also, the STA associated with the other three segments of the multi-segment foot model, the medial forefoot, the lateral forefoot and the hallux, need to be quantified. The use of skin markers is one of the limitations of the other studies in this dissertation due to STA.

The other main limitation for the running shoe studies was the small sample size. As noted in the study chapters, this is a common issue in foot research that use multi-segment foot models. The post-analysis for these studies is very cumbersome which generally restricts studies to examining low numbers of subjects. The use of traditional statistics is also difficult with this population, not only because of the small sample size, but also because of the high variability within subjects and **between** subjects. As noted in the study chapters, this is partly due to the STA, which is influenced by the vibration and inertial motion of the marker clusters which has been shown to increase with increased speeds such as during running.

The results and limitations of the previous three methodological studies were considered during the design of the two clinical studies. The first of these two studies examined the effect of longitudinal torsion stiffness (LTS) and forefoot flexion on foot kinematics and only found a statistical difference for the hindfoot motion between the Nike Free control shoe condition and the Nike Free with the

forefoot plate, which happens to be the two shoe conditions that are similar in LTS and FFlex. However, majority of the shoe conditions compared to the barefoot condition during running for the hindfoot and the hallux angles were greater than the MID. Although not significant, the shoe with the forefoot plate did tend to restrict the motion of the forefoot which increased the motion of the hindfoot and medial longitudinal arch since they remained free to move, whereas the shoe with the full length plate tended to minimize the ROM in most inter-segmental joints compared to the barefoot condition. On average, the foot motion when the subject was wearing the Nike Free tended to mimic barefoot running pattern quite well compared with the other two shoe conditions, with the exception of the hallux motion. It appears that the three shoe conditions were unable to dramatically perturb the foot's range of motion pattern differently. This is seen in the joint motion curves found in chapter 5.

The second clinical study investigated the motion of the foot during cutting and during running and concluded that a directional change influenced the motion of the foot since the joint angles were greater than the MID. Examining the inter-segmental joint curves from the two clinical studies, it is obvious that a directional change dramatically alters the movement of the foot compared to a change in the LTS or FFlex of the shoe, mostly in the hindfoot and the midfoot. This infers that during a straight path, the foot may have a pre-determined range of motion (ROM) and joint pattern that is unable to be perturbed by a change in LTS, but is perturbed by a change in direction. Considering the results from chapter 3 as well, which examined the change in the neutral position, it appears that the shoes

may modify the absolute joint angular motion of the foot but do not disrupt the joint pattern. This may be an important result for injury mechanisms and the idea of end-of-range. This is best explained with an example. A subject's end-of-range for a certain soft tissue is considered to be located at 25 degrees of eversion in the hindfoot. This same subject runs in a pair of shoes and has a hindfoot eversion of 5 degrees to 20 degrees (ROM = 15 degrees) throughout stance phase. If this same subject runs in a different pair of running shoes which positions the subject's hindfoot in an absolute range of 15 degrees to 30 degrees of eversion throughout stance phase, the ROM is still equal to 15 degrees, but now the subject has surpassed the end-of-range for the joint. If the subject continues to run in this second pair of shoes, it is speculated that over time the increased stress on soft tissue constraints of the joint will cause weakening and eventually an over-use injury may occur. This concept needs to be investigated further, including the development of a method for dynamically testing end-of-range and the examination of how per-condition static trials versus single static trials affect the dynamic trials of different shoe conditions.

Future research should also examine the joints proximal to the foot when the longitudinal torsion stiffness of the footwear is altered or during a directional change. The joints proximal to the subtalar joint are influenced by the motion of the foot joints via the kinetic chain during a closed chain exercise. The model used in this dissertation is compatible with the Helen Hayes marker set that is commonly used in most gait laboratories, consequently all foot joints and lower extremity joints can be examined simultaneously. Pressure and kinetic data

should also be captured to examine whether LTS, FFlex or a direction change affect these measures. It is suspected that since the carbon plates change the hardness of the shoe, there will be a pressure change that may or may not be due to a change in LTS.

Overall, these studies demonstrate that it is possible to test the motion of a foot within a shoe during a variety of activities, including running, walking and cutting, and during a variety of shoe conditions when using a multi-segment foot model and optical motion capture. The objective of this dissertation was not to develop a foot model but to develop and test a clinical method to investigate various shoe conditions. The following section demonstrates one possible usage of this method to assist researchers in their quest to discover the mechanism behind how the foot adapts to perturbation.

7.1 Addition to current research – The theory of Excessive Pronation

The theory that excessive pronation of the foot produces running related injuries was developed from retrospective studies examining biomechanical abnormalities of injured groups compared to control groups²⁻⁶. When more pronated feet were observed in an injured group compared to a control group, it was concluded that having pronated feet was a risk of injury for a runner^{5, 7, 8}. Studies concluded that 58-68% of these injuries were obtained by subjects who had moderate to severe pronated feet^{5, 8}. Injuries due to excessive pronation of the foot during the stance phase of running were shown to occur in the foot as

well as other segments and joints proximal to the foot including the hip, knee, and Achilles tendon ⁷.

Certain injuries were thought to occur in athletes with a certain foot type. The following chart, created by MacKenzie ⁶, shows the different injuries related to each foot type. Injuries of athletes with pes cavus feet were suspected to be caused by a lack of shock attenuation ability ⁶. A pes cavus foot was suspected to be unable to achieve the necessary pronation position in the early stages of the gait cycle to adapt to the terrain and be flexible enough to adequately shock absorb. Pes planus feet tended to lead to injuries due to abnormal rotation of the foot, ankle, tibia and continue up the kinetic chain ⁶. This foot type is suspected to be unable to form the necessary rigid lever needed for propulsion in the later stages of stance phase.

Table 7.1. Table of injuries related to foot type ⁶

Pes Cavus (high-arch, over supinated)	Pes Planus (low-arch, over pronated, flat foot)
Iliotibial band friction syndrome	Tibial stress syndrome
Planter fasciitis	Patellofemoral pain syndrome
Stress fractures	Posterior tibialis tendonitis
Achilles tendonitis	Achilles tendonitis
Gastroc/soleus muscle strain	Plantar fasciitis
Trochanteric bursitis	
Peroneal tendonitis	
Metatarsalgia	

Running shoe companies tend to design running shoes for these specific foot types, promoting either motion control features to prevent excessive pronation or extra cushioning to assist supinators ⁹. However, in recent bone pin studies, and even skin-mounted marker studies, it appears that despite an intervention (orthotic/shoe), the foot joint motion remains consistent if the path of motion is straight, such as it is in running. This is shown in the running study and the

cutting study in this dissertation. The range of motion and joint pattern of the foot joints remained unchanged despite the shoe condition changing during level running. However, when the path of motion is changed, as in the cutting versus running study, the joint angles did deviate from the optimized joint pattern observed during the running trials.

These results have challenged the thinking of foot biomechanists. In the last decade, new research has been able to specifically contradict the previously published foot kinematic research. The results of several recent studies have begun to challenge accepted theory that excessive pronation and high impact peaks lead to injury¹⁰.

A few new paradigms were included as possible rationale for the study observations throughout the proceeding chapters. The issue is whether the foot kinematics are unaltered by a footwear perturbation, but why does the subject's pain decrease with the use of an orthotic or a change in running shoes that have been prescribed to change the foot kinematics. One possible theory is that the foot has a pre-determined movement pattern that is controlled by muscle activation. Therefore, orthotics and motion control shoes rescue the muscles and soft tissues by supporting the bones in the foot. The joint's ROM remains constant but the strain on the soft tissue is decreased, as is the pain. The fact that kinetics and electromyography (muscle activity) were not captured during the studies in this dissertation is a limitation since they might have answered some of these questions.

The second possibility that was discussed was that the foot is a structurally redundant system. With technology advances, researchers should be able to decrease the number of bones per segment in multi-segment foot models until the articulations of each bone can be individually measured reliably. Then the true motion of the foot when disrupted by a footwear perturbation could be known.

The last possibility was discussed in chapter 3. One of the major problems with conducting research on the foot is that inter-subject variability is very high, as seen throughout this dissertation. This means that small sample sizes that are often used in this type of research are not often generalizable. However, perhaps this subject variability is the exact underlying theory that needs to be analyzed in order to discover the mechanism behind foot injuries and orthotic or shoe prescription.

One potential possibility is that everyone is different. Each person has a different neutral zone where they remain pain free. If the subject remains within the neutral zone by not surpassing their active boundary (or end-of-range), they will avoid injury, as discussed in chapter 3 and above. If for whatever reason, such as too much training, weak muscles, or harder running surface, the subject is unable to maintain joint motion within the desired neutral zone, they may experience pain. If an orthotic or shoe can correct the malalignment, then they remain injury-free. The ROM may remain the same but rather than moving through an absolute angle outside the subject's neutral zone, the subject now moves within the joint end-of-range.

The subject variability becomes important when discussing the limits of an individual's end-of-range. An example would be two runners that have the same injury and receive the same orthotic but one becomes injury-free while the other does not. It is speculated that the injury-free athlete had a larger neutral zone range before crossing their end-of-range than did the other athlete.

In conclusion, researchers need to be conscious of soft tissue artifact errors when planning their methodologies. Other methodological considerations include hole sizes for the windows cut into the shoe and the single versus per-condition static trials for establishing neutral positions. The studies performed in this dissertation should assist researchers with these questions. Using chapter 2, the validation study, a valid window size was determined. The chart accompanying chapter 3 should assist researchers in their decision on single versus pre-condition neutral trials depending on their research objective.

Foot research is in its infancy. The foot is a difficult body segment to study methodologically, compared to the knee for example. The foot, comprised of 26 bones, has only small joint excursions which makes tracking motion difficult. However, the foot is a very important segment since it is the segment that contacts the ground. Therefore much of what happens in the foot influences the joints that are more proximal in a closed kinetic chain. Hopefully with technological advances and novel foot models, such as the one used in this dissertation, analysis of the foot will become easier and more reliable so that some of the hypothesis addressed in this dissertation can become standard foot theories.

7.2 Reference

1. Stacoff, A., Reinschmidt, C. & Stussi, E. The movement of the heel within a running shoe. *Med Sci Sports Exerc* 24, 695-701 (1992).
2. Nawoczinski, D. A., Saltzman, C. L. & Cook, T. M. The effect of foot structure on the three-dimensional kinematic coupling behavior of the leg and rear foot. *Phys Ther* 78, 404-16 (1998).
3. Barr, K. P. & Harrast, M. A. Evidence-based treatment of foot and ankle injuries in runners. *Phys Med Rehabil Clin N Am* 16, 779-99 (2005).
4. Lutter, L. Injuries in the runner and jogger. *Minn Med* 63, 45-51 (1980).
5. Shorten, M. R. The energetics of running and running shoes. *J Biomech* 26 Suppl 1, 41-51 (1993).
6. McKenzie, D. C., Clement, D. B. & Taunton, J. E. Running shoes, orthotics, and injuries. *Sports Med* 2, 334-47 (1985).
7. Clarke, T. E., Frederick, E. C. & Hamill, C. L. The effects of shoe design parameters on rearfoot control in running. *Med Sci Sports Exerc* 15, 376-81 (1983).
8. Busseuil, C., Freychat, P., Guedj, E. B. & Lacour, J. R. Rearfoot-forefoot orientation and traumatic risk for runners. *Foot Ankle Int* 19, 32-7 (1998).
9. Yamashita, M. H. Evaluation and selection of shoe wear and orthoses for the runner. *Phys Med Rehabil Clin N Am* 16, 801-29 (2005).
10. Nigg, B. M. The role of impact forces and foot pronation: a new paradigm. *Clin J Sport Med* 11, 2-9 (2001).